Alan J. A. McBride

Studies on DNA Supercoiling and Potential *Z*-DNA Forming Sequences in Streptomycetes

A thesis submitted to the University of Manchester

Institute of Science and Technology

for the degree of Ph.D.

1995

Department of Biochemistry and Applied Molecular Biology

ABSTRACT

The superhelical density of the *Streptomyces* plasmid, pIJ486, was determined by estimating the linking difference (ΔLk) from a range of topoisomers *in vitro*. The superhelical density was observed to vary from —0.057 up to —0.073, among the highest values reported for plasmids isolated from eubacteria to date. Given the high G+C content (ca.74 mol%) of *Streptomyces* DNA this was perhaps not unexpected; during DNA-protein interactions, negative supercoiling provides an inherent energy source and G+C rich DNA templates would require more energy to separate the strands compared to DNA with a low G+C content.

A standard pIJ486 sample, of known ΔLk, allowed the variation in superhelical density of pIJ486 to be investigated throughout the growth phases of *Streptomyces coelicolor* MT1110(pIJ486). In contrast to observations made in *Escherichia coli*, the superhelical density of pIJ486 was maintained at a high level (> —0.064) throughout exponential growth and well into stationary phase. Surface grown cultures in particular maintained a superhelical density of ca.—0.07 with the loss of only two negative supercoils for at least 50 h into stationary phase. The sharpest change in the linking difference of pIJ486, isolated from surface grown cultures, was observed during the transition phase to aerial hyphae formation. The number of potentially unrestrained negative supercoils rose by up to ca.20%. During liquid growth the topological distributions of some plasmid samples were observed to be bimodal, with two distinct topoisomer populations. This appeared to coincide with cannibalistic regrowth of the culture during late stationary phase and was limited to liquid grown cultures.

In the glycerol operon of *Streptomyces coelicolor* and *Streptomyces lividans* there are potential *Z*-DNA forming sequences within the —35 region of *gylP*1 and midway between *metH*p and *gylR*p, which are divergently transcribed. The possibility that these sequences could adopt a left-handed *Z*-DNA conformation on recombinant plasmids *in vivo* was investigated. Gradient plate analysis of *neo* expression suggested that disruption of these *Z-form* sequences does relieve expression from vector-borne *gyl*P1/P2. However, the APHII enzyme assay data did not confirm these observations, possibly due to recombination between the plasmid and chromosome during the liquid growth for the preparation of cell-free extracts. It should be noted that this recombination occurred in an orientation-specific fashion and may be linked to increased expression from *gylR*p.

A model is presented to explain the results observed for expression from *metH*p in the *Z*-DNA mutants. On a recombinant plasmid the 23 bp *Z-form* sequence between *metH*p and *gylR*p appears to enhance expression from *metH*p, possibly by adopting *Z*-DNA to relieve transcription-induced supercoiling *in vivo*.

DECLARATION

No portion of the work referred to in this thesis has been submitted in support of an application for another degree or qualification of this or any other institution of learning.

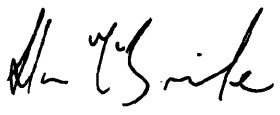

Acknowledgements

Firstly, I would like to thank my supervisor, Colin Smith, for providing me this opportunity, for the invaluable discussions and advice over the last few years.

Thanks also to the other members of the *gyl* group, Zoe Hindle, Mark Paget, Fiona Davies and those who passed through F28, particularly Fiona, Jackie, Giselda, Diana, and Roseanna, for the hands on help and alternative points of view.

There are many others in the department who deserve thanks, to name but a few, Glynn, Phil, Tony and Dave for help with the bioreactors, and Simon for help with the computers.

Thanks also to my parents who provided the best place to write this thesis, hope I did not disrupt things too much.

Lastly, I would like to thank Zoe again, if you had not been there I would never have finished this, I owe you a lot.

Abbreviations

A	adenine
ADP	adenosine diphosphate
amp	gene encoding β-lactamase
ATP	adenosine triphosphate
att	attachment site
bp	base pair(s)
cAMP	cyclic adenosine monophosphate
cat	gene encoding chloramphenicol acetyltransferase
ccc	covalently closed circular
CIAP	calf intestinal alkaline phosphatase
ChQ	chloroquine
C	cytosine
DNaseI	deoxyribonuclease I
ds	double stranded
EtBr	ethidium bromide
DTT	dithiothreitol
G	guanine
kb	1000 bp
ΔLk	linking difference
mRNA	messenger RNA
NADH	β-nicotinamide adenine dinucleotide, reduced form
neo	aminoglycoside phosphotransferase isolated from Tn*5*
oc	open circular
oligo	oligonucleotide(s)
ORF	open reading frame
ori	origin of replication
PolIk	*E. coli* DNA polymerase I, Klenow (large) fragment
^{R}	[superscript] resistance/resistant
ss	single stranded
σ	superhelical density or specific linking difference
T	thymine
t_D	doubling time(s)
Top	topoisomer(s)
TopI	DNA topoisomerase I
tsr	thiostrepton resistance gene
U	units

Table of Contents

Chapter One

Introduction

1.1: Preamble

The genus *Streptomyces* consists of Gram positive eubacteria, unusual among prokaryotes because of their complex cycle of morphological development and the exceptional number of useful secondary metabolites they produce. Streptomycetes are also being exploited for the over-production of economically important endogenous and heterologous proteins.

Streptomycetes surface-colonise substrates through an extensive, branched, vegetative mycelium that, possibly upon nutrient limitation, differentiates to form aerial hyphae and eventually, pigmented spores for dispersal. The production of secondary metabolites is temporally co-ordinate with differentiation and may be an attempt to protect the lysing vegetative mycelium, a potential nutrient source, from other scavenging bacteria (Chater and Merrick, 1979), and/or export toxic intermediates that could otherwise kill the cell (see, e.g., Zähner, 1979).

Due to the low levels of antibiotics produced by wild-type actinomycete strains and acquired immunity by target organisms the pharmaceutical industry is constantly looking for ways to improve yields and isolate novel compounds. This was originally achieved through classical strain improvement programmes (random mutation and selection, media

and bioreactor optimisation), and the screening of randomly selected isolates from around the world. However, this empirical approach is likely to be of finite use (Chater, 1990); the screening of isolates is a very labour intensive and costly process, therefore recently there has been a trend towards the application of qualitative techniques to overcome these problems.

As the biosynthetic pathways of various antibiotics are cloned and studied the preferential synthesis of a desirable product has become possible (Doull and Vining, 1990; Hobbs *et al.*, 1992). The manipulation of biosynthetic pathways using blocked mutants and precursor analogues has been used to synthesise new compounds (reviewed by Okami and Hotta, 1988). Other techniques for the production of novel compounds include direct crossing, protoplast fusion and genetic engineering.

The actinorhodin (*act*) gene cluster of *Streptomyces coelicolor* A3(2) has been used to create novel hybrid antibiotics (Hopwood *et al.*, 1985b). The overexpression of the activator genes of specific biosynthetic pathways leading to increased yields has been achieved (e.g., *redD*, Takano *et al.*, 1992; *act*II-ORF4, Gramajo *et al.*, 1993).

At present this more rational approach is being jointly undertaken in Europe (e.g. EC BRIDGE *Streptomyces* project), by investigating microbial physiology through the study of primary metabolic pathways. Studies of carbon catabolism have led to a basic understanding of gene regulation which can be applied to other metabolic pathways and the generation of useful genetic tools such as expression vectors (e.g., *tipA*, Murakami *et al.*, 1989).

One such pathway in *S. coelicolor* A3(2) is the peripheral carbon catabolic pathway for glycerol utilization; the glycerol (*gyl*) operon (section 1.7) is glycerol inducible, glucose repressed and regulated by GylR (Seno and Chater, 1983; Seno *et al.*, 1984; Smith, 1986; Smith and Chater, 1988a, b; Hindle and Smith, 1994). Catabolite repression control mechanisms are also known to be involved in the regulation of antibiotic biosynthesis and morphological differentiation (Chater and Merrick, 1979; Martin and Demain, 1980) and may provide insights into the regulation of secondary metabolism. Although lacking commercial interest *S. coelicolor* A3(2) and its close relative *S. lividans* 66 are the best characterised streptomycetes and have become the "control" strains in studies of primary metabolism.

An aspect of *Streptomyces* molecular biology so far overlooked, indicated by published literature, is how the biological consequences of DNA-protein interactions (see above) and DNA topology relate to each other. Studies in *E. coli*, *Salmonella* spp. and *Bacillus subtilis* have provided an increasing amount of information on the interaction between the superhelical density (σ) of DNA and many DNA-protein interactions. For example, the enzymes that control the level of σ, DNA gyrase (*gyrA* and *gyrB*), and DNA topoisomerase I (*topA*), are transcriptionally regulated by DNA supercoiling at their loci (section 1.8.3).

This thesis describes the structure and regulation of the *gyl* operon of *S. coelicolor* and studies of DNA supercoiling and *Z*-DNA formation. Previous work on the *gyl* operon and gene regulation in *Streptomyces* DNA topology and its biological significance in prokaryotes is discussed below.

1.2: The *Streptomyces* genome

Actinomycetes contain one major genetic linkage group and a range of extrachromosomal elements, not all of which are circular. The use of heteroclones and the fertility factors of *S. coelicolor* A3(2) has produced a detailed circular linkage map of the chromosome (Hopwood and Kieser, 1990). With the advent of pulsed-field gel electrophoresis (PFGE) a combined physical-genetic map of *S. coelicolor* M145 was obtained (Kieser *et al.*, 1992). Unexpectedly, a recent publication demonstrated that the chromosome is physically linear (Lin *et al.*, 1993).

The use of PFGE has so far provided the most accurate size estimation of the *S. coelicolor* genome, at ca.8 Mb (8 X 10^6 bp), which is 75% larger than the *E. coli* genome (Kieser *et al.*, 1992). This work also revealed that the two genetically almost silent regions are physically long and not recombination hotspots. Streptomycetes have a biased base composition, 70-74 mol% G+C, and there is a very marked preference for G+C rich codons in the structural genes (Wright and Bibb, 1992).

Another unusual feature of the *S. coelicolor* linkage map is the dyad symmetry of some gene clusters, whereby the genes of a biosynthetic pathway are diametrically separated, possibly as a result of a doubling of the chromosome (Hopwood, 1967). This evolutionarily historic doubling was probably followed by a progressive loss of one of the duplicated genes at either site on the map. The *Streptomyces* genome is also genetically unstable; deletions of up to 800 kb associated with tandem amplifications of chromosomal DNA have been reported (see references in Hopwood and Kieser, 1990).

1.3: Gene expression and regulation

This section summarises the basic cellular components and signals known to play a role in gene expression and regulation.

1.3.1: Transcription and RNA polymerase

Early work by Westpheling *et al.* (1985) suggested that *Streptomyces* probably use a number of alternative sigma factors to recognise promoters. RNA polymerase purified from *S. coelicolor* was studied and two different holoenzymes were identified (Westpheling *et al.*, 1985). One form, σ^{35}, was found to recognise the *veg* promoter from *B. subtilis* which is very similar to the *E. coli* σ^{70} consensus sequence ($E\sigma^{70}$). The other, σ^{49}, recognised the *endoH* promoter of *S. plicatus* and *ctc* of *B. subtilis*. To date seven RNA polymerase holoenzymes have been identified which suggests that sigma factors occupy a central role in regulation of gene expression in *Streptomyces* (Buttner, 1989). Protection studies with the *S. coelicolor* RNA polymerase indicate that it interacts with a promoter region in a way similar to the *E. coli* holoenzyme (Reznikoff *et al.*, 1985).

The isolation of such a variety of holoenzymes suggests that *Streptomyces* regulate transcription in a manner more akin to *Bacillus* spp. than to *E. coli*. The majority of *E. coli* promoters fall into two categories, recognised by $E\sigma^{70}$ or $E\sigma^{54}$ sigma factors (Gralla, 1991), whereas there are eight known holoenzymes of *B. subtilis*, six of which are involved in morphological development (Losick and Straiger, 1992). In *S. coelicolor* a similar situation exists where a single gene (*dagA*) is transcribed from four promoters

recognised by at least three different sigma factors (Buttner *et al.*, 1988). Support for the theory that sigma factors may be involved in the morphological development of *Streptomyces* spp. was provided by studies of *whiG*. This gene is essential for sporulation in *S. coelicolor* and the predicted protein σ^{WhiG}, is similar to three sigma factors, σ^{D} of *B. subtilis*, σ^{F} of *S. typhimurium* and *Pseudomonas aeruginosa* (Chater, 1993), and see below. Four other genes have been isolated from *S. coelicolor* which have homology to *rpoD*, namely *hrdA* to *hrdD*. *hrdB* appears to be essential, therefore it has been suggested to encode the principle *S. coelicolor* sigma factor σ^{66} (σ^{HrdB}) (Brown *et al.*, 1992). *hrd* genes have also been isolated from *S. aureofaciens* and expression of the genes appears to be temporally regulated during differentiation. Transcription initiates from *hrdA* only at the start of aerial hyphae formation and from *hrdD* only during early mycelial growth (Kormanec and Farkašovský, 1993).

1.3.2: *Streptomyces* spp. promoters

Various attempts have been made to find a consensus-like promoter sequence in the manner of that for *E. coli* (Hawley and McClure, 1983), although *Streptomyces* spp. promoters vary widely in sequence and transcriptional patterns (Hütter and Eckhardt, 1988; Strohl, 1992). A recent review of streptomycete promoters by Strohl (1992) suggests two major groupings: (a) promoters with sequences similar to those transcribed by $E\sigma^{70}$ and whose —10 and —35 hexamers are 16-18 bp apart; (b) promoters with non-consensus-like sequences and whose —10 and —35 hexamers are separated by more than 18 bp. The majority of promoters fall into the latter group with the promoters of the housekeeping genes in the former group, this is probably a reflection of the popularity of the non-

housekeeping genes as more "interesting" targets. The Eσ^{70}-like streptomycete promoters include the *gyl*P1 promoter of the *S. coelicolor gyl* operon and would include *gylR*p and *gyl*P2 if a hexamer spacing of 19 bp was allowed. Mutational studies on streptomycete promoters show that the spacing is more important than the —35 hexamer in some cases, e.g. *ermE*p1 and *gal*p1 (see Strohl, 1992). Studies on the —10 hexamer of *gyl*P1 and *gyl*P2 have demonstrated its essential role (F.J. Davies and C.P. Smith, personal communication).

1.3.3: Translation

Initiation occurs in a typical prokaryote manner, although streptomycete ribosomes need only a small amount of complementarity between the Shine-Dalgarno sequences and the 3' end of the 16S rRNA to initiate (Strohl, 1992). Streptomycetes do not fit the rules proposed by McLaughlin *et al.* (1981) for Gram positive bacteria; *B. subtilis* complementarity is very stringent. AUG is the usual start codon but GUG is also used and for the majority of streptomycete genes the ORF is around 100 bp from the transcription start site. Given some of the distances involved it has been proposed that the significant secondary structures in some 5' mRNA leaders are regulatory, e.g. antiterminators. Several *Streptomyces* genes are known to translate without an RBS, transcription and translation often starting at the same b (see Strohl, 1992). As mentioned in section 1.2, *Streptomyces* show a very biased codon usage with up to 90% of the third position of translated codons being G or C (Wright and Bibb, 1992). This is probably a consequence of the mutational bias that resulted in the high G+C content of the chromosome. This bias does not however extend to all genes, TTA codons occur in

occur in genes expressed at low levels, e.g. regulatory genes like *act*II-ORF4 (Gramajo *et al.*, 1993; and see below).

1.3.4: Secretion

As mentioned in section 1.1, *Streptomyces* spp. secrete a variety of proteins such as exoenzymes, protease inhibitors, regulatory molecules (e.g. Factor-C) and heterologous proteins (e.g. proinsulin). From the identified amino-terminal signal-sequence-like structure of several genes streptomycetes appear to use the same secretory mechanism as *E. coli* and *Bacillus* spp. (Silhavy *et al.*, 1983). During secretion the signal sequence is cleaved by a signal peptidase and the mature protein is secreted directly into the medium. The signal sequence consists of three domains: a hydrophilic amino-terminus; a hydrophobic trans-membrane region and a signal cleavage site. Arginine residues are the preferred charged amino-acids in the hydrophilic region, possibly because *Streptomyces* spp. prefer G+C rich codons over the A+T rich lysine codons preferred by *E. coli* and *Bacillus* spp.

Another mechanism of secretion may exist in streptomycetes as some secreted proteins lack a signal sequence (e.g. tyrosinase of *S. antibioticus*; Bernan *et al.*, 1985).

1.4: Antibiotic synthesis in *Streptomyces spp.*

Streptomyces spp. produce a vast array of secondary metabolites and many of them are antibiotics and other pharmacologically active compounds. In liquid media production is usually limited to stationary phase or cultures with low growth rates (Demain *et al.*, 1983); in solid media it seems to be temporally co-ordinate with differentiation, with some genes involved in both processes (Chater, 1993). Isolation of pleiotropic mutants of *S. coelicolor* indicate that the antibiotic genes are globally as well as specifically regulated (see, e.g., Champness *et al.*, 1992; Chater, 1993). *S. coelicolor* A3(2) produces at least four chemically distinct antibiotics: actinorhodin (*act*); undecylprodigiosin (*red*); methylenomycin (*mmy*) and a calcium dependant antibiotic (CDA). The biosynthetic pathways, including structural, regulatory and resistance genes are usually clustered on the chromosome, the methylenomycin genes are however clustered on the giant linear plasmid SCP1 (reviewed by Chater, 1990).

1.4.1: Antibiotic specific regulation

Various pathway-specific activators have been identified: *redD* in undecylprodigiosin biosynthesis (Narva and Feitelson, 1990) and *act*II-ORF4 in actinorhodin biosynthesis (Fernández-Moreno *et al.*, 1991), in *S. coelicolor*; *strR* in streptomycin biosynthesis in *S. griseus* (Distler *et al.*, 1987); *brpA* in bialaphos biosynthesis (Raibaud *et al.*, 1991); and *dnrI* in daunorubicin biosynthesis in *S. peucetius* (Stutzman-Engwall *et al.*, 1992). The actual mechanism of regulation still remains unclear although there is evidence that a reduction in growth rate from exponential to stationary phase kinetics

stimulates transcription of some activators. Indeed, when *redD* or *act*II-ORF4 are present on multicopy vectors the overexpression of each respective antibiotic occurs during exponential growth; suggesting that the presence of activator is the only limiting factor for expression under the conditions described (*redD*, Takano *et al.*, 1992; *act*II-ORF4, Gramajo *et al.*, 1993). In both cases there is no evidence for a repressor protein being titrated out by the vector.

One possible method for regulation of the activator genes was thought to be through the temporal regulation of *bldA* (Leskiw *et al.*, 1993) as all the activators above (except *redD*) contain the rare TTA codon and *bldA* encodes the necessary $tRNA_{UUA}$ for efficient translation (but see below). The expression of *redD* was suggested to be increased by changes in superhelical density when plasmid-borne (Takano *et al.*, 1992), another possible mode of regulation.

Antibiotic resistance genes, which protect the antibiotic-producing organism from self-destruction (Hopwood, 1988), may be regulated through the expression of the biosynthetic structural genes (Janssen *et al.*, 1989). The promoters of the resistance and structural genes often overlap, are divergent and probably interact topologically. However, some resistance genes respond to the appearance of the antibiotic in the environment, presumably at sub-inhibitory concentrations e.g. *mmr* in the methylenomycin cluster (Hobbs *et al.*, 1992). Others are regulated by a repressor protein e.g. the export genes (*act*II-ORF2/3) of actinorhodin are regulated by the repressor encoded by *act*II-ORF1 (Caballero *et al.*, 1991), the promoter of which is divergent to the export genes, allowing a topological interaction between them.

1.4.2: Pleiotropic regulation of antibiotic pathways

Developmental mutants, blocked in antibiotic biosynthesis have been identified and placed into two groups: (i) mutations that block both antibiotic biosynthesis and differentiation (e.g. *bldA-D* and *bldG-H*, reviewed by Chater, 1993; Chater and Bibb, 1995) and (ii) mutations that block antibiotic biosynthesis but permit differentiation (reviewed by Chater and Bibb, 1995; *absA* and *absB*, Champness *et al.*, 1992; *afsR* and *afsB*, Hara *et al.*, 1983; Horinouchi *et al.*, 1983; and *abaA*, Fernández-Moreno *et al.*, 1992).

bldA is the only *bld* mutation with a known gene product, namely $tRNA_{UUA}$ that recognises the TTA codon (Lawlor *et al.*, 1987). As the *act*II-ORF4 sequence contains TTA codons (Fernández-Moreno *et al.*, 1991), this provides a reason why *bldA* mutants cannot produce actinorhodin. When however, *act*II-ORF4 is present on a multicopy vector actinorhodin is produced (Passantino *et al.*, 1991). This is assumed to occur through mistranslation of the UUA codon beyond the threshold level of ACTII-ORF4 required for actinorhodin production. Loss of undecylprodigiosin production in *bldA* mutants does not occur through *redD* as it contains no TTA codons, suggesting that there are additional genes, containing TTA codons, required for *redD* expression.

The role of *bldA* in the regulation of actinorhodin production is unclear. Under one set of conditions *bldA* is temporally regulated, no mature, active $tRNA_{UUA}$ is present until stationary phase (Leskiw *et al.*, 1993); under another set of conditions there is active $tRNA_{UUA}$ in young vegetative mycelium and *act*II-ORF4 still was not expressed until the transition to stationary phase (Gramajo *et al.*, 1993). Leskiw *et al.* (1993) suggest that

the culture conditions may determine which regulatory elements are predominant in regulating secondary metabolism.

The *abs* loci encode genes required in the production of all four antibiotics produced by *S. coelicolor* (Adamidis and Champness, 1992). *abs* mutations block the production of these antibiotics but allow sporulation suggesting, given that the mutants are genetically competent in all the biosynthetic pathways, that the *abs* loci represent mechanisms of specific global antibiotic regulation. During complementation studies a DNA fragment was repeatedly isolated that caused overproduction of actinorhodin in AbsB$^-$ mutants, and was identified as *act*II-ORF4. As *act*II-ORF4 and *redD* have significant homology to each other (Takano *et al.*, 1992), the *abs* genes may regulate *redD* in *bldA* mutants, although no common DNA-binding motif in the amino-acid sequence of the activators has been identified.

1.5: Differentiation and morphological development of *Streptomyces* spp.

Streptomycetes undergo both physiological and morphological differentiation. Secondary metabolism is described as physiological differentiation as it occurs after the main period of vegetative and metabolic growth. The interaction between antibiotic biosynthesis and morphological development has been described in section 1.4. This section describes what is known concerning the interaction between aerial hyphae formation and sporulation during morphological differentiation.

Streptomycetes grow by extension of the hyphal tips and quasiexponential branching to form a vegetative mycelial mat. As the mycelia age storage compounds are accumulated, secondary metabolites are produced and eventually the mycelium lyses. Meanwhile aerial hyphae develop after a stalling in macromolecular synthesis (Granozzi *et al.*, 1990), and solubilization of the storage compounds (e.g. glycogen). The resultant increase in osmotic pressure is proposed to encourage aerial hyphae to form (Chater, 1989a, b), the directionality of which is provided by condensation of surface molecules peculiar to aerial hyphae, Saps, (spore associated proteins). Saps may help to disrupt surface tension to allow extension of the hyphae and act as an anti-desiccant by covering the surface of the hyphae (Willey *et al.*, 1991). After extension ceases, possibly by a reappearance of glycogen deposits and resultant decrease in osmotic pressure (Chater, 1989b), unigenomic compartmentalization of the aerial hypha occurs. Two classes of mutants have been isolated in the attempt to unravel the genetically basic but regulatory complex interactions of differentiation; the *bld* and *whi* mutants. *bld* mutants fail to produce aerial hyphae and most are defective in antibiotic production, the *whi* mutants produce aerial hyphae but fail to develop the pigment associated with mature spores.

1.5.1: Aerial hyphae-deficient mutants

To date there have been no *bld* mutations isolated that are not unaffected in secondary metabolism, suggesting that those involved solely in aerial hyphae formation must be essential for vegetative growth. Saps are absent from most *bld* mutants and they are defective in storage compound metabolism (see Chater, 1993). *bldA, bldB, bldD* and *bldG* have been cloned, but as mentioned in section 1.4, only the gene product of *bldA* is

known; the $tRNA_{UUA}$ that recognises TTA codons (Lawlor *et al.*, 1987). *bldA* can be deleted, presumably no essential vegetative genes contain the TTA codon; interestingly 80% of TTA codons identified are in specific regulatory or resistance genes of antibiotic biosynthetic pathways (Leskiw *et al.*, 1991). It has been noted, through promoter-probing and S1 mapping studies, that mature *bldA* transcripts increase in abundance during aerial hyphae formation or early stationary phase in liquid growth (Leskiw *et al.*, 1993). This suggests that *bldA* may temporally regulate genes containing the TTA codon. However, Gramajo *et al.* (1993) found abundant levels of mature transcript in young cultures and no increase during aerial hyphae formation or early stationary phase. It should be noted that different hosts and growth conditions were used, Leskiw and co-workers used rich media; Gramajo and co-workers used minimal media. Leskiw *et al.* (1993) also reported the existence of an antisense transcript from within the tRNA-encoding sequence of *bldA* which may be involved in mRNA processing or stability *in vivo*.

The study of *S. griseus bldA* mutants has indicated a potential target for *bldA* regulation, namely *orf*1590 (Babcock and Kendrick, 1990), which contains a TTA codon, as does the *S. coelicolor* homologue. *orf*1590 contains two promoters and may be involved in postranslational regulation of sporulation on top of any regulation by *bldA* (McCue *et al.*, 1992). SapB, a non-ribosomally synthesised protein (see Chater, 1993), diffuses around producing colonies, and can restore aerial hyphae formation to *bldA-D, bldG-I* and *bld-261* mutants when grown close to a producing strain or supplemented by the purified SapB protein (Willey *et al.*, 1991).

However, all the *bld* mutants can produce aerial hyphae on minimal media (containing mannitol) and under these conditions SapB is not detected (Willey *et al.*, 1991). Thus, aerial hyphae formation can proceed by alternate pathways with SapB only detected when grown on rich media. Interestingly, under these conditions *bldA* may be temporally regulated and SapB is thought to contain leucine residues but this may be irrelevant if SapB is synthesised non-ribosomally.

Another diffusible compound is A-factor, in *S. griseus* it regulates sporulation and secondary metabolite formation by inactivating a cytoplasmic-binding repressor protein. A-factor-like compounds are widespread in *Streptomyces* and a role in differentiation has been demonstrated in only a few strains so far (reviewed by Horinouchi and Beppu, 1992).

1.5.2: Sporulation deficient mutants

The formation of the grey spore-associated pigment is determined by genes involved in early spore formation, the *whi* genes. Through the morphology of double mutants an epistatic sequence for the five loci defective in sporulation was suggested: *whiG* → *whiH* → *whiA,B* → *whiI*, other results have shown however, that it is not due to a simple linear regulatory cascade (Chater, 1975). Moreover, the mutant phenotypes do not reflect the intermediate stages of normal sporulation.

Some of the *whi* genes have been cloned and sequenced, the following is a brief description of what this information has provided.

The putative sigma factor σ^{WhiG} has homologues in all *Streptomyces* spp. and other sporulating actinomycetes screened so far. Multiple copies of *whiG* cause early and abnormal sporulation, indicating its role in confining sporulation to aerial hyphae (Chater *et al.*, 1989b). Transcription from *whiG* is limited to cultures undergoing aerial hyphae formation (see Chater, 1993), and two promoters have been isolated that require σ^{WhiG} for expression. Neither of which are located close to or are from known *whiG* genes (Kieser *et al.*, 1992).

The *whiB* gene has been sequenced and encodes a small, charged polypeptide. Homologues have been isolated from non-sporulating actinomycetes and WhiB may be a transcriptional activator and part of novel protein family. Two promoters were found, with *whiB*P2 showing much stronger activity during aerial hyphae formation.

The *whiE* locus consists of seven ORFs, six of which encode proteins with homology to proteins involved in the synthesis of polyketide antibiotics (Davis and Chater, 1990). Transcription from *whiE*P1 coincides with the visible appearance of aerial hyphae.

Chater (1993) has reviewed this information in much greater detail and has proposed a model for sporulation based on genetical and biochemical regulation.

1.6: Carbon catabolism in *Streptomyces* spp.

There are many problems inherent to the study of primary metabolism in *Streptomyces* spp., mainly due to their life-cycle. A biomass sample from a *Streptomyces* sp. surface culture

would contain a range of morphologically and physiologically distinct mycelia. *Streptomyces* spp. do not grow in a synchronous manner and tend to pellet in liquid resulting in a range of differentiated mycelial states. Determining which active metabolic pathways belong to which phenotype is likely to be very difficult. Primary metabolism has recently been reviewed (Hodgson, 1994) and includes what is known about the central pathways of glucose metabolism and how they differ from those of *E. coli*.

Streptomyces spp. produce a number of extracellular enzymes to degrade the many complex carbohydrates they encounter in their natural habitat, e.g. cellulose, starch and chitins. A number of such pathways have been cloned and are under investigation, this section describes some of them. Carbon catabolite repression in prokaryotes and what is known about it is also summarised. The peripheral pathway of glycerol catabolism is discussed in detail in section 1.7.

1.6.1: Cellulose and cellulase

Cellulose is a glucose polysaccharide and in nature is complexed with hemicellulose to provide the most abundant organic compound on earth, its degradation is vital to the ecology. There is also a good deal of interest in the production of single-cell protein (SCP) and ethanol from waste wood and other natural sources (Crueger and Crueger, 1982). Streptomycetes produce a complex range of enzymes to achieve cellulose degradation and little is known about their regulation. This range includes endoglucanase (C_x cellulase), exo-glucanase (C_1 cellulase), and specific cellobiases. Straw was demonstrated to be an efficient inducer of these enzymes. Cellobiose is a repressor of

endoglucanase production, glycerol and amino acids also repress cellulase production (Godden *et al.*, 1989). This regulation varies from strain to strain, in some isolates cellobiose stimulated cellulase production and there may be a regulatory region upstream of a cellulase gene in *S. halstedii* (see Hodgson, 1994).

1.6.2: Starch and α-amylases

Starch is another abundant plant polysaccharide, hydrolysed by amylases which are used in the food industry in the production of sweeteners. The *aml* gene has been cloned from *S. limosus* and is maltose induced but not glucose repressible, however, when in an *S. coelicolor* or *S. lividans* background it is glucose repressible (Virolle and Bibb, 1988). The *S. venezuelae aml* gene is glucose repressed, this depends on the glucose kinase gene (see below), which is absent or not regulated by glucose in *S. limosus*. The *aml* gene is transcribed from an $E\sigma^{70}$-like promoter in all the hosts (Virolle *et al.*, 1988).

1.6.3: Chitin and chitinases

Chitins are also common to the natural environment of *Streptomyces* spp. in the form of insect exoskeletons and fungal cell walls and streptomycetes are very efficient at breaking them down. The chitinase genes have been cloned and studied from some *Streptomyces* spp. (Miyashita *et al.*, 1991; Robbins *et al.*, 1992). The promoters of two chitinase genes from *S. plicatus* were studied in *S. lividans* and were found to be induced by chitin and repressed by glucose (Delic *et al.*, 1992). The *chi63* promoter is $E\sigma^{70}$-like and direct repeat sequences flank the —35 region. Disruption of the repeat sequences results in

constitutive expression and loss of glucose sensitivity. This would seem to imply that glucose repression is mediated through inducer exclusion, however the *chi63* gene is not glucose repressed in *S. plicatus*.

1.6.4: Catabolite repression

Prokaryotes and eukaryotes prevent unnecessary metabolism via peripheral carbon catabolite pathways by repressing them when a rapidly assimilable carbon source, such as glucose, is available. This mechanism is known as catabolite repression (CR) and is usually exerted by two or more regulatory processes for repression of any particular pathway. The mechanism of CR is best understood in the enteric bacteria where a phosphoenolpyruvate (PEP):carbohydrate phosphotransferase system (PTS) regulates the uptake of substrates and modulates the synthesis of cyclic AMP (cAMP). What follows is a brief summary of what is known about CR in *E. coli* and a description of CR in *Streptomyces* spp.

1.6.4.1: Catabolite repression in *E. coli*

This subject has been extensively reviewed (Saier Jr, 1993; Postma *et al.*, 1993) and is summarised briefly below.

The PEP:PTS functions via inducer exclusion, preventing the uptake of non-PTS carbohydrates (e.g., glycerol, lactose and Krebs cycle intermediates) or leading to repression of specific catabolic genes by their repressor. The uptake of all PTS

carbohydrates (e.g., glucose, fructose and mannose) is regulated by the first two enzymes of the PEP:PTS; the phosphate group of PEP is transferred to enzyme I (EI), then to the HPr protein (P~Hpr) and onto the incoming carbohydrate in the presence of a carbohydrate-specific enzyme complex (EII). For glucose, the complex consists of the diffusible protein, IIA^{glc} (previously III^{glc}), and the membrane bound protein, $IICB^{glc}$, in *E. coli*. As glucose is assimilated IIA^{glc} is probably in the dephosphorylated form as the phosphate is transferred to an incoming glucose molecule. IIA^{glc} is the central regulatory molecule in CR; in its non-phosphorylated state it can bind to and inhibit the non-PTS carbohydrate carriers or, in the case of glycerol, glycerol kinase itself (section 1.7). The phosphorylated state of IIA^{glc} is balanced between phosphorylation, via P~HPr to $P\sim IIA^{glc}$, and its dephosphorylation via $IICB^{glc}$ in the presence of glucose. Also, the other PTS carbohydrates can dephosphorylate $P\sim IIA^{glc}$; P~HPr will phosphorylate the specific EIIA protein, and as the phosphorylation of IIA^{glc} by P~HPr is reversible, IIA^{glc} will probably exist in the non-phosphorylated state, resulting in inducer exclusion of non-PTS carbohydrates. It has been suggested that $P\sim IIA^{glc}$ activates adenylate cyclase resulting in the generation of cAMP (see, e.g., Postma *et al.*, 1993). cAMP interacts with the cAMP receptor protein (CRP) which then stimulates transcription of many CR-sensitive genes (reviewed by Kolb *et al.*, 1993).

1.6.4.2: Catabolite repression in *Streptomyces* spp.

It has only recently been demonstrated that some *Streptomyces* spp. contain the first two enzymes of the PTS. However, only the transport of fructose seems to occur via the PTS in the streptomycetes examined (Titgemeyer *et al.*, 1994). Also, there is no correlation

between cAMP production and carbon source assimilation in streptomycetes (reviewed by Hodgson, 1994) suggesting that CR in streptomycetes is different to that in *E. coli* . It is suggested that the PTS proteins in streptomycetes function generally in the regulation of carbon metabolism and secondary metabolite biosynthesis and/or excretion by a novel mechanism (Titgemeyer *et al.*, 1994). A number of both inducible and constitutive carbohydrate uptake systems in streptomycetes have been identified. Hodgson (1982) demonstrated that the uptake systems for glycerol and arabinose were substrate induced and glucose repressed at the transcriptional level. This glucose inhibited uptake of glycerol or arabinose was only observed when the mycelia were pre-grown on either carbon source in the presence of glucose. This suggested that the mechanism of glucose inhibition of sugar uptake could be glucose induced. By selecting for resistance to 2-deoxyglucose (DOG) in the presence of arabinose, Hodgson (1982) isolated non-CR mutants. These mutants had lost the ability to grow on glucose due to the loss of glucose kinase (*glk* mutants; Seno and Chater, 1983). Seno and Chater (1983) also demonstrated that in these mutants the glycerol catabolic genes were no longer glucose sensitive. The *glk* mutants were complemented by a DNA fragment and the activity localised to a 2.9 kb fragment (Ikeda *et al.*, 1984a). The sequence of this fragment was found to contain two complete open reading frames, ORF2 and ORF3, and a partial one, ORF1. ORF3 (*glkA*) alone complemented the *S. coelicolor* DOG mutants and restored glucose kinase activity and CR; it encodes GlkI, a glucose kinase protein as opposed to an activator of the *glk* gene (Angell *et al.*, 1992). *glkA* mutants are relieved for CR in several catabolic pathways including glycerol, agar and starch (Hodgson, 1982; Seno and Chater, 1983; Ikeda *et al.*, 1984a; Virolle and Bibb, 1988; Angell *et al.*, 1992). In a *glkA* mutant, CR of glycerol kinase and agarase activity is relieved on several carbon sources even though

these sources are not metabolized via glucose kinase. This suggested that CR is regulated by glucose kinase itself rather than the catalytic activity of the protein (i.e., not by synthesising a metabolite involved in glucose repression) (Kwakman and Postma, 1994). This is supported by results indicating that a structurally unrelated glucose kinase restores glucose assimilation but not CR in a *glkA* mutant (Angell *et al.*, 1994). It is likely that other controlling mechanisms for CR exist in *S. coelicolor* and not just glucose kinase. Hodgson (1982) showed that *glkA* mutants grew well on galactose and fructose, but were repressed if glucose was present as well. CR, via inducer exclusion, of the glycerol utilization operon is considered in section 1.7.1.3.

1.7: Glycerol catabolism

The use of glycerol as a sole carbon and energy source by bacteria is well known and has been comprehensively reviewed (Lin, 1976). It is only dissimilated by two routes, and the end product of each is the glycolytic intermediate, dihydroxyacetone phosphate (DHAP). In the major route, glycerol is phosphorylated to glycerol-3-phosphate (G3P) which is then oxidised to DHAP. In the second route, glycerol is oxidised to dihydroxyacetone and then phosphorylated to DHAP. Glycerol utilization by *S. coelicolor* is via the former route and involves two catabolic enzymes, ATP-dependent glycerol kinase and G3P dehydrogenase (Seno and Chater, 1983). This system has provided an amenable model for studying regulated streptomycete gene expression. What follows is a description of what is known about the structure and regulation of the glycerol (*gyl*) operon of *S. coelicolor*.

1.7.1: Glycerol catabolism in *Streptomyces spp.*

1.7.1.1: Cloning of the glycerol operon

Glycerol non-utilizing mutants were used to clone the catabolic genes and were classified into three phenotypes: Gyl^s mutants, sensitive to glycerol and lacking G3P dehydrogenase activity; Gyl$^-$ mutants, tolerant to glycerol and lacking both catabolic enzyme activities; Gyl^x mutants, slightly inhibited by glycerol but containing wild-type levels of glycerol kinase and G3P dehydrogenase activities. The Gyl^x mutations did not map close to the other mutations and are not discussed any further. The co-ordinate induction of both enzymes, by glycerol, and the lack of one or both of these enzymes in mutants unable to grow on glycerol indicates they are the primary enzymes of glycerol catabolism in *S. coelicolor* (Seno and Chater, 1983).

The Gyl^s mutations were thought to lie in the structural gene of the G3P dehydrogenase, glycerol sensitivity being due to an accumulation of toxic levels of G3P; a similar effect was reported for *E. coli* and *B. subtilis*. The Gyl$^-$ mutations were thought to lie in either the glycerol kinase gene, with G3P as the specific inducer (as in *E. coli*), or in an activator gene (Seno and Chater, 1983; and references therein). The relatively high uninduced glycerol kinase activity in Gyl^s mutants suggested that G3P was the specific inducer. Although it appears that *S. coelicolor* cannot transport it as it cannot grow on G3P as the sole carbon-source. The co-ordinate CR of glycerol kinase (*gylA*) and G3P dehydrogenase (*gylB*) in *S. coelicolor* led Seno and Chater (1983) to believe that the genes were clustered within the same operon.

Thus, as expected, complementation of the Gyl^s and Gyl$^-$ mutations indicated they were closely linked, mapping close to the *argA* locus of *S. coelicolor* (Seno *et al.*, 1984). Two, extensively, overlapping DNA fragments, 2.74 and 2.84 kb long, restored wild-type enzyme activity to all the Gyl^s and some Gyl$^-$ mutants. The results obtained suggest that neither of the two cloned *gyl* DNA fragments contained the promoter of the operon, complementation being achieved through recombination between the cloned and the chromosomal *gyl* DNA sequences (Seno *et al.*, 1984).

To clone the entire *gyl* operon a cosmid library was probed and three cosmids were isolated that spanned ca.69 kb of the *S. coelicolor* M138 genome, with the *gyl* operon near the centre (Smith and Chater, 1988a).

1.7.1.2: Organisation of the *gyl* operon

The organisation of the *S. coelicolor gyl* operon is presented in Figure 1.1. Two glycerol-inducible transcripts, 5.4 and 4.3 kb long, were detected by Northern blotting of mRNA isolated from *S. coelicolor* cultures grown on glycerol. Furthermore, S1 nuclease mapping using cloned *gyl* DNA revealed the 3' end of the 4.3 kb transcript, t_1 (Smith and Chater, 1988a). As t_1 coincided with the termination of sequences essential for glycerol utilization (Seno *et al.*, 1984) the 1.1 kb sequence, extending further downstream in the 5.4 kb transcript, was considered a non-essential gene (*gylX*), possibly encoding the glycerol facilitator protein; as glycerol is known to passively diffuse into the cell its disruption would be irrelevant (Smith and Chater, 1988a). However, the predicted N-terminal region of the first gene of the operon (*gylC*) has since been shown to have good

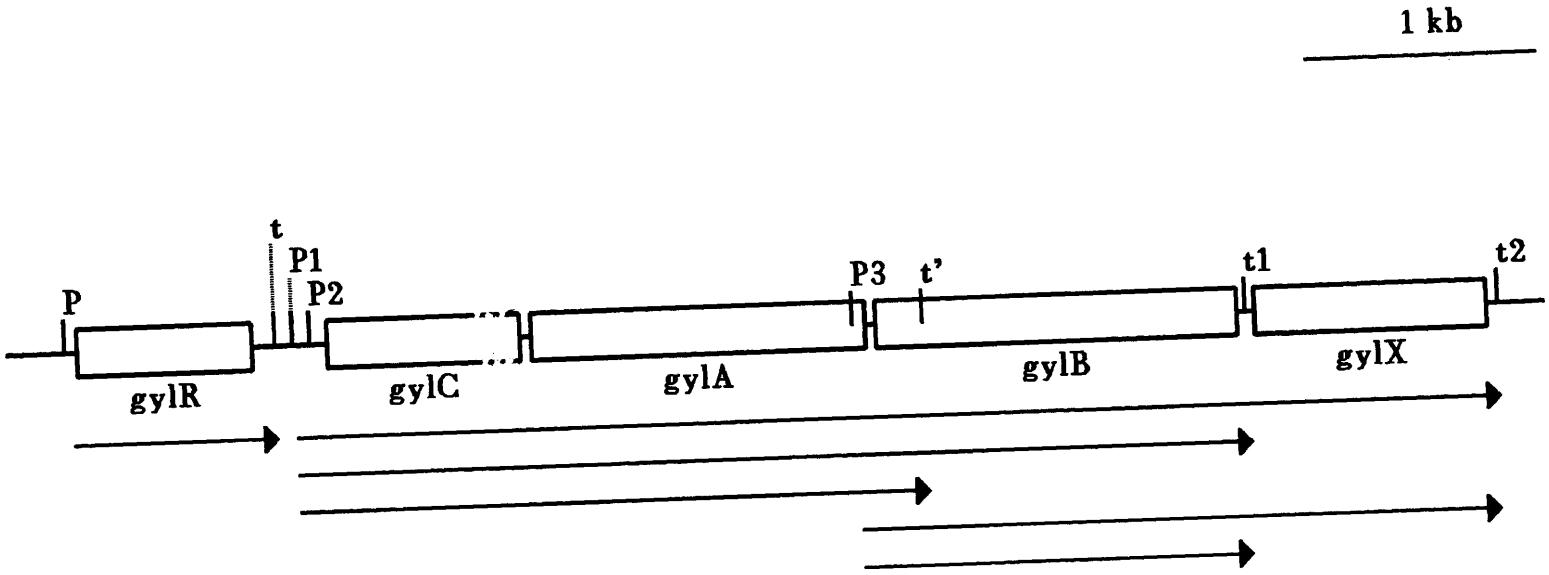

Figure 1.1: Transcriptional organisation of the glycerol catabolic genes of *S. coelicolor*

The arrows indicate transcripts and the boxed regions indicate the open reading frames. The dotted lines in the boxes of *gylC* and *gylA* indicate that the 3' end of *gylC* and the 5' end of *gylA* have not yet been mapped. The *gyl* promoters "P" are shown, as are the terminators "t" (see text). *gylR* encodes the repressor protein; *gylC* encodes the glycerol facilitator; *gylA* encodes glycerol kinase; *gylB* encodes G3P dehydrogenase; *gylX* encodes a protein of unknown function.

homology to the glycerol facilitator of *E. coli*. The *gylX* gene has been sequenced and its predicted 332 amino acid sequence has no significant homology to any known proteins (F.J. Davies and C.P. Smith, personal communication). The sequence upstream from *gylX* revealed the 3' end of an ORF (*gylB*) with a predicted amino acid sequence similar to *E. coli* G3P dehydrogenase, as expected from genetic studies (see above). The predicted transcriptional terminators, t_1 and t_2, flanking *gylX* were found to have typical intrinsic terminator-like sequences, with t_2 probably functioning in both orientations (F.J. Davies and C.P.Smith, personal communication). In addition to t_1 and t_2 a third 3' end was revealed from S1 nuclease mapping studies, t'. t_1 and t' (Figure 1.1) were thought to coincide with the end of cistrons (*gylB* and *gylA* respectively) from gene disruption studies and *in vivo* protein labelling studies (Smith, 1986; Smith and Chater, 1988a). Thus, the gene order of the glycerol operon is *gylCABX*.

Upstream from *gylC* a glycerol-inducible 0.9 kb transcript was detected by Smith and Chater (1988a). This was later designated *gylR* and it transcribes in the same direction as the *gylCABX* operon. It was found to encode a protein with the classical α-helix-turn-α-helix domain typical of some DNA-binding proteins (Smith and Chater, 1988b). GylR has homology to the transcriptional repressor proteins, IclR of *E. coli* (Nègre *et al.*, 1991) and KdgR of *Erwinia chrysanthemi* (Reverchon *et al.*, 1991).

1.7.1.3: Regulation of the *gyl* operon

The *gylCABX* operon is transcribed from tandem promoters, *gyl*P1 and *gyl*P2 (Figure 1.2), which are separated by ca.50 bp, induced 60-fold by glycerol and are glucose

(a) *gylR* promoter region:

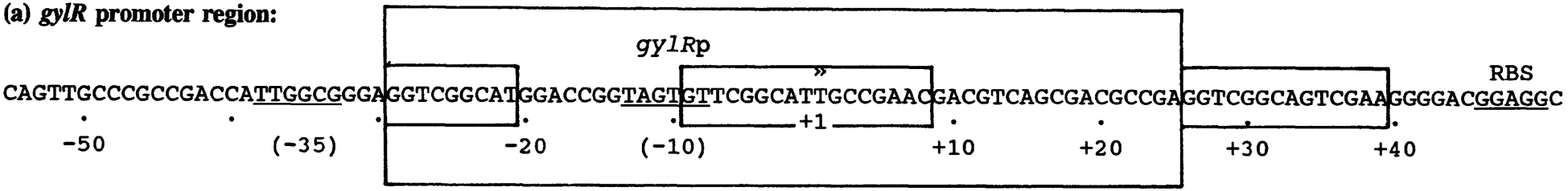

(b) *gylCABX* promoter region:

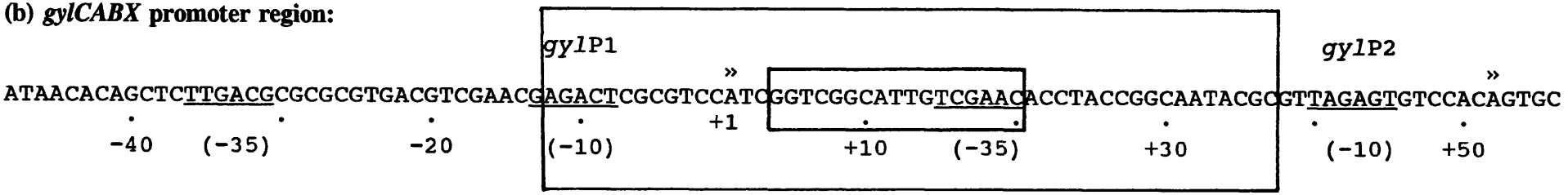

(c) Related operator sequences (indicated in smaller boxes above), [partially duplicated segments within *gylR*p are also indicated]

```
gylRp      (-29) 5′-G-G-T-C-G-G-C-A-T-
gylRp      (- 9) 5′-G-t-T-C-G-G-C-A-T-T-G-c-C-G-A-A-C-
                  ---------------> <---------------
gylRp      (+26) 5′-G-G-T-C-G-G-C-A-#-#-G-T-C-G-A-A-
gylP1/P2   (+ 4) 5′-G-G-T-C-G-G-C-A-T-T-G-T-C-G-A-A-C-
```

Figure 1.2: Features of the *gylR* and *gylCABX* promoter regions

The -10 and -35 regions of *gylR*p, *gyl*P1 and *gyl*P2 are underlined and the transcription start-sites are indicated by "»"; DNA sequences are numbered relative to the start-sites of *gylR*p and *gyl*P1 respectively; the *gylR* RBS is underlined. Operator elements (described in (c) above) and related sequences are indicated by small boxed regions; large boxed regions indicate the footprint protected from DNaseI by GylR *in vitro*.

repressible, (Smith and Chater, 1988b). *gylP*1 is a typical Eσ^{70}-like streptomycete promoter, *gylP*2 would be included in this group if a hexamer spacing of 19 bp was permitted (Strohl, 1992). Mutation of the —10 hexamer totally abolishes transcription initiation from the relevant promoter while the other remains unaffected (F.J. Davies and C.P. Smith, personal communication). A third promoter, *gylP*3, has recently been identified within the *gylA* C-terminal sequence (Figure 1.1) and which resembles *gylP*2 in structure (F.J. Davies and C.P. Smith, personal communication). This promoter may allow differential expression of *gylB*; possibly preventing toxic levels of G3P accumulating in the cell, or when transcription terminates at t' (see above).

The 0.9 kb upstream region (*gylR*) of *gylCABX* is transcribed by *gylR*p, an Eσ^{70}-like promoter similar to *gylP*2 in structure. *gylR*p is induced 10-fold by glycerol and is weakly glucose repressible. Another promoter, *gylR*p', was detected ca.250 bp upstream from *gylR*p, close to the *Sma*I(4)[1] site (Smith and Chater, 1988b). Overlapping the *gylR* and *gyl* promoter regions are very similar 17 bp operator-like elements (Figure 1.2). The operator element at *gylR*p differs from the one at *gylP*1/P2 by only 2 bp (Smith and Chater, 1988b). *gylR* has been over-expressed in *E. coli* and purified, DNaseI footprint studies using the purified GylR have revealed that GylR binds to both operator sequences (Figure 1.2; Z. Hindle and C.P. Smith, personal communication).

Originally GylR was thought to be a transcriptional activator in the presence of inducer and a repressor in the absence of inducer. This was based on a number of observations:

---

[1]The number in parenthesis after a restriction enzyme refers to the restriction sites shown in Figure 2.5.

gylR is specifically induced by glycerol and two glycerol non-utilizing mutants were complemented by DNA from the *gylR* region (Smith, 1986). However, since then a deletion of the chromosomal copy of *gylR* has indicated that GylR is not essential for glycerol utilization. GylR is in fact the repressor of the *gylCABX* operon and functions as a negative autoregulator (Hindle and Smith, 1994). GylR was also found to be similar to other transcriptional repressors (see above). The non-utilizing mutants that mapped to *gylR* mentioned above are probably inducer insensitive "super-repressors". When *gylR* was placed *in trans* at the phage ϕC31 *att* site the mutants were not complemented (C.P. Smith, personal communication). Complementation of the super-repressors probably occurred by recombination.

In section 1.6.4.2 it was mentioned that the *gyl* operon is glucose repressed; expression from *gyl*P1 is reduced ca.7-fold and from *gyl*P2 ca.2.5-fold when cultures are grown in equimolar concentrations of glycerol and glucose (Smith and Chater, 1988b). That GylR could be implicated in this CR was indicated by the *gylR* null-mutants; the *gyl* promoters were no longer glucose repressed (Hindle and Smith, 1994). This led Hindle and Smith (1994) to suggest that glucose metabolism via glucose kinase could somehow inhibit glycerol kinase activity, thus reducing the amount of inducer in the cell. This would lead to repression of *gylCABX* by GylR (i.e. inducer exclusion).

Another interesting feature of the *gyl* promoter region is the presence of alternating purine-pyrimidine tracts with the potential to form left-handed, Z-DNA (Figure 4.1; Smith and Chater, 1988b). When a *gyl*P1/P2-containing fragment was sub-cloned into the promoter-probe vector pIJ425 constitutive expression was observed. However, when *gylR*

was contiguous with *gyl*P1/P2 expression was abolished on all carbon sources tested (Smith, 1986). This phenomenon is referred to as unconditional repression and was considered paradoxical at the time as GylR was considered to be the transcriptional activator of *gyl*P1/P2 (see above). A possible role for Z-DNA formation (possibly due to differences in DNA supercoiling between the plasmid and chromosome) in the unconditional repression was suggested and an investigation into the *Z-form* sequences upstream from *gyl*P1 and *gylR*p is described in Chapter Four. Z-DNA and DNA supercoiling are discussed in section 1.8.

Since the demonstrationthat *gylR* encodes the repressor of the *gyl* operon the unconditional repression of *gyl*P1/P2 mentioned above has been regarded in a different light and a model has been proposed to explain it (Paget, 1994). Multiple copies of *gylR* will raise the concentration of GylR in the cell and repress *gylR*p expression, thus reducing the amount of GylR in the cell. However, the effect on chromosomal- and vector-borne *gyl*P1/P2 expression would probably be larger and more immediate compared to *gylR*p expression if GylR is constantly controlling them. A reduction in expression of the *gyl* operon will reduce the levels of glycerol kinase in the cell and hence the inducer, G3P, concentration. This will result in an increase in the proportion of repressor unbound to inducer (active) in the cell and thus, further repress the *gyl* operon. The multiple copies of *gylR* could therefore be shifting a balanced system towards a "repression cycle", gradually leading to a complete shut-down of *gyl*P1/P2 expression. Indeed, cells containing multiple copies of *gylR* grow poorly on glycerol as the sole carbon source (Paget, 1994), and glycerol kinase activity in such cells is undetectable in the cell-free

extracts (this study; data not shown). The reader is referred to Paget (1994) for a more critical discussion of this model.

1.8: DNA topology

Ever since the elucidation of the basic structure of the double helix of DNA (Watson and Crick, 1953) its importance has never been in doubt. However, the various alternative forms described in this section and their biological ramifications have only recently been considered. The following sections will attempt to summarise the salient points known at present concerning DNA topology.

1.8.1: DNA structure

Before considering the higher order structures of DNA the primary and secondary structure of DNA will be considered. DNA consists of repeated units, the nucleotides, that are in turn built up from three components: a sugar, 2'-deoxyribose; phosphate; and one of four bases. The bases consist of two purines, adenine and guanine, and two pyrimidines, thymine and cytosine. The chain is made by linking the sugars via a 3'-5' phophodiester bond and the bases are attached at the 1' position of the sugar. This constitutes a polynucleotide chain and is the primary structure of DNA.

From X-ray diffraction and chemical data the double helix structure of DNA was predicted. The two strands of the duplex are antiparallel, linked via hydrogen bonds between the bases and are coiled around each other in a right-handed twist. The bases

always bind specifically, adenine:thymine and guanine:cytosine. This represents the secondary structure of DNA and is known as *B-form* DNA, probably the most common form of DNA inside a cell. The helical repeat (number bp/turn) is usually estimated at 10.5 bp/turn for DNA in solution (see, e.g., Peck and Wang, 1981).

A-form DNA has been identified from X-ray diffraction studies (Franklin and Gosling, 1953) but has not been demonstrated *in vivo*, however, it has been suggested to exist in dormant spores of *Bacillus* spp. (Setlow, 1992; see below). *A*-DNA differs from *B*-DNA in the conformation of the sugar and has a helical repeat of 11 bp/turn.

Z-form DNA was the first structure to be elucidated by X-ray crystallography (Pohl and Jovin, 1972; Wang *et al.*, 1979). *Z*-DNA has a left-handed double helix with a helical repeat of 12 bp/turn and the sugar-phosphate backbone zig-zags, hence the name. *Z*-DNA has been demonstrated to occur *in vivo* (Jaworski *et al.*, 1987) and will be discussed in more detail in section 1.8.4.

Cruciforms can occur in sequences of dsDNA containing inverted repeats and formation of this structure involves intra-strand pairing. The formation of cruciforms has only been demonstrated on negatively supercoiled plasmids *in vitro* (Greaves *et al.*, 1985).

Another structure, *H*-DNA, formed in the DNA sequence $d(TC)_n$, occurring in eukaryotic DNA, has been demonstrated. Although the exact structure is not yet known it may consist of a triple stranded and ss region of DNA which then forms a kink (Bernués *et al.*, 1989).

DNA also demonstrates varying degrees of curvature of the helix, known as the intrinsic curvature of DNA and DNA bending. Intrinsic curvature has been demonstrated to occur when the DNA contains short runs of adenine bases every 10-11 bp (per helical repeat). This sequence has been found in kinetoplast DNAs of trypanosomes (Wells *et al.*, 1988). DNA bending can be of two types, isotropic and anisotropic. Isotropic bending can occur in any direction whereas anisotropic bending has a preferred bending path. DNA bending is related to sequence and is important in DNA-protein interactions, e.g. the interaction of CRP with DNA causes the DNA to bend by ca.90°, changes in the DNA sequence of the CRP binding site alter CRP binding and the degree of the bend (Schultz *et al.*, 1991).

For most of these conformations to exist, *in vitro* or *in vivo*, the energy supplied through DNA supercoiling is required for the deformation of the DNA helix. DNA supercoiling is considered in the following section.

1.8.2: DNA supercoiling

Supercoiled DNA was first described as a "twisted circular form" and referred to the major component of polyoma DNA (Vinograd *et al.*, 1965), since then supercoiling to some extent has been demonstrated in all ccc and constrained DNAs contained within a cell. DNA supercoiling is a result of either, introducing or removing, a full 360° twist in cccDNA or linear DNA if the ends are constrained relative to one another. Thus, negative supercoiling occurs when two complementary strands in a duplex ring are underwound, (positive supercoiling occurs when the strands are overwound). Once the two strands are covalently rejoined the level of supercoiling can only be altered by a

strand breakage event. This is often demonstrated with rubber tubing, if the ends are twisted relative to one another and rejoined the tubing coils up upon itself. DNA supercoiling has been quantified by various mathematical models (Bauer and Vinograd, 1968; White, 1969) and is explained briefly below.

The linking number (*Lk*) is the basic parameter of DNA supercoiling and is defined as the number of times one strand of DNA goes around the other in a double stranded ring in which both strands are continuous, i.e. the number of double helical turns; *Lk* must be an integer. A given cccDNA molecule has an inherent number of double helical turns due to its structure. This number is the length of the DNA, *N*, in bp divided by the number of bp per turn of the helix, *h*; *h* depends on the conditions but is usually 10.5 bp/turn (see above). This is not an integer but the twisting required to join the ends of the DNA correctly is minimal over thousands of bp. Thus, a completely relaxed plasmid, e.g. pIJ486, has an *Lk* which is the closest integer to *N/h*. This is known as Lk_m; thus formula [1.1]:

$$Lk_m \approx \frac{N}{h} \approx \frac{N}{10.5}$$

In the case of pIJ486, $N = 6211$ bp, and the Lk_m is +592 when *h* is 10.5 bp/turn. This number is constant and will not change unless the strands are broken and rejoined. When such a change occurs it is known as the linking difference, ΔLk, and is $Lk\text{-}Lk_m$, and can be either positive or negative. However, ΔLk is calculated from a completely relaxed plasmid and as the value described by Lk_m is slightly strained the exact number of double helical turns, *N/h*, is used to determine the actual ΔLk which is not an integer. This

value is known as $Lk°$ and allows supercoiling to be quantified; thus formula [1.2]:

$$\Delta Lk = Lk - Lk°$$

In the case of pIJ486, $Lk°$ is 591.5 when h is 10.5 bp/turn. As a given ΔLk will cause more torsional stress in a smaller plasmid compared to a larger one, superhelical density (σ) is used to normalise the size factor; thus formula [1.3]:

$$\sigma = \frac{Lk-Lk°}{Lk°} = \frac{\Delta Lk}{Lk°}$$

This value is also known as the specific linking difference and allows comparisons between DNAs isolated from different sources. For an excellent explanation of how the geometry and topology of DNA interact mathematically the reader is referred to the section on DNA supercoiling in Bates and Maxwell (1993).

Negatively supercoiled DNA is associated with excess free energy which may be utilized in many cellular processes. Any process that removes negative supercoils or stabilizes them is more favourable in negatively supercoiled DNA compared to relaxed DNA. Such processes include replication and transcription of DNA, the binding of intercalating dyes, e.g. EtBr, the formation of nucleosomes and other DNA-protein interactions. Structural changes in the DNA such as *Z*-DNA formation and cruciforms occur more favourably in negatively supercoiled DNA. Such processes are discussed in more detail in section 1.8.5.

1.8.3: Bacterial DNA topoisomerases

DNA topoisomerases appear to control the level of DNA supercoiling inside the cell, probably by the competing activities of DNA gyrase and DNA topoisomerase I in prokaryotes (Wang, 1985; Drlica, 1992; Luttinger, 1995). In bacteria the chromosome is negatively supercoiled (Worcel and Burgi, 1972) as are plasmids (reviewed by Drlica, 1992). However, in the extreme thermophilic archaebacteria positively supercoiled plasmids have been isolated and a reverse gyrase that introduces positive supercoils has been identified as the major topoisomerase activity in these species (Bouthier de la Tour *et al.*, 1991; Charbonnier and Forterre, 1994).

Four types of DNA topoisomerases have been found in *E. coli*: Type I topoisomerases, consisting of DNA topoisomerase I (TopI; Wang, 1971) and DNA topoisomerase III (TopIII; Dean *et al.*, 1983); and Type II topoisomerases, consisting of DNA gyrase (Gellert *et al.*, 1976) and DNA topoisomerase IV (TopIV; Kato *et al.*, 1990). Type I topoisomerases act by transiently breaking a single-strand of DNA and passing another piece of DNA (single-stranded or double-stranded) through the gap. Type II topoisomerases make transient double-stranded breaks for the passage of DNA strands.

TopI and DNA gyrase are thought to regulate the levels of supercoiling in bacteria; TopI by relaxing negative supercoils and DNA gyrase by introducing them. TopI is encoded by *topA* and does not appear to be essential, although mutations in *topA* lead to slow growth and elevated levels of supercoiling. Interestingly, suppressor mutations were mapped to the DNA gyrase genes in viable, fast growing, *topA* deletion strains (DiNardo

et al., 1982; Pruss *et al.*, 1982). These studies indicate that TopI relaxes negative supercoils and DNA gyrase introduces them *in vivo*, and that vigourous growth occurs within a ± 15% range of supercoiling. DNA gyrase is encoded by *gyrA* and *gyrB* and forms a tetramer (A_2B_2), uniquely (so far) it can add negative supercoils to plasmids *in vitro* in the presence of ATP. In the absence of ATP, gyrase removes both positive and negative supercoils (see, e.g., Wang, 1985). In the presence of gyrase inhibitors, e.g. novobiocin, DNA isolated from cells was more relaxed than normal (Drlica and Snyder, 1978). In concert with DNA relaxation, expression from *gyrA* and *gyrB* is increased and *topA* expression is decreased, suggesting the genes are regulated by supercoiling at their loci (Menzel and Gellert, 1983; Tse-Dinh, 1985). Studies of gyrase mutants have indicated that the enzyme has several roles in the cellular processes that occur within bacteria, including transcription and the initiation, elongation and termination of DNA replication (Pruss *et al.*, 1982 ; Filutowicz and Jonczyk, 1983).

To date there is little evidence that TopIII and TopIV are required for regulation of DNA supercoiling in the cell, although overexpression of TopIV can suppress the slow growth of a *topA* mutant (Kato *et al.*, 1990). TopIII (*topB*) and TopIV (*parC* and *parE*) may be involved in the segregation of the chromosome during replication (reviewed by Luttinger, 1995).

It is likely that the DNA topoisomerases found in *E. coli* are representative of those in other bacteria, indeed TopI and DNA gyrase have been found in a number of other species including *Streptomyces* spp. (Thiara and Cundliffe, 1993; Hoggarth *et al.*, 1994).

Given that DNA gyrase utilizes ATP (see above) and that changes in the [ATP]/[ADP] ratio alter the level of negative supercoiling *in vitro* (Westerhoff *et al.*, 1988), it was not surprising that supercoiling was found to vary under different growth conditions, possibly due to changes in cellular energetics (Hsieh *et al.*, 1991a, b). The transition to anaerobic growth in *E. coli* results in a rapid drop in both the [ATP]/[ADP] ratio and the level of negative supercoiling, the level of negative supercoiling then recovers to a higher level than that seen during aerobic growth. Alternatively, when *E. coli* cells are transferred to a medium of high salt both the [ATP]/[ADP] ratio and negative supercoiling rise rapidly. It appears that the balance of gyrase activity shifts towards the relaxation of supercoils when the [ATP]/[ADP] ratio is reduced and the reverse when it increases (reviewed by Drlica, 1992). Mutations in *gyrB* or *topA* that are non-lethal have been used to mimic the effect of changing environment on negative supercoiling. The relative abundance of a group of proteins was monitored in these mutants and was found to change compared to the wild-type. Thus, changes in negative supercoiling associated with changes in the environment, e.g. aerobic to anaerobic growth, have a widespread impact on gene expression (Steck *et al.*, 1993). In support of the idea that negative supercoiling and its variation can effect a number of cellular processes; Balke and Gralla (1987) grew *E. coli* in various media, known to influence global gene expression. The effect of changing the cellular environment on the superhelical density on a plasmid, pBR322, was determined in each culture. Significant changes in supercoiling occur when *E. coli* switches its metabolism in response to changes in the nutritional content of a given medium. Interestingly there did not appear to be any correlation between growth rate and changes in the superhelical density of pBR322 (see above). However, once the *E. coli* cells were in stationary phase the plasmid lost up to 10 supercoils within a few hours, corresponding

to ca.68% of unrestrained supercoils (Balke and Gralla, 1987). As *Streptomyces* spp. produce a large amount of secondary metabolites during stationary phase (see above) an investigation was undertaken, see Chapter Three, to see if a similar situation exists in *S. coelicolor*.

Negative supercoiling of DNA is partitioned *in vivo* in bacteria by the binding of histone-like proteins to 50-60% of the negative supercoils (Pettijohn and Pfenninger, 1980; Sinden *et al.*, 1980; Lilley, 1986; Bliska and Cozzarelli, 1987). It is the unrestrained negative supercoils (i.e. not bound to histone-like proteins) that are altered rapidly during the changes in the environment described above, e.g., salt shock (McClellan *et al.*, 1990). Thus, changes in negative supercoiling are likely to have an effect on DNA-protein interactions, e.g. transcription and replication (see below) as it is within the unrestrained supercoils that the interactions occur (Bliska and Cozzarelli, 1987). In eukaryotic DNA, negative supercoiling is due to the left-handed winding of the DNA around the histones, the positive supercoils generated as a result of this winding are removed by topoisomerases and there is no evidence of unrestrained supercoiling (Laskey *et al.*, 1978). Chromatin must be decondensed before cellular processes such as transcription and replication can utilize the energy inherent in the negatively supercoiled DNA (reviewed by Roth and Allis, 1992). Histone-like proteins have been found in bacteria, namely the abundant HU and H-NS (or H1) proteins. HU, encoded by *hupA* and *hupB*, is capable of wrapping DNA and restraining negative supercoils and is likely to be associated with the condensation of bacterial DNA in the nucleoid (reviewed by Drlica and Rouvière-Yaniv, 1987). H-NS, encoded by *hns*, also appears to compact DNA, negative supercoiling is reduced in *hns* mutants and it seems to influence

transcription *in vivo* (Tupper *et al.*, 1994). The bacterial chromosome is thought to be compacted into 40-50 negatively supercoiled domains, possibly with each domain superhelically distinct (Worcel and Burgi, 1972; Higgins *et al.*, 1988). However, recent data has suggested that the domains do not differ in their superhelical density, although only a small, random, number of domains were examined (Miller and Simons, 1993; Pavitt and Higgins, 1993).

1.8.4: Left-handed or *Z*-DNA

This DNA conformation is of particular interest due to the potential *Z*-DNA sequences in the glycerol operon (section 1.7.1.3). The structure of *Z*-DNA is very different to that of *B*-DNA (see above) and is likely to prevent some DNA-protein interactions, e.g. RNA polymerase initiation, at the site of the deformation (Peck and Wang, 1985; Glikin *et al.*, 1991). Since it was observed *in vitro* (Pohl and Jovin, 1972) and *Z*-DNA-binding proteins were recognised (Nordheim *et al.*, 1982; Leith *et al.*, 1988) there have been many attempts to assign *Z*-DNA a role *in vivo*.

In an alternating sequence of purine-pyrimidine bases in the *Z-form* the bases are on the outside of the sugar-phosphate backbone; the pyrimidines have an *anti* conformation about the glycosidic bond and the purines adopt the unusual *syn* conformation about the glycosidic bond. The double helix is left-handed and the helical repeat is now 12 bp/turn (McLean and Wells, 1988). Thus, the DNA structure and topology is very different compared to that of *B*-DNA.

The adoption of *Z*-DNA by a DNA sequence is sequence dependent, but it does not require a complete purine-pyrimidine alternation of all the bases, *B-Z* and *Z-Z* junctions exist (Klysik *et al.*, 1981). The existence of *Z*-DNA in recombinant plasmids was demonstrated under a variety of conditions, usually high salt; the experiments cited above used high salt to assist the formation of *Z*-DNA. However, it was subsequently shown that *Z*-DNA could exist under physiological ionic conditions when its formation was induced by DNA supercoiling (Singleton *et al.*, 1982). The level of negative supercoiling needed to form *Z*-DNA was dependent on the length of the $d(C\text{-}G)_n$ (Peck and Wang, 1983).

The most energetically favourable sequence is a run of alternating CG bp, the shortest sequence found to adopt *Z*-DNA was $d(C\text{-}G)_4$ (McLean *et al.*, 1986). However, long runs of $d(C\text{-}G)_n$ do not occur very often in nature, but the DNA sequence $d(T\text{-}G)_n \cdot d(C\text{-}A)_n$ (which is common) was found to form *Z*-DNA *in vitro* (Haniford and Pulleyblank, 1983; Trifonov *et al.*, 1985). Thus, the *Z-form* sequences in the glycerol operon meet the sequence requirements to adopt *Z*-DNA. *Z*-DNA can also be transmitted through intervening sequences to form the longest left-handed helix possible (McLean *et al.*, 1988) suggesting that *Z-form II* (Figure 4.1), in the glycerol operon, could adopt *Z*-DNA 23 bp long.

That *Z*-DNA exists *in vivo* was first demonstrated using a biochemical-genetic assay. The assay was based on the finding that a target site for a temperature sensitive methylase is not methylated or restricted when the target site is in or near to *Z*-DNA. Thus, plasmid DNA isolated from cells grown at the permissive temperature and whose target site was

"protected" by *Z*-DNA formation could be linearized and then restricted with *Eco*RI (Jaworski *et al.*, 1987). Since then the *in vivo* existence of *Z*-DNA has been suggested often (Hoheisel and Pohl, 1987; Rahmouni and Wells, 1989; Zacharias *et al.*, 1990; Jaworski *et al.*, 1991). However, some *Z*-DNA-binding proteins (see above) that, initially, strongly supported an *in vivo* role for *Z*-DNA may in fact be phospholipid-binding proteins and not involved in gene regulation at all (Krishna *et al.*, 1990). Whether *Z*-DNA plays a role in the expression of the glycerol utilization genes is investigated in Chapter Four.

1.8.5: The biological impact of DNA topology

The observation that transcription and DNA supercoiling are inter-related was based on investigations into a promoter mutation (*leu-500*) of the *leuABCD* operon. Mutants that exhibited phenotypic reversion were isolated, not all of which mapped in the *leu* operon (Mukai and Margolin, 1963). Some of the complementary mutations were mapped to *supX*, which was later found to be the structural gene for DNA topoisomerase I, *topA* (see above; Margolin *et al.*, 1985). *leu-500* is a point mutation in the —10 region of the *leuABCD* promoter and is sensitive to supercoiling. Adjacent, divergent, transcription suppresses this mutation (Tan *et al.*, 1994). Such transcription has been suggested to increase negative supercoiling behind the RNA polymerase:DNA complex (see below) and therefore around the *leu-500* promoter. Other studies involving the inhibition of DNA gyrase have shown that transcription is differentially affected; lowering the negative supercoiling inside a cell inhibits the transcription of some, but not all, operons (reviewed by Smith, 1981).

Supercoiled DNA in prokaryotes consists of free, unrestrained, supercoils and supercoils constrained by histone-like binding proteins (see above). However, it is now known that transcription can locally alter the degree of supercoiling around an actively transcribing gene, beyond normal, controlled levels. pBR322 isolated from a *topA* mutant was significantly more negatively supercoiled than that isolated from the wild-type host (Pruss, 1985). Furthermore, inactivation of *tetA* transcription on pBR322, in the *topA* mutant, prevented the high supercoiling (Pruss and Drlica, 1986) and inhibition of DNA gyrase in the wild-type led to the isolation of positively supercoiled pBR322 (Lockshon and Morris, 1983). These results were suggested to be the result of transcription *per se*, rather than a change in superhelical density causing expression of the gene (Liu and Wang, 1987). They speculated that, effectively, the RNA polymerase, nascent mRNA chain, and the binding of ribosomes to the mRNA would hold it in a fixed position relative to the DNA. The rotation of the DNA about its axis as it translocates around the RNA polymerase would result in the generation of negative supercoils behind the complex and positive supercoils in front, the "twin-supercoiled-domain" model (Wu *et al.*, 1988). As the supercoils are equal and opposite they would be expected to diffuse around the DNA and cancel each other out. However, if the DNA includes other active genes the supercoils are unable to diffuse around the DNA. Thus, the DNA topoisomerases, TopI and DNA gyrase, act to relax and to introduce negative supercoils behind and in front of the transcription complex respectively.

Other work has indicated an alternative hypothesis for RNA polymerase movement, whereby the RNA polymerase appears to assume an apical position on the DNA and then translocates the DNA, maintaining its apical location (ten Heggeler-Bordier *et al.*, 1992).

Such a model allows for twin-supercoiled-domains as the nascent mRNAs tend to adhere to one another and prevent the newly generated supercoils cancelling each other out, resulting in transcription-induced supercoiling. As DNA gyrase and TopI appear to act differentially (reviewed by Wang, 1985) on the twin-supercoiled-domains the superhelical density of the plasmid will be altered, seen as an increase or decrease in linking number *in vitro*. This model was further supported when *Z-form* sequences were cloned upstream and downstream from the *tetA* gene in pBR322. *Z*-DNA, in *Z-form* sequences as short as 14 bp, was formed upstream from the *tetA* promoter, and only when it was transcribing (Rahmouni and Wells, 1992). Thus, the negative supercoils generated behind the *tetA* transcription complex allowed the *Z-form* sequence to adopt *Z*-DNA. Given that *Z*-DNA formation is enhanced with increased negative supercoiling and that transcription-induced supercoiling can cause *Z*-DNA formation, the initial importance attached to *Z*-DNA (and other DNA structures) *in vivo* is more creditable.

Further evidence of the interaction between transcription and DNA supercoiling was shown with the divergent *malEp* and *malKp* promoters of the maltose regulon on a recombinant plasmid. An *in vitro* system was developed to mimic the *in vivo* promoter activity. The system demonstrated the dependence of the promoters on negative supercoiling for formation of the transcription initiation complex and its subsequent stability (Richet and Raibaud, 1991). The effect of DNA supercoiling on promoter activity is very complex, variations in the spacing of the —10 and —35 regions suggest that it is the overall structure of the promoter that responds to changes in supercoiling (Jyothirmai and Mishra, 1994). Perhaps the best studied promoter responses to supercoiling are those of *topA*, *gyrA* and *gyrB*. Increased negative supercoiling increases

transcription initiation from *topA* (Tse-Dinh, 1985) and reduces it in the gyrase genes (Menzel and Gellert, 1983). The effect on the gyrase promoters is unexpected as increased negative supercoiling usually enhances RNA polymerase binding and unwinding of the promoter regions (Drew *et al.*, 1985). This phenomenon has been shown to depend on the sequence at the site of initiation of RNA synthesis. It is thought that a reduction in negative supercoiling prevents abortive cycling by RNA polymerase, leading to elongation of the transcription complex (Menzel and Gellert, 1987).

Replication of circular DNA, in the *E. coli* chromosome as well as plasmids, initially involves an unwinding of the DNA duplex at the origin of replication and is favoured by negatively supercoiled DNA. In *E. coli*, DnaA binds at *oriC* and unwinds the DNA at an AT-rich region and this process is dependent on negative supercoiling of the DNA template (Bramhill and Kornberg, 1988). This requirement has also been reported for bacteriophage lambda DNA replication (Furth *et al.*, 1977). In yeast, the ability of autonomously replicating sequences (ARS) to unwind is related to their efficiency as origins of replication *in vivo* and is enhanced by negative supercoiling (Umek and Kowalski, 1988). As replication proceeds positive supercoils build up ahead of the replication forks, and in *E. coli*, the removal of these supercoils is probably by the action of DNA gyrase or TopIV (see above). In eukaryotes, topoisomerases I and II can relax positive supercoils, and in *Saccharomyces cerevisiae* the inhibition of both leads to reduced DNA synthesis (Kim and Wang, 1989). Type II topoisomerases are also required to segregate the daughter chromosomes after replication terminates in *E. coli* (see above). In yeast, topoisomerase II appears to be involved in decatenation as catenanes of plasmids (interlinked ds circular DNA) build up in its absence and it is

required during mitosis (DiNardo *et al.*, 1984). *E. coli* mutants that increase the negative supercoiling of the chromosome had no effect on DNA replication when compared to mutants with reduced negative supercoiling. The more relaxed chromosomal *oriC* template resulted in asynchronous replication. This could be explained by the altered affinity of DnaA for the "DnaA boxes" in the *oriC* region (von Freiesleben and Rasmussen, 1992).

The influence of DNA topology on DNA rearrangements has been reviewed (Ikeda, 1990), this section summarises what is known about illegitimate recombination in *E. coli* and includes what is known about similar events in *Streptomyces* spp. DNA rearrangement between non-homologous and non-specific DNA sequences is known as illegitimate recombination and results in deletions, duplications, insertions, and inversions. It is known to occur in bacteriophages, plasmids, eukaryotic cells and bacteria.

The deletion event is usually independent of the key gene involved in homologous recombination, e.g., *recA* in *E. coli*, and none of the other genes involved in recombination and DNA repair seem to be involved either, e.g., *recB, recC, uvrB, uvrC* in *E. coli*. This suggests that illegitimate recombination is the cause of the deletion. Duplication of DNA is usually seen as tandem duplications in both phage and bacterial DNA and is most likely due to illegitimate recombination between various sites in the genome. These tandem duplication events are also known to occur independently of the homologous recombination systems. The mechanisms behind illegitimate recombination are not yet fully understood, but DNA topoisomerases are likely to be

involved. *In vitro* systems developed for studying illegitimate recombination (see, e.g., Ikeda *et al.*, 1981) suggest that DNA gyrase is involved. Ikeda and co-workers found that recombination occurred between sites with homology of only 4 bp or less supporting the assumption that the recombination event was illegitimate. To determine whether DNA gyrase is involved in illegitimate recombination in *E. coli*, *gyrA* mutants were examined for recombination events. Excision of DNA from λ*plac*-plasmid hybrids was reduced by up to 100-fold in the *gyrA* mutants. Also, oxolonic acid (an inhibitor of DNA gyrase that stabilizes an enzyme-DNA complex) was found to increase recombination 13-fold and by preventing ATP reaching gyrase this increase in recombination was prevented, suggesting DNA gyrase is definitely involved in the recombination event. Temperature sensitive *gyrA* mutants also demonstrated reduced recombination events (Miura-Masuda and Ikeda, 1990). DNA gyrase is known to cleave DNA preferentially *in vitro* and *in vivo* (Lockshon and Morris, 1985) and there does seem to be some (limited) specificity for gyrase at known recombination sites (Ikeda *et al.*, 1984).

A model for illegitimate recombination was proposed by Ikeda *et al.* (1982) and involves gyrase sub-unit exchange. DNA gyrase (A_2B_2; section 1.8.3) binds to DNA and cleaves it in a double strand break, generating an intermediate; the gyrase is bound to each 5' end of the DNA. Two such gyrase:DNA complexes then join to form A_4B_4, the subsequent dissociation back to the normal tetramer form could occasionally result in the gyrase sub-unit-DNA complexes (AB) exchanging, resulting in illegitimate recombination once the break is rejoined. Alternatively, the A_2B_2-DNA complex could dissociate to the AB-form and re-associate with another AB-form, again resulting in illegitimate recombination upon strand rejoining. This model can also explain the secondary recombination often seen at

the site of the first recombination event both *in vitro* and *in vivo*; if the gyrase fails to dissociate from the DNA after the first rejoining event and undergoes further rounds of sub-unit exchange with other gyrase-DNA complexes (Naito *et al.*, 1984).

Inverted repeats are unstable in *E. coli* and often result in deletions, two models have been proposed to explain this event. The first (Glickman and Ripley, 1984), suggested that cruciform extrusion provides a substrate for exonuclease activity (encoded by *sbcC*); inverted repeats are stable in *recBC sbcB sbcC* mutants. Alternatively, there is some evidence of DNA gyrase promoting deletion events in long inverted repeats of plasmid DNA (Saing *et al.*, 1988).

DNA topoisomerases are also likely to be involved in DNA amplifications *in vivo*, such amplification events are usually represented by an extension of the "onion skin model" (Botchan *et al.*, 1979; Roberts *et al.*, 1983). Unscheduled replication can lead to multi-eyed structures in the DNA that can be resolved into tandem repeats by either homologous or illegitimate recombination. TopI cleavage sites have been found at the junctions of amplifications and DNA gyrase is known to be associated with replication (see above). As both processes are stimulated by negatively supercoiled DNA it is possible they may be linked through transcription-induced supercoiling (see above; Dröge, 1994). In *Streptomyces* spp. genetic instability is very common and involves gene amplification and deletions and a model has been proposed to explain it, based on rolling circle replication and recombination (Young and Cullum, 1987). Interestingly, in a study using DNA gyrase inhibitors similar results to those reported for illegitimate recombination in *E. coli* were reported (Volff *et al.*, 1993). Oxolonic acid was found to

increase genetic instability (presumably because the gyrase was stabilized on the DNA by the oxolonic acid), as did novobiocin, although to a lesser extent. Volff and co-workers (1993) suggested that DNA gyrase could be involved in the mechanism of genetic instability in *Streptomyces* spp. through illegitimate recombination and replication. However, as yet there is no consensus sequence for gyrase cleavage sites, nor has there been any reported consensus sequence found in the deletion junctions (Birch *et al.*, 1991).

DNA supercoiling is known to affect the expression of a variety of genes and has been proposed as a regulatory response mechanism to environmental changes, mediated through "stress-regulated" genes (Ni Bhriain *et al.*, 1989). Perhaps one of the most studied supercoiling-sensitive genes to date is *proU* in *E. coli* and *S. typhimurium*. *proU* is expressed in response to osmotic changes in the extracellular environment and causes the uptake of glycine betaine, an osmoregulant (see e.g., Booth and Higgins, 1990). The expression of *proU* increases 100-fold and is correlated with the increase of potassium ions in the cytoplasm under conditions of high osmolarity, but the mechanism for this was unclear. Interestingly, under conditions of high osmolarity the negative superhelical density ($-\sigma$) of plasmids isolated from these hosts was elevated (Higgins *et al.*, 1988). This led Higgins and co-workers to suggest that the *proU* promoter may be sensitive to changes in DNA topology. It contains 3 GC bp in the −10 region which may make it more sensitive to changes in $-\sigma$ (Richardson *et al.*, 1988). Indeed, when *proU* expression was examined in *topA* mutants it was increased even under conditions when it would not normally be expressed. The *topA* mutation seemed to be mimicking an increase in osmolarity by raising the $-\sigma$ of the DNA. One possible mechanism for this regulation of *proU* could be that potassium ions alter the TopI or DNA gyrase activities

by changing their conformation. The potassium concentration rises from 100 mM to 400 mM during the response to high osmolarity, such increases in salt concentration can effect the structural conformation of proteins (Booth and Higgins, 1990). Complementary mutations for increased *proU* activity under conditions of low osmolarity mapped to *topA* and *osmZ*. The *osmZ* locus has since been identified as the structural gene of H-NS (*hns*), the histone-like binding protein (May *et al.*, 1990), which is known to alter DNA topology *in vivo* (Tupper *et al.*, 1994). These mutations were pleiotropic and affect (amongst others) the porin genes, *ompC* and *ompF*, the expression of which is altered when *proU* is expressed. However, these results have been challenged (Ramirez and Villarejo, 1991), they suggest that the regulatory signal for *proU* expression *is* potassium glutamate accumulation, albeit *in vitro*, and could see no correlation between $-\sigma$ and *proU* expression.

OmpC and OmpF are outer membrane porins and respond to many different stimuli in *E. coli*; osmotic stress, pH, temperature and anaerobiosis (Graeme-Cook *et al.*, 1989). The expression of *ompC* and *ompF* is regulated by OmpR and EnvZ, but there is no clear mechanism for this. However, it has been suggested by Graeme-Cook *et al.* (1989) that EnvZ (the "sensor" protein) could not respond to, nor sense, all the different stimuli that the *ompC* and *ompF* genes are known to be sensitive to (see above). Changes in DNA supercoiling have been demonstrated to alter their expression, e.g. in *topA* mutants or in the presence of gyrase inhibitors (Graeme-Cook *et al.*, 1989). Thus, *ompC* and *ompF* have been suggested to belong to the "stress-regulated" group of genes (see above).

Expression of *tonB*, which is increased in stationary phase and repressed during anaerobic growth, is required for the uptake of iron chelates and vitamin B_{12} in *E. coli* (see Dorman *et al.*, 1988). Interestingly, *tonB* expression is repressed when the locus is more negatively supercoiled than normal, both *in vitro* and *in vivo*. Interestingly, during anaerobic growth negative supercoiling appears to be increase after the initial drop (Dorman *et al.*, 1988; Hsieh *et al.*, 1991a). Dorman and co-workers suggested that TopI or DNA gyrase activity could be affected under these conditions and that changes in DNA supercoiling could be the switch for anaerobic growth. Earlier reports had indicated that some DNA gyrase mutants could not grow under anaerobic conditions and that *topA* mutants could not grow aerobically (Yamamoto and Droffner, 1985). However, these mutants may have included additional, unknown, mutations; well defined *topA* deletion mutants are viable under aerobic conditions (see above), indicating that supercoiling changes could not be solely responsible for the switch to anaerobic growth (Dorman *et al.*, 1988). Also, the regulation of colicin gene expression in *E. coli* appears to be mediated by environmentally induced variations in DNA supercoiling. Under anaerobic growth colicin gene expression was increased significantly (Malkhosyan *et al.*, 1991).

Another possible member of the "stress-regulated" group is *oxrC*, encoding phosphoglucose isomerase in *E. coli*, which seems to be required to regulate some genes expressed during anaerobic growth. Some 50 additional proteins are induced during the switch to anaerobic growth, some of which require the *oxrC* gene product and others the Fnr protein (which resembles the CRP) for activation (Spiro and Guest, 1987). *oxrC* mutations are pleiotropic and reduce the expression of anaerobically expressed genes dependant on phosphoglucose isomerase. These mutants probably mimic carbon

starvation (phosphoglucose isomerase is required for carbon flux through the glycolytic pathway); this effect causes a reduction in negative supercoiling in *E. coli* (see above; Balke and Gralla, 1987).

Ni Bhriain *et al.* (1989) suggest that the "stress-regulated" genes could provide a mechanism for responding to changes in the environment, mediated through DNA supercoiling. After the basic response, initiated by changes in supercoiling, the specific regulators would be involved in "fine-tuning" the processes, e.g. OmpR and EnvZ. However, the topoisomerases are unlikely to be involved in regulating DNA supercoiling *per se*, they appear to respond rather to changes in the homeostatic norm (but see below). Transcription-induced changes are more likely to alter DNA supercoiling such that gene expression is then affected.

In Gram-positive bacteria similar effects have been reported, the expression of epidermolytic toxins, encoded by *eta*, is both growth phase dependent and supercoiling sensitive in *Staphylococcus aureus* (Sheehan *et al.*, 1992). A reduction in DNA supercoiling, by sub-inhibitory concentrations of novobiocin, caused the *eta* promoter to be strongly induced. This suggests that DNA supercoiling is reduced during stationary phase growth, similar to that seen in *E. coli* (Balke and Gralla, 1987).

In *Bacillus subtilis* one response to a shiftdown in temperature is the increased synthesis of unsaturated fatty acids. Inclusion of novobiocin during the shiftdown prevented the induction of the unsaturated fatty acids (Grau *et al.*, 1994). Interestingly, DNA gyrase expression in *E. coli* appears to increase during the cold-shock response, possibly due to a

transcriptional activator, CS7.4 (a major *E. coli* cold-shock protein), enhancing *gyrA* and *gyrB* expression (Jones *et al.*, 1992). A cold-shock protein, CspB, with good homology to CS7.4, has been identified in *B. subtilis* (Willimsky *et al.*, 1992). It will be interesting to see if it activates the gyrase genes during the cold-shock response.

During sporulation of *B. subtilis*, plasmid DNA isolated from the forespore compartment shows a dramatic increase in negative supercoiling *in vitro* (Nicholson and Setlow, 1990). This is presumably caused by small, acid-soluble spore proteins (SASPS) wrapping the DNA in a left-handed manner, introducing negative supercoils which are then stabilized by TopI (Nicholson *et al.*, 1990). Alternatively, it has been suggested that the DNA could be in an *A*-DNA conformation, DNA gyrase would introduce negative supercoils as the helical repeat of *A*-DNA is 11 bp/turn and would therefore be more relaxed *in vivo* (see above; reviewed by Setlow, 1992). This altered DNA conformation may prevent UV damage to spores (Nicholson *et al.*, 1990).

1.9: Aims of this project

One of the main aims of this project was to determine the superhelical density of the *Streptomyces* sp. plasmid pIJ486. Given that *Streptomyces* spp. have a GC-rich genome it was expected that they would maintain their DNA at a higher superhelical density than species with lower GC-rich genomes, e.g. *E. coli*.

This "standard" pIJ486, of known linking number, was then be used to determine the variation in superhelical density throughout the growth phases of *S. coelicolor*

MT1110(pIJ486). Previous data suggested that the superhelical density of plasmid DNA decreased rapidly during stationary phase growth in *E. coli* and probably in *S. aureus* as well (see above). However, as *Streptomyces* spp. produce a significant amount of secondary phase metabolites, many synthesised during the stationary phase and regulated at the transcription level, this reduction in superhelical density was not expected.

Another objective was to test the hypothesis that Z-DNA formation, in the *Z-form* sequences of the glycerol operon, causes aberrant, unconditional repression of *gyl*P1/P2 when plasmid-borne.

Chapter Two

Materials and Methods

2.1: Strains and plasmids

The bacterial strains used in this study are listed in Table 2.1. Plasmids used in this study are listed in Table 2.2. Some of the restriction maps of vectors, upon which many of the plasmid constructs described in this thesis were based, are shown in Figures 2.1 to 2.4.

2.2: Chemicals, enzymes and reagents

2.2.1: Chemicals and reagents

Acrylamide (Biorad, Electrophoresis grade)
Adenosine triphosphate (ATP), disodium salt (Sigma); for APHII assay
Agarose (Sigma, Type I: low EEO)
Agarose (Sigma, Type II: medium EEO); for 1D and 2D ChQ gels
Agarose (Sigma, low melting point)
Amino acids (Sigma)
Ammonium persulphate (APS) (BRL, Ultra-pure)
Bis-acrylamide (N,N'-methylene-) (BRL, Ultra-pure)
Bromophenol blue (Sigma)
Bovine serum albumin (BSA) (Sigma)
Caesium chloride (CsCl) (BDH, AnalaR)
Chloroquine (ChQ) (Sigma)
Deoxyribonucleotide triphosphates (dNTPs) (Pharmacia)
Dimethyldichlorosilane (BDH)
Dimethylsulphoxide (DMSO) (BDH, AnalaR)
Dithiothreitol (DTT) (Sigma)
Ethidium bromide (EtBr) (Sigma)
EtBr (Calbiochem); for generation of topoisomers

8-Hydroxyquinoline (Sigma)
Isoamyl alcohol (Sigma)
Junlon (Honeywill and Stein Ltd., Surrey)
β-Nicotinamide adenine dinucleotide, reduced form, disodium salt (NADH) (Sigma)
Orange G (G.T. Gurr Ltd.)
Phenol (BDH, AnalaR)
Phospho-enol-pyruvate (PEP), potassium salt (Sigma)
Phosphoric acid (BDH)
Polyethylene glycol (PEG) 1000 (Koch-Light)
PEG 6000 (BDH, AnalaR)
Radiochemicals ([^{35}S]-dNTPs; 600 Ci/m/mol and [^{32}P]-dNTPs; 3000 Ci/m/mol) (Amersham)
N,N,N',N'-tetramethylethylenediamine (TEMED) (BRL, Ultra-pure)
Triethanolamine, potassium salt (Sigma)
Tris (Boehringer Mannheim)
Urea (BRL, Ultra-pure)
Xylene cyanol FF (Sigma)

All other chemicals and reagents used were from commercial suppliers.

2.2.2: Enzymes

Calf intestinal alkaline phosphatase (CIAP) (Pharmacia)
DNA Polymerase I, Klenow fragment (Amersham or Boehringer Mannheim)
DNA Topoisomerase I (TopI) (Promega, wheatgerm)
Lactate dehydrogenase (Boehringer Mannheim)
Lysozyme (Sigma, Grade VI for general use; Grade I for protoplasting)
Pyruvate kinase (Boehringer Mannheim)
Restriction endonucleases (BRL, Promega, Amersham, Boehringer Mannheim or Pharmacia)
Ribonuclease A (RNase) (Sigma)
T4 DNA ligase (BRL)
T4 DNA polymerase (Boehringer Mannheim)
T4 polynucleotide kinase (Boehringer Mannheim or Promega)
T7 DNA polymerase sequencing kit (Promega)
Taq DNA polymerase sequencing kit (Promega)

2.2.3: Miscellaneous materials

Cellophane discs, 325p (Courtaulds Cannings, Bristol)
Mineral oil (Sigma)
X-ray film (Amersham, β-max or Hyperfilm-MP)

Table 2.1: Bacterial strains used in this study

Strain	Genotype/Plasmid status	Reference
Derivatives of *S. coelicolor* A3(2) strain 1147[1]		
MT1101[2]	wild-type, SCP1$^+$, SCP2$^+$	Hopwood *et al.* (1985a)
MT1110	wild-type, SCP1$^-$, SCP2$^-$	C. Frazer, personal communication
Derivatives of *S. lividans* 66		
1326[3]	wild-type	Lomovskaya *et al.* (1972)
TK24	*str-6* (SLP2$^-$, SLP3$^-$)	Hopwood *et al.* (1983)
1326 Δ*gylR1*	Δ*gylR1* derivative of 1326	Z. Hindle, personal communication[4]
Derivatives of *E. coli* K-12 (relevant markers only)		
"CS1"[5]	Δ(*lac-proAB*), (*φ80d*Δ(*lacZΔM15*)), *strA*, *recA*, F$^-$	Rüther *et al.* (1981)
ET12567	*dam*-13::Tn*9*, *dcm*-6, *hsdR*, *recF*	MacNeil *et al.* (1992)
GM33	*dam*-3, *str*, F$^-$	From M. G. Marinus
WK6	Δ(*lac-proAB*), *galE*, *strA*(*F'lacI*^{q}, *lacZΔM15*, *proA*$^+$*B*$^+$)	Zell and Fritz (1987)
WK6 *mutS*	WK6 *mutS*::Tn*10*	as WK6

Notes:
1. *S. coelicolor* A3(2) is a misnamed *S. violaceoruber* strain (Kutzner and Waksman, 1959) and should not be confused with *S. coelicolor* Muller.
2. UMIST stock number for 1147.
3. John Innes stock number for *S. lividans* 66.
4. *S. coelicolor* derivatives carrying the Δ*gylR1* mutation are described in Hindle and Smith (1994).
5. This strain was named: F$^-$, *Z*$^-$*ΔM15*, *recA* by Rüther *et al.* (1981) but is designated "CS1" in this thesis for brevity.

Table 2.2: Plasmids used in this study

Plasmid	Details (marker)[1,2]	Reference or Figure
Plasmids not constructed in this work		
pIJ2925	Derivative of pUC18 (*amp*)	Janssen and Bibb, 1993; (Figure 2.1)
pIJ2211	*S. coelicolor* M138 *gyl* DNA (*BclI*(1-13) fragment) cloned into pBR327 (*amp*)	Smith, 1986; (Figure 4.2)
pIJ486	multicopy promoter-probe, based on pIJ101 (*tsr*, promoter-less *neo*)	Ward *et al.*, 1986; (Figure 2.2)
pMa	Phasmid for oligonucleotide directed mutagenesis (*amp*)	Stanssens *et al.*, 1989; (Figure 2.3)
pMc	Phasmid for oligonucleotide directed mutagenesis (*cat*)	as pMa; (Figure 4.2)
pMT3000	*Xho*I linker introduced into the *Bam*HI site of pIJ2925 (amp)	Paget, 1994; (Figure 4.4)
pMT3007	*gyl* DNA ([*Eco*RI]*Cla*I(10)-*Sma*I(11)) isolated by PCR and cloned into pMT3000	Paget *et al.*, 1994
pSK2.3	*S. coelicolor* M138 *gyl* DNA (*Sph*I(2)-*Kpn*I(12)) cloned into pIJ2925 (*amp*)	C.P. Smith, personal communication; (Figure 2.4)
pSK2.3 (*gylR10*)	pSK2.3 with a 4 bp deletion at the *Xho*I(6) site	C.P. Smith, personal communication
pSK2.3 (*gylR13*)	pSK2.3 with a 4 bp insertion at the *Xho*I(6) site	C.P. Smith, personal communication
pSK2.3 (*gylR20*)	pSK2.3 with a 14 bp deletion at the *Pvu*II(7) site	C.P. Smith, personal communication
pSK2.3 (*gylR25*)	pSK2.3 with a silent (point) mutation at the *Pvu*II(7) site	C.P. Smith, personal communication

Table 2.2 continued..

Plasmid	Details (marker)	Section or Figure
Plasmids constructed in this work		
pJAM10	*Z-form I* from pIJ2211 (*Pvu*II(7)-*Sma*I(11)) cloned in pMc (*cat*)	4.2 (Figure 4.2)
pJAM11	*Z-form I* region in pJAM10 disrupted, new *Apa*I site (*amp*)	4.2 (Figure 4.2)
pJAM20	*Z-form II* from pIJ2211 (*Sma*I(4)-*Pvu*II(7)) cloned in pMc (*cat*)	4.2 (Figure 4.2)
pJAM21	*Z-form II* region in pJAM20 partially disrupted, new *Sma*I site (*amp*)	4.2 (Figure 4.2)
pJAM22	*Z-form II* region from pJAM21 cloned in opposite orientation to pJAM20 in pMa (*amp*)	4.2 (Figure 4.2)
pJAM23	*Z-form II* region in pJAM21 disrupted, new *Sca*I site (*cat*)	4.2 (Figure 4.2)
pJAM24	*Sma*I(4-11), containing *Z-form II* in opposite orientation to pJAM20, partially disrupted with NM6, new *Sca*I site (*cat*)	4.2 (Figure 4.3)
pJAM30	*Sma*I(4-11) fragment from pSK2.3 cloned in pMT3000 (*amp*)	4.3 (Figure 4.4 and 4.5(c))
pJAM35	*Sma*I(4-11) fragment from pSK2.3(*gylR10*) cloned in pMT3000 (*amp*)	4.3 (Figure 4.4)
pJAM40	*gyl* DNA ([*Eco*RI]*Cla*I-*Sma*I) from pMT3007 cloned in pMT3000 (*amp*)	4.3 (Figure 4.4)
pJAM50	(*Cla*I(10)-*Sma*I(11)) *gyl* fragment from pJAM11 used to replace same region in pSK2.3 (*amp*)	4.4.1 (Figure 4.5(b))
pJAM51	as for pJAM50	
pJAM60	(*Cla*I(10)-*Sma*I(11)) *gyl* fragment from pJAM11 used to replace same region in pJAM30 (*amp*)	4.4.1 (Figure 4.5(c))
pJAM65	(*Cla*I(10)-*Sma*I(11)) *gyl* fragment from pJAM11 used to replace same region in pJAM40 (*amp*)	4.4.1
pJAM70	(*Bst*EII(5)-[*Bam*HI[14]]) *gyl* fragment from pJAM23 replaced same region in pJAM30 (*amp*)	4.4.2

Table 2.2 continued..

Plasmid	Details (marker)	Section or Figure
Plasmids constructed in this work		
pJAM80	(*Bst*EII(5)-[*Bam*HI[14]] *gyl* fragment from pJAM23 replaced same region in pJAM60 (*amp*)	4.4.2 (Figure 4.6(a))
pJAM100	(*Bst*EII(5)-[*Bam*HI[14]]) *gyl* fragment from pJAM23 replaced same region in pJAM30 (*amp*)	4.4.2 (Figure 4.6(b))
pJAM110	[*Bgl*II] fragment from pSK2.3 cloned into pIJ486, α^3 (*tsr*)	4.5
pJAM111	[*Bgl*II] fragment from pSK2.3 cloned into pIJ486, β (*tsr*)	4.9
pJAM112	[*Bgl*II] fragment from pJAM50 cloned into pIJ486, α (*tsr*)	4.5 (Figure 4.7(a))
pJAM113	[*Bgl*II] fragment from pJAM50 cloned into pIJ486, β (*tsr*)	4.9
pJAM115	[*Bgl*II] fragment from pSK2.3(*gylR10*) cloned into pIJ486, α (*tsr*)	4.5
pJAM116	[*Bgl*II] fragment from pSK2.3(*gylR10*) cloned into pIJ486, β (*tsr*)	4.9
pJAM120	[*Bgl*II] fragment from pJAM30 cloned into pIJ486, α (*tsr*)	4.5
pJAM121	[*Bgl*II] fragment from pJAM30 cloned into pIJ486, β (*tsr*)	4.9
pJAM125	[*Bgl*II] fragment from pJAM35 cloned into pIJ486, α (*tsr*)	4.5
pJAM126	[*Bgl*II] fragment from pJAM35 cloned into pIJ486, β (*tsr*)	4.9
pJAM130	[*Bgl*II] fragment from pJAM40 cloned into pIJ486, α (*tsr*)	4.5
pJAM131	[*Bgl*II] fragment from pJAM40 cloned into pIJ486, β (*tsr*)	4.9
pJAM135	[*Bgl*II] fragment from pJAM80 cloned into pIJ486, α (*tsr*)	4.5 (Figure 4.7(b))

Table 2.2 continued..

Plasmid	Details (marker)	Section or Figure
Plasmids constructed in this work		
pJAM136	[*Bgl*II] fragment from pJAM80 cloned into pIJ486, β (*tsr*)	4.5
pJAM140	[*Bgl*II] fragment from pJAM60 cloned into pIJ486, α (*tsr*)	4.5
pJAM141	[*Bgl*II] fragment from pJAM60 cloned into pIJ486, β (*tsr*)	4.5
pJAM145	[*Bgl*II] fragment from pJAM70 cloned into pIJ486, α (*tsr*)	4.5
pJAM146	[*Bgl*II] fragment from pJAM70 cloned into pIJ486, β (*tsr*)	4.9
pJAM150	[*Bgl*II] fragment from pJAM65 cloned into pIJ486, α (*tsr*)	4.5 (Figure 4.7(c))
pJAM151	[*Bgl*II] fragment from pJAM65 cloned into pIJ486, β (*tsr*)	4.9
pJAM160	[*Bgl*II] fragment from pSK2.3(*gylR13*) cloned into pIJ486, α (*tsr*)	4.8.1
pJAM161	[*Bgl*II] fragment from pSK2.3 (*gylR13*) cloned into pIJ486, β (*tsr*)	4.8.1
pJAM165	[*Bgl*II] fragment from SK2.3(*gylR20*) cloned into pIJ486, α (*tsr*)	4.8.1
pJAM166	[*Bgl*II] fragment from pSK2.3(*gylR20*) cloned into pIJ486, β (tsr)	4.8.1
pJAM170	[*Bgl*II] fragment from pSK2.3 (*gylR25*) cloned into pIJ486, α (*tsr*)	4.8.1
pJAM171	[*Bgl*II] fragment from pSK2.3(*gylR25*) cloned into pIJ486, β (*tsr*)	4.8.1
pJAM180	(*Bgl*I(9)PolIk[4])-*Sma*I(11) *gyl* fragment from pJAM30 cloned into *Sma*I-digested pMT3000	3.4

Notes to Table 2.2:

1. The numbers in parenthesis after the restriction sites refer to those shown in Figure 2.5.

2. Those restriction sites in square brackets refer to sites in the polylinker region of the vector.

3. α or β refers to the orientation of the insert in PIJ486; α indicates a *gyl*P1/P2::*neo* fusion; β indicates a *metH*p::*neo* fusion or, in the case of pJAM131 and pJAM151, the opposite orientation to α.

4. PolIk indicates that the end generated from the restriction digest was blunt-ended.

Figure 2.1

Restriction map of PIJ2925 showing polylinker region.

Figure 2.2

Restriction map of the promoter-probe vector PIJ486. The position of the polylinker region allows the cloning of fragments in front of the *neo* (*aph*II) gene.

Figure 2.1

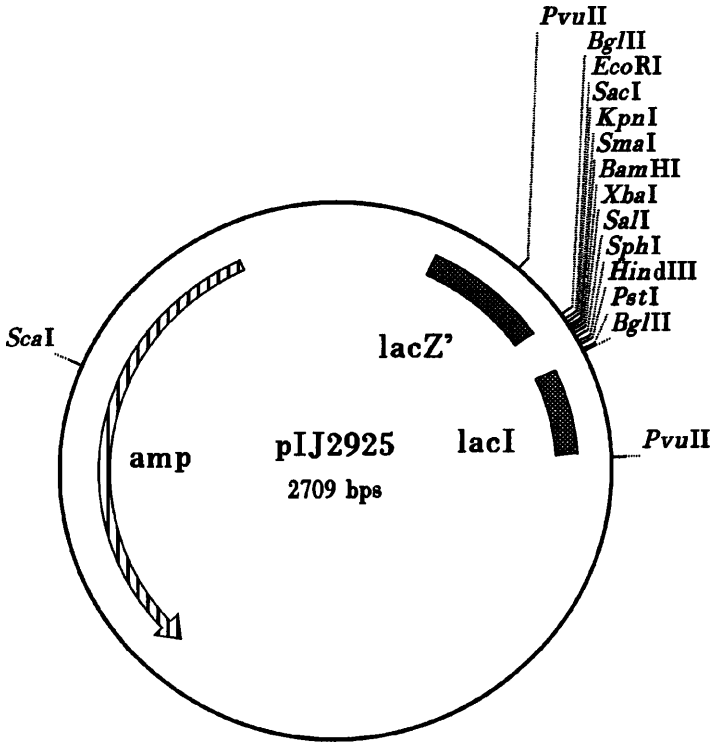

Figure 2.2

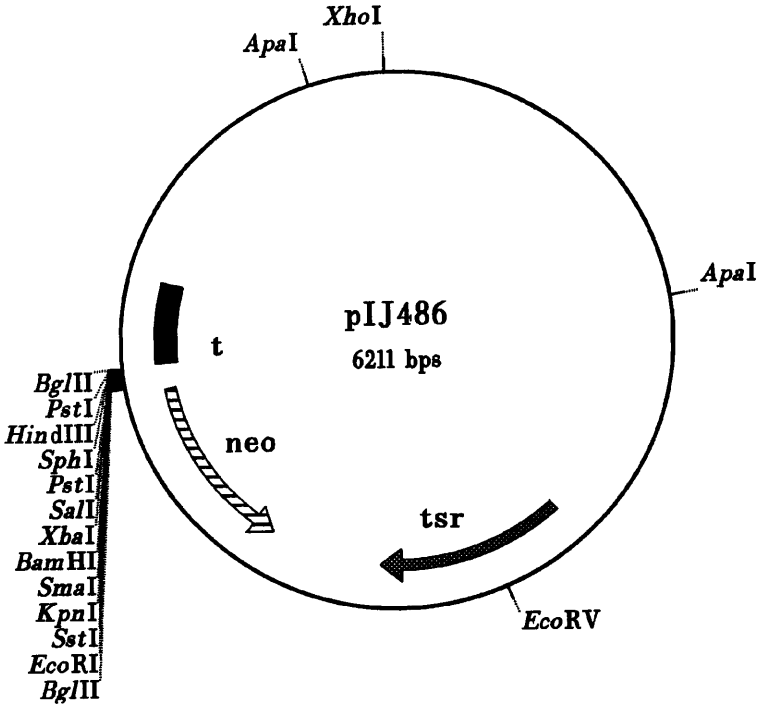

Figure 2.3

Restriction map of pMac reproduced from Stanssens *et al.* (1989). The position of the *amp* and *cat* gene, the origin of replication (*ori*), the filamentous phage origin (*f1 ori*) and the phage transcription termination signal (*fdt*) are indicated. The positions of the amber mutations in pMc (the *amp* gene does not contain the *Sca*I site) and pMa (the *cat* gene does not contain the *Pvu*II site) are indicated.

Figure 2.4

Restriction map of pSK2.3 showing the *gyl* DNA and the relevant restriction sites.

Figure 2.3

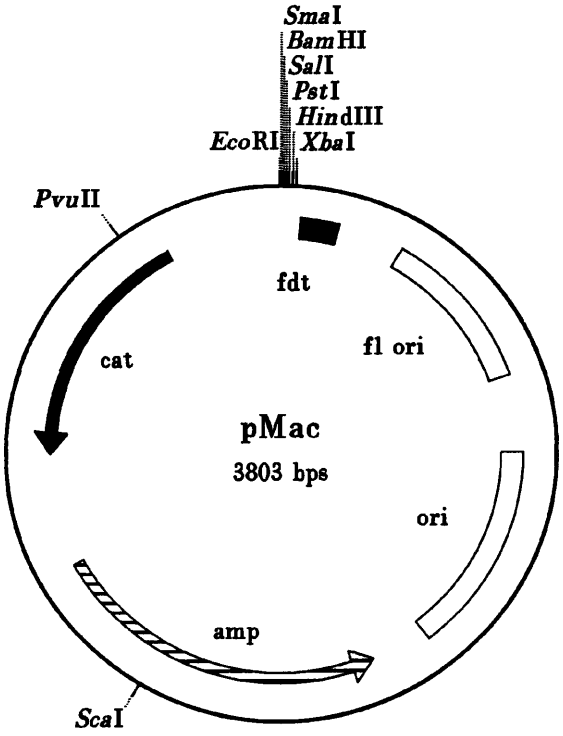

Figure 2.4

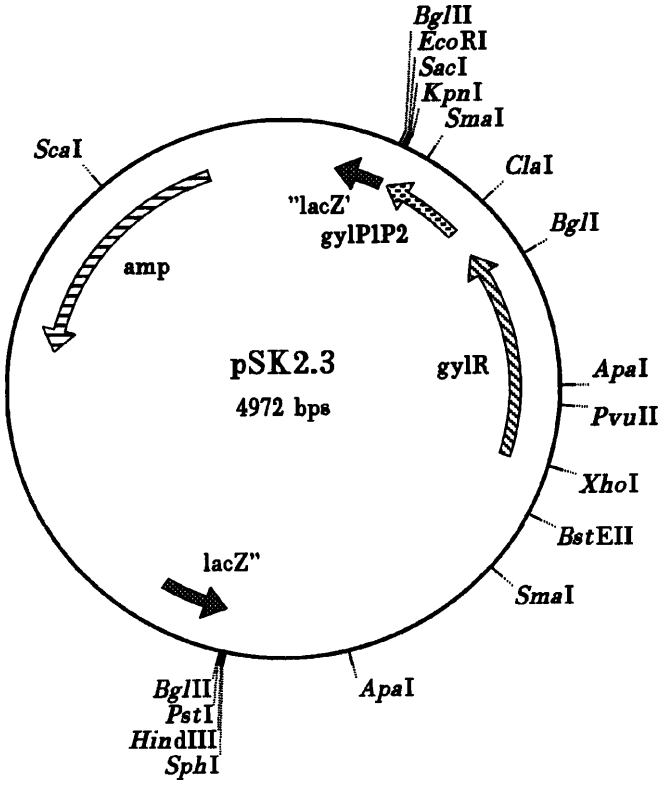

Figure 2.5: Restriction map of the glycerol operon

The restriction sites relevant to this study are indicated. The transcriptional organisation, including the *gyl* promoters *gylR*p and *gyl*P1/P2, and *metH*p are also indicated. The *gylCABX* transcription unit (dashed arrow) extends downstream from *BclI*(13) for a further 4.84 kb. The divergent *metH* transcription unit (left-slanting arrow) extends upstream from *BclI*(1) for an, as yet, undetermined distance. The *gylR* transcription unit is indicated by right-slanting arrow.

Figure 2.5

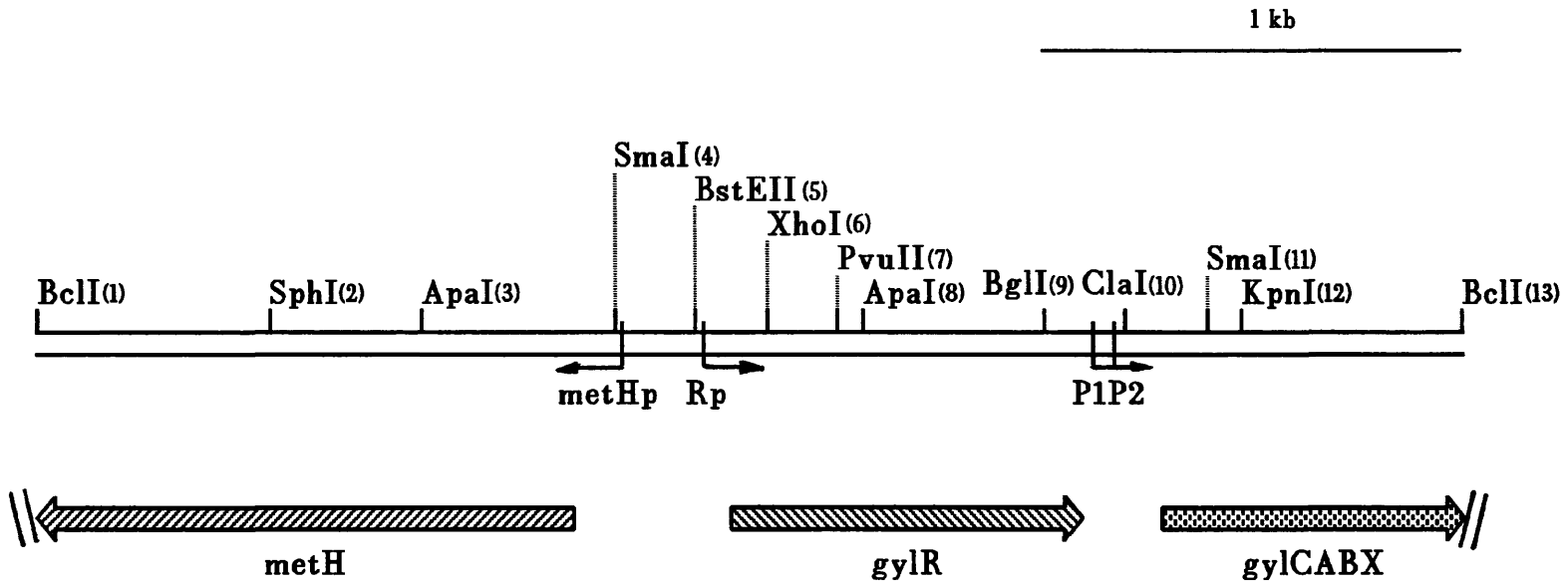
1 kb
SmaI (4)
BstEII (5)
XhoI (6)
PvuII (7)
ApaI (8)
BglI (9)
ClaI (10)
SmaI (11)
KpnI (12)
BclI (1)
SphI (2)
ApaI (3)
BclI (13)
metHp
Rp
P1P2
metH
gylR
gylCABX

2.3: Growth and maintenance of bacterial strains

2.3.1: Growth media

Streptomyces:

The strains were propagated using media described previously (Hopwood *et al.*, 1985a) except for the following:

MS agar: 20 g mannitol, 20 g soya bean meal/flour, 16 g Oxoid agar No.3 per litre of tap water, autoclaved 2 X.

HMM for production of methylenomycin, as described previously (Hobbs *et al.*, 1992).

HMM agar: HMM with Junlon excluded and LabM agar added to 1% (w/v).

TSB: 17 g Difco bacto-tryptone, 3 g Difco bacto-soytone, 5 g NaCl, 2.5 g K_2HPO_4, 2.5 g glucose per litre dH_2O, pH to 7.3 with HCl.

E. coli:

2T3Y: 16 g Difco bacto-tryptone, 15 g Difco bacto-yeast extract, 5 g NaCl per litre dH_2O.

DYT and DYT agar: 16 g tryptone, 10 g yeast extract, 5 g NaCl per litre dH_2O. For DYT agar LabM agar was added to 1.6% (w/v).

Minimal medium: 400 ml dH_2O containing 8 g LabM agar, 80 ml 6 X Spizezen salts (12 g $(NH_4)_2SO_4$, 84 g K_2HPO_4, 36 g KH_2PO_4, 6 g sodium citrate, 1.2 g $MgSO_4$ per litre dH_2O, autoclaved), autoclave then add 0.5 ml thiamine (10 mg/ml stock), 0.625 ml 1 M $MgSO_4$, 2 ml 50% glucose. Supplements were added as described in section 2.3.2.

2.3.2: Supplements to growth media

Amino acid supplements

When required, amino acids were added to growth media to a final concentration of 7.5 μg/ml unless indicated otherwise. Stock solutions were prepared in dH_2O as 1000 X solutions, autoclaved and stored at 4°C for up to 6 months.

Antibiotic supplements

All antibiotic stock solutions were prepared and the final concentrations used as described in Hopwood *et al.* (1985a). The stock solutions were stored at —20°C except thiostrepton (a gift from The Squibb Institute for Medical Research, Princeton, NJ) which was stored at 4°C.

2.3.3: Growth of bacterial strains and phages

Streptomyces:

For the preparation of spore suspensions strains were grown on MS agar for 5-7 d at 30°C and processed as described in Hopwood *et al.* (1985a). For high density spore suspensions however, spore tubes were not used. Instead care was taken during the scraping off of the spores so that no agar was disturbed and transferred to the suspension. The suspension was then sonicated in an ultrasonic waterbath for 10 min prior to centrifugation (B&T: 3,000 rpm; 10 min) and resuspended in either sterile dH_2O or 20% glycerol.

Liquid cultures were grown in sprung shake flasks on orbital shakers (180-200 rpm) at 30°C as described in Hopwood *et al.* (1985a). Strains containing plasmids were grown with antibiotic selection unless otherwise indicated.

E. coli:

All strains were grown in 2T3Y or DYT broth/agar overnight at 37°C unless otherwise indicated.

Phages:

M13K07 helper phage was grown as described in the manufacturers method sheet.

2.3.4: Storage of bacterial strains and phages

Short term storage

Both *Streptomyces* and *E. coli* strains were maintained as streaks on agar plates at 4°C. *Streptomyces* high density spore suspensions were stored in dH_2O at 4°C for up to 1 month, this allowed for more reproducible growth curves.

Long term storage

Streptomyces strains were stored as spores in 20% glycerol at either —20 or —70°C. *E. coli* strains were stored in 20% glycerol at —20°C or as stabs in nutrient agar.

2.4: Buffers and solutions

All buffers and solutions not described in this study were prepared as described previously (Hopwood *et al.*, 1985a; Sambrook *et al.*, 1989).

10 X TPE: 60.6 g Tris base, 3.7 g EDTA per litre dH_2O; pH to 8.0 with phosphoric acid.

Phenol: 300 g of phenol was melted at 68°C, 8-hydroxyquinoline was added to 0.1% (w/v) and the phenol neutralised with 100 ml 1 M Tris (pH8). The aqueous phase was then discarded, 500 ml 10 mM Tris (pH8) added, mixed, and when it was confirmed that

the aqueous phase pH was >7.6, the phenol was aliquoted in 10 ml volumes and stored at —20°C.

2.5: General methods

2.5.1: Centrifugation

Large scale centrifugation was carried out in either a Baird & Tatlock (B&T) Mark IV bench top centrifuge (up to 50 ml) or in a Sorvall RC-5B Refrigerated Superspeed Centrifuge (up to 500 ml) using GS-3, GSA or SS34 fixed angle rotors or HB4 swing-out rotor as appropriate. The rotor, speed and time used are specified in each method and all were carried out at room temperature unless indicated otherwise.

Centrifugation of volumes up to 1.5 ml were carried out in either a MSE Micro Centrifuge, an Eppendorf Microfuge (variable and fixed speed) or a Heraeus Biofuge (variable speed). Unless otherwise indicated the speed was always 13,000 rpm.

2.5.2: Phenol/chloroform/isoamyl alcohol extractions (P/C/I)

An equal volume (not less than 300 μl) of buffered phenol/chloroform/isoamyl alcohol (25:24:1) was added to the DNA solution and the phases mixed by vortexing. The phases were separated by centrifugation (B&T: 3,000 rpm; 5 min or microfuge: 2 min). The aqueous phase was transferred to a fresh tube and the DNA precipitated with isopropanol.

2.5.3: Isopropanol precipitation

Sodium acetate was added to the DNA solution to a final concentration of 0.3M (1/9 volume of 3M stock), 1 volume of isopropanol was added and the tube vortexed for 1-2 min. For samples containing a small amount of DNA (<1 μg) carrier tRNA (ca.5-10 μg) was added to ensure efficient precipitation of the DNA. The DNA was recovered by centrifugation (microfuge: 2-10 min or SS34: 5,000 rpm; 10 min). The supernatant was discarded, the pellet washed in 70% ethanol, dried and resuspended in TE (pH8).

2.5.4: Spectrophotometry

Optical density measurements were made using a Cecil Instruments CE292 Digital Ultraviolet Spectrophotometer, Beckman DU-8 Spectrophotometer or a Varian Cary 1 UV-Visible Spectrophotometer.

2.6: Isolation of DNA

2.6.1: *Streptomyces* plasmid DNA

Large scale preparation

500 ml YEME containing thiostrepton to 5 μg/ml was inoculated with 0.2 ml of a dense spore suspension and incubated with shaking at 30°C for 40-48 hours. The culture was processed using a variation of the alkaline lysis method detailed in Sambrook *et al.* (1989) as follows:

The mycelia were harvested by centrifugation (GSA: 8,000 rpm; 10 min) and resuspended in 18 ml Solution I (50 mM glucose, 25 mM Tris pH8, 10 mM EDTA). 2 ml of 10 mg/ml lysozyme stock solution was added and the solution mixed gently by inversion and incubated at 37°C for 30 min. 40 ml of freshly prepared Solution II (0.2 M NaOH, 1% SDS) was added, mixed well by shaking and incubated at room temperature for 5-10 min. 15 ml Solution III (3 M KOAc, pH4.8) was added, mixed well by shaking and incubated on ice for 10 min. The supernatant was cleared by centrifugation (GSA: 4,000 rpm; 15 min; 4°C) and transferred, by filtering through cheesecloth to prevent any carry over of precipitate, to fresh tubes containing 0.6 volume isopropanol. The solutions were mixed well by vortexing and the DNA recovered by centrifugation (SS34: 5,000 rpm; 15 min). The pellet was dried and resuspended in 2 ml TE (pH8) and extracted with phenol/chloroform/isoamyl alcohol until there was no interphase (2-3 X). The DNA was precipitated with isopropanol and resuspended in TE (pH8) and further purified by

caesium chloride-ethidium bromide gradient centrifugation (see section 2.6.4) if necessary.

Small scale preparation

10 ml of TSB containing 5 μg/ml thiostrepton was inoculated with spores and incubated with shaking for 36 h at 30°C in universals. The mycelial pellets were harvested using a Gilson P1000 with a "cut off" 1 ml blue tip and the plasmid isolated using one of the following methods (method II was the preferred procedure as it was faster and gave a good yield of DNA):

Method I: The alkaline lysis procedure 2 as described in Hopwood *et al.* (1985a) was used with the following modifications: after step 7a the DNA pellet was washed with 80% ethanol, dried and resuspended in TE (pH8) and stored at —20°C.

Method II: A modification of a method described previously (Hopwood *et al.*, 1987): 100 μl of Solution I (50 mM glucose, 25 mM Tris (pH8), 10 mM EDTA, lysozyme: 2 mg/ml) was added to the mycelia and incubated at 37°C for 30 min. 200 μl of ice-cold Solution II (0.2 M NaOH, 1% SDS) was added, mixed by inversion and incubated on ice for 5-10 min. Then 150 μl of Solution III (3 M KOAc, pH4.8) was added, mixed by inversion and kept on ice for 5 min. The supernatant was cleared by centrifugation (microfuge: 2 min) and 400 μl transferred to a fresh tube. The supernatant was extracted with 100 μl P/C/I and the aqueous phase recovered to a fresh tube. 800 μl of cold (—20°C) ethanol was added, the solution mixed by inversion and left at room temperature

for 2 min. The DNA was precipitated by centrifugation (microfuge: 2 min) and the supernatant discarded. The pellet was resuspended in 50 μl 100 mM NH_4OAc, vortexed to completely resuspend the DNA and 150 μl of cold ethanol was added, mixed by inversion and left at room temperature for 2 min. The DNA was precipitated by centrifugation (microfuge: 10 min), the pellet was washed in 70% ethanol, dried and resuspended in 50 μl TE (pH8) containing 10 ng/μl RNAse. RNA was digested by incubation at 65°C for 15 min and the preparations stored at 4°C or at —20°C.

2.6.2: *E. coli* plasmid DNA

Large scale preparation

500 ml DYT containing the relevant antibiotic was inoculated with 0.1 ml of the *E. coli* glycerol stock, incubated at 37°C for 12-16 h and processed as follows:

The large scale method described in section 2.6.1 was used with the following modifications: lysozyme was not used and the cells were resuspended in 20 ml of Solution I prior to incubation for 5 min. This method was scaled down 10-fold for 50 ml cultures.

Small scale preparation (minipreps)

10 ml of DYT containing the relevant antibiotic was inoculated with cells from an agar plate or glycerol stock and processed as follows: Method II, described in section 2.6.1, with the following modifications: 1 ml of the culture was transferred to an eppendorf tube

and the cells pelleted (microfuge: 2 min) before resuspension in Solution I. Lysozyme was not used.

2.6.3: M13K07 (Helper phage) single stranded DNA

The method used was as described in section 2.9.

2.6.4: Caesium chloride-ethidium bromide gradient centrifugation

The caesium chloride was dried at 90°C and 4.4 g added to 4 ml DNA in TE plus 400 μl of 10 mg/ml EtBr, mixed well and incubated on ice for 20 min. This step removed excessive quantities of RNA, the RNA-EtBr complexes were pelleted by centrifugation (B&T: 8,000 rpm; 10 min). The solution was loaded into a 5.1 ml heat sealable ultracentrifuge tube. The tubes were balanced in pairs, topped up with paraffin oil and sealed. The gradient was formed by ultracentrifugation (Beckman L5-50B or LB-70 ultracentrifuge, VTi65: 45,000 rpm; 16-20 h; 20°C). The cccDNA was recovered as described previously (Sambrook *et al.*, 1989). EtBr was extracted with isoamyl alcohol, the sample diluted 5-fold and the DNA precipitated with isopropanol and the pellet resuspended in 0.5-1 ml TE (pH8).

2.6.5: Quantitation of DNA, RNA and oligonucleotides

Spectrophotometric and EtBr fluorescence comparisons were used to estimate concentrations and purity of nucleic acid samples (see, e.g. Hopwood *et al.*, 1985a).

2.7: *In vitro* DNA manipulation

2.7.1: Restriction endonuclease digestion of DNA

The standard reaction mixture contained 1 μl 10 X enzyme buffer, up to 8 μl DNA (50-500 ng DNA), $\leq$0.5 μl enzyme (4-10 U/μl) and dH_2O to a final volume of 10 μl. The tube was mixed by flicking, pulse centrifuged (microfuge) and incubated at the appropriate temperature for at least 1 h. The recommended reaction conditions supplied with each enzyme were followed.

2.7.2: Removal of 5' phosphate groups from DNA

5'-phosphate groups were removed from linear DNA using calf intestinal alkaline phosphatase (CIAP, from Pharmacia) according to the method described in the Promega Protocols and Applications Guide (1991).

2.7.3: Converting sticky ends of DNA fragments to blunt ends

Filling-in recessed 3' termini

3' recessed termini were filled-in using PolIk. The standard reaction mixture consisted of 0.1-4 μg DNA, 1 μl of 0.5 mM dNTP s (0.5 mM of dATP, dCTP, dGTP and dTTP), 1-5 U of PolIk in a restriction endonuclease buffer (1 X) and dH_2O up to 20 μl. The

mixture was incubated at 30°C for 15 min and the reaction stopped by the addition of 1 μl 0.5 M EDTA. The DNA was isopropanol precipitated and resuspended in TE (pH8).

Blunt ending recessed 5' termini

The method was as described in the section above except that T4 DNA polymerase was used in place of PolIk.

2.7.4: DNA ligation

The standard reaction mixture consisted of the following: 2 μl 5 X ligation buffer, 1 U of T4 DNA ligase, vector and insert DNA fragments (1:3 molar ratio, ca.100 ng vector DNA), dH_2O to 10 μl. The tube was flicked to mix, pulse centrifuged (microfuge) and incubated at room temperature for 4 h or at 15°C for 12-16 h. The reaction was stopped by heat inactivation (65°C; 15 min) and the ligation checked on a minigel (section 2.7.5). Up to 5 μl of the mixture was used to transform competent cells (section 2.8).

2.7.5: Agarose gel electrophoresis

Agarose gel electrophoresis was carried out using submerged, horizontal gel tanks essentially as described in Hopwood *et al.* (1985a). Gel concentrations ranged from 0.5-1.5% agarose (w/v) dissolved in either 1 X TBE or 1 X TAE running buffer by boiling in a microwave oven. EtBr (0.5 μg/ml) was incorporated in the agarose and running buffer

to allow instant visualisation of the DNA (using a UV transilluminator, 375nm). Electrophoresis was performed in perspex tanks constructed at UMIST.

The DNA samples were prepared as follows: 25-1000 ng DNA, dH_2O to 10 μl and 2 μl 10 X loading buffer (50% sucrose, 1% Orange G, 5 mM EDTA) for large gels. For minigels: 10-250 ng DNA, dH_2O to 5 μl and 1 μl loading buffer were used. In order to estimate DNA fragment sizes in agarose gels DNA size standards were used, either λ *Hin*dIII markers or ϕX174 *Hae*III markers (see Appendix 2.1). Gels were run at 1-5 V/cm until the dye approached the bottom of the gel. Photographs of gels were taken using Polaroid 665 and 667 film or with a video imaging system.

It should be noted that *S. lividans* DNA underwent degradation when electrophoresed at low voltages for extended periods of time, due to the presence of contaminating iron in the buffer (Zhou *et al.*, 1988). If EDTA was excluded from the buffer used this was prevented.

2.7.6: Recovery of DNA fragments from agarose gels

This was carried using one of two methods, electroelution into dialysis tubing or a modification of the freeze-squeeze method (Tautz and Renz, 1983).

Electroelution into dialysis tubing

As described previously (Hopwood *et al.*, 1985a) with the following modifications: after step 9 the pellet was washed with 70%, then 95% ethanol (microfuge: 2 min) and dried under vacuum. The pellet was resuspended in 20 μl TE (pH8), vortexed briefly, pulse centrifuged (microfuge) and the supernatant (containing the DNA) recovered to a fresh tube. The pellet remaining contained most of the impurities from the agarose. The concentration of the DNA fragment was calculated as described in section 2.6.5.

Squeeze Method (Heery *et al.*, 1990)

This was the preferred method for recovery of DNA fragments up to 5 kb as it was much faster and provided DNA of good enough quality to perform ligations with. The band of interest was excised from a LMP gel using a scalpel blade (while visualised on a UV transilluminator). The gel slice was transferred to a 0.5 ml eppendorf tube which had been pierced at the end (by a 19G needle) and plugged with siliconised glass wool. The lid was cut off and the tube containing the gel slice was put into a 1.5 ml eppendorf tube and the DNA (in solution) centrifuged away from the agarose gel slice (microfuge: 6,000 rpm; 10 min). The DNA was made up to at least 300 μl and extracted with P/C/I until there was no more material visible at the interphase. The DNA was precipitated with isopropanol, washed with 70% ethanol, dried and resuspended in 20 μl TE (pH8). The concentration and quality of the DNA was assessed as described in section 2.6.5.

2.8: Preparation and transformation of competent cells

2.8.1: *Streptomyces* protoplasts

Protoplasts were prepared and transformed essentially as described (Hopwood *et al.*, 1985a), with the following modifications: After step 5 of the transformation procedure 0.5 ml of 25% PEG 1000 (in P-buffer) was added to the protoplasts and DNA using a 1 ml pipette, mixed by trituration once and then immediately 0.1 ml aliquots were spread out onto dried R5 plates. The spreader was made from a pasteur pipette; the thin end was sealed in the flame of a bunsen and then heated and bent to form the L-shaped spreader.

2.8.2: *E. coli* cells

Transformation was carried out using either the traditional $CaCl_2$ method or a high efficiency method.

Traditional method

The method used was a modification by Smith (1986) of a method described previously (Dagert and Ehrlich, 1979).

High efficiency method (J. Parkhill, personal communication)

Preparation: From an overnight culture 0.4 ml of cells were used to inoculate a flask containing 200 ml DYT and the cells were incubated at 37°C until an OD_{550} of ca.0.1 was reached. The cells were harvested (B&T: 5,000 rpm; 10 min), the cells resuspended in 20 ml TFB I (10 mM $RbCl_2$, 50 mM $MnCl_2$, 30 mM KoAc, 10 mM $CaCl_2$, 15% (v/v) glycerol, pH to 5.8 with 0.2 M CH_3COOH) and incubated on ice for 30 min. The cells were harvested by centrifugation (SS34: 5,000 rpm; 10 min; 4°C) and resuspended in 4 ml TFB II (10 mM MOPS (pH7), 10 mM $RbCl_2$, 75 mM $CaCl_2$, 15% v/v glycerol). The cells were aliquoted in 200 μl volumes into eppendorf tubes, snap frozen in dry-ice ethanol and stored at —70°C for 3-4 months.

Transformation: The cells were thawed at room temperature until just liquid, placed on ice and the transforming DNA added, the cells were mixed gently and incubated on ice for 10-60 min. The cells were heat-shocked at 42°C for 1.5 min and returned to ice. 1 ml of pre-warmed DYT was added and the cells incubated at 37°C for 1 h before the cells were plated out in 0.1 ml aliquots onto DYT agar containing the relevant antibiotic.

2.9: Oligonucleotide-directed mutagenesis

The method used was as described previously (Stanssens *et al.*, 1989) with the following modifications:

Step 1: after infection with M13KO7 the cells were shaken at ca.50 rpm for 30 min and then 250-300 rpm for 4-5 h. The culture was transferred to a centrifuge tube and the cells spun down (HB4: 10,000 rpm; 10 min). The supernatant was transferred to a fresh tube, 250 μl of PEG solution (20% PEG 6000; 2.5 M NaCl) was added and the supernatant incubated on ice for 15 min. The phages were harvested by centrifugation (HB4: 8,000 rpm; 10 min), the supernatant removed and the tubes re-spun (B&T: max. rpm; 5 sec) and the remaining supernatant removed. The pellet was resuspended in 300 μl TE (pH8), 1 volume P/C/I was added and mixed by vortexing intermittently for ca.10 min. The tube was centrifuged (microfuge: 3 min), the aqueous phase removed to a fresh tube, re-extracted with chloroform/isoamyl alcohol (24:1), centrifuged again (microfuge: 3 min) and the aqueous phase transferred to a fresh tube. The phage ssDNA was precipitated with 1/9 volume 5 M $NaClO_4$ and 1 volume isopropanol, mixed by vortexing, harvested by centrifugation (microfuge: 20 min) and the pellet dried. The ssDNA was dissolved in 50 μl TE (pH8) and stored at 4°C.

Step 2: The gapped duplex (gd) DNA was prepared by mixing 0.1 pmol of the fragment with 0.5 pmol of ssDNA, 5 μl 10 X hybridisation buffer (1.5 M KCl, 100 mM Tris-HCl, pH7.5) was added and the volume adjusted to 40 μl with dH_2O in a screw-cap eppendorf tube. The tube was incubated first in a boiling water-bath for 4 min and then at 65°C for 5-10 min.

Step 3: 4-8 pmol of the phosphorylated mutagenic oligo was mixed with 8 μl of gdDNA in an eppendorf tube and incubated in 500 ml dH_2O at 90°C which was left to cool to

room temperature. The gdDNA (with annealed oligo) was filled-in for 30 min as described and then the enzymes inactivated at 67°C for 10 min.

2.10: DNA sequencing

Sequencing was carried out using a variation of the dideoxy chain termination method first described by Sanger *et al.* (1977).

2.10.1: Labelling reaction

Nucleic acid sequencing was carried out using the Two-Step Extension/Labelling Protocol as described in the Promega Protocols and Applications Guide (2nd Ed., 1991). Both Promega T7 and *Taq* DNA Polymerase sequencing kits were used and the reactions were labelled with [^{35}S]dCTP.

2.10.2: Sequencing gels

The sequencing gels were prepared as described in Sambrook *et al.* (1989), to a concentration of 8%.

2.11: Large scale (10 l) preparation of pIJ486

The medium used was YEME + 10% sucrose, and 5 μg/ml thiostrepton; the usual concentration of 34% would have caramelised during autoclaving (P. Butler, personal

communication). The medium and 5 ml of antifoam were added to a 20 l bioreactor which was sterilised for 2 h at 10 lb/sq.in. The inoculum was prepared by inoculating 25 ml YEME + 34% sucrose with 0.3 ml of a dense spore suspension and incubated with shaking at 30°C for ca.36 h. The exponential (non pigmented) culture was then used to inoculate 500 ml of YEME + 34% sucrose, incubated with shaking at 30°C until the culture was in exponential phase (ca.36 h), to provide the 5% seed inoculum for the 10 l culture. The inoculum was added to the 20 l bioreactor via a bottom side-arm flask and thiostrepton was injected to a final concentration of 5 μg/ml. The culture was aerated at a rate of 10 l/min, stirred at 1,000 rpm and maintained at 30°C $\pm$ 2°C. The growth of the culture was monitored using a spectrophotometer (OD_{550}) and at 31 h, during exponential phase, the culture was harvested into 1 l flasks. The mycelia were harvested by centrifugation (Beckman J-6B Centrifuge: 4,200 rpm; 20 min) and stored overnight at 4°C. The plasmid was isolated by scaling up the large scale method described in section 2.6.1 2 X for each 1 l sample. The total plasmid DNA precipitate was resuspended in 10 ml TE (pH8). The plasmid DNA was further purified by 2 X gradient centrifugation (see section 2.6.4). The DNA was stored at 4°C after removal of the EtBr and CsCl.

2.12: Growth of MT1110(pIJ486) in a chemically defined liquid medium

The batch cultures were grown in a 3 l bioreactor (Life Science Laboratories Ltd.) in 2.5 l volumes of HMM (containing alanine) as described previously (Hobbs *et al.*, 1992) with the following modifications: the bioreactor batch cultures were stirred at 1,000 rpm and the medium was inoculated to 2 X 10^7 spores/ml from a high density spore suspension prepared as described in section 2.3.3. The spore suspension was resuspended for 10 min

in an ultrasonic waterbath prior to inoculation. The CO_2 output was used as an indicator of growth and the bioreactor was sampled from mid exponential to stationary phase as described in section 3.3.1.

2.13: Growth of MT1110(pIJ486) on a chemically defined solid medium

The medium used was HMM agar (containing alanine as the nitrogen source), ca.25 ml medium per plate, the plates were dried for 1 h in a flow cabinet and a cellophane disc placed on the surface of each agar plate. The cellophane discs were prepared by layering ca.150 discs into a beaker of water, heating it over a bunsen until boiling, the water changed and the discs re-boiled. The water was changed again, the discs autoclaved in the water and stored in the dark at room temperature. Before being placed on the agar excess water was drained off each disc. The plates were inoculated with 1 X 10^7 spores/plate and incubated face down at 30°C.

At each time point, 5 plates were selected and the cellophane discs removed from the agar, placed flat on a glass plate and the mycelia scraped off with a razor blade. The mycelia were washed off the glass plate into a sintered glass filter funnel containing a pre-weighed Whatmann Glass microfibre GF/C filter (4.7 cm ∅) and attached to a side-arm flask. A vacuum was applied to the flask and the mycelia were retained on the filter. The mycelia and filter were then dried in a microwave oven (full power) for 15 min (P. Butler, personal communication) and weighed to determine the average dry weight at each time point. The pH of the medium was determined from agar plugs sampled using a cork borer from each plate (after the mycelia and cellophane disc were removed). Each agar

plug was placed in a 0.5 ml eppendorf tube (the lid was cut off; the end pierced with a 20G needle; and a siliconised glass wool plug inserted to support the agar), the small eppendorf was placed inside a 1.5 ml eppendorf tube and centrifuged (microfuge: 6,000 rpm; 3 min) to collect the liquid in the agar. The pH of this liquid was measured using a micro pH probe. When the plates were harvested for plasmid isolation up to 15 plates were used to provide enough mycelia. The morphology of the culture was recorded using a camera attached to a microscope, see section 3.3.2.

2.14: Isolation of pIJ486 for 1D ChQ gel analysis

The method used was a modification of that described by Pruss (1985) as follows:

2.14.1: Bioreactor samples

Step 1: The bioreactor was sampled into a conical flask containing 0.5 volume frozen HMM (without Junlon) to quickly reduce the temperature of the sample. The mycelia were harvested by centrifugation (B&T: 4,000 rpm; 5 min) and resuspended in 1/50 volume STET (8% sucrose (w/v), 5% Triton X-100 (v/v), 50 mM EDTA, 50 mM Tris.HCl (pH8)). The suspension was transferred to a boiling tube, heated over a bunsen until just boiling, vortexed, and incubated in a boiling waterbath for 40 seconds. The tube was again vortexed and kept on ice until the next step of the isolation.

Step 2: The suspension was transferred to a 50 ml centrifuge tube, 4 ml STET containing lysozyme (0.67 mg/ml) was added and the tube incubated at 37°C for 30 min. Non

cccDNA (e.g. chromosomal DNA) was denatured by the addition of 10 ml Solution II (0.2 M NaOH, 1% SDS), the suspension was triturated 3 X with a 10 ml pipette and incubated on ice for 10 min. Cell debris was removed by the addition of 7.5 ml Solution III (3 M KOAc, pH4.8), the tube incubated on ice for 10 min and the precipitate pelleted by centrifugation (B&T: 3,000 rpm; 10 min). The supernatant was transferred through muslin to a fresh tube and the plasmid DNA was precipitated by the addition of 0.6 volume isopropanol and harvested by centrifugation (SS34: 5,000 rpm; 15 min). The supernatant was discarded and the pellet resuspended in 2 ml TE (pH8).

Step 3: The DNA was extracted with P/C/I until there was no material at the interphase (3-4 X), precipitated with isopropanol and the pellet resuspended in 1 ml TE (pH8). The Junlon did not resuspend immediately, therefore after vortexing the tube was pulse centrifuged (microfuge) and the supernatant containing the plasmid DNA recovered to a fresh tube leaving the Junlon pellet behind. The DNA was further purified by the addition of 0.8 volume 5 M NH_4OAc and 2 volumes ice cold ethanol, mixed, incubated on crushed dry-ice for 5 min and the DNA precipitated by centrifugation (B&T: 5,000 rpm; 10 min). The pellet was washed in 1 ml 70% ethanol (B&T: 5,000 rpm; 5 min), resuspended in 100 μl TE (pH8) containing 10 ng/μl RNase and incubated at 65°C for 10 min.

Step 4: The plasmid DNA was further purified by a modification of the method described by Saunders and Burke (1990):

100 mg CsCl and 100 μl EtBr (10 mg/ml) were added to 100 μl of the plasmid DNA, the tube was vortexed and then centrifuged (microfuge: 2 min). The volume was made up to 400 μl with TE (pH8) and the EtBr was extracted with isoamyl alcohol until the upper phase was clear. The DNA was precipitated with isopropanol, the pellet washed with 70% ethanol, dried, the pellet was checked under longwave UV light for any remaining bound EtBr and resuspended in 50 μl TE (pH8). The plasmid samples were checked on a minigel for purity and concentration before being analyzed by 1D ChQ gel electrophoresis.

2.14.2: Plate samples

The cellophane discs were lifted off each plate and the mycelia carefully scraped and washed off (see section 2.13) into a 50 ml tube containing 20 ml frozen HMM (without Junlon). The mycelia were pelleted (B&T: 5,000 rpm; 5 min) and then processed in an identical manner to mycelia sampled from bioreactors.

2.15: Determination of the superhelical density of pIJ486 by the band counting method

The technique involved generating a series of overlapping topoisomers of pIJ486 *in vitro* using DNA Topoisomerase I in the presence of varying concentrations of EtBr as described by Singleton and Wells (1982). Plasmid DNA (ccc) ca. 1-10 μg was mixed with EtBr (0-60 μM) and incubated with enough TopI to cause complete relaxation of the

cccDNA. This technique allowed a range of topoisomers to be generated, varying in superhelical density, from 0 to —0.165.

2.15.1: Complete relaxation of pIJ486 cccDNA

The 3 X assay buffer (0.15 M Tris-HCl (pH7.9), 3 mM EDTA, 3 mM DTT, 0.15 M NaCl) used was that recommended by Promega for TopI isolated from wheatgerm. The various reaction volumes (μl) used are listed in Table 2.3. After all the components were added each tube was flicked to mix, pulse centrifuged (microfuge) and incubated at 37°C for 4 h. The results are presented in section 3.2.1.

2.15.2: Generation of an overlapping distribution of topoisomers of pIJ486

The reaction conditions were scaled up to 1 ml volumes from those described in section 2.15.1 and from the results presented in section 3.2.1 the incubation time was increased to 5 h. The range of EtBr concentrations used to generate the topoisomers of pIJ486 are shown in Table 2.4. TopI was used at a concentration of 1 U/μg cccDNA with the stock diluted to 0.2 U/μl (1 X assay buffer was used to dilute the enzyme). The reaction conditions are shown in Table 2.5, after all the components were added each tube was flicked to mix, pulse centrifuged (microfuge) and incubated at 37°C for 5 h. After incubation the EtBr and TopI were removed by extraction 2 X with P/C/I. The DNA was isopropanol precipitated, washed in 70% ethanol (microfuge: 2 min), the pellet resuspended in 20 μl TE (pH8) and analyzed by agarose gel electrophoresis (see Figure 3.2).

Table 2.4: Generation of topoisomers of pIJ486

Topoisomer	EtBr (μM)	EtBr (μg/ml)	EtBr (μl)	EtBr [Stock]	dH_20 (μl)
1	0	0	0	/	547.7
2	0.5	0.2	20	10 μg/ml	527.7
2a	1.0	0.4	40	"	507.7
3	1.5	0.59	5.9	100 μg/ml	541.8
4	2.0	0.79	7.9	"	539.8
5	2.9	1.18	11.8	"	535.9
6	4.0	1.58	15.8	"	531.9
7	6.9	2.76	5.5	500 μg/ml	542.2
8	11.9	4.73	9.5	"	538.2
9	13.9	5.52	11.0	"	536.7
10	18.9	7.49	15.0	"	532.7
11[1]	0	0	0	/	647.7

Notes.
1. Topoisomer #11 was a control for the reaction conditions and contained no TopI.

Table 2.5: Reaction conditions for generation of topoisomers

Components	Volume (μl)	Addition order
pIJ486 (20 μg)	19	3rd
3X TopI buffer	333.3	1st
TopI (0.2 U/μl)	100	5th
EtBr	see Table 2.4	4th
dH_2O	see Table 2.4	2nd

Table 2.3: Conditions used to determine complete relaxation of pIJ486

Units of TopI	0	0.1	0.25	0.5	1.0	5
pIJ486 (0.5 μg)[1]	10	10	10	10	10	10
3X TopI buffer	8.3	8.3	8.3	8.3	8.3	8.3
dH_2O	6.7	6.2	5.4	4.2	1.6	1.7
TopI (0.2 U/μl)	0	0.5	1.25	2.5	5.0	0.2[2]

Notes:
1. The volumes in Table 2.3 are in μl.
2. The stock concentration for this reaction was 10 U/μl.

2.16: Chloroquine (ChQ) gels

2.16.1: One dimensional ChQ gels

The method used was a modification of a previously described method by Shure *et al.* (1977).

The gel was prepared using Sigma Type II agarose (300 ml 1.2% in 1 X TPE) and boiled in a microwave oven to dissolve the agarose. The agarose was cooled to ca.55°C, ChQ was added to the desired concentration, mixed and the molten agarose poured into a horizontal glass mould (27 x 19.8 x 0.4 cm) in a coldroom. The gel comb was supported 4 mm above the surface of the mould and was of the following dimensions: 10 teeth 1 mm apart; each tooth being 10 x 10 x 1 mm. The horizontal gel tank (30 x 20 x 7 cm) was of the type with individual reservoirs at each pole and a raised table to support the gel. The tank was filled with buffer such that the surface of the gel was covered by 5 mm. Under each end of the tank a magnetic stirrer was used to mix the buffer (with a 2 cm flea) in each reservoir at a slow speed. The gel was pre-run at 1.8 V/cm for ca.2-4 h in 1 X TPE (containing the same concentration of ChQ as the gel) with recirculation of the buffer (15 ml/min) in a coldroom. The average temperature of the buffer and gel was 8°C.

The plasmid samples (1 μg each) were loaded in 30 μl volumes + 6 μl loading buffer, the samples were "run in" at a high voltage for 15 min and the voltage reduced to 1.8 V/cm for ca.40 h. The gel was removed from the tank and washed in 2 l dH_2O, then 2 l

1mM $MgSO_4$ and finally 2 l dH_2O (ca.20 min for each wash). The gel was then stained in EtBr (1 μg/ml) overnight at 4°C. Prior to photography the gel was destained in dH_2O for 20 min. The DNA was visualised using a transilluminator and photographed using Polaroid 665 (positive/negative) film, typical exposure was 15 sec at f5.6.

2.16.2: Two dimensional ChQ gels

The method used was as described previously (Bowater *et al.*, 1992).

2.16.3: Densitometric scanning of a distribution of a topoisomer population

Each topoisomer distribution was scanned (from the negative taken as described in section 2.16) using a Beckman DU-8 spectrophotometer with a compusat SLABGEL accessory. The method was carried out as described in the accompanying literature and using the program presented in Appendix 2.2.

2.17: Enzyme assays

2.17.1: Kanamycin patch plate assay

A master plate (MS plus 50 μg/ml thiostrepton) was inoculated with the *Streptomyces* strains to be tested and incubated until the patches (ca.1 cm^2) of growth had sporulated. A range of test plates were prepared from MMT plus kanamycin at concentrations of 0, 50, 100, 300 μg/ml and were inoculated by replica-plating from the master plate. The plates were incubated at 30°C for 2-3 days and then scored for growth.

2.17.2: Kanamycin gradient plate assay

The level of kanamycin resistance was determined by a modification of the gradient plate assay as described previously (Ward *et al.*, 1986). The gradient plates were inoculated either directly as described (Ward *et al.*, 1986), or by replica-plating from a master-plate. The master plates were prepared using MS agar plus 50 μg/ml thiostrepton. The spores were streaked onto the MS agar and allowed to sporulate before replica-plating to the gradient plates.

2.17.3: Aminoglycoside phosphotransferase (APHII) assay

The method used was a modification of previously described methods (Seno *et al.*, 1983; M.J. Bibb, personal communication).

Step 1: The spore suspensions of each *Streptomyces* strain were prepared by spreading primary transformants onto MS agar and incubating the plates until a confluent lawn of spores was visible (5-7 d). The spores were then gently scrapped off the agar, washed in dH_2O and resuspended in sterile dH_2O and stored at 4°C.

Step 2: The above spore suspensions were pre-germinated as described previously (Hopwood *et al.*, 1985a) and used to inoculate 50 ml NMMP containing L-arabinose as a neutral carbon source and 5 μg/ml thiostrepton. The cultures were grown with shaking at 30°C to an OD_{450} of 0.8-1.0 and harvested (B&T: 3,500 rpm; 7 min). Each mycelial pellet was resuspended in 5 ml NMMP (no carbon source), split in 2, one volume was added to 22.5 ml of NMMP plus 0.5% glycerol, 5 μg/ml thiostrepton, and the other to 22.5 ml NMMP plus 0.5% L-arabinose, 5 μg/ml thiostrepton. The cultures were incubated with shaking at 30°C for 2 h, harvested (B&T: 5,000 rpm; 5 min) and processed immediately or stored at —70°C until step 3.

Step 3: The mycelia were washed in 20 ml RS buffer (10 mM Tris.HCl (pH7.6), 10 mM $MgCl_2$, 0.21% 2-mercaptoethanol (v/v), 50 mM NH_4Cl, dH_2O to 100 ml and stored at 4°C) and re-pelleted (B&T: 3,000 rpm; 10 min).

Step 4: The cells were resuspended in 1.5 ml RS buffer and sonicated (MSE Soniprep 150) using the fine probe in an ethanol/ice bath for 3 X 15 sec with 15 sec intervals at a power setting of 18 μ.

Step 5: The sonicate was then transferred to a 5 ml open top ultracentrifuge tube, filled and balanced with mineral oil and the cell debris pelleted by centrifugation (Beckman L5-50B ultracentrifuge, SW50.1: 40,000 rpm; 1.5 h at 4°C).

Step 6: ca.1 ml of the sonicate was transferred to an eppendorf on ice and either assayed immediately or frozen at —70°C.

Step 7: The following reagents were prepared: TEAK buffer (50 mM Triethanolamine (pH7.4), 10 mM $MgCl_2$, dH_2O to 100 ml and stored at 4°C); NADH (35.47 mg β-NADH in 2 ml Na buffer (80 mM Na_2CO_3, 20 mM $NaHCO_3$) and stored at —70°C); ATP (242.8 mg ATP in 2 ml Na buffer and stored at —70°C); PEP (41.22 mg PEP in 1 ml dH_2O and stored at —70°C); PAN (240 μl NADH, 240 μl ATP, 180 μl PEP and stored at —70°C). For each assay the following reagents were mixed in a universal: 2 ml TEAK (at 25°C), 50 μl PAN, 3.2 U pyruvate kinase, 11 U lactate dehydrogenase and 100 μl sonicate. This was split into 2 X 1 ml disposable plastic cuvettes and the OD_{340} monitored in a dual beam spectrophotometer (Varian Cary 1 UV-Visible Spectrophotometer). The assay was initiated by the addition of 2.5 μl kanamycin (50 mg/ml) to the reference cuvette. The rate of decrease of NADH at OD_{340} was then followed as a positive slope. The Cary program used to run the assay is presented in Appendix 2.3.

Step 8: The protein concentration in each sonicate sample was determined using the Biorad micro assay, the standard curve was determined using bovine immunoglobulin G.

Step 9: The APHII activity was calculated using the following formula:

μmol NADH oxidised/min/mg protein = (OD/min)/6.22/(mg protein/assay)

2.17.4: Glycerol kinase assay

The assay was performed on sonicates isolated from cultures grown in NMMP plus 0.5% glycerol as described in section 2.17.3. The only difference between the two assays was: firstly, the sonicate sample was allowed to equilibrate at 25°C for 1 h prior to the assay; the enzyme is unstable at 0°C. Secondly, glycerol was added as the substrate, in Step 7, to a final concentration of 10 mM (3.7 μl of a 25% stock).

Chapter Three

Results I: DNA Supercoiling in *Streptomyces* spp.

3.1: Introduction

Prior to this study there have been no published investigations of DNA supercoiling in streptomycetes. Since *Streptomyces* spp. need to maintain active metabolism in stationary phase for secondary metabolic processes (and because it is known that many of these metabolites are under transcriptional control), the maintenance of a significant level of supercoiling was expected. It was therefore of interest to determine DNA supercoiling levels at different growth phases.

S. coelicolor A3(2) produces four known antibiotics, all of which are globally regulated at the transcriptional level (Chater and Bibb, 1995). Changes in DNA supercoiling could also have a role to play in the environmental signalling involved in the developmental expression of the *bld*, *sap* and *whi* genes involved in aerial hyphae formation and sporulation. It has also been speculated that DNA supercoiling may be involved in catabolite repression as loss of the glucose kinase gene leads to a reduction in supercoiling (Hodgson, 1994), similar to the loss of *oxrC* in *E. coli* (see section 1.8.5).

As a step towards investigating DNA supercoiling in streptomycetes, the superhelical density (σ), of the multicopy plasmid, pIJ486, isolated from both liquid and surface

grown cultures, was determined *in vitro*. HMM, which causes the exclusive production of methylenomycin by MT1101, was used. Since the genes for the synthesis of and resistance to, methylenomycin are extrachromosomally encoded on SCP1 (and are regulated at the transcriptional level), any changes in the activity of DNA topoisomerases, in response to environmental or developmental signals regulating methylenomycin synthesis, would probably be reflected by changes in the σ of pIJ486. Thus, any role involving DNA supercoiling in the response to such signals could be assessed by monitoring the σ of pIJ486 at different growth phases. The liquid cultures provided information on how the growth conditions for the production of methylenomycin affected supercoiling (as also did the surface grown cultures). The surface grown cultures allowed the determination of supercoiling levels at different stages of morphological development (which also provided information on aerial hyphae formation and the σ of pIJ486). These studies also indicated whether the σ might be high enough for *Z*-DNA to form in the plasmid-borne *gyl* promoter fragments (see Chapter Four).

3.2: Determination of the superhelical density of pIJ486 *in vitro*

The method of determining superhelical density involved the generation of a set of overlapping topoisomer populations of pIJ486 and the band-counting method of Keller (1975). The ΔLk (section 1.8.2) of a plasmid sample is analogous to an extendable ladder which represents the set of overlapping topoisomer populations. Each topoisomer population within the set is represented by each individual ladder, and the distribution within each topoisomer population is represented by the rungs of each ladder. Therefore, the ΔLk of the overlapping set of topoisomers is analogous to the number of rungs from

top to bottom in the fully opened, extendable, ladder. The resolution of each topoisomer population into "rungs on a ladder" was achieved by 1D ChQ gel electrophoresis (see section 2.16.1). The determination of the σ of pIJ486 achieved two things. First, it indicated the likelihood that the potential *Z*-DNA forming sequences of the *gyl* operon could adopt left-handed DNA *in vivo* (section 4.1), and secondly, it provided a standard preparation of pIJ486 of known ΔLk. This standard was then used as a reference for the 1D ChQ gel analysis of pIJ486 samples isolated across the growth phase of MT1110(pIJ486).

3.2.1: Generation of a set of overlapping topoisomers of pIJ486

The amount of TopI required to completely relax the plasmid cccDNA was first determined. A range of concentrations of the enzyme was used in the reaction conditions described in section 2.15.1. The samples were analyzed by gel electrophoresis (Figure 3.1). Incomplete relaxation (a completely relaxed plasmid cccDNA sample has similar mobility to ocDNA), was observed for samples in lanes 2-4. A concentration of 1 U TopI per μg DNA appeared to completely relax the cccDNA (lane 5), and to ensure this, the TopI incubation time was increased to 5 h.

Due to the large amount of plasmid cccDNA required for this study a large scale pIJ486 preparation was isolated from a 10 l batch culture as described in section 2.11. The plasmid was purified by double CsCl gradient centrifugation to remove chromosomal and linear DNA as well as minimising the amount of ocDNA present in the sample. The plasmid sample was stored at 4°C in TE (pH8), to prevent any mechanical shearing that

Figure 3.1: Complete relaxation of cccDNA by TopI: Agarose gel electrophoresis of pIJ486 relaxed to varying degrees

Electrophoresis was carried out with 1.2% agarose (w/v), in 1 X TAE buffer at 2 V/cm for ca.14 h with recirculation of the buffer (10 ml/min). The agarose did not contain EtBr, the gel was stained after electrophoresis with EtBr (0.5 μg/ml), for 30 min and de-stained in 1 Mm $MgSO_4$ for 20 min before photographing. Samples of pIJ486 were treated with "x" Units (U), of TopI unless otherwise indicated (see Table 2.3). Lanes: 1, pIJ486 untreated; 2, 0.1 U; 3, 0.25 U; 4, 0.5 U; 5, 1.0 U; 6, 5.0 U; 7, 0.0 U; 8, pIJ486 untreated; 9, λ *Hin*dIII marker. Relaxation causes the cccDNA to have a similar mobility as the ocDNA in lane 1. On the original photograph lanes 2 to 4 show some cccDNA running below the ocDNA position indicating incomplete relaxation, on this basis the concentration of TopI used in lane 5 was used to completely relax pIJ486 cccDNA.

Figure 3.2: Analysis of a set of topoisomers of pIJ486 by agarose gel electrophoresis

Electrophoresis was carried out with 1.0% agarose (w/v), in 1 X TBE buffer containing EtBr (0.5 μg/ml), at 4 V/cm for ca.5 h. All samples were treated with TopI unless otherwise indicated. Lanes: 1, λ *Hin*dIII marker; 2, Top 1; 3, Top 2; 4, Top 3; 5, Top 4; 6, Top 5; 7, Top 6; 8, Top 7; 9, Top 8; 10, Top 9; 11, Top 10; 12, pIJ486 control (no TopI). The $-\sigma$ of the topoisomers increased from left to right; this reduced their mobility as the more supercoiled plasmids could bind increasing amounts of EtBr; EtBr removes supercoils and therefore lowers the mobility of the plasmids in that sample.

Figure 3.1

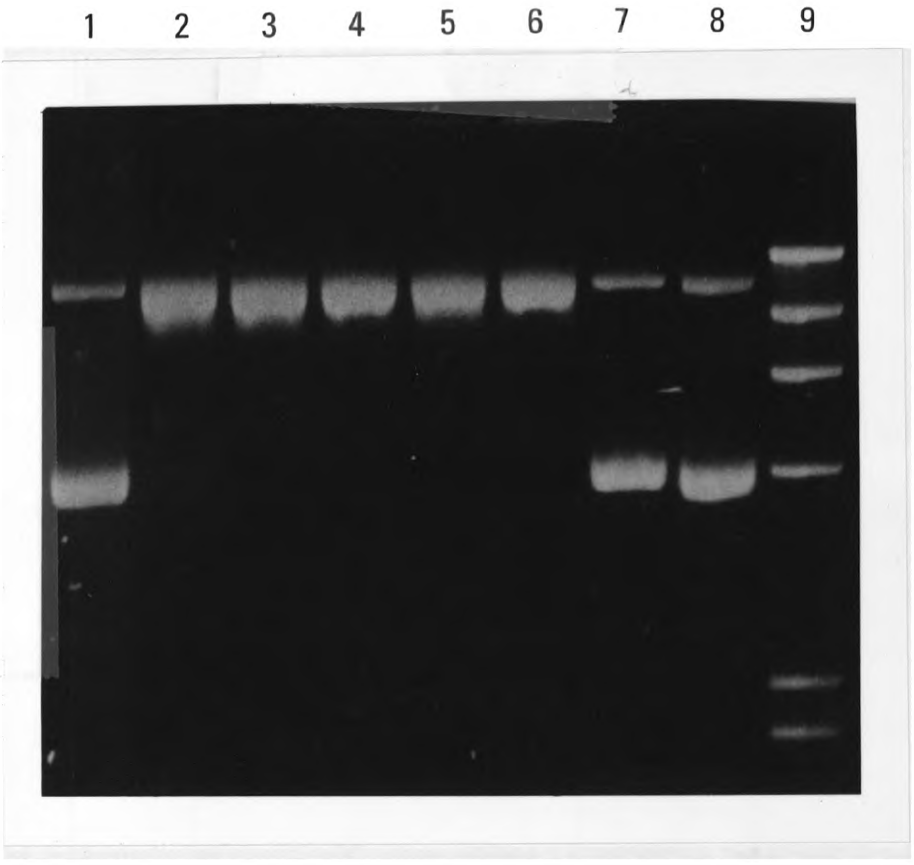

Figure 3.2

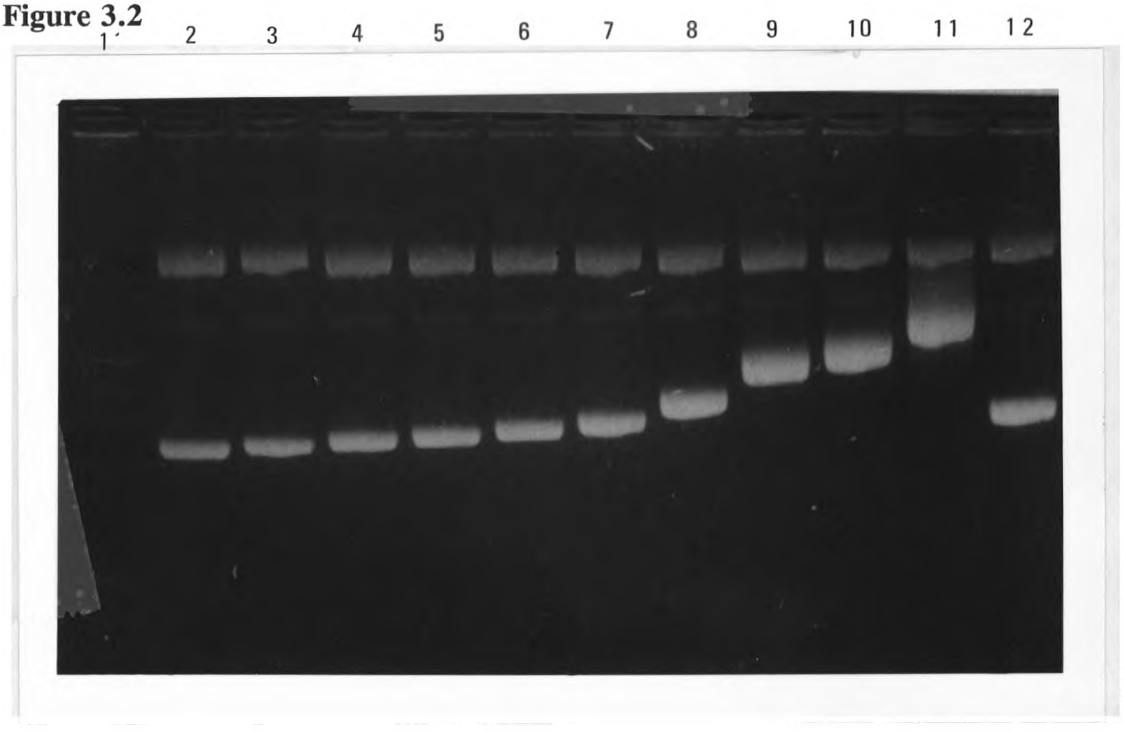

may otherwise have occurred during freeze/thaw cycling, if it was stored at —20°C. A set of topoisomers was generated using the EtBr concentrations in Table 2.4 and the method described in section 2.15.2, each topoisomer population was analyzed by agarose gel electrophoresis (Figure 3.2). The removal of the EtBr, after complete relaxation, caused the DNA helix of each sample to be underwound by an amount directly proportional to the concentration of EtBr in that sample. This underwinding resulted in an increase in the number of negative (—) supercoils which therefore increased the $-\sigma$.

3.2.2: Analysis of the overlapping set of pIJ486 topoisomers

Any one topoisomer population contained a distribution of plasmids varying in σ due to the thermal fluctuations that occurred during the strand cleavage/re-ligation reaction with TopI (Bates and Maxwell, 1993). In order to resolve the distribution ("rungs"), of each topoisomer population, ranging from the topoisomer with 0 supercoils to that with the same σ as the pIJ486 sample, and to find the overlap between each population of topoisomers, 1D ChQ gels containing varying amounts of ChQ were used (see section 2.16.1). Topoisomers 1 to 6 and a native sample of pIJ486 were partially resolved by electrophoresis in a gel containing 12.5 μg/ml ChQ (Figure 3.3). Each band below the ocDNA in Figure 3.3 represents a topoisomer that differs from the one above or below by $\pm$ 1 supercoil. At this ChQ concentration not all the topoisomers were resolved into discrete bands (see, e.g., lanes 1 and 4 in Figure 3.3). Also, the populations of topoisomers 2 and 3 did not overlap; therefore another topoisomer population, 2a, was generated using a concentration of EtBr between that used to generate topoisomers 2 and 3 (Table 2.4). Complete resolution of topoisomer 1 and the overlap between topoisomers

Figure 3.3: Resolution of the distributions of topoisomers by 1D ChQ gel electrophoresis

Electrophoresis was carried out as described in section 2.16.1. The concentration of ChQ used was 12.5 μg/ml. All samples were treated with TopI unless otherwise indicated. Lanes: 1, Top 1; 2, Top 2; 3, Top 3; 4 Top 4; 5, Top 5; 6, Top 6; 7, pIJ486 native sample #1, untreated.

The pIJ486 sample was harvested from the 10 l batch culture described in section 2.11.

The gels presented in Figure 3.3 and Appendices 3.1-3.3 were resolved in agarose containing ChQ rather than EtBr as it has a lower affinity for DNA compared to EtBr (Shure *et al.*, 1977). This was important as the degree of resolution of the topoisomers was found to be highly sensitive to minor variations in experimental conditions and concentration of DNA per lane when EtBr was used. The cccDNA in lanes 1 to 3 is positively supercoiled, that in lane 4 is almost completely relaxed and in lanes 5 to 7 the cccDNA is negatively supercoiled. This is due to the binding of ChQ to the cccDNA during electrophoresis; although all the samples are negatively supercoiled orginally (see section 2.15.2) the binding of ChQ to the samples in lanes 1 to 3 removes all the negative supercoils and introduces positive supercoils, dependent on the initial degree of negative supercoiling. Thus, at this ChQ concentration the sample in lane 4 has lost virtually all negative supercoils and those in lanes 5 to 7 contained sufficient negative supercoils such that some, but not all, negative supercoils were removed by the binding of ChQ during electrophoresis.

Figure 3.3

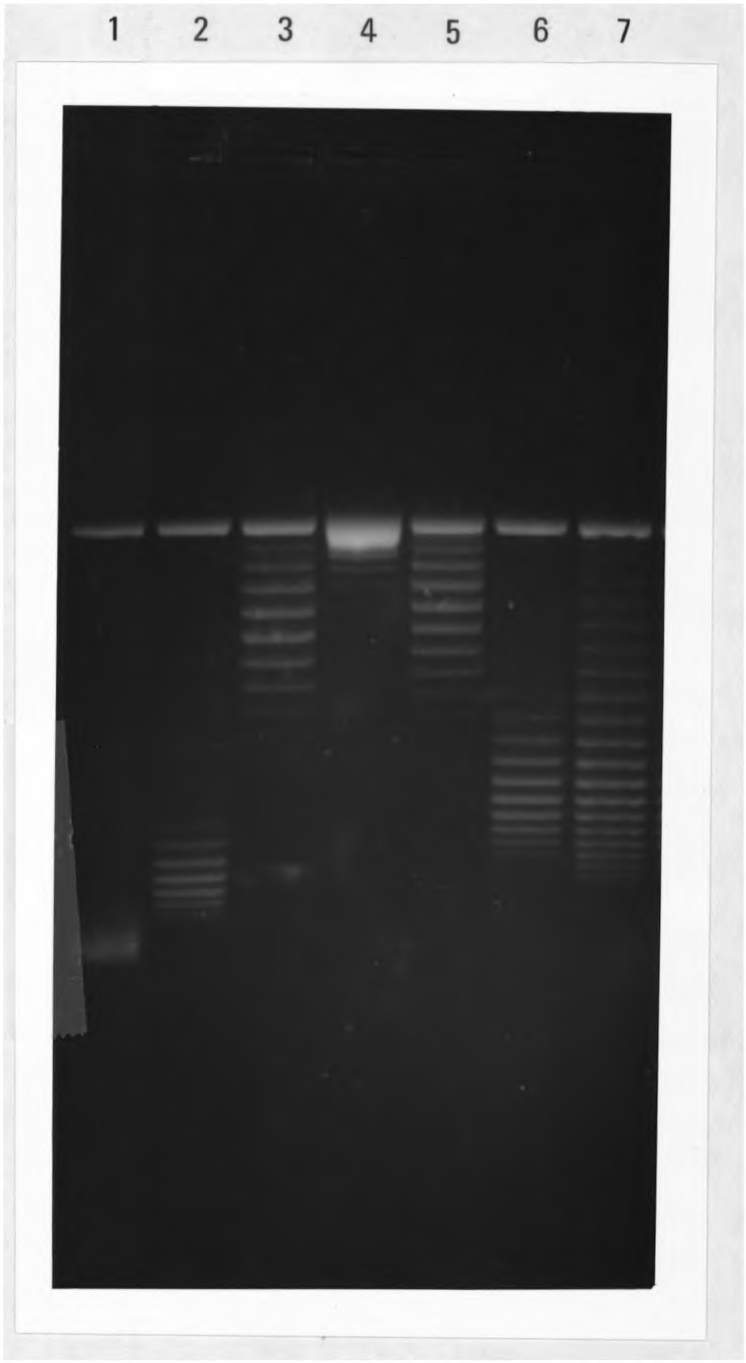

2a, 3 and 4 was obtained with a ChQ concentration of 2.5 μg/ml (Appendix 3.1). The overlap between topoisomers 1, 2 and 2a was determined with a ChQ concentration of 10 ng/ml (Appendix 3.2), while the overlap between topoisomer 4 and 5 was resolved at a ChQ concentration of 10 μg/ml (Appendix 3.3). To accurately analyze the overlapping topoisomer populations the gels were photographed and the Polaroid negatives were scanned as described in section 2.16.3. Using the position of the ocDNA as the reference point, the scans of adjacent lanes of topoisomers were compared and the position of the overlaps noted. Two such scans are presented in Figure 3.4, showing the overlap between topoisomers 5 and 6 (Figure 3.3). As the mean of the population of topoisomers could only change by a strand cleavage/re-ligation event it was a constant under the conditions used to resolve the topoisomers. Under these conditions four different concentrations of ChQ were used to determine the ΔLk of pIJ486 and the error was estimated to be $\pm$ 1.5 supercoils as described previously (Keller, 1975). This overlapping set of topoisomers allowed the ΔLk of pIJ486 to be determined by counting the number of bands from the mean of topoisomer 1 (lane 1, Figure 3.3), to the mean of the topoisomer 6, which had the same mean mobility as the native pIJ486 sample. The ΔLk of the pIJ486 sample in lane 7 of Figure 3.3 was found to be -38 ± 1.5. This was composed of the differences between the means of the various overlapping topoisomers as seen in Table 3.1. Using formula [1.1] in section 1.8.2 the $Lk°$ of pIJ486 is 591.5, and from formula [1.3] the σ or specific linking difference of pIJ486 sample #1 was -0.064 ± 0.002. This pIJ486 sample, of known ΔLk, was used as the standard for all subsequent determinations of $-\sigma$ described in this study.

Figure 3.4: Densitometric scans of Top 5 and Top 6 showing the overlapping topoisomer populations

The distributions of the topoisomers were densitometrically scanned as described in section 2.16.3. The scans are aligned at the position of the ocDNA.

TOP 5

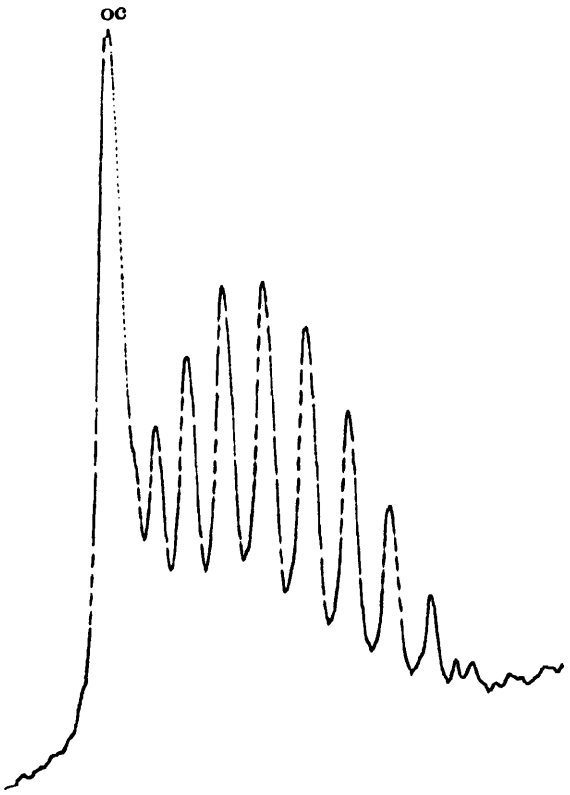

Figure 3.4

TOP 6

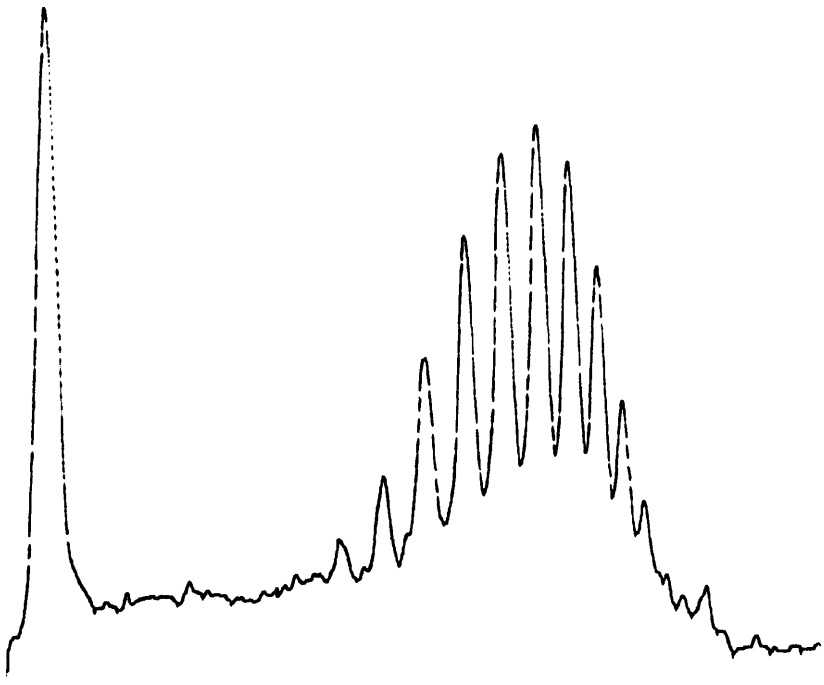

Table 3.1:

Topoisomer[1]	ΔLk
1-2	−5
2-2a	−6
2a-3	−6
3-4	−5
4-5	−8
5-6	−8
6-pIJ486 #1	0

Notes:
1: Indicates the overlap between each topoisomer population.
2: ΔLk indicates the linking difference between the means of each overlapping topoisomer population.

3.3: Variation of the superhelical density of pIJ486 across the growth curve of *S. coelicolor* MT1110(pIJ486)

The variation in the σ of pIJ486 isolated from surface and liquid grown cultures was studied using HMM (containing alanine). This medium was chemically defined for the exclusive production of methylenomycin in the parent strain of MT1110, *S. coelicolor* MT1101 (Hobbs *et al.*, 1992). It has also been suggested by Hobbs *et al.* (1992), that methylenomycin production may be a stress response due to profound changes in the environment of the culture. As discussed in section 1.8.5, transcription and supercoiling are closely linked and sensitive to the environment. Any relationship between observed changes in the medium, and DNA topology, could be determined by following the σ of pIJ486.

3.3.1: Variation in the σ of pIJ486 when MT1110(pIJ486), was cultured in liquid HMM

MT1110(pIJ486) was grown in HMM, that is, under the physiological conditions used for the exclusive production of methylenomycin by MT1101. However, MT1110 does not produce methylenomycin since it is SCP1$^-$. The experiments were carried out in a 3.5 l bioreactor as described in section 2.12. Production of CO_2 was logged and used as an indicator of biomass to determine the growth phase of the culture. The bioreactor was sampled for mycelia from which plasmid DNA was isolated by the method described in section 2.14.1. The ΔLk was determined by resolving the plasmid samples and the standard pIJ486 (of known ΔLk), in gels containing 5-10 μg/ml ChQ as described in section 2.16.1. The change in the position of the mean of the topoisomer distributions between the standard and the bioreactor samples was calculated from densitometric scans. Four batch cultures were prepared under the same physiological conditions; data obtained from one such culture is presented in Figure 3.5 and that from two of the others is presented in Appendices 3.4 and 3.5.

3.3.1.1: Growth kinetics of MT1110(pIJ486) in liquid batch culture

Batches 1, 2 (Appendices 3.4 and 3.5), and 4 (data not shown), all had similar growth kinetics with average doubling times (t_D), of 4.3 h; batch 3 however, had a t_D of 7.1 h. Batches 1, 2, and 3 were carbon limited whereas batch 4 was not, probably due to the presence of more utilizable carbon in the medium used for batch 4. Batch 4 entered stationary phase in stepwise decrements (as judged from %CO_2 evolution), which

Figure 3.5: Variation in superhelical density of pIJ486 across the growth curve of MT1110(pIJ486), cultured in liquid HMM

"Batch culture 3" was prepared as described in section 2.12. $\%CO_2$ evolution, pH of the medium and superhelical density of pIJ486 sampled from the culture, are shown.

Figure 3.5

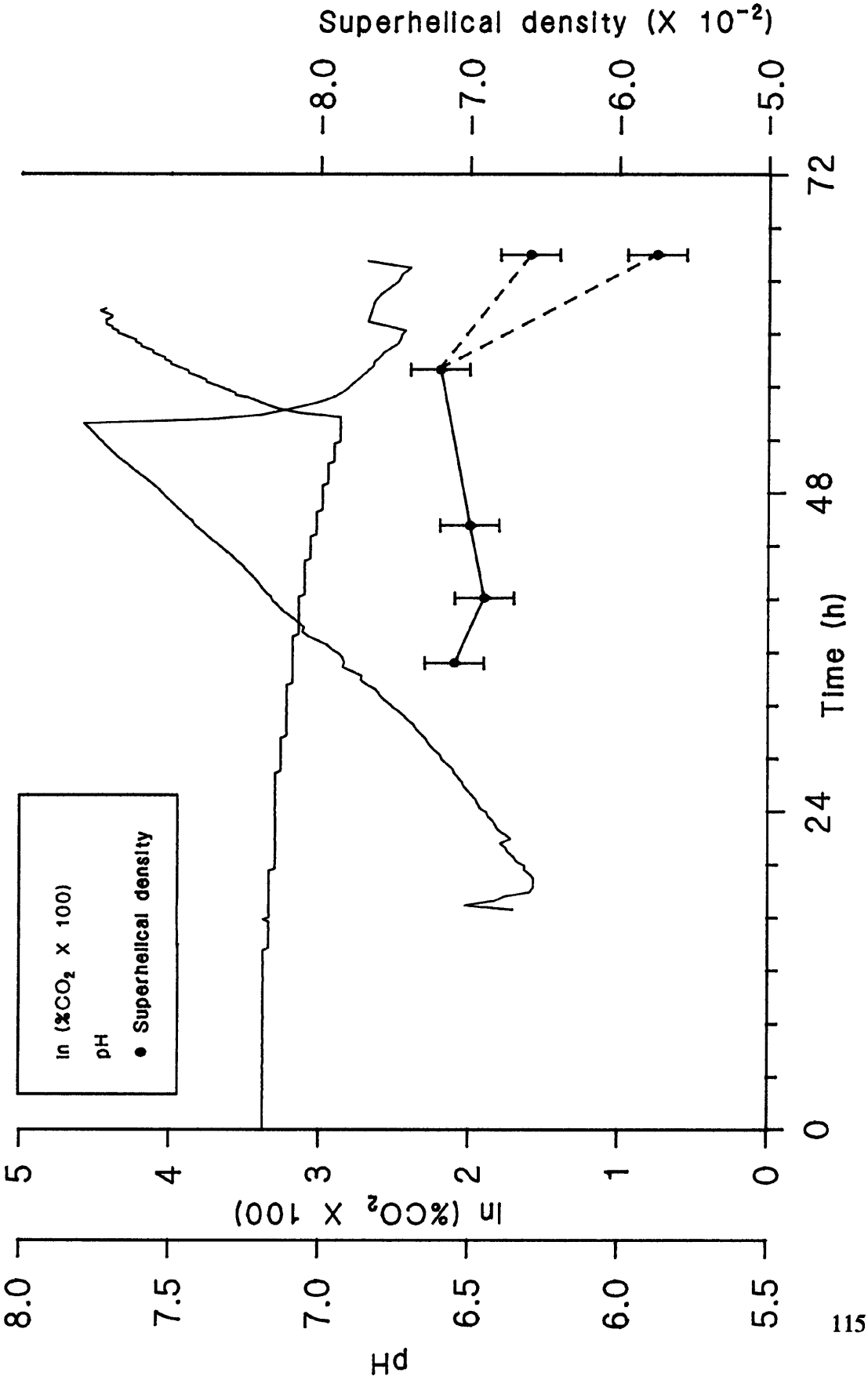
Superhelical density (X 10^{-2})
-8.0
-7.0
-6.0
-5.0
72
48
24
0
Time (h)
ln (%CO_2 X 100)
pH
• Superhelical density
5
4
3
2
1
0
8.0
7.5
7.0
6.5
6.0
5.5

indicated the presence of an available carbon source, in contrast to the near vertical drop in $\%CO_2$ evolution associated with carbon source exhaustion (see, e.g., batch 3, Figure 3.5). The differences in available carbon was attributed to the variable effects of autoclaving on the carbon and nitrogen sources; HMM has since been modified to ensure carbon-limitation (P. Butler, personal communication). Batch 1 had an erratic CO_2 plot possibly due to non-synchronous growth, as a seed culture was used as the inoculum. The other batch cultures were each inoculated with a high density spore preparation (section 2.3.3), to achieve more synchronous growth.

3.3.1.2: ΔLk of pIJ486 sampled across the growth curve of MT1110(pIJ486)

Plasmid samples from the batch cultures were isolated (see section 2.14.1), resolved by 1D ChQ gel electrophoresis (Figure 3.6(a)), and the ΔLk determined as described previously. All of the plasmids isolated from each batch culture, from mid to late exponential phase, showed an initial average ΔLk of -41 ± 1.5 ($\sigma = -0.069 \pm 0.002$), which was maintained with fluctuations of $\pm$ 2 supercoils until stationary phase. As seen from batch 3 (Figure 3.5), the σ was maintained for at least 4 h into stationary phase, followed 6.7 h later by a topoisomer population which was bimodal, with ΔLk of -39 and -34 ($\sigma = -0.066 \pm 0.002$ and -0.057 ± 0.002). The 1D ChQ gel in Figure 3.6(a) and the scan of lane 6, Figure 3.6(b) shows clearly the bimodal distribution of the latter. The last sample from batch 1 (Appendix 3.4), was harvested ca.6 h into stationary phase and also contained a bimodal plasmid population, with ΔLk of -41 and -35 (σ of -0.069 ± 0.002 and -0.059 ± 0.002). Batch 4 (data not shown), was sampled ten times between mid exponential phase and the onset of stationary phase and demonstrated

Figure 3.6: pIJ486 samples from batch 3 resolved by 1D ChQ gel electrophoresis

(a) Electrophoresis was carried out as described in section 2.16.1 in an agarose gel containing 12.5 μg/ml ChQ. Lanes: 1, pIJ486 #1 standard (of known ΔLk); 2, sample #1; 3, sample #2; 4, sample #3; 5, sample #4; 6, sample #5; 7, pIJ486 #1 standard.

(b) The densitometric scan of lane 6 showing the bimodal distribution of topoisomers in sample #5.

Figure 3.6

a

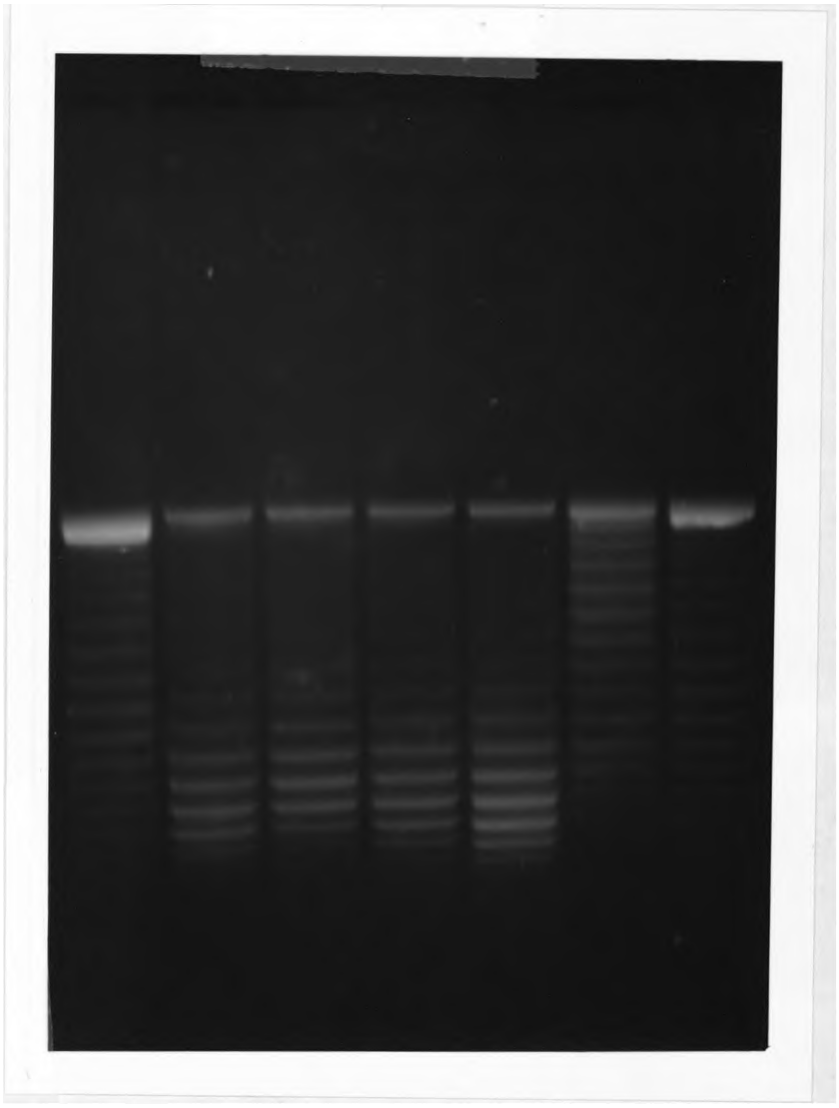

(b)

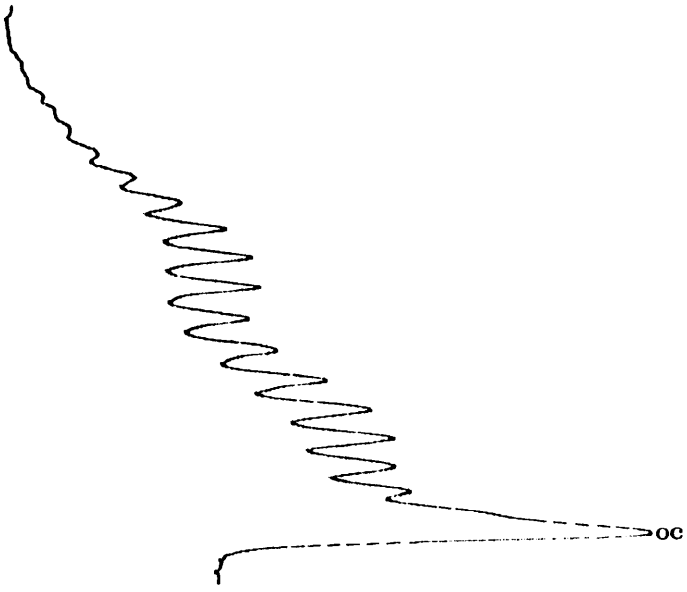

that a variation of 2 supercoils could occur within a 0.75 h period (or 1/6 of a t_D).

3.3.1.3: The σ of pIJ486 isolated from a culture grown in the absence of thiostrepton

Thiostrepton was used to maintain selection in the above bioreactor batch cultures, but it is known to induce synthesis of additional proteins and have a wide range of physiological effects (Murakami *et al.*, 1989). To determine whether the presence of thiostrepton may have influenced the level of σ a batch culture identical to the others, but containing no thiostrepton, was studied (batch 5; see Appendix 3.6). The average t_D for batch 5 was similar to the others, at ca.4.3 h, although the lag phase was shorter compared to the four batches containing thiostrepton. The culture was carbon limited and was sampled nine times from mid exponential to early stationary phase. The initial ΔLk was -41 ± 1.5 ($\sigma = -0.069 \pm 0.002$), and fluctuated by $\pm$ 1 supercoil until the transition phase to linear growth kinetics when the ΔLk dropped to -38 ± 1.5 ($\sigma = -0.064 \pm 0.002$); within 1.3 h however, the plasmid had regained the lost supercoils. It was concluded that thiostrepton did not significantly influence the level of σ under the growth conditions used.

3.3.2 Variation in the σ of pIJ486 when MT1110(pIJ486) was surface grown on HMM agar medium

HMM was adapted for surface growth by the addition of 1% (w/v), agar and the exclusion of Junlon. The plates were prepared and inoculated as described in section 2.13. At each time point, 5 plates were sampled to determine the average dry weight of

mycelia and the pH of the medium. Plasmid was isolated from 5-15 plates and processed using the method described in section 2.14.2. Two experiments were carried out under identical conditions and the influence of the growth phase on the σ of pIJ486 in experiment 2 is presented in Figure 3.7 (the data from experiment 1 is presented in Appendix 3.7).

3.3.2.1: Growth kinetics of surface grown MT1110(pIJ486) cultures

The kinetics of growth in both experiments were fairly similar. The t_D of the culture in experiment 1 was 6.7 h (at mid exponential phase), and that in experiment 2 was 5.9 h; although the characteristic pH drop associated with HMM cultures prior to entering stationary phase was only seen in experiment 2 it may have occurred in experiment 1, but been missed during sampling. In experiment 2, the transition from vegetative mycelium to aerial hyphae formation began at ca.40 h and growth seemed to stall at this point until ca.44 h, when exponential growth was resumed. The transition phase from vegetative mycelium to aerial hyphae formation is portrayed in the montage presented in Figure 3.8. Although the time at which the transition phase occurred was not accurately determined in experiment 1, when the two log plots (dry weight), were aligned for exponential growth (Appendix 3.9), and the photographs of morphology were compared (experiment 2, Figure 3.8; experiment 1, Appendix 3.8), it could be seen that at ca.57 h in experiment 1 growth stalled for 4 h. Given the longer t_D of experiment 1 it was probable that this point represented the transition phase.

Figure 3.7: Variation in the superhelical density of pIJ486 isolated from surface grown MT1110(pIJ486): experiment 2

Experiment 2, prepared as described in section 2.13, showing the dry weight, pH and variation in the σ of pIJ486 across the growth curve of the culture.

Figure 3.7

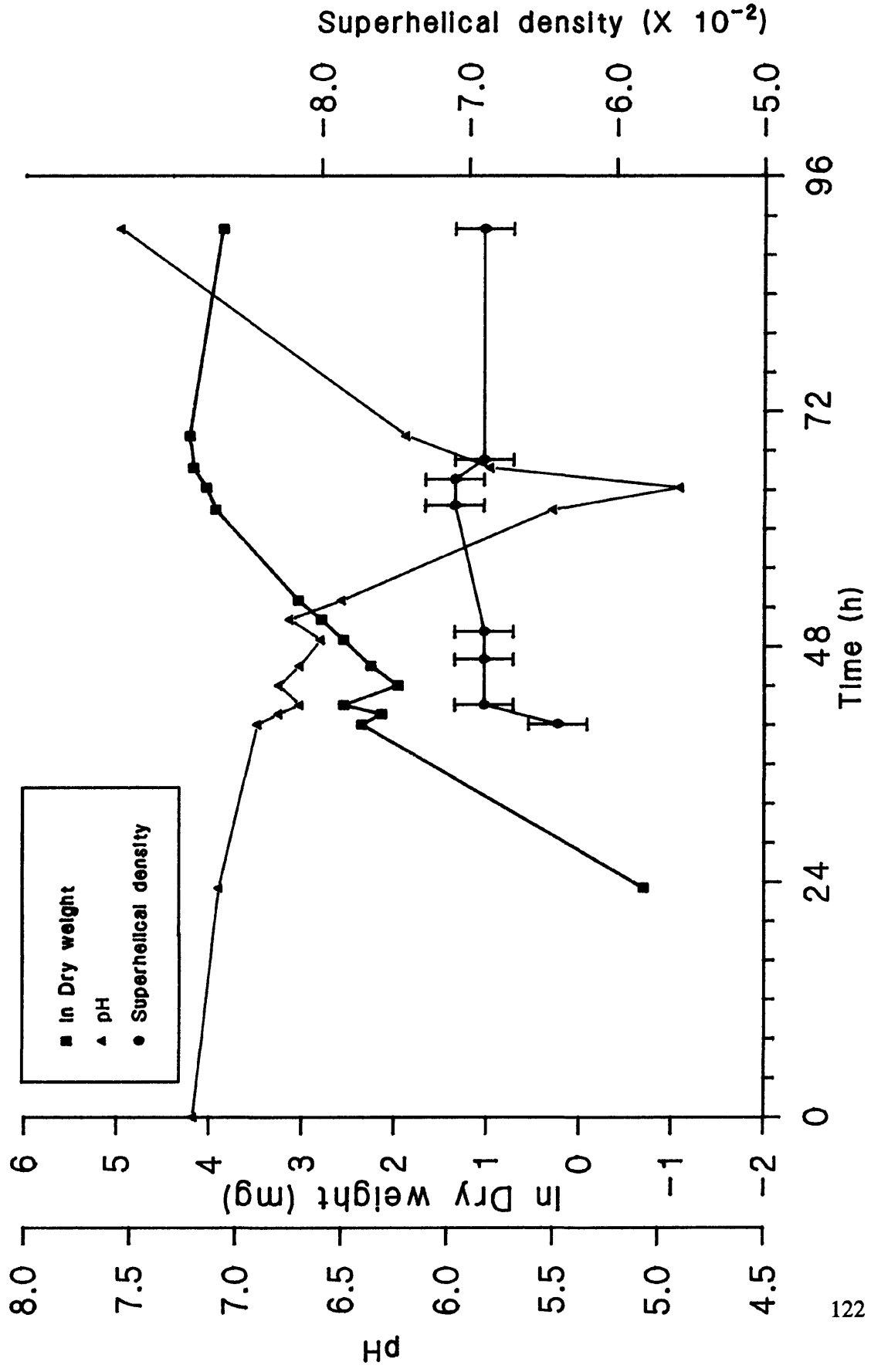
Superhelical density (X 10^{-2})
-8.0
-7.0
-6.0
-5.0
96
72
48
24
0
Time (h)
■ ln Dry weight
▲ pH
● Superhelical density
6
5
4
3
2
1
0
-1
-2
ln Dry weight (mg)
8.0
7.5
7.0
6.5
6.0
5.5
5.0
4.5
pH

Figure 3.8: Surface grown MT1110(pIJ486) culture (experiment 2): a montage showing the transition phase from vegetative mycelia to aerial hyphae formation

The mycelia were photographed through a X32, long focal length, microscope objective. The microscope was a Leitz Laborlux 12 and the camera was a Wild MP551, exposure was controlled with a Wild Photoautomat MP545.

(a) 24 h after inoculation. Note the confluent vegetative mycelial mat.

(b) 46 h after inoculation. Note the dark spots that indicate the beginning of the transition phase to aerial hyphae formation.

(c) 49 h after inoculation. Note the presence of mycelial "towers" (bottom right) pushed up from the basal vegetative mat, and aerial hyphae formation.

(d) 51 h after inoculation. Note the denser appearance of the mycelium.

(e) 62 h after inoculation. Note the increase in aerial hyphae formation; the majority of the vegetative mycelium had undergone the transition phase to aerial hyphae at this point.

(f) 65 h after inoculation. Note the appearance of spores at the tips of some of the aerial hyphae.

Figure 3.8

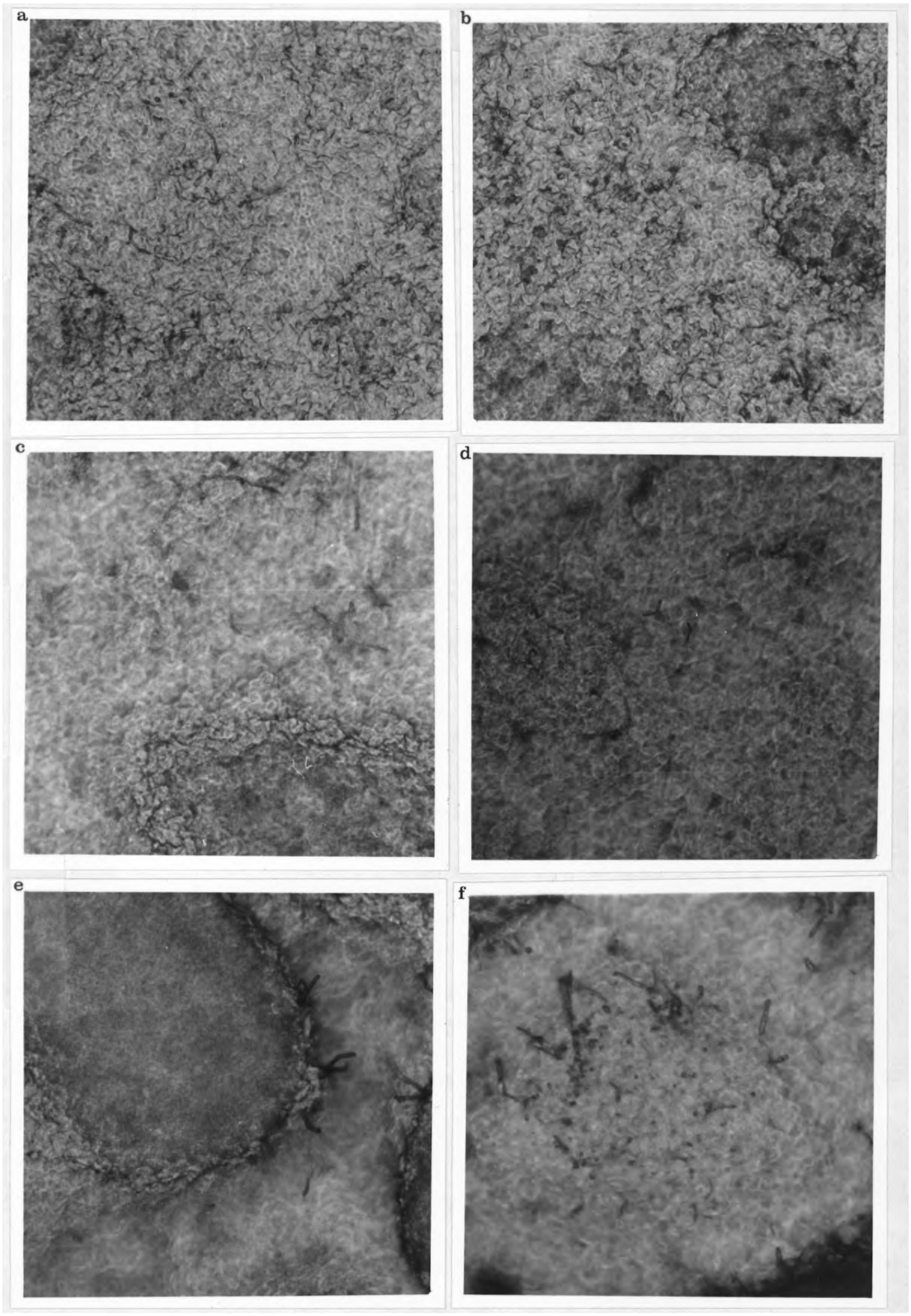

3.3.2.2: ΔLk of pIJ486 sampled across the growth curve of surface grown MT1110(pIJ486)

The plasmid samples from experiments 1 and 2 were isolated and resolved in gels containing 10 μg/ml ChQ (see, e.g., Figure 3.9). The initial pre-transition phase ΔLk of pIJ486 was —41 $\pm$ 1.5 (σ = —0.069 $\pm$ 0.002) for experiment 1 and —38 $\pm$ 1.5 (σ = —0.064 $\pm$ 0.002) for experiment 2.

During the transition to aerial hyphae formation in experiment 1 (Appendix 3.8), there was an increase in ΔLk of 2 negative supercoils (σ = —0.073 $\pm$ 0.002). This was followed by a decrease in ΔLk of 1 supercoil when the pH of the medium was at its lowest recorded point and the culture had just entered stationary phase. The ΔLk was then maintained at —42 (σ = —0.071 $\pm$ 0.002), for at least 28 h into stationary phase, 22 h later there was a decrease in ΔLk of 2 negative supercoils to —40 (σ = —0.068 $\pm$ 0.002). Similarly, in experiment 2 there was an increase in ΔLk of 3 negative supercoils to —41 (σ = —0.069 $\pm$ 0.002), during the transition to aerial hyphae formation. This was maintained for up to 24 h whereupon the ΔLk increased to —42 (σ = —0.071 $\pm$ 0.002), and then dropped to —41 (σ = —0.069 $\pm$ 0.002), on entry to stationary phase (where the pH was at its lowest point). This was maintained for at least 24 h. There was no evidence of a bimodal distribution of topoisomers, in any of the plasmid samples harvested during stationary phase, in either of the surface grown cultures, in contrast to the liquid cultures of MT1110(pIJ486) (see, e.g., Figure 3.6).

Figure 3.9: pIJ486 samples from a surface grown culture (experiment 2), resolved by 1D ChQ gel electrophoresis

Electrophoresis was carried out as described in section 2.16.1 in an agarose gel containing 10 μg/ml ChQ. Lanes: 1, pIJ486 #1 standard; 2, pIJ486 #2 standard; 3, sample #1; 4, sample #2; 5, sample #3; 6, sample #4; 7, sample #5; 8, sample #6; 9, sample #7; 10, sample #8.

Figure 3.9

3.4: Z-DNA formation by *Z-form I in vitro*

gyl DNA (*BglI*(9)-*Sma*I(11)[1] fragment) containing *Z-form I* (see Figure 4.1), was subcloned from pJAM30 into pMT3000 (see Figure 4.5), and the resulting construct designated pJAM180. A range of topoisomers of pJAM180 were prepared using the same method described in section 2.15.2 with a range of concentrations of EtBr (data not shown). The topoisomers were pooled and analyzed by two-dimensional ChQ gel electrophoresis as described in section 2.16.2. Preliminary data presented in Appendix 3.10(a) shows the pattern of pJAM180 topoisomer migration under the conditions used. Appendix 3.10(b) depicts a migration pattern of topoisomers of a plasmid (electrophoresed under the same conditions as the gel in (a)), containing a *Z-form* DNA sequence, $(CG)_8$, that has adopted a left-handed conformation. From the gel in (a) it can be inferred that a σ of —0.031 is not enough for *Z-form I* to adopt a left-handed conformation, under the conditions used. The level of resolution by the 2D ChQ gel in Appendix 3.10(a) does not however, indicate the σ at which *Z-form I* would adopt such a conformation. Thus, the preliminary data suggest that the potential Z-DNA sequence upstream from *gyl*P1 (*Z-form I*), would not adopt a left-handed conformation *in vivo* unless the negative superhelical density was higher than 0.031.

---

[1]The numbers in parenthesis after the restriction enzymes refer to the restriction sites in Figure 2.5

3.5: Discussion

This chapter was mainly concerned with the study of how the superhelical density (σ) of pIJ486 varied under the culture conditions that are used for the exclusive production of methylenomycin. The growth medium incorporates an organic nitrogen source (alanine) and a high concentration of phosphate, with glucose as the principal carbon source; both liquid batch and surface grown cultures were studied. The plasmid samples isolated from these cultures were analyzed against the pIJ486 #1 standard (of known ΔLk), described in section 3.2.2, Figure 3.3.

The linking difference (ΔLk), of the pIJ486 standard was -38 ± 1.5, which is equivalent to a σ of -0.064 ± 0.002, under the conditions used for resolution of the topoisomers. However, the 1D ChQ gel electrophoresis was carried out at 8°C, and Keller (1975), demonstrated that a decrease in temperature increased the $-\sigma$ of plasmid DNA. To take into account the effect of temperature on DNA supercoiling the conversion factor to correct the ΔLk by determining the change in rotation angle of the DNA double helix due to temperature (—0.010°/°C/bp), was used (Duguet, 1993; Charbonnier and Forterre, 1994). This would equate (by extrapolation) to a difference of 3.8 supercoils in pIJ486 between 8°C and 30°C. Therefore, the estimated *in vivo* superhelical density of pIJ486 isolated from MT1110, cultured at 30°C in YEME + 10% sucrose, harvested in the late exponential phase would be -0.058 ± 0.002. This value, as expected, is among the higher levels of σ so far reported for eubacteria (+0.015 to —0.063; Charbonnier and Forterre, 1994). [*Streptomyces* DNA has a high G+C content (average ca.74 mol%; Gladek and Zakrzewska, 1984), and therefore requires a greater amount of energy to

unwind the double helix (in the binding of RNA polymerase for example), compared to *Bacillus* DNA which has a low G+C content.]

It should be noted that more than half of these supercoils could be sequestered by various histone-like proteins such as HU and H-NS (or H1a), (section 1.8.3), the unrestrained σ of pIJ486 could therefore be ca.—0.024. This assumption is used below, where the number of unrestrained supercoils is referred to. *Streptomyces* probably contain similar histone-like proteins as *E. coli*, since they package their DNA in similar sized nucleoids (Gumpert *et al.*, 1986). Any change in the ΔLk of pIJ486 by DNA topoisomerases only takes place within unrestrained DNA, and therefore has a much greater impact on supercoiling-sensitive reactions/interactions compared to protein free plasmids (see section 1.8).

The growth kinetics of the liquid batch cultures were generally reproducible; the exception was batch 3 which had a t_D of 7.1 h compared to an average 4.3 h for the other batch cultures. This was most likely due to some component(s) of the medium as it "foamed up" to a greater extent in batch 3 and subsequently more antifoam was added. This could have reduced the amount of dissolved O_2 in the medium and therefore slowed down the growth rate of the culture and increased the t_D (Crueger and Crueger, 1982).

Previous work by Hobbs *et al.* (1992), suggested that methylenomycin production began during the transition from exponential to linear growth kinetics and could be initiated by an acid-shock in the medium. However, in all the batch cultures studied only batch 2 (Appendix 3.5), underwent an acid-shock where the pH dropped to 5.74. The number of

potentially unrestrained supercoils increased during this period by ca.11%, but batch 1 (Appendix 3.4), underwent a similar change when the pH dropped to only 7.03. In batch 3 the pH did not drop below 6.9 (there was no pH plot available for batches 4 and 5). But, as there was no significant change in the variation of the σ of pIJ486 during the pH changes it would seem that pH does not affect methylenomycin production through changes in DNA supercoiling, at least under these growth conditions.

From the results described in section 3.3.1, the variation in the σ of the pIJ486 samples harvested during mid exponential to stationary phase did not change significantly from batch to batch. The initial σ was -0.069 ± 0.002, which, corrected to 30°C, would be equivalent to -0.063 ± 0.002 *in vivo*. This would represent an unrestrained σ of ca.-0.026 which varied by $\pm$ 11% during exponential growth of batches 1-4 (see, e.g., Figure 3.5). The σ was also independent of the growth rate of MT1110(pIJ486), e.g., see batches 1 and 2 (Appendices 3.4 and 3.5), compared to batch 3 (Figure 3.5). This observation supports similar results found for the σ of plasmid DNA isolated from *E. coli*(pBR322) (Balke and Gralla, 1987). Additionally, there was no significant effect of thiostrepton on the σ of pIJ486; see batch 5 (Appendix 3.6). Although towards the end of exponential growth the σ of the unrestrained supercoils dropped by 17% within 1.5 h, it regained the supercoils 1.3 h later.

In *E. coli* it was found that the σ of plasmids decreased dramatically when the host was subjected to nutrient starvation (Balke and Gralla, 1987). In *Streptomyces* however, such a loss of supercoils could conceivably interfere with transcription of secondary or stationary phase metabolic genes. Interestingly then, a relatively high $-\sigma$ was maintained

into early stationary phase during the growth of *S. coelicolor* (see, e.g., Figure 3.5). This would be consistent with the findings, described in section 1.4, that antibiotic production by *S. coelicolor* A3(2) is regulated at the transcriptional level. If the DNA began to lose negative supercoils like *E. coli* (e.g., ca.40% of unrestrained supercoils lost within a few hours; Balke and Gralla, 1987), there may not be sufficient transcription of global regulators, e.g., *absA* and *absB*, or the specific activator genes (e.g., *act*II-ORF4; *redD*), for expression of the biosynthetic genes, or even the biosynthetic genes themselves.

Later, in the stationary phase, a bimodal distribution of topoisomers in the liquid batch cultures 1 and 3 was noted (see, e.g., Figure 3.6). This unusual distribution seemed to coincide with a resumption of growth; the CO_2 output had started to fluctuate, possibly as a result of fresh nutrients made available by mycelial lysis. Another explanation for the bimodal distributions could be the heterogeneous, pelleted nature of the culture (the Junlon did not completely overcome the tendency of the culture to pellet). As there would have been differing levels of nutrients and O_2 within such a pellet this could have caused plasmids isolated from the centre of a pellet to have a different σ to plasmids isolated from the actively growing mycelia. Changes in O_2 concentration have been shown to effect the σ of plasmids, probably by interfering with the ATP/ADP ratio and hence DNA gyrase activity (section 1.8.3). This could also explain why not all of the topoisomers within each plasmid sample comprised a normal distribution. A bimodal distribution of topoisomers was also reported in samples of pBR322, isolated from *E. coli* host cells after prolonged starvation, which suggests that re-growth maybe the reason for the bimodal distribution as *E. coli* cultures are physiologically homogeneous.

The results from the surface grown cultures also demonstrated that the growth kinetics of the culture and the pH of the medium had little or no effect on the $-\sigma$ of pIJ486 (see Figure 3.7). The surface grown cultures grew more slowly than the majority of the liquid batch cultures, with average t_D of 6.3 h and 4.3 h (not including batch 3), respectively. The most significant difference between the liquid and surface grown cultures was the maintenance of the $-\sigma$ of pIJ486 in stationary phase. The $-\sigma$ was maintained for over 48 h with the loss of only ca.11% of potentially unrestrained supercoils once the culture entered stationary phase (Appendix 3.7). Neither of the two surface grown cultures showed evidence of bimodal distributions of topoisomers in any of the pIJ486 samples. This was even though mycelium from experiment 1 had started to lyse (data not shown), from around 106 h. It is possible that the phenomenon was dependant on suspended growth.

Interestingly, during the transition to aerial hyphae formation both cultures showed an increase of ca.12-19% in the potentially unrestrained σ of pIJ486 (see, e.g., Figure 3.7). This represented the greatest change in σ in all of the cultures studied in this work. This corresponded with a stalling in the growth of each culture which is associated with the solubilization of macromolecules such as glycogen, potentially to provide osmotic pressure to drive the formation of aerial hyphae (reviewed by Chater, 1993). Changes in osmotic pressure have been suggested to alter the σ of DNA (section 1.8.5). Thus, the observed change in $-\sigma$ of pIJ486 could be as a result of increased osmolarity in the mycelia, this is further discussed in Chapter Five. The genetics involved in the formation of aerial hyphae are not yet fully understood but temporal transcription of *bldA* has been suggested to be involved (Leskiw *et al.*, 1993). *bldA* encodes the rare $tRNA_{UUA}$ and the

TTA codon has been found mainly in genes expected to be expressed late in the growth of the organism; for example, the activator gene required for *act* expression, *act*II-ORF4. *bldA* was thought to be temporally regulated, with the appearance of active $tRNA_{UUA}$ delayed until stationary phase (Leskiw *et al.*, 1993). However, work by Gramajo *et al.* (1993), demonstrated the presence of active $tRNA_{UUA}$ during early stages of growth (section 1.4.2). Both groups agree however, that the $tRNA_{UUA}$ transcript is present in early cultures; this rules out any involvement of the changes in σ described above in the regulation of *bldA* transcription; at least under the conditions described in this study.

The observed changes in the superhelical density of pIJ486 (maximum 19% increase), may suggest a role for DNA supercoiling in the global regulation of secondary metabolism. Changes of 15-30% in the level of supercoiling have been shown to have significant effects on transcription *in vitro* (Borowiec and Gralla, 1985; Brahms *et al.*, 1985). Global antibiotic regulatory genes, such as *absA* and *absB*, may be targets for regulation, mediated through DNA supercoiling, in response to morphological and/or environmental changes.

Preliminary data, see Appendix 3.10(a), would seem to indicate that the potential *Z*-DNA forming sequence upstream from *gyl*P1 (*Z-form I*), is unlikely to adopt a left-handed conformation under physiological conditions. Assuming an unrestrained superhelical density of —0.03 for pIJ486 *in vivo* (see above), and the evidence that *Z-form I* is unlikely to adopt a *Z*-DNA conformation at a superhelical density that low (see section 3.4), probably rules out a role for *Z-form I Z*-DNA in the unconditional repression of *gyl*P1/P2 when plasmid-borne on pIJ486, but see Chapter Four.

This study did not attempt to assign a specific positive or negative role for DNA supercoiling in antibiotic production or development in *Streptomyces*. It was undertaken firstly to determine the σ of a *Streptomyces* plasmid and secondly, to study how variations in environmental conditions altered the superhelical density of the plasmid. The results reported here may or may not reflect how the topology of the chromosome is altered under these conditions. However, these results do not demonstrate that changes in the environment alter DNA supercoiling and that these changes in supercoiling then regulate gene expression. Supercoiling may be a passive response to any or all of the conditions described in this study.

Chapter Four

Results II: Studies on the potential *Z*-DNA forming sequences found in the glycerol operon

4.1: Introduction

Earlier work showed that when *gylR-gyl*P1/P2 is displaced from its usual chromosomal location, on a multicopy plasmid, the vector-borne *gyl* promoters are not expressed normally (C.P. Smith, personal communication). On the multicopy promoter-probe vectors, pIJ425 and pIJ486, *gyl*P1/P2-containing fragments were expressed at a moderate constitutive level. However, when *gylR* was contiguous with *gyl*P1/P2 (*Bcl*I(1-13)[1] and *Sph*I(2)-*Kpn*I(12) fragments) on the plasmids, transcription from vector-borne *gyl*P1/P2 was effectively zero even in the presence of glycerol. These results were unexpected since, under these conditions, chromosomal *gyl*P1/P2 transcription is induced 60-fold (Smith and Chater, 1988b). This unexpected regulation of vector-borne *gyl*P1/P2 has been termed "unconditional repression". This unconditional repression was thought to be unusual when this project was started; GylR appeared to be the transcriptional activator of *gyl*P1/P2 (see section 1.7). However, it has since been found that the role of GylR, with respect to the *gyl* operon, is to repress transcription (section 1.7.1; Hindle and Smith, 1994). Interestingly, when a frameshift mutation was introduced into the vector-borne

---

[1]The numbers in parenthesis after restriction enzymes refer to the restriction sites shown in Figure 2.5.

gylR (*gylR10*) *gyl*P1/P2 expression on the plasmid was found not only to be derepressed but to be 3-fold higher than that from vector-borne *gyl*P1/P2 alone. This finding suggested that it was possible that *cis*-acting sequences, within the *gylR-gyl*P1/P2 fragment, as well as GylR, were involved in the unconditional repression of vector-borne *gyl*P1/P2.

What causes this unconditional repression? Does the topology of the plasmid contribute to aberrant binding by GylR? Is the unconditional repression due to specific *cis*-acting sequences downstream or upstream of *gyl*P1/P2?

As mentioned in section 1.7.1, there are potential *Z-form* DNA sequences upstream from *gylR*p and *gyl*P1/P2 (see Figure 4.1). It has been suggested that these regions could be capable of adopting a Z-DNA conformation under physiological conditions (M.J. McLean, personal communication to C.P. Smith; J. McClellan, personal communication). The topology of pIJ486 was investigated in Chapter Three and the results indicate that pIJ486 has a high negative superhelical density in *S. coelicolor* MT1110 (section 3.3.2.2). With values as high as —0.073, Z-DNA formation, especially when assisted by transcription mediated supercoiling, was considered possible, but see section 3.5 and Chapter Five. The adoption by the *Z-form* sequences of left-handed Z-DNA structures could significantly interfere with transcription from *gyl*P1/P2; *Z-form I* overlaps the —35 region of *gyl*P1. Therefore, perhaps Z-DNA formation could contribute to the observed unconditional repression.

In order to investigate the role of these potential *Z-form* sequences, they were disrupted

Figure 4.1: The *gylR* and *gylCABX* promoter regions showing the potential *Z*-DNA sequences

The potential *Z*-DNA sequences are indicated in boldface and are separated from the sequences on either side by one space. The mutagenic oligonucleotide sequences (lower case) are aligned above their respective complementary regions; capitalised bases indicate site specific changes introduced to disrupt the purine-pyrimidine alternation of the wild-type sequence or to generate new restriction sites. The new restriction sites are indicated above the relevant oligonucleotide. The —10 and —35 regions of *gylR*p, *gyl*P1 and *gyl*P2 are underlined and the transcription start-sites are indicated by "»"; DNA sequences are numbered relative to the start-sites of *gylR*p and *gyl*P1 respectively.

Figure 4.1:

(a) *gylR* promoter region:

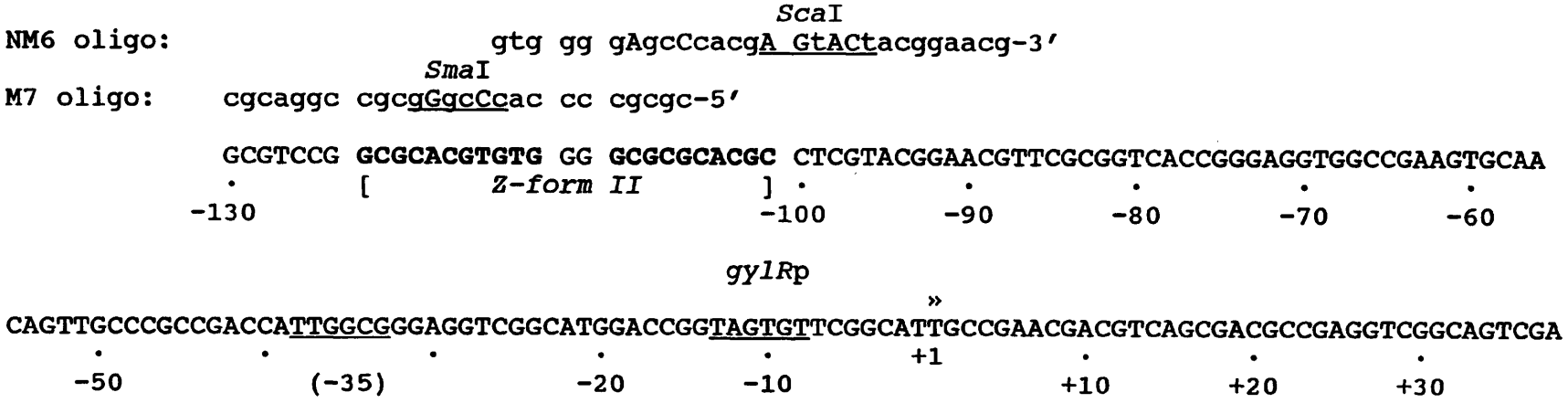

(b) *gylCABX* promoter region:

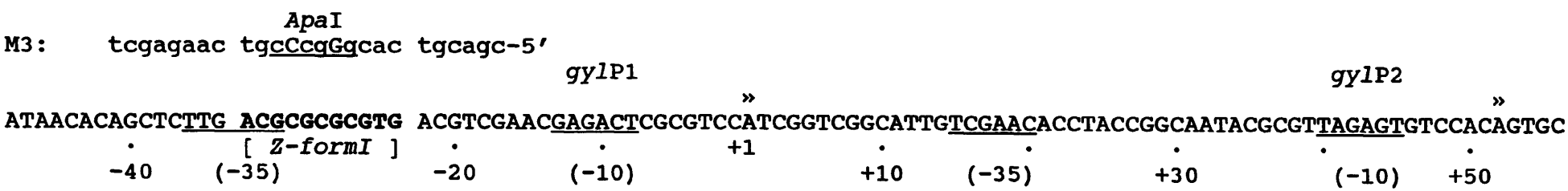

by oligonucleotide-directed mutagenesis. The effect of the mutations on promoter expression was analyzed using transcriptional fusions to the *neo* reporter gene of pIJ486. The effect of the potential *Z-form II* sequence upstream of *gylR*p on the divergent promoter of the *metH* homologue (Paget, 1994), was also studied.

In the earlier work, the sequence downstream of *gyl*P1/P2, on the *Cla*I(10)-*Bcl*I(13), *Bcl*I(1-13) and *Sph*I(2)-*Kpn*I(12) fragments that were used, contained the RBS of *gylC*. It is possible that the RBS could interfere with translation of the *neo* transcript in the following manner: when transcribed, the 5' leader of the *neo* mRNA would include the RBS of *gylC* which may interfere with the translation of the downstream reporter gene. The translation initiation region of *gylC* is very well conserved between *Streptomyces* spp. and could therefore have important regulatory functions (Paget, 1994). Thus, the inclusion of the additional downstream *gyl* DNA could significantly interfere with expression of *gyl*P1/P2. The 5' ends of the *neo* mRNAs were also different in two of the above constructs, therefore processing of the mRNA may have been affected. This alone however, would not account for the virtually undetectable expression of vector-borne *gyl*P1/P2 in the *Bcl*I(1-13) and *Sph*I(2)-*Kpn*I(12) fragments; the *Cla*I(10)-*Bcl*I(13) fragment, containing *gyl*P1/P2 alone, gave 15-45 μg/ml Km^R. In this study the *gyl* DNA fragments were recloned such that each downstream insert-vector junction was identical. In each case the *gyl* DNA was fused to *neo* at *Sma*I(11), 52 bp from *gyl*P2; thus, no RBS or *gyl* coding sequence was present, avoiding any possibility of translational interference. Expression of the mutant constructs was examined in five different strains to determine any background effects due to host specific factors.

4.2: Mutagenesis of the potential *Z*-DNA sequences

The potential *Z*-DNA sequence upstream from *gyl*P1, *Z-form I* (see Figure 4.1), was subcloned from pIJ2211 into the unique *Sma*I site of pMc to generate pJAM10, and the potential *Z*-DNA sequence upstream from *gylR*p, *Z-form II* (see Figure 4.1), was also subcloned into the *Sma*I site of pMc to generate pJAM20 as described in Figure 4.2.

To disrupt the *Z*-DNA sequences three mutagenic oligonucleotides were designed that interrupted the alternating purine-pyrimidine nature of the sequences but did not alter the spacing of each region. Restriction sites were incorporated in the oligonucleotides as markers for each mutation. Using the oligonucleotide-directed mutagenesis method described in section 2.9, one marker was introduced into *Z-form I*, pJAM11, and two markers were introduced into *Z-form II*, pJAM23, as shown in Figure 4.2.

4.2.1: Screening of pJAM11, pJAM21 and pJAM23 for mutations

The *gyl*P1/P2 region of pJAM10, pJAM11 and the *gylR*p regions of pJAM20, pJAM21 and pJAM24 (mutagenised in *Z-form II* only; see Table 2.2) containing the desired restriction site markers were sequenced (Figure 4.3); pJAM23 was also sequenced (data not shown). This confirmed that *Z-form I* and *Z-form II*, in the respective plasmids, were disrupted and no undesired mutations had been introduced into the segment of *gyl* DNA that was subsequently cloned into the promoter-probe constructs (section 4.4).

Figure 4.2: Subcloning and mutagenesis of the potential *Z*-DNA regions of *gyl*

Step 1. pIJ2211 was digested with *Sma*I and then *Pvu*II, the two *gyl* fragments (*Pvu*II(7)-*Sma*I(11), *Z-form I*; *Sma*I(4)-*Pvu*II(7), *Z-form II*) were gel purified and ligated (separately), into dephosphorylated *Sma*I-digested pMc; the ligation mix was used to transform *E. coli* WK6 (*su*$^-$). Clones were isolated that contained the *gyl* DNA transcribing into the *fd* terminator of pMc (the α-orientation); phasmid containing truncated *gylR-gyl*P1/P2 was designated pJAM10, and phasmid containing *gylR*p designated pJAM20.

Step 2. Single-stranded DNA of pJAM10 and pJAM20 was prepared as described in section 2.9. pMa was digested with *Eco*RI and *Hin*dIII and the 3.77 kb pMa backbone fragment was gel purified. The pMa backbone fragment was annealed to the ss pJAM10 and pJAM20 DNA as described (section 2.9), to form gdDNA. The mutagenic oligo M3 was hybridised to the gdDNA of pJAM10 and oligo M7 to the gdDNA of pJAM20.

Step 3. gd pJAM10 was filled-in with PolIk and T4 DNA ligase and used to transform *E. coli* WK6*mutS*; transformants were selected for ampicillin resistance. After overnight growth, phasmid was isolated, checked for the presence of the new *Apa*I site and segregated in WK6 (see section 2.9). A phasmid containing the new *Apa*I site was designated pJAM11.

Step 4. gd pJAM20 was filled-in and segregated as above. A phasmid containing the new *Sma*I site was designated pJAM21.

Step 5. To incorporate the second mutant NM6 oligo into pJAM21 the *gyl* DNA from pJAM21 was first recloned in the opposite orientation to that of pJAM20 and designated pJAM22. pJAM22 was then mutagenised as described above and in section 2.9. A phasmid containing the new *Sca*I site was designated pJAM23.

NB. The respective plasmids are drawn to different scales and not all the restriction sites are shown.

Figure 4.2

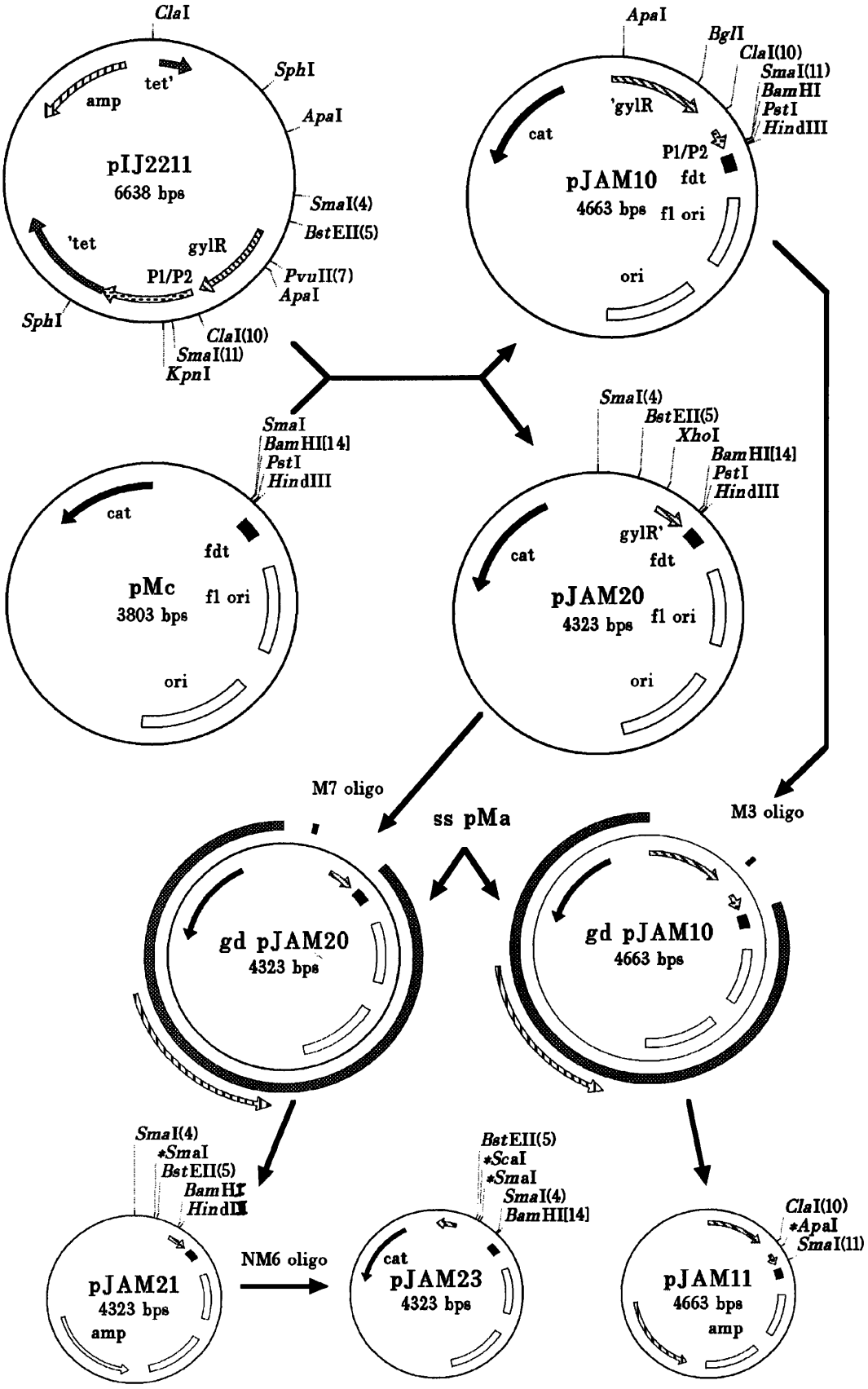
ClaI
SphI
ApaI
SmaI(4)
BstEII(5)
PvuII(7)
ApaI
ClaI(10)
SmaI(11)
KpnI
SphI
tet'
amp
pIJ2211
6638 bps
'tet
gylR
P1/P2
ApaI
BglI
ClaI(10)
SmaI(11)
BamHI
PstI
HindIII
'gylR
cat
P1/P2
pJAM10
fdt
4663 bps
f1 ori
ori
SmaI
BamHI[14]
PstI
HindIII
cat
fdt
pMc
3803 bps
f1 ori
ori
SmaI(4)
BstEII(5)
XhoI
BamHI[14]
PstI
HindIII
gylR'
cat
fdt
pJAM20
4323 bps
f1 ori
ori
M7 oligo
ss pMa
M3 oligo
gd pJAM20
4323 bps
gd pJAM10
4663 bps
SmaI(4)
*SmaI
BstEII(5)
BamHI
HindIII
BstEII(5)
*ScaI
*SmaI
SmaI(4)
BamHI[14]
ClaI(10)
*ApaI
SmaI(11)
pJAM21
4323 bps
amp
NM6 oligo
cat
pJAM23
4323 bps
pJAM11
4663 bps
amp

Figure 4.3: Sequence of wild-type and mutant *Z-form* regions

(a) pJAM10: sequence showing the wild-type *Z-form I* region.

(b) pJAM11: sequence showing disruption of alternating purine-pyrimidines of the *Z-form I* region.

(c) pJAM20: sequence showing the wild-type *Z-form II* region.

(d) pJAM21: sequence showing disruption of *Z-form II* by oligo M7.

(e) pJAM24: sequence showing disruption of *Z-form II* by oligo NM6.

Figure 4.3

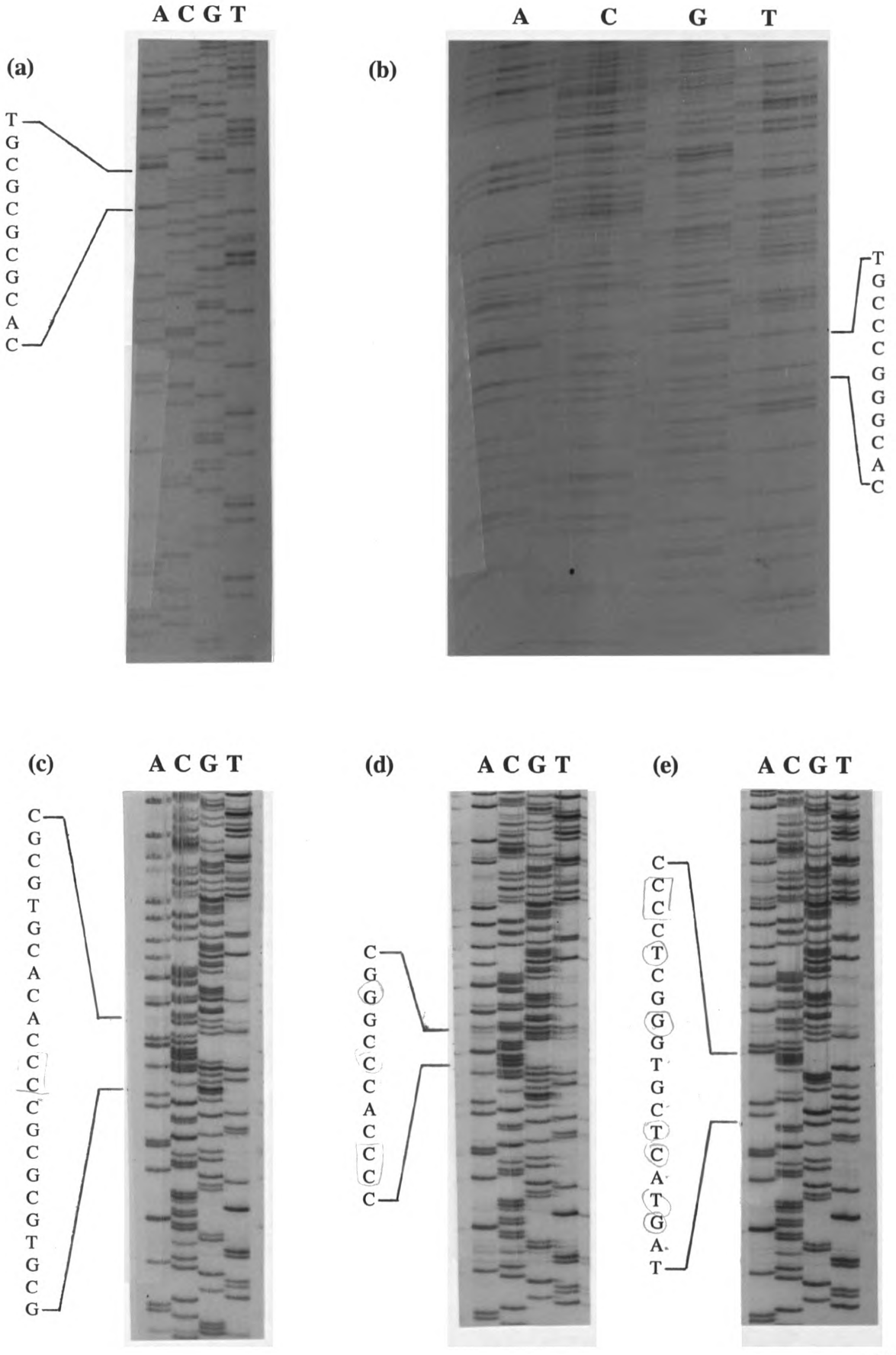
A C G T
(a)
T
G
C
G
C
G
C
G
C
A
C
A C G T
(b)
A C G T
(c)
C
G
C
G
T
G
C
A
C
A
C
C
C
C
G
C
G
C
G
T
G
C
G
A C G T
(d)
C
G
G
G
C
C
C
A
C
C
C
C
A C G T
(e)
C
C
C
C
T
C
G
G
G
T
G
C
T
C
A
T
G
A
T

4.3: Subcloning of the *gyl* promoter fragments into pMT3000

The plasmid, pMT3000, was used as an intermediate cloning vector, since *gyl* DNA could then be removed as a *Bgl*II fragment and cloned directly into pIJ486. As mentioned earlier, the original promoter-probe constructs contained DNA fragments, which included the RBS of *gylC*, with different insert-vector junctions. The various *gyl* promoter fragments were therefore recloned (described in Figure 4.4), such that the sequence downstream of *gylR*p and *gyl*P1/P2 was known, and it contained no structural features which could be predicted to interfere with expression of *gyl*P1/P2.

4.4: Reconstitution of the *Z-form* mutations into pSK2.3, pJAM30 and pJAM40

4.4.1: *Z-form I* mutation

pJAM11 (Figure 4.2), was used to transform *E. coli* GM33 and the *Z-form I* mutation was excised as a 0.2 kb *Cla*I-*Sma*I fragment, gel purified, and subcloned into pSK2.3 (Figure 2.4), as a direct replacement of the wild-type *Cla*I(10)-*Sma*I(11) region. This involved a triple ligation since partial *Sma*I digestion of pSK2.3 always resulted in the left-most *Sma*I(4) site (Figure 4.4), being cleaved first. To this end GM33-propagated pSK2.3 plasmid was digested to completion first with *Cla*I and then with *Sma*I. The 3.6 kb *Sma*I backbone fragment, containing the vector, and the 1.2 kb *Sma*I(4)-*Cla*I(10) fragment were recovered separately by gel purification; the 3.6 kb backbone fragment was then dephosphorylated with CIAP prior to the ligation. Initially the mutant *Cla*I-*Sma*I fragment was ligated with the 1.2 kb *Sma*I(4)-*Cla*I(10) fragment from pSK2.3 and the

Figure 4.4: *S. coelicolor* promoter fragments used in this study

pSK2.3: 2.3 kb *Sph*I(2)-*Kpn*I(12) fragment subcloned into pIJ2925. Boxed regions marked by right-slanting lines indicate *gylR*, *t* indicates the *gylR* terminator and boxed regions marked by dashed lines indicate *gyl*P1/P2. Arrows indicate the direction of transcription from *gylR*p and *gyl*P1/P2.

pSK2.3(*gylR10*): Frameshift mutation introduced into pSK2.3 at the *Xho*I(6) site as a 4 bp deletion, resulting in the loss of the *Xho*I site (indicated by "*F").

pJAM30: 1.4 kb *Sma*I(4-11) fragment from pSK2.3 subcloned into the *Sma*I site of pMT3000, see polylinker region indicated at the bottom of the figure. The orientation has *gyl*P1/P2 transcribing in the direction of the *Hin*dIII site in the polylinker.

pJAM35: *Sma*I fragment from pSK2.3(*gylR10*) subcloned into the *Sma*I site of pMT3000, in the same orientation as pJAM30.

pJAM40: The 0.2 kb fragment containing *gyl*P1/P2 was isolated by PCR (see Notes) and incorporates an *Eco*RI site to the left of *Cla*I(10) that enabled the fragment to be subcloned into the unique *Eco*RI and *Sma*I sites of pMT3000, in the same orientation as pJAM30. "Z-DNA II" indicates the *Z-form II* region from Figure 4.1.

Notes:

The original wild-type *Sph*I(2)-*Kpn*I(12) fragment cloned in pSK2.3 was isolated from pIJ2211, which contains the *BclI*-*BclI* fragment from *S. coelicolor* M138 (Smith and Chater, 1988a).

The equivalent fragment containing a frameshift mutation in *gylR* (*gylR10*), was generated from pSK2.3; it contains a 4 bp deletion at the *Xho*I(6) site (Paget *et al.*, 1994).

The [*Eco*RI]*Cla*I(10)-*Sma*I(11) fragment was a PCR product, sequenced and proved to be identical to the wild-type *S. coelicolor* sequence (Paget *et al.*, 1994).

The arrow below the pMT3000 polylinker region indicates the direction of transcription of the *lac* promoter.

Figure 44

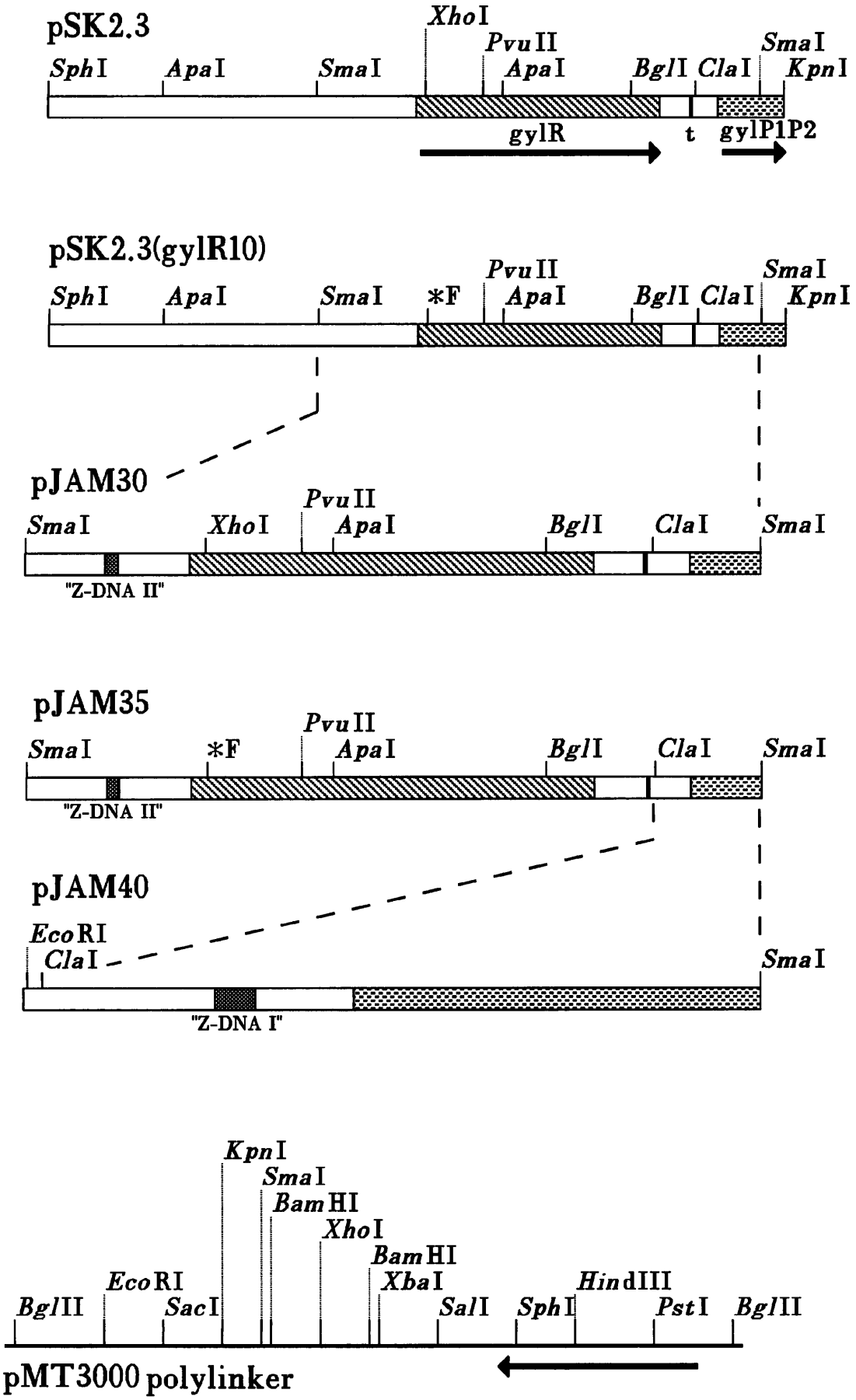
pSK2.3
XhoI
PvuII
SmaI
SphI
ApaI
SmaI
ApaI
BglI
ClaI
KpnI
gylR
t
gylP1P2
pSK2.3(gylR10)
PvuII
SmaI
SphI
ApaI
SmaI
*F
ApaI
BglI
ClaI
KpnI
pJAM30
PvuII
SmaI
XhoI
ApaI
BglI
ClaI
SmaI
"Z-DNA II"
pJAM35
PvuII
SmaI
*F
ApaI
BglI
ClaI
SmaI
"Z-DNA II"
pJAM40
EcoRI
ClaI
SmaI
"Z-DNA I"
KpnI
SmaI
BamHI
XhoI
BamHI
XbaI
HindIII
EcoRI
BglII
SacI
SalI
SphI
PstI
BglII
pMT3000 polylinker

resultant fragments of 1.4 kb were gel purified. These fragments were then ligated with the 3.6 kb *Sma*I backbone fragment and used to transform *E. coli* CS1. A recombinant plasmid with the correct restriction pattern was chosen and designated pJAM50 (Figure 4.5(a & b)). The 1.4 kb *gyl Sma*I fragment was excised from pJAM50 and subcloned into dephosphorylated *Sma*I-digested pMT3000, a clone with the same orientation as pJAM30 (Figure 4.4), was designated pJAM60, (Figure 4.5(c)). The same 0.2 kb *Cla*I-*Sma*I fragment from pJAM11 was used to replace the *Cla*I(10)-*Sma*I(11) fragment of pJAM40 (Figure 4.4). A recombinant plasmid containing the new *Apa*I site was designated pJAM65.

4.4.2: *Z-form II* mutation

The *Z-form II* mutation in pJAM23 (Figure 4.2), was excised as a *Bst*EII(5)-*Bam*HI[14] 0.2 kb fragment (the *Bam*HI end was blunt-ended with PolIk) and gel purified. pJAM30 and pJAM60 (Figure 4.5(c)), were digested with *Eco*RI, blunt ended with PolIk, digested with *Bst*EII and dephosphorylated. The 0.2 kb fragment, containing the *Z-form II* mutation, was ligated with the resulting backbone fragments of pJAM30 and pJAM60 and used to transform CS1. Plasmid containing the *Z-form I* and *Z-form II* mutations was designated pJAM80, and plasmid containing wild-type *Z-form I* and the *Z-form II* mutations was designated pJAM100. Plasmid maps of these constructs are shown in Figure 4.6(a) and (b), respectively.

Figure 4.5: Restriction analysis of pJAM50 (*Z-form I* mutant) and the restriction map of pJAM60

(a): Agarose gel electrophoresis of pSK2.3 and pJAM50 showing presence of the new *Apa*I site

Electrophoresis was carried out with 0.8% agarose (w/v) in 1 X TBE buffer at 3 V/cm for ca.3 h. All samples were cut with *Apa*I unless otherwise indicated. Lanes: 1, λ *Hin*dIII marker; 2, pSK2.3 uncut; 3, pSK2.3; 4, sample 1; 5, pJAM50; 6, sample 3; 7, sample 4; 8, sample 5; 9, pJAM51; 10, λ *Hin*dIII marker.

Notes:
1. **pSK2.3** digested with *Apa*I yields two fragments, 3.9 and 1.06 kb in size.
2. **pJAM50** digested with *Apa*I yields three fragments, 3.2, 1.06 and 0.7 kb in size.
3. If the 1.4 kb *Sma*I(4-11) fragment had ligated in the opposite orientation this would result in three fragments, 3.66, 0.7 and 0.64 kb in size.

From the restriction pattern of samples in lanes 5 and 9 it was clear that the mutant *Z-form I* region had been successfully cloned.

(b): Restriction map of pJAM50

"*" indicates new *Apa*I site (*Z-form I* mutation).

(c): Restriction map of pJAM60 [and pJAM30]

Note the orientation of the *gyl* DNA is opposite to that in pJAM50. The new *Apa*I site is indicated with "*". [pJAM30] refers to a restriction map lacking the new **Apa*I site; i.e. it would represent the wild-type, pJAM30, restriction map if the **Apa*I site was not shown.

Figure 4.5

(a)

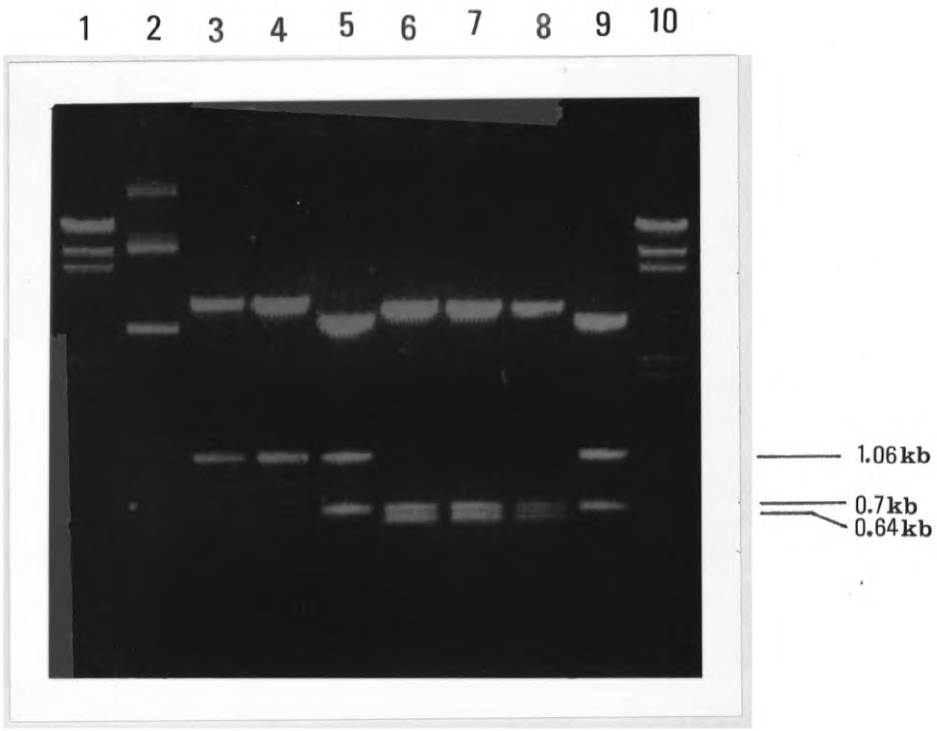

(b)

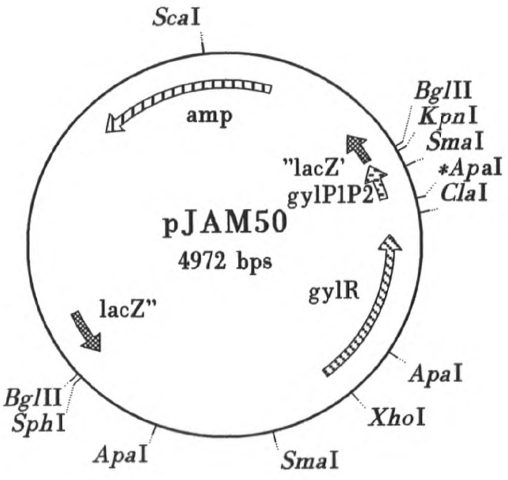

(c)

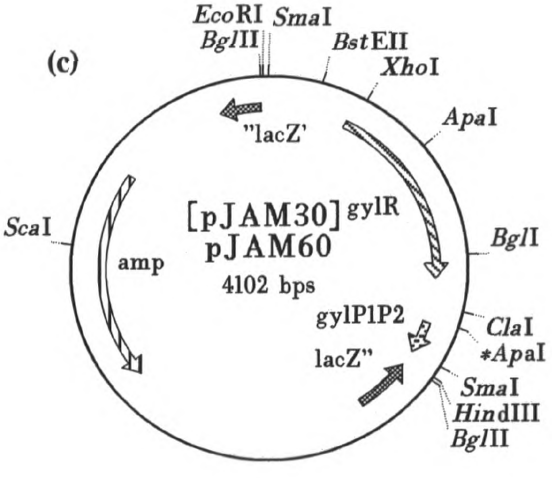

Figure 4.6: Plasmid maps of pJAM80 and pJAM100

(a): pJAM80

Restriction sites used in the construction (see text) are detailed; the three restriction sites indicating disruption of *Z-form I* and *Z-form II* are shown, prefixed with "*".

(b): pJAM100

Restriction sites used in the construction (see text) are detailed; the two restriction sites indicating disruption of *Z-form II* are shown, prefixed with "*".

Figure 4.6

(a)

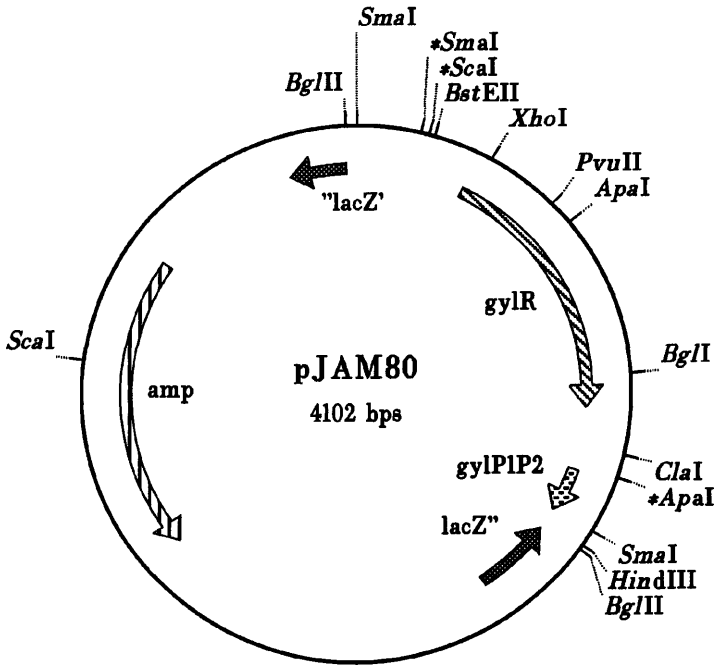
SmaI
*SmaI
*ScaI
BstEII
XhoI
PvuII
ApaI
BglII
"lacZ'
gylR
ScaI
amp
pJAM80
4102 bps
BglI
gylP1P2
ClaI
*ApaI
lacZ"
SmaI
HindIII
BglII

(b)

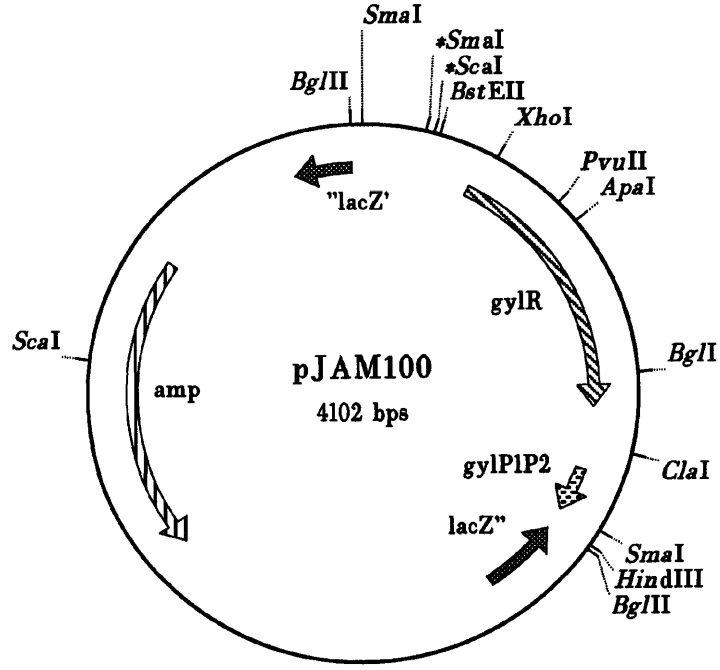
SmaI
*SmaI
*ScaI
BstEII
XhoI
PvuII
ApaI
BglII
"lacZ'
gylR
ScaI
amp
pJAM100
4102 bps
BglI
gylP1P2
ClaI
lacZ"
SmaI
HindIII
BglII

4.5: Sub-cloning of the wild-type and mutant *gyl* DNA fragments into the promoter-probe vector pIJ486

For ease of construction, the *gyl* DNA fragments were excised as *Bgl*II fragments (see, e.g., Figure 4.6), and ligated non-directionally into the *Bgl*II-digested backbone fragment of pIJ486, for subsequent screening in *Streptomyces*. The ligation mixes were used to transform *S. lividans* 1326. When *gyl*P1/P2 is transcriptionally fused to the *neo* gene of pIJ486, this is termed the α-orientation, whereas the opposite orientation is referred to as the β-orientation. Both orientations were obtained for each fragment and the respective plasmids were designated pJAM110 to 151 (see, e.g., Figure 4.7 and Table 2.2 for details). Different *Streptomyces* strains were transformed with each plasmid.

4.6: Analysis of the *gyl* promoters in pIJ486

The use of *S. coelicolor* MT1101 was discontinued at an early stage since it was impossible to determine activity levels for *gyl*P1/P2 before rearrangements and/or recombination occurred (see section 4.8.3), due to the presence of SCP1. The use of *S. lividans* TK24 was also discontinued at an early stage; the wild-type *S. lividans* 1326, was used in preference.

Expression of *gyl*P1/P2 (the α-orientation), in the various constructs conferred kanamycin resistance (Km^R) to the host strain. Km^R was determined either by patch plates or gradient plates as described in section 2.17. The results obtained with the various fusions

Figure 4.7: pJAM112, pJAM135 and pJAM150 promoter-probe constructs in pIJ486

(a) pJAM112: 2.3 kb *Bgl*II fragment from pJAM50 (*Z-form I* mutant) was used to replace the *Bgl*II polylinker fragment of pIJ486. When *gyl*P1/P2 is transcriptionally fused to the *neo* gene (as shown) the *gyl* DNA is in the α-orientation; when the reverse is true, and *metHp* is fused to the *neo* gene the *gyl* DNA is in the β-orientation (see Table 2.2). The new *Apa*I site is prefixed with "*".

(b) pJAM135: 1.48 kb *Bgl*II fragment from pJAM80 (*Z-form I* and *II* double mutant) was used to replace the *Bgl*II polylinker fragment of pIJ486. The construct shown is in the α-orientation and the new restriction sites are prefixed with "*".

(c) pJAM150: 0.28 kb *Bgl*II fragment from pJAM65 (*Z-form I* mutant) was used to replace the *Bgl*II polylinker fragment of pIJ486. The construct shown is in the α-orientation and the new *Apa*I site is prefixed with "*".

Figure 4.7

(a)

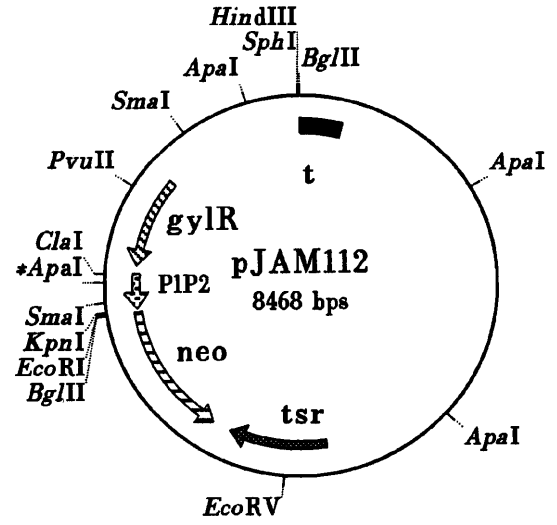

(b)

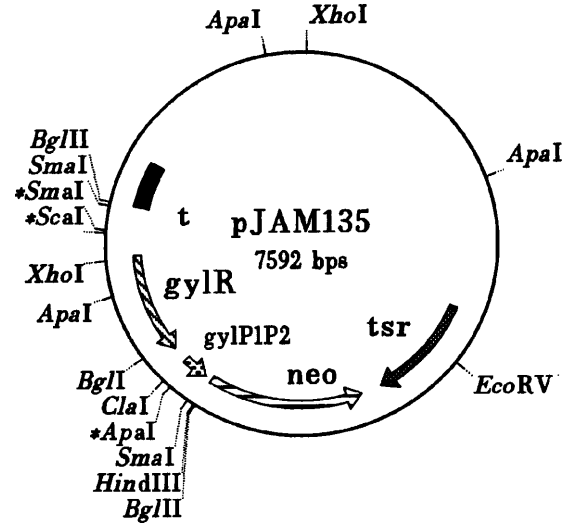

(c)

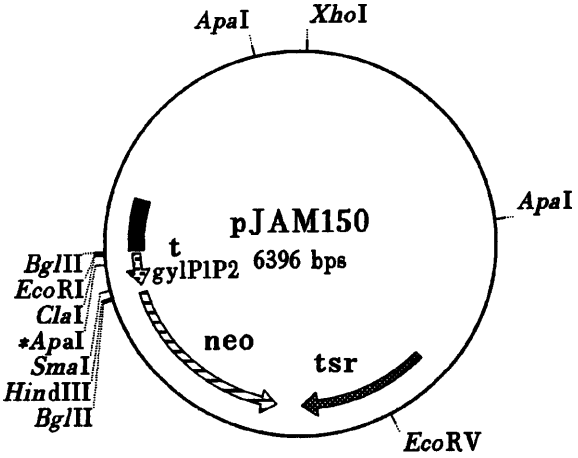

in a variety of host strains are presented in Table 4.1. An example of the gradient plate assay for the 1326Δ*gylR1* host is presented in Appendix 4.1.

The carbon source used in the experiments presented in Table 4.1 was glycerol. It has consistently been shown that expression of *gyl*P1/P2, on a multicopy plasmid, is carbon source independent (when *gyl*P1/P2 is fused to *neo* (data not shown), or *xyl*E, the reporter gene of pMSP1060 (Paget, 1994)).

As can be seen from Table 4.1, *gyl*P1/P2 alone (pJAM130) gave an average Km^R across all the strains (except MT1101) of ca.104 ± 21 μg/ml, but with *gylR* upstream (pJAM110, *Sph*I(2)-*Kpn*I(12) fragment) resistance was virtually zero in strains 1326 and TK24. However, when the *gylR-gyl*P1/P2 region was recloned as the *Sma*I(4-11) fragment (pJAM120) the average Km^R was ca.104 ± 6 μg/ml in all strains tested. The main difference between pJAM110 and pJAM120 was the presence of the RBS and amino terminal coding sequences of *gylC* in the *gyl* DNA which would be fused to the 5' end of the *neo* coding sequence. In contrast, the *gylR10* mutations (pJAM115 and pJAM125) showed resistance levels of ≥300 μg/ml in all the host strains studied regardless of the presence or absence of additional 5' *gyl* sequences. [It should be noted that in another study (e.g. Paget, 1994; Paget *et al.*, 1994), *gyl*P1/P2 expression from the "*Sma*I(4-11)" fragment was undetectable using *neo*, *mel* and *xylE* fusions; note: the *xylE* fusion data were not reproducible. However, in this case the "*Sma*I" fragment had been altered, with ca.10 bp additional sequence being introduced. The *gyl* insert-vector junction sequences were also different, therefore these results may not be directly comparable with the present study.]

Table 4.1: Analysis of the promoter-probe constructs fused to the *neo* gene of pIJ486

Fusion[1]	*gylR*[2]	*Z-form* mutant	Kanamycin resistance (μg/ml)				
			1326[3]	TK24[4]	MT 1101[3]	MT 1110[5]	1326Δ*gylR1*[6]
pJAM130	NO	wt.[7]	90	125	57	103	100
pJAM150	NO	*I*	80	109	300	104	100
pJAM110	YES	wt.	1	0	30	ND[8]	ND
pJAM112	YES	*I*	<10	0	29	ND	ND
pJAM115	*gylR10*	wt.	≥300	ND	ND	ND	ND
pJAM120	YES	wt.	110	ND	ND	102	101
pJAM135	YES	*I, II*	100	ND	ND	279	≥300
pJAM140	YES	*I*	75	ND	ND	230	223
pJAM145	YES	*II*	300	ND	ND	260	≥300
pJAM125	*gylR10*	wt.	≥300	ND	ND	≥300	≥300
pIJ486	/	/	<10	<10	<10	12	8

Notes:

1: All the constructs were in the α-orientation (see Table 2.2 for a detailed explanation of the plasmid fusions and Figures, where available).
2: "YES" indicates the presence of *gylR* upstream of *gyl*P1/P2; "*gylR10*" indicates a frameshift mutation in *gylR*.
3: Average of 4 independent isolates.
4: Average of 8 independent isolates.
5: Average of 6 independent isolates.
6: Average of at least 6 independent isolates.
7: "wt." indicates wild-type *Z-form*.
8: "ND" indicates not determined.

When the *Z-form I* region of *gyl*P1/P2 was disrupted (pJAM150) there was no significant difference in the average Km^R (ca.98 $\pm$ 18 μg/ml) compared to the wild-type (pJAM130); in 1326 and TK24 hosts the activity was lower, but only by ca.12%. The same disruption in pJAM112 had no effect on the activity of *gyl*P1/P2. In strain 1326, the *Z-form I* and *II* double mutation (pJAM135) had no discernable effect compared to the wild-type (pJAM120). However, in strains MT1110 and 1326Δ*gylR1* the activity of *gyl*P1/P2 in pJAM135 was nearly 3-fold higher. In 1326, the *Z-form I* mutation (pJAM140) reduced activity by ca.32% compared to *gylR-gyl*P1/P2 (pJAM120) yet in strains MT1110 and 1326Δ*gylR1* the activity of *gyl*P1/P2 in pJAM135 was greater than 2-fold higher compared to pJAM120. The *Z-form II* mutation (pJAM145) in the strains tested showed an increase of nearly 3-fold over pJAM120, as did the *gylR10* mutation (pJAM125) in all strains tested.

To rule out the effects of copy number on Km^R, the plasmids were isolated from the various strains. The yields were found to be comparable suggesting that the differences in activity were unlikely to be due to copy number, but see Chapter Five. The negative controls containing pIJ486 alone, showed only low background levels of activity. Levels above this can be attributed to *gyl*P1/P2 activity and not from promoters within pIJ486, transcribing through to the *neo* gene.

4.7: Determination of APHII specific activity

Cell extracts from 1326Δ*gylR1* transformants containing the various constructs were assayed for APHII activity for comparison with the Km^R plate assay results. The assay was carried out as described in section 2.17.3.

4.7.1: APHII activity across the growth curve

APHII activity generated from the *gyl*P1/P2::*neo* fusions was found to vary over the growth phase, with the greatest activity being observed during mid to late exponential growth. After this period it was found to decrease rapidly as the culture entered stationary phase. This was true for both surface grown (data not shown) and liquid grown cultures (see Appendix 4.2). In surface grown cultures the greatest activity was found before aerial hyphae were visible (10-13 h, MMT plus 0.5% glycerol). In agreement with these findings, high resolution S1 nuclease mapping of chromosomally encoded *gyl*P1/P2 indicated that transcription from *gyl*P1/P2 decreased from early stationary phase onwards (M.S.B. Paget and C.P. Smith, personal communication).

4.7.2: APHII assay results

To minimise the possibility of recombination between the plasmid constructs and the chromosome 1326Δ*gylR1* was used as the host. In addition, plasmid preparations of the constructs containing mutations were used to transform each host immediately prior to the

assay as described in section 2.17.3. The results from the various promoter-probe constructs tested are presented in Table 4.2.

Table 4.2: APHII assay results in 1326Δ*gylR1*

Fusion[1]	*gylR*	*Z-form* mutant	APHII Specific activity (Units[2]/min/mg protein) uninduced[3]	induced
pJAM130	NO	wt.	17.68	16.21
pJAM150	NO	*I*	18.25	13.91
pJAM120	YES	wt.	18.14	16.68
pJAM135	YES	*I, II*	25.57	21.66
pJAM140	YES	*I*	11.85	13.62
pJAM145	YES	*II*	24.39	22.02
pJAM125	*gylR10*	wt.	83.89	77.32
pIJ459	/	/	261.83	158.48
pIJ486	/	/	1.15	3.62

Notes:

1: See Table 2.2 for a detailed explanation of the plasmid fusions and Figures, where available.
2: "Units" indicates nmoles NADH oxidised.
3: "uninduced" indicates the neutral carbon source L-arabinose and "induced" indicates glycerol as the carbon source.

The results are the averages obtained using two independent clones of each construct, and each cell extract was assayed twice. The specific activities of the positive control (pIJ459, containing *ermE*p1/p2), were in good agreement with those published previously

(Ward *et al.*, 1986), although the promoters appear to be partially glycerol repressible. The negative control (pIJ486) showed only low background levels of activity.

Firstly, there appeared to be no significant difference between APHII activity levels from induced (grown on glycerol) and uninduced (grown on arabinose) cultures containing the *gyl* DNA constructs. As observed in the gradient plate assays the presence of *gylR* upstream of *gyl*P1/P2 (1.4 kb *Sma*I(4-11) fragment) had no obvious effect on activity levels and neither did the *Z-form I* mutation (pJAM150) on vector-borne *gyl*P1/P2. Secondly, when the effect of the *Z-form* mutations was examined the APHII specific activities did not correlate with the plate assays. Previously (see Table 4.1) these mutants conferred a similar level of Km^R to that of the *gylR10* mutant (pJAM125) whereas the APHII specific activity from pJAM125 was over 3-fold higher than the mutants. To examine the possibility of strain dependence on the APHII activity levels some of the constructs were screened in other host strains.

4.7.3: Strain variation and the APHII assay

Various promoter-probe constructs were used to transform MT1110 and 1326; their APHII specific activities are presented in Table 4.3.

In 1326 and MT1110, in contrast to previous results, *gyl*P1/P2 (pJAM130) showed slightly higher levels of activity when grown on glycerol. This was also demonstrated by the *gylR10* construct, even more strikingly, in MT1110 and to a lesser extent in 1326. However, the vector control (pIJ486) also showed a similar increase in MT1110

Table 4.3: Strain dependence and the APHII assay

Fusion	*gylR*	*Z-form* mutant	Host	APHII Specific activity (Units/min/mg protein) uninduced	induced
pJAM130	NO	wt.	1326 MT1110	17.31 9.38	26.79 12.37
pJAM120	YES	wt.	1326 MT1110	37.51 ND	34.16 17.54
pJAM125	*gylR10*	wt.	1326 MT1110	90.43 58.95	107.72 136.04
pIJ486	/	/	1326 MT1110	ND 7.42	ND 9.35

suggesting these results were probably not significant. In 1326 the specific activities of all the constructs, except pJAM125, were slightly higher compared to MT1110 and 1326Δ*gylR1* hosts.

The various constructs were also assayed in MT1110 grown on solid medium (MMT plus 0.5% glycerol; see Appendix 4.3). The APHII specific activities were found to be of similar levels to those seen in Tables 4.2 and 4.3. These results were unexpected when compared to those of the gradient plates. A possible role for plasmid/chromosome recombination, in influencing vector-borne *gyl*P1/P2 activity in the mutant constructs, was investigated.

4.8: Recombination in the *gyl* DNA::*neo* fusions

From the APHII specific activities (and the varied results of the Km^R assays) it was considered possible that the vector-borne (mutant) *gyl* DNA may have undergone gene conversion (recombination) with the chromosome. If this was the case the majority of the plasmids could have contained wild-type DNA, resulting in the lower than expected levels of APHII activity, i.e the wild-type phenotype.

4.8.1: Recombination, orientation and the *gylR* frameshift mutations

Efficient recombination between the promoter-probe constructs and the chromosome was first revealed with plasmid pJAM115 (Table 2.2), which carries the frameshift mutation *gylR10*. The amount of recombination was assessed by restricting the plasmid DNA with *Xho*I and estimating the proportion of the plasmid preparation that contained both *Xho*I sites (the *Xho*I site in *gylR* is disrupted in the *gylR10* mutation). It was found that when ca.10% of the plasmid population had re-acquired the wild-type *gylR* by recombination, the Km^R fell to almost zero (data not shown). Further work using pJAM160 (which contains a 4 bp insertion at the *Xho*I site in *gylR*); pJAM165 (a 14 bp deletion at the *Pvu*II site in *gylR*); and pJAM170 (a "silent" point mutation resulting in the loss of the *Xho*I site), see Table 2.2 for details, indicated that recombination between the plasmid and the chromosome was only detectable when the *gyl* DNA was inserted in one orientation, the α-orientation. Figure 4.8 illustrates the variations in the level of recombination, as judged by re-acquisition of the *gylR Xho*I site.

Figure 4.8: Restriction analysis of the various frameshift mutant constructs in pIJ486 showing the degree of recombination with the chromosome

Plasmids were isolated from *S. lividans* TK24, grown in TSB liquid medium.

(a) Agarose gel electrophoresis of various constructs showing the re-acquisition of the *Xho*I site in *gylR*

Electrophoresis was carried out with 0.8% agarose (w/v) in 1 X TBE buffer at 1 V/cm for ca.14 h. All samples were cut with *Xho*I unless otherwise indicated. Lanes:
1, λ *Hin*dIII marker; 2, pIJ2211 uncut; 3, pIJ2211; 4, pIJ486 uncut; 5, pIJ486;
6, pJAM115(α-1) uncut; 7, pJAM115(α-1); 8, pJAM116(β-1); 9, pJAM115(α-2);
10, pJAM116(β-2); 11, pJAM115(α-3); 12, pJAM116(β-3); 13, pJAM115(α-4);
14, pJAM115(α-5); 15, pJAM161(β-1); 16, pJAM161(β-2); 17, pJAM160(α-1);
18, pJAM161(β-3); 19, pJAM160(α-2); 20, pJAM160(α-3); 21, pJAM160(α-4);
22, pJAM170(α-1); 23, pJAM170(α-2); 24, pJAM171(β-1); 25, pJAM170(α-2);
26, pJAM171(β-2); 27, pJAM170(α-3); 28, pJAM171(β-3); 29, pJAM170(α-4);
30, pJAM110(α-1) uncut; 31, pJAM110(α-1); 32, λ *Hin*dIII marker.

(b) Agarose electrophoresis of various constructs showing the reacquisition of the *Pvu*II site in *gylR*

Electrophoresis was carried out with 0.8% agarose (w/v) in 1 X TBE buffer at 1 V/cm for ca.17 h. All samples were cut with *Pvu*II unless otherwise indicated. Lanes:
1, λ *Hin*dIII marker; 2, pIJ2211 uncut; 3, pIJ2211; 4, pIJ486 uncut; 5, pIJ486;
6, pJAM110 uncut; 7, pJAM110(α-1); 8, pJAM165(α-1); 9, pJAM166(β-1);
10, pJAM165(α-2); 11, pJAM165(α-3); 12, pJAM165(α-4); 13, pJAM165(α-5);
14, pJAM165(α-6); 15, pJAM165(α-7); 16, pJAM165(α-8); 17, λ *Hin*dIII marker.

Note:
The details of each of the plasmid constructs mentioned above are described in Table 2.2.

Figure 4.8

(a)

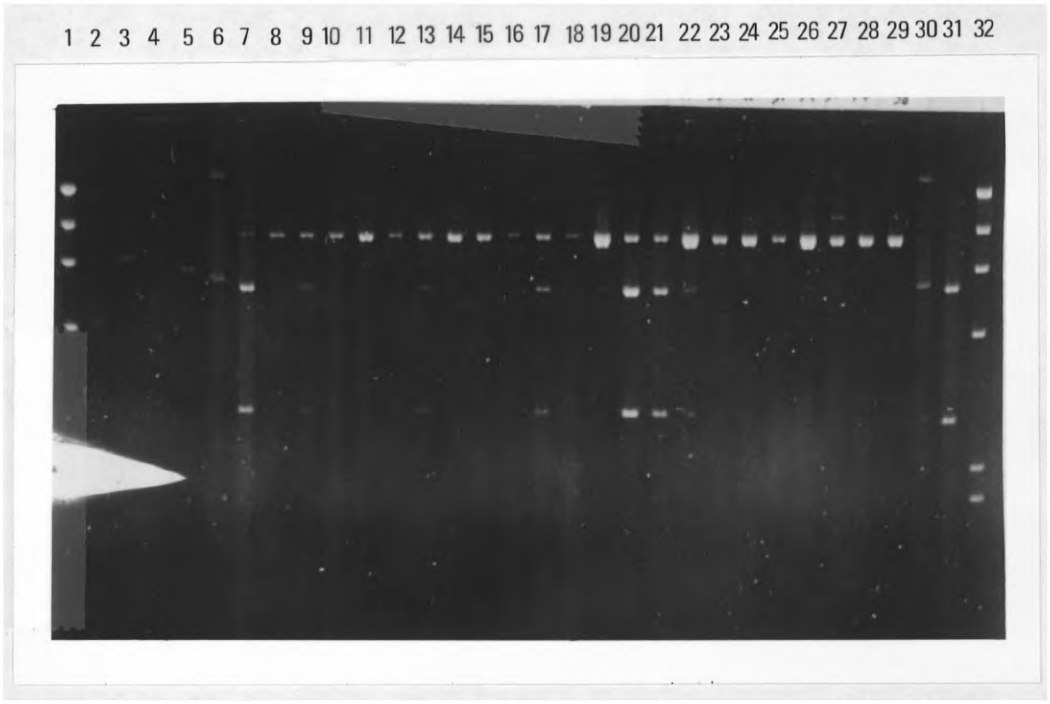
1 2 3 4 5 6 7 8 9 10 11 12 13 14 15 16 17 18 19 20 21 22 23 24 25 26 27 28 29 30 31 32

(b)

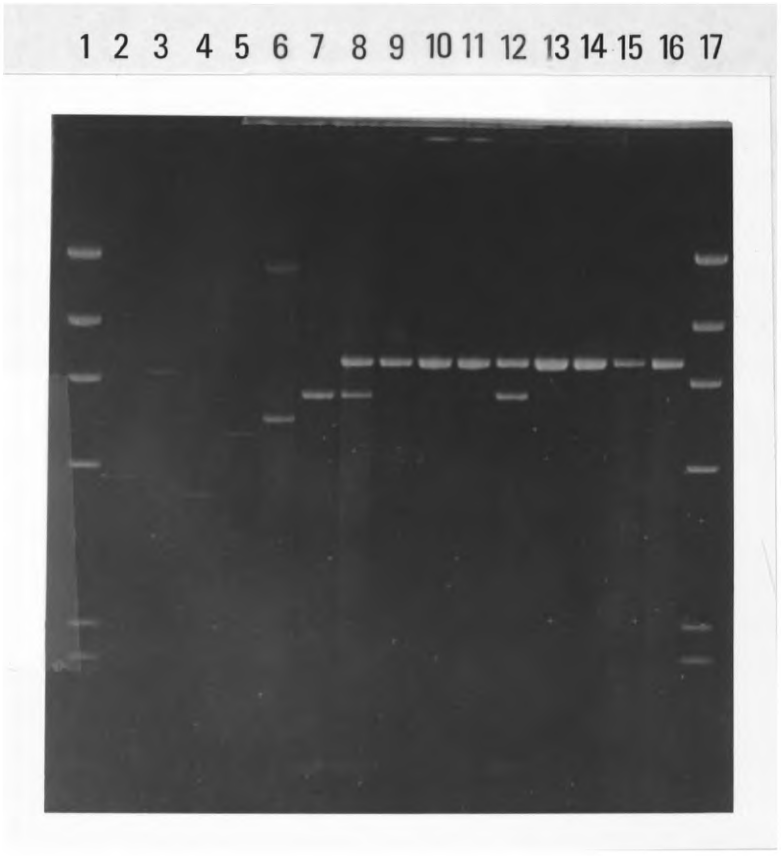
1 2 3 4 5 6 7 8 9 10 11 12 13 14 15 16 17

When ca.10% of the plasmids had recombined with the chromosome, in transformants containing pJAM115 (*gylR10*) in the α-orientation (lanes 9 and 13, Figure 4.8(a)) wild-type *gyl*P1/P2 levels of Km^R were noted. When the level of recombination was much lower than 10% (see lane 14, Figure 4.8(a)) Km^R was as expected, ca.300 μg/ml. When pJAM160 (*gylR13*) was examined however, levels of recombination as high as ca.60% (lane 20, Figure 4.8(a)) had no apparent effect on Km^R; it remained ca.300 μg/ml. Interestingly, only one of the transformants containing pJAM170 (*gylR25*) had re-acquired the *Xho*I site from the chromosome (lane 22, Figure 4.8(a)) and, as expected, there was no change in *gyl*P1/P2 activity (ca.10 μg/ml). The level of recombination in transformants containing pJAM165 (*gylR20*) also had no effect on levels of Km^R, although all of the plasmids had undergone some degree of recombination in this case (see lanes 8 and 10-16, Figure 4.8(b)). This is considered further in the discussion (section 4.10).

As mentioned previously (section 4.6 and above), none of the plasmids in the β-orientation showed any visible degree of recombination (see lanes 8, 10, 12, 15, 16, 18, 24, 26 and 28, Figure 4.8(a) and lane 9, Figure 4.8(b)), and the levels of Km^R were reproducible. This could be due to such a recombination event being lethal to the host strain.

4.8.2: Recombination and the *Z-form* mutations

Due to the results from the promoter-probing studies in MT1101 (see Table 4.1) and the effect of recombination on vector-borne *gyl* expression, a strain containing a *gylR* null-mutation (1326Δ*gylR1*) was used as the host to minimise recombination between the

plasmids and the chromosome. The homology between the *gyl* DNA in the chromosome and the plasmids was reduced to 0.6 kb (0.26 kb upstream of *gylR*p and 0.34 kb downstream; Hindle and Smith, 1994); homology of less than 1 kb (non-interrupted), has been demonstrated to substantially reduce the frequency of recombination in *S. coelicolor* and *S. lividans* (Z. Hindle and C.P. Smith, personal communication).

Due to the disparity in the results between the plate and the APHII assays, even in 1326Δ*gylR1*, the vector-borne *Z-form* mutations were examined for recombination. The subculturing of strains was kept to a minimum. Thus, spores were taken from primary transformant colonies and were used to inoculate an MS plate and 5 mls TSB. The TSB culture was grown for ca.36 h and the plasmid DNA isolated by the "miniprep" method (see section 2.6.1). Spores from the MS plate were used to inoculate the gradient plates and NMMP for the APHII assays; it was hoped that this approach would minimise the chances of recombination between the plasmid and the chromosome. As each *Z-form* mutation introduced a restriction site the loss of that site was used to indicate recombination. Figure 4.9 presents the results of the diagnostic restriction digests performed on the various *Z-form* mutant promoter-probe constructs. The *Z-form I* mutation introduced an *Apa*I site which results in the generation of an additional 0.68 kb band, in pJAM135 and pJAM136; an additional 1.47 kb band in pJAM150; an additional 1.6 kb band in pJAM151 (see Table 2.2 and Figure 4.9) on digestion with *Apa*I compared to the wild-types. As seen in Figure 4.9(a), all of the plasmid minipreps, except pIJ486, showed a partial digest. This suggested that recombination had occurred as the positive control, pIJ486, had digested to completion, although the plasmid miniprep could have been contaminated, resulting in the partial digest. The *Z-form II* mutation introduced a

Figure 4.9: Restriction analysis of plasmids containing the various *Z-form* mutations to estimate the degree of recombination with the chromosome

(a) Agarose gel electrophoresis of various constructs to determine any loss of the *Apa*I site of the *Z-form I* mutation

Electrophoresis was carried out with 0.8% agarose (w/v) in 1 X TBE buffer at 4 V/cm for ca.4 h. All samples were cut with *Apa*I unless otherwise indicated. Lanes: 1, λ *Hin*dIII marker; 2, pJAM150(α-1) uncut; 3, pJAM150(α-1); 4, pJAM150(α-2); 5, pJAM151(β-1); 6, pJAM151(β-2); 7, pJAM130(α-1); 8, pJAM135(α-33) uncut; 9, pJAM135(α-33); 10, pJAM135(α-34); 11, pJAM136(β-37); 12, pJAM136(β-38); 13, pJAM120(α-22); 14, pIJ486; 15, pIJ486 uncut; 16, λ *Hin*dIII marker.

(b) Agarose electrophoresis of various constructs to determine any loss of the *Sma*I site of the *Z-form II* mutation

Electrophoresis was carried out under the same conditions as described in (a). All samples were cut with *Sma*I unless otherwise indicated. Lanes: 1, λ *Hin*dIII marker; 2, pJAM135(α-33) uncut; 3, pJAM135(α-33); 4, pJAM135(α-34); 5, pJAM136(β-37); 6, pJAM136(β-38); 7, pJAM145(α-42); 8, pJAM145(α-43); 9, pJAM120(α-22); 10, pIJ486; 11, pIJ486 uncut; 12, λ *Hin*dIII marker.

(c) Agarose electrophoresis of various constructs to determine any loss of the unique *Sca*I site of the *Z-form II* mutation

Electrophoresis was carried out under the same conditions as described in (a). All samples were cut with *Sca*I unless otherwise indicated. Lanes: 1, λ *Hin*dIII marker; 2, pJAM135(α-33) uncut; 3, pJAM135(α-33); 4, pJAM135(α-34); 5, pJAM136(β-37); 6, pJAM136(β-38); 7, pJAM145(α-42); 8, pJAM135(α-43); 9, pJAM120(α-22); 10, pIJ486; 11, pIJ486 uncut; 12, λ *Hin*dIII marker.

Figure 4.9

(a)

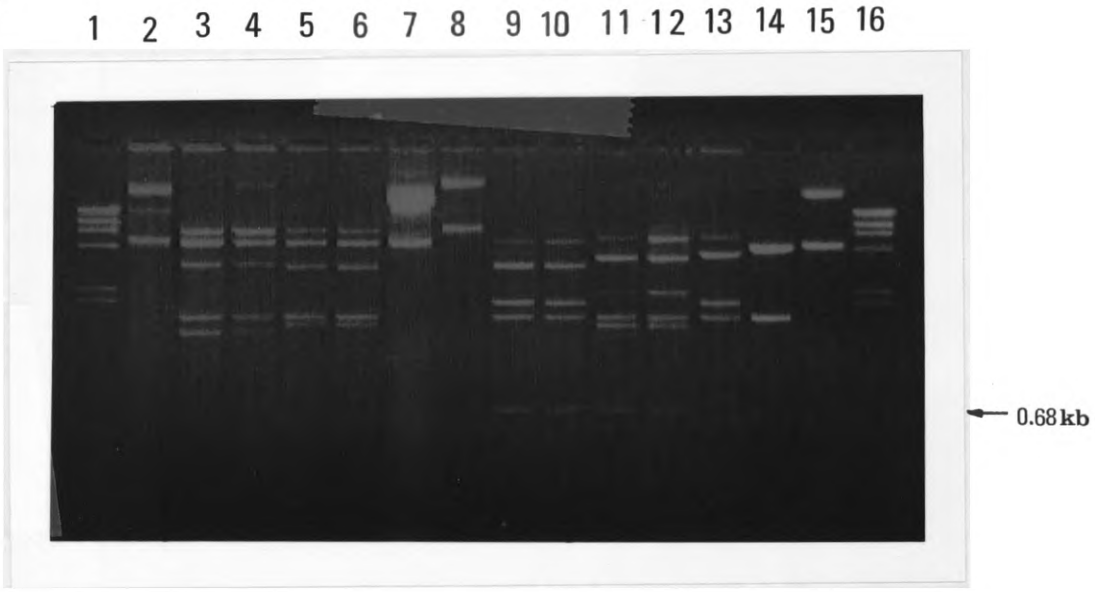

(b)

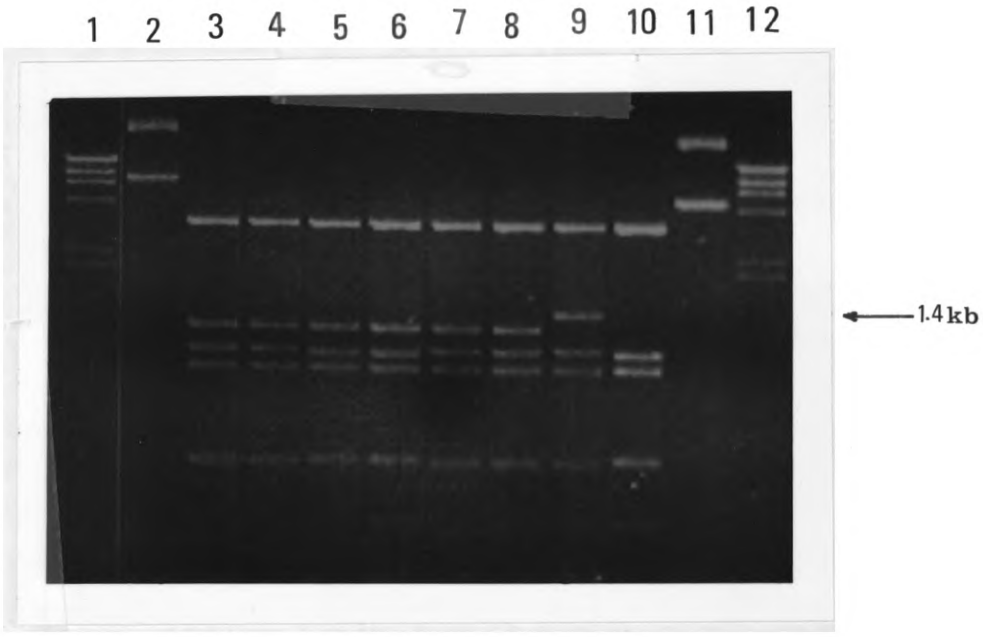

(c)

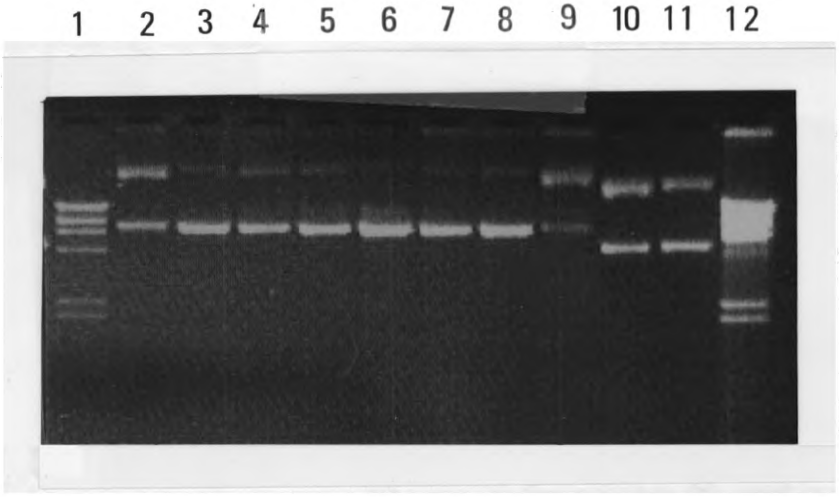

*Sma*I and *Sca*I site in plasmids pJAM135 and pJAM145, resulting in the loss of the 1.4 kb band seen in pJAM120 (lane 9, Figure 4.9(b)) when those plasmids were digested with *Sma*I, or linearisation when digested with *Sca*I. From the restriction analysis shown in Figure 4.9(b) any recombination with the chromosome would have resulted in the appearance of a 1.4 kb band; since this was not visible in the samples it was assumed that recombination had not occurred in those plasmid samples tested. Figure 4.9(c) also indicated that the *Sca*I site had not been lost from the plasmids tested, again suggesting recombination had not occurred.

4.8.3: Recombination and rearrangement between MT1101 and pIJ486

From the initial results with the *gyl* constructs, in pIJ486, when the host was MT1101, (see Table 4.1) it was realised that the presence of SCP1 in MT1101 was having a significant effect on Km^R. Figure 4.10 presents pIJ486 plasmid minipreps from MT1101 analyzed on an agarose gel. From the number of bands in lanes 3 to 8 (Figure 4.10) it was apparent that there had been substantial rearrangements of pIJ486. The use of MT1101 as a host for promoter-probe constructs, based on pIJ486, was discontinued.

4.9: Analysis of *metH*p-containing fragments in pIJ486

Divergent promoter activity upstream from *gylR*p had previously been observed (Smith, 1986). The promoter is located 20 bp downstream from the *Sma*I(4) site (Figure 2.5). The region downstream of this promoter was subsequently sequenced and the presence of an ORF homologous to *E. coli* MetH was demonstrated (Paget, 1994). Using the *Z-form*

Figure 4.10: Analysis of pIJ486 minipreps isolated from MT1101

Electrophoresis was carried out with 0.8% agarose (w/v) in 1 X TBE buffer at 3 V/cm for ca.4 h. All samples were uncut unless otherwise indicated. Lanes: 1, λ HindIII marker; 2, pIJ486; 3, pIJ486#1; 4, pIJ486#2; 5, pIJ486#3; 6, pIJ486#4; 7, pIJ486#5; 8, pIJ486#6.

The "#nos." indicates a plasmid sample isolated from MT1101. Spores from an MS plate were used to inoculate 5 mls of TSB and the culture was grown for ca.36 h before the plasmid was harvested.

Figure 4.10

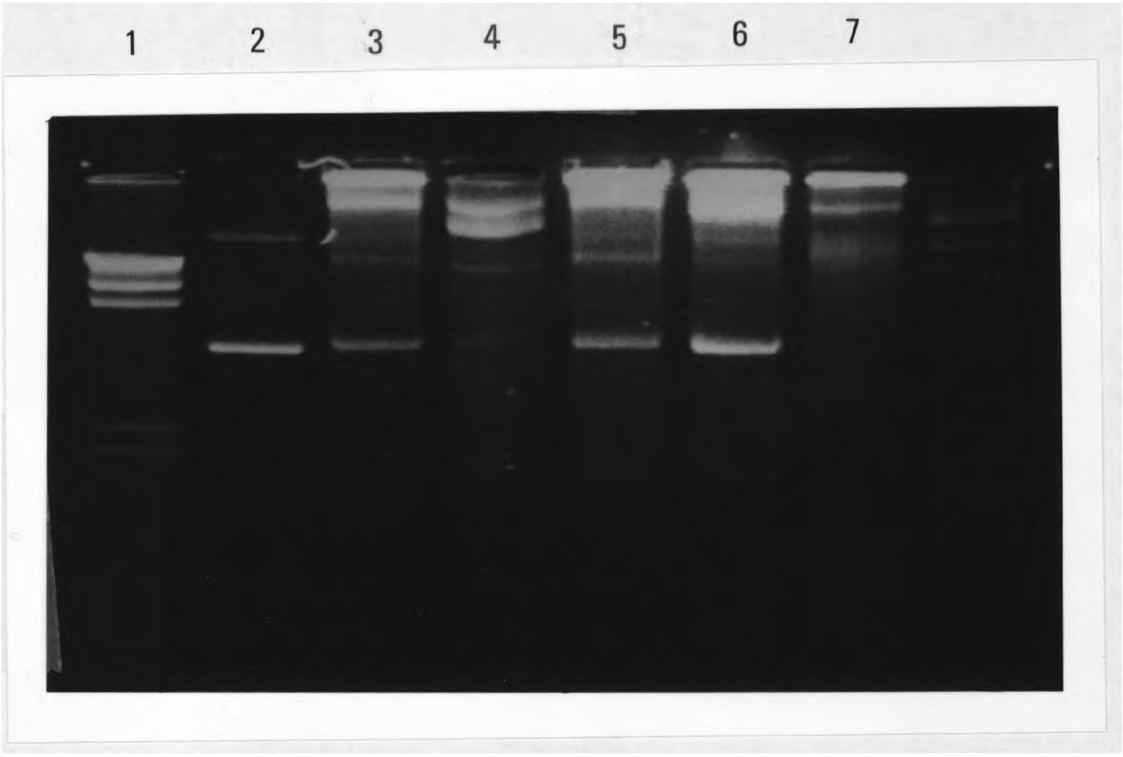

mutations (β-orientation) in pIJ486 their effect on *metH*p activity was investigated. The results from patch and gradient plate assays are presented in Table 4.4.

Table 4.4: Studies on the effect of the *Z-form* mutations on *metH*p activity

Fusion[1]	*gylR*	*Z-form*	Kanamycin resistance (μg/ml)		
			1326[2]	MT1110[3]	1326Δ *gylR1*[4]
pJAM131	NO	wt.	<10	4	5
pJAM151	NO	*I*	<10	5	3
pJAM111	YES	wt.	≥ 300	ND	ND
pJAM113	YES	*I*	≥ 300	ND	ND
pJAM116	*gylR10*	wt.	≥ 300	ND	ND
pJAM121	YES	wt.	120	>50	109
pJAM136	YES	*I, II*	82	ND	84
pJAM141	YES	*I*	100	>50	≤ 100
pJAM146	YES	*II*	42	25	53
pJAM126	*gylR10*	wt.	ND	>50	≥ 300
pIJ486	/	/	3	4	4

Notes:

1: All the constructs contained the *gyl* DNA in the β-orientation (see Table 2.2 for a detailed explanation of the plasmid fusions and Figures, where available).
2: Average of 3 independent isolates.
3: Average of 4 independent isolates.
4: Average of 6 independent isolates.

The constructs pJAM131 and pJAM151 acted as internal controls for vector initiated transcription as there are no promoters that transcribe into *neo* in that orientation. Their

activity and that of pIJ486 showed that the levels of Km^R seen in the other constructs were due to the activity of *metH*p. Interestingly, when the constructs where in the β-orientation the reproducibility of gradient plate assays improved. The constructs containing the *Sph*I(2)-*Kpn*I(12) fragment (pJAM111, pJAM113, pJAM116) show much higher levels of activity than the *Sma*I fragment; possibly due to sequences downstream of *metH*p, the additional *metH* sequences in the fusion transcript could either stabilise the transcript or enhance translation of *neo*. The construct with both *Z-form* regions disrupted (pJAM136) showed ca.70% of the activity levels of the wild-type construct (pJAM121). However, when the *Z-form II* region alone was disrupted (pJAM146) *metH*p expression was reduced almost 3-fold in 1326 and by at least one half in MT1110 and 1326Δ*gylR1*. The results from the disruption of the *Z-form I* region (pJAM141) indicate that it has little or no significant effect on *metH*p expression. The *gylR10* construct (pJAM126) in 1326Δ*gylR1*, showed the highest levels of activity (ca.300 μg/ml) suggesting that in the wild-type (pJAM120) GylR may repress *metH*p, or that the derepressed transcription from *gylR*p (Hindle and Smith, 1994) in the plasmid carrying *gylR10*, was inhibiting the divergent *metH*p topologically (see section 4.10).

The same constructs were assessed for APHII activity and the results are presented in Table 4.5. Again, lower than expected levels for *metH*p activity were demonstrated although they were more consistent than those for the α-orientation. The APHII specific activities are consistent with the results from gradient plate analysis (Table 4.4). The presence of the *gylR10* frameshift mutation on the plasmid, pJAM125, again enhanced expression from *metH*p. The *Z-form II* mutation reduced expression in all strains tested,

but to a lesser extent when the *Z-form I* region, in the same plasmid, was disrupted as well.

Table 4.5: Analysis of *metH*p activity when fused to *neo*

Fusion	*Z-form* mutant	Host	APHII Specific activity (Units/min/mg protein) L-arabinose	glycerol
pJAM121	wt.	1326Δ*gylR1* MT1110	16.9 ND	17.0 22.9
pJAM136	*I, II*	1326Δ*gylR1* MT1110	18.6 ND	16.3 11.2
pJAM141	*I*	1326Δ*gylR1* MT1110	22.2 ND	17.8 22.3
pJAM146	*II*	1326Δ*gylR1* MT1110	8.1 ND	9.2 9.6
pJAM126	*gylR10*	1326Δ*gylR1*	58	43.2
pIJ486	/	1326Δ*gylR1* MT1110	1.2 ND	3.8 2

4.10: Discussion

As discussed in section 4.1, the potential Z-DNA forming regions upstream of *gyl*P1 and *gylR*p were studied using the reporter gene *neo*, to determine their possible influence on the expression of *gyl*P1/P2 on multicopy plasmids. When *gyl*P1/P2 was subcloned into pIJ425, the relatively low constitutive level of expression (15-45 μg/ml Km^R), was abolished when *gylR* was contiguous with *gyl*P1/P2 (*BclI*(1-13) and *SphI*(2)-*KpnI*(12) fragments; see section 4.1), regardless of the carbon source (Smith, 1986). This

phenomenon is referred to as "unconditional repression". However, when the *gyl* fragments were recloned as a *Sma*I(4-11) fragment, *gyl*P1/P2 was expressed at elevated levels (ca.100 μg/ml Km^R), irrespective of the presence of upstream *gylR* (see Table 4.1). One possible explanation for this was the presence of additional *gyl* sequences between *gyl*P2 and *neo*, including a RBS for *gylC* in the fragments used by Smith (1986). Alternatively, the different *gyl* sequences could have resulted in the creation of a "junction promoter" between the *gyl* DNA and the polylinker of pMT3000, subcloned into pIJ486. This may explain why pJAM120, containing *gylR-gyl*P1/P2, gave the same level of expression from vector-borne *gyl*P1/P2 as pJAM130; pJAM130 does not contain *gylR*. A junction promoter would not be unconditionally repressed by GylR. Promoter-probe vectors utilising alternative reporter genes, *xylE* in pMSP1060 and *mel* in pMT3010, as well as some *neo* fusions, found that the presence of contiguous *gylR* abolished expression of vector-borne *gyl*P1/P2 (Paget, 1994; Paget *et al.*, 1994). However, the *xylE* fusions were not reproducible (Paget, 1994; C.P. Smith, personal communication). It is important to note that these results may not be directly comparable; the *Sma*I(4-11) fragments used in pIJ486 were different (see section 4.6). The additional 10 bp could have caused an important change in the spacing of *cis*-acting sequences in the vector-borne *gyl* DNA. Alternatively, the discrepancies between the expression of *gyl*P1/P2, in each vector system, could be due to differences in the DNA topology of the respective promoter-probe vectors; such that GylR could not repress *gyl*P1/P2 when carried on pIJ486. *gyl*P1/P2 expression was relieved/enhanced by a frameshift mutation introduced at the *Xho*I site of *gylR* (*gylR10*) in plasmids pJAM115 and pJAM125; Km^R was ca.300 μg/ml. Interestingly the inclusion of the RBS of *gylC*, in pJAM115, in the 5' end of *neo* transcript had no effect on Km^R in this case, possibly due

to a topological effect (see below). The level of Km^R was reproducibly carbon source independent.

It was considered that topological differences between the vector-borne *gyl* DNA and the chromosomal *gyl* region might play a role in the aberrant unconditional repression of *gyl*P1/P2. For example, if vector-borne *gyl* promoters are more negatively supercoiled than the chromosome *gyl* region, then perhaps the formation of Z-DNA in the former would interfere with transcription. The *gyl* DNA-containing fragments with mutations in the *Z-form* regions upstream of *gyl*P1, *gylR*p (and the divergent *metH*p) were studied to assess whether these *Z-form* regions influenced *gyl*P1/P2 expression. *Z-form I* overlaps the -35 region of *gyl*P1; left-handed Z-DNA formation at this position would undoubtedly have a profound effect on expression of *gyl*P1 (section 1.8.4); RNA polymerase holoenzymes are known to contact both the —10 and —35 hexamers (reviewed by Strohl, 1992). The *Z-form II* sequence has the potential to form the largest stretch of Z-DNA in the *gyl* promoter regions, 23 bp, and is fairly central between the two divergent promoters *gylR*p and *metH*p (see Figure 4.1). The topological studies on the superhelical density of pIJ486 (Chapter Three), suggest that the *Z-form* regions could adopt Z-DNA *in vivo*; the maximum reported superhelical density of pIJ486 was —0.073, but see section 3.5 and Chapter Five.

Initial results from the Km^R assays (see Table 4.1) implicated disruption of the *Z-form* regions in relief of unconditional repression of *gyl*P1/P2. When the *Z-form* double mutant, pJAM135, and the *Z-form II* mutant, pJAM145, were analyzed expression of *gyl*P1/P2 increased nearly 3-fold, similar to that of the *gylR10* mutant, pJAM125. This

provided some physiological evidence of a role for the *Z-form* regions in influencing *gyl*P1/P2 expression on multicopy plasmids. There was also some evidence of strain dependence; *S. lividans* 1326 only showed increased expression of *gyl*P1/P2 when *Z-form II* was disrupted. *S. coelicolor* MT1110 and *S. lividans* 1326Δ*gylR1* showed similar levels of relief with individual and combined *Z-form* disruptions. It could be inferred from these observations that GylR-mediated repression in *S. lividans* 1326 might be different to that of *S. coelicolor* MT1110. The yields of plasmid DNA from each construct and strain were comparable, suggesting that copy number was not the cause of these differences in activity, but see Chapter Five. Levels of activity from the negative control (pIJ486) indicated that the *gyl*P1/P2::*neo* fusion (or junction promoter), was responsible for Km^R and not internal vector sequences.

The patch and gradient plate assays were not always consistent and therefore the constructs were further characterized by assaying the enzyme activities of APHII. APHII activity was found to vary across the growth curve of both *S. lividans* and *S. coelicolor* with maximum activity around mid to late exponential phase, in either solid or liquid media (see Appendix 4.2). As mentioned in section 4.7.1, this is attributable to decreased levels of *gyl* transcript on entry to stationary phase (M.S.B. Paget and C.P. Smith, personal communication). The APHII assay was carried out on sonicates of 1326Δ*gylR1* containing the various pIJ486 constructs (see Table 4.2). The enzyme levels were lower than expected, on both neutral (L-arabinose) and inducing (glycerol) carbon sources. The presence of *gylR* upstream of *gyl*P1/P2 had no discernable effect on APHII activity (as expected from the Km^R data). However, neither did any of the *Z-form* disruptions. The *gylR10* mutant (pJAM125) did show the expected increase in vector-

borne *gyl*P1/P2 expression compared to the wild-type (pJAM120) in the Km^R assay; this was seen on L-arabinose and glycerol carbon sources. The very strong activity of the positive control, pIJ459, ruled out the possibility of any components in the assay (eg. ATP, NADH) being rate limiting. The negative control (pIJ486) indicated that the enzyme levels were due to promoters within the *gyl* DNA and not the vector. The fact that all the *gyl*::*neo* fusion transcripts had the same 5' ends rules out differences in stability of the message as the reason for the unexpected APHII levels in Table 4.2.

Some of the constructs were used to transform MT1110 and 1326 and assayed for APHII activity (see Table 4.3). Unlike the Km^R plate assays, vector-borne *gyl*P1/P2 expression (pJAM130) was slightly higher on glycerol in both 1326 and MT1110; this was also seen in the *gylR10* frameshift mutation (pJAM125) in MT1110 and, to a lesser extent, in 1326 hosts. However, this may have been background NADH oxidase activity as the negative control was also elevated to a similar extent on glycerol. Interestingly, *gyl*P1/P2 expression in pJAM120 and pJAM130 was ca.2-fold higher in the 1326 host compared to 1326Δ*gylR1* (see Table 4.3). APHII activities from the various constructs in MT1110 surface grown cultures, harvested before aerial hyphae formation (see Appendix 4.3), were comparable to those seen in Table 4.3.

Transcription-induced supercoiling (section 1.8.5) would result in raised levels of negative supercoiling behind the transcription complex initiating at *gyl*P1/P2. This increased supercoiling could then drive the formation of Z-DNA at *Z-form I*, probably preventing further transcription from *gyl*P1 by structurally altering its —35 region. This deformation of the vector-borne *gyl* DNA could also prevent GylR binding in a repressive manner to

the operator site at *gylP*1/P2 (Figure 1.2). If GylR could bind to the operator site at *gylR*p and repress *gylR*p as normal this could explain why the wild-type *Sma*I(4-11) *gylR-gylP*1/P2-containing fragment, pJAM120, showed similar levels of activity as the *Cla*I(10)-*Sma*I(11) *gylP*1/P2-containing fragment, pJAM130, when they were vector-borne (Tables 4.1 and 4.2). In a *gylR* null-mutant background chromosomal *gylR*p expression is derepressed 2-fold (Hindle and Smith, 1994) and this could lead to transcription-induced supercoiling. Thus, in the *gylR-gylP*1/P2 fragment containing the *gylR10* frameshift mutation, pJAM125, the positive supercoils generated in front of the transcription complex, at the derepressed *gylR*p, could prevent the formation of *Z*-DNA at *gylP*1 and increase the expression from *gylP*1/P2 to levels greater than that seen from *gylP*1/P2 in pJAM130. Possibly because there is likely to be increased transcription initiation at *gylP*1/P2. This is due to increased expression from *gylR*p; the RNA polymerase holoenzymes could either fail to terminate at *t* (Figure 1.1) and read through to *gylP*1/P2, or terminate at *t* and therefore increase their concentration around *gylP*1/P2; thus, increasing transcription initiation at *gylP*1/P2.

These studies indicate that, if the *Z-form* regions do influence *gylP*1/P2 expression by adopting *Z*-DNA, it is in a negative manner as the disruptions appear to increase *gylP*1/P2 expression when the promoters are vector-borne. In contrast, analysis of *metH*p expression (see Table 4.4) indicates that disruption of *Z-form II* reduces expression by almost 3-fold in 1326 and by one half in MT1110 and 1326Δ*gylR1*. GylR also showed signs of repressing *metH*p as the *gylR10* mutation, pJAM126, increased vector-borne *metH*p activity nearly 3-fold compared to pJAM121 in 1326Δ*gylR1*. Another explanation for pJAM126 expression involves the derepressed (see above), divergent, expression of

vector-borne *gylR*p in pJAM126; the change in topology associated with this transcription (increased negative supercoiling behind the DNA-RNA polymerase complex), could possibly enhance expression of vector-borne *metH*p. The data for *metH*p expression are reproducible and consistent between the Km^R and APHII assays probably due to the lack of recombination in this (β) orientation. An explanation for the inhibition of vector-borne *metH*p, by the *Z-form II* disruption, again involves transcription-induced supercoiling (see section 1.8.5) and a model for this is presented below.

Relief from transcriptional inhibition caused by supercoiling

Z-form II is almost exactly in the middle of the two divergent promoters *metH*p and *gylR*p, ca.140 and 110 bp upstream from their —10 hexamers respectively. Normally, negative supercoils are generated behind a DNA-RNA polymerase complex and an equal amount of positive supercoils are generated in front; the twin-supercoiled-domain model proposed by Liu and Wang (1987). The supercoils normally cancel each other out by diffusing around the plasmid. However, divergent transcription would provide a block to the diffusion of the supercoils around the plasmid and lead to domains of different superhelical density (Liu and Wang, 1987; Wu *et al.*, 1988); transcription from *metH*p and *gylR*p is an example of this phenomenon. Interestingly, this would result in two converging "waves" of negative supercoils meeting in the *Z-form II* region. It is possible that the formation of left-handed Z-DNA at this position could relieve this "bottleneck" of negative supercoiling; the switch to the left-handed conformation causes a loss of negative supercoils (section 1.8.4). The disruption of *Z-form II* may result in a build up of negative supercoils that would inhibit *metH*p and *gylR*p. Thus, preventing further

transcription until the positive supercoils generated in front of the earlier DNA-RNA polymerase complexes are relaxed by TopI. Normally, the superhelical density of DNA in the cell is controlled by TopI and DNA gyrase to prevent such artificially high (or low), regions of supercoiling. However, in a cell containing multiple copies of a plasmid, such as pIJ486, unnaturally high levels of negative supercoiling could exist transiently within the plasmid population. The topoisomerases being "outnumbered" by the plasmids. The transient levels of supercoiling could be enough to inhibit expression from *metH*p. This role for *Z-form II* is supported by results from the *gyl*P1/P2 plate assay (see Table 4.1). The double *Z-form* mutant, pJAM135, gave similar levels of Km^R as the *Z-form II* mutant, pJAM145, and the *gylR10* frameshift mutation, pJAM125. Thus, it would appear that these *Z-form* mutations have a similar effect as a vector-borne *gylR* null-mutation. One explanation for this is that disruption of *Z-form II* causes a topological inhibition of *gylR*p expression, similar to that described for *metH*p above. This could prevent GylR binding at the *gylR* operator site, leading to derepression of *gylR*p and thus an increase in *gyl*P1/P2 expression in pJAM145 as described for pJAM120 above. The negative controls pIJ486, pJAM131 and pJAM151 showed that internal vector sequences were not responsible for APHII activity. The 5' ends of the *neo* mRNAs were identical which would rule out processing or stability of the transcripts as an alternative explanation to the above results. However, a possible alternative suggestion is that the *Z-form II* disruption alters a non-topologically acting *cis*-acting sequence required by *metH*p (or *gylR*p).

Results from glycerol kinase assays (performed as described in section 2.17.4) on sonicates from a 1326Δ*gylR1* host containing various pIJ486 *gyl* constructs (data not

shown), provided evidence of complete repression of chromosomal *gyl*P1/P2 by GylR *in trans* when *gylR* was carried on a multicopy vector (e.g. pJAM120, pJAM135 or pJAM145), in the presence of inducer. This is not without precedents, the *gal* and *lac* operons of *E. coli* are completely repressed when their respective repressor genes (*galR* and *lacI*) are placed on multicopy plasmids (Haber and Adhya, 1988). Compared to moderately high, vector only, glycerol kinase activity, pJAM130 (containing *gyl*P1/P2 alone) showed a 3-fold increase in glycerol kinase activity. This suggests that a *trans*-acting repressor molecule, not GylR as there is none in this system, was being titrated out by the plasmid. However, this result was not always reproducible. These findings support the view that GylR may not be solely responsible for unconditional repression of vector-borne *gyl*P1/P2.

The disparity between the Km^R assay data and the APHII assay data is probably attributable to differences in the level of recombination between the plasmid and the chromosome. As described in section 4.8.1 this was first noted in pJAM115, when only ca.10% of the plasmid had recombined, wild-type levels of Km^R were recorded. Also described was the fact that the plasmid DNA containing the *gylR13* mutation showed ca.60% recombination but plate assays showed that Km^R was still ca.300 μg/ml. In this case, the recombination event probably occurred while the transformant was cultured for plasmid isolation, and not during growth in the gradient plate assay. Thus, the pIJ486 constructs for the APHII assay could have undergone recombination with the chromosome during growth in NMMP in the preparation of cell-free extracts. The plasmids described in section 4.8.2, although having tested negative for recombination, were probably not a true reflection of the plasmids in the mycelium harvested for the APHII assay. In any

future assays it would be necessary to isolate the vector-borne *gyl* DNA directly, by PCR, from gradient plates and to sample the mycelium prior to sonication to provide an accurate picture of the level of recombination between the plasmid constructs and the chromosome. The hosts were transformed just prior to the assay with plasmids that had been checked beforehand for recombination (see section 2.17.3) to try to minimise this. However, high frequency recombination could explain why the *Z-form* disruptions had no apparent effect on *gyl*P1/P2 APHII activity. This could also explain why MT1110 sonicates (Table 4.3 and Appendix 4.3) showed similar levels of APHII activity as 1326Δ*gylR1* sonicates. 1326Δ*gylR1* was used to minimise recombination as there is less homology between the plasmids and chromosome, see section 4.8.2. However, as long as the minimum percentage of plasmids (possibly $\leq$ 10%, see section 4.8.1) necessary to cause the wild-type phenotype to be exhibited, had recombined in 1326Δ*gylR1*, greater levels of recombination between the plasmid and the chromosome in MT1110, which was likely, would have no apparent phenotypic effect on *gyl*P1/P2 APHII activity. The results from the pJAM170, *gylR25* point mutation, show that the recombination event may be enhanced when transcription from *gylR*p is increased (see section 4.8.1). All the other frameshift mutations (data not shown) prevent the production of GylR and Hindle and Smith (1994) have shown that this probably leads to derepression of *gylR*p by ca.2-fold. Assuming this occurs on the plasmids as well, the *Z-form II* region will probably be in the Z-DNA conformation and may assist in the recombination event (see section 1.8.4; and Chapter Five).

In summary, on the basis of these results, the *Z-form* regions may have a negative (repressing), *cis*-acting, regulatory role when *gyl*P1/P2-containing *gyl* DNA is vector-

borne. This is supported by results from Chapter Three showing pIJ486 has a high level of superhelical density (up to —0.073) which would facilitate the *Z-form* DNA adopting a *Z*-DNA conformation *in vivo*, but see section 3.5 and Chapter Five. Moreover, *Z-form II*, upstream from *metH*p, may be involved in a more positive manner, disruption of this region leads to repression of the promoter. It should be noted that *gyl* DNA, containing *Z-form I* and *Z-form II* regions, from various *Streptomyces* species were isolated by PCR and sequenced; the *Z-form I* region was somewhat conserved (Appendix 4.4). However, the sequence containing the *Z-form II* region, which demonstrated relief of *gyl*P1/P2 and repression of *metH*p when disrupted (see Table 4.1), was conserved only in *S. coelicolor*, the other species appeared to have deleted this region (M.S.B. Paget and C.P. Smith personal communication). This is however, still consistent with the model for relief of transcriptional inhibition caused by supercoiling described above. The *metH*p and *gylR*p promoters are separated by 60-90 bp in the species lacking the *Z-form II* region; the DNA::RNA polymerase complex could encompass both promoter regions when bound to either promoter. Thus, there would be no "bottleneck" of converging "waves" of negative supercoils, they would diffuse normally around the plasmid (see Chapter Five).

Chapter Five

General Discussion and Future Work

The main objective of this study was to determine the superhelical density (σ) of the *Streptomyces* plasmid, pIJ486, and how it varied during the growth of *S. coelicolor*; firstly, because there is no information on DNA supercoiling in streptomycetes; and secondly because this information would also indicate the likelihood of the *Z-form* sequences in the glycerol operon adopting a *Z*-DNA conformation.

An interesting observation made during this study was the apparent correlation between an increase in negative supercoiling and the onset of aerial hyphae formation (section 3.3.2). This is even more interesting given the hypothesis that aerial hyphae formation is initiated/accompanied by an increase in osmolarity within the mycelium (see, e.g., Chater, 1993). Supercoiling is known to be sensitive to changes in osmolarity (Higgins *et al.*, 1988; Ni Bhriain *et al.*, 1989; Graeme-Cook *et al.* 1989; Dorman *et al.*, 1990); an increase in osmolarity of the environment leads to an increase of osmolarity inside the cell and a corresponding increase in DNA supercoiling (see also section 1.8.5).

The correlation between aerial hyphae formation and increased supercoiling could be more accurately determined by following the rate of macromolecular synthesis, since it is known to slow down appreciably just before aerial hyphae formation (Granozzi *et al.*, 1990); this would identify when the transition to aerial hyphae formation begins.

Increased sampling of mycelia for plasmid isolation around this transition period would also indicate whether the increase in supercoiling is gradual and if it corresponds to changing osmolarity within the mycelia (correlated with the disappearance of glycogen). One problem with such an investigation in *Streptomyces* spp. is however, their heterogeneous growth. Even in a lawn of mycelia derived from pre-germinated spores some areas will have sporulated before the majority of mycelia have even formed aerial hyphae. But this could be overcome by removing such areas before harvesting the mycelia.

A speculative hypothesis, based on the preliminary results, is that increased supercoiling leads to a switching on of the late developmental genes in some manner. The change in DNA topology could allow the recognition of hitherto untranscribed genes by sigma factors such as σ^{WhiG} and σ^{HrdA} (Chater, 1993; Kormanec and Farkašovský, 1993), or perhaps even lead to the transcription of *whiG* or *hrdA* themselves. This hypothesis could be investigated using continuous cultures to correlate changes in osmolarity with gene expression; the medium in the bioreactors could be manipulated to mimic the increased osmolarity associated with aerial hyphae formation. RNA samples harvested at various time points could be screened for the early appearance of *whiG*, *hrdA* or other known late developmental gene transcripts and correlated with the superhelical density of pIJ486. Also, surface grown cultures could be transferred to a medium of high osmolarity and samples taken for screening as above. DNA gyrase inhibitors such as novobiocin could be added at various concentrations to surface grown cultures to determine their effect on DNA supercoiling and late developmental gene expression. Concentrations of DNA gyrase inhibitor that only prevent the rise in unrestrained supercoils associated with aerial

hyphae formation, accompanied by a failure to sporulate or produce antibiotics could be easily screened for. Side effects due to novobiocin acting on targets other than DNA gyrase could be ruled out using *Streptomyces* transformants carrying pGL103; this plasmid contains the novobiocin resistance determinant from the novobiocin producer *S. niveus* (Hoggarth *et al.*, 1994). This could establish a causal link between negative DNA supercoiling and developmental gene expression. These experiments might indicate whether the inferred ca.20% increase in the number of unrestrained supercoils was significant during the transition to aerial hyphae formation. Changes of 15-30% have been shown to have significant effects on transcription *in vitro* (Brahms *et al.*, 1985; Boroweic and Gralla, 1987).

Another interesting discovery was that *S. coelicolor*(pIJ486) maintains a high level of σ well into stationary phase, especially when surface grown; a σ of —0.064 was maintained for at least 24 h into stationary phase (section 3.3.2.2). Over a 48 h period, from onset of stationary phase, *S. coelicolor*(pIJ486) lost only 10% of unrestrained supercoils in pIJ486 (Appendix 3.7). *E. coli*(pBR322) in comparison, lost ca.40% of unrestrained supercoils from the plasmid within 4 h (Balke and Gralla, 1987). These time periods from the onset of stationary phase are equivalent to ca.8 t_D and 6 t_D, respectively; thus, the apparent differences are likely to be significant. Such differences, between *E. coli* and *S. coelicolor*, are not unexpected due to the number of transcriptional processes initiated in stationary phase by *Streptomyces* spp. The maintenance of an optimal negative (—) σ is probably necessary for transcription initiation and elongation (Wu *et al.*, 1988; Jyothirmai and Mishra, 1994). This optimal —σ is maintained by the differential activities of DNA gyrase and DNA topoisomerase I (section 1.8.3). To investigate

whether or not DNA gyrase is still active in the stationary phases of *S. coelicolor* and *E. coli*, RNA samples, harvested at various time points throughout their growth cycles, could be probed with the relevant *gyrB* sequences to determine the level of expression of the respective gene at each locus. This would indicate whether DNA gyrase is still transcribed during stationary phase. Alternatively, the protein could have a longer half-life in *S. coelicolor* compared to *E. coli*.

The study indicated that pIJ486 has a high $-\sigma$, up to 0.073 (section 3.3.2.2), in *S. coelicolor* MT1110 (at least in its purified state). At this level of $-\sigma$ alternating purine-pyrimidine DNA sequences can adopt a left-handed *Z*-DNA conformation (McLean and Wells, 1988). The preliminary two-dimensional chloroquine gel analysis of *Z-form I* (Appendix 3.10) indicated that *Z-form I* does not adopt the *Z*-DNA conformation up to a $-\sigma$ of 0.031 (section 3.4). It is expected that, at slightly higher levels of $-\sigma$, it would adopt the *Z*-DNA conformation. The resolution of the 2D ChQ gel did not allow the determination of the $-\sigma$ value at which the transition would occur. Thus, *Z-form I* appears to be capable of existing as *Z*-DNA in pIJ486 and, as *Z-form II* is longer than *Z-form I* (Figure 4.1) it too could adopt this conformation when carried on pIJ486; longer stretches of alternating purine-pyrimidine bases require less negative supercoiling to form *Z*-DNA (see, e.g., Rahmouni and Wells, 1989). However, bacterial DNA is thought to sequester some 60% of supercoils by binding histone-like proteins (see, e.g., McClellan *et al.*, 1990); and it is only within the free, unrestrained, supercoils of DNA that secondary structures such as *Z*-DNA and cruciforms can occur (see, e.g., Bliska and Cozzarelli, 1987). By analogy with the above, the maximum unrestrained σ of pIJ486 would therefore be ca.—0.028 *in vivo*. Thus, *Z-form I* borne on pIJ486 is unlikely to

exist as *Z*-DNA *in vivo*; a certain threshold level of superhelical density is required to facilitate the adoption of an alternative secondary structure by *B*-DNA (Lilley and Hallam, 1984), but see below. Further work is necessary to determine whether *Z*-DNA exists *in vivo* at the *Z-form* sequences of the glycerol operon. This could be achieved by *in situ* probing for the *Z-Z* or *B-Z* junctions (that exist upon *Z*-DNA formation) using potassium permanganate (e.g., as described by Jiang *et al.*, 1991), or osmium tetroxide (e.g., as described by Rahmouni and Wells, 1992). The $-\sigma$ at which each of the *Z-form* regions form *Z*-DNA could also be determined by two-dimensional chloroquine gel electrophoresis. This could provide evidence that *Z-form II* forms *Z*-DNA more easily than *Z-form I*. It may also support the *in situ* *Z*-DNA probing data if the $-\sigma$ at which *Z*-DNA is formed is similar to those found *in vivo*.

Interestingly, the *Z-form II* mutation reduced expression from vector-borne *metH*p (section 4.9) suggesting an upstream regulatory sequence had been disrupted or that *Z*-DNA formation somehow enhanced expression. This has led to the development of a hypothesis whereby *Z-form II* and possible *Z*-DNA formation are implicated in the relief of transcriptional inhibition caused by supercoiling (section 4.10). Although speculative at present, this could be the first evidence of a regulatory role for *Z*-DNA *in vivo*. This could be further investigated by replacing the imperfect alternating purine-pyrimidine *Z-form II* sequence with a "perfect", longer $(GC)_n$ (where $n \geq 12$) sequence without changing the spacing. Expression from *metH*p and *gylR*p could be followed; if it increased, and *Z*-DNA formation could be demonstrated *in situ* (see above), this would provide strong evidence of a biological role for *Z*-DNA, albeit on a recombinant plasmid. The longer region of *Z*-DNA would reduce the level of negative supercoiling to a greater

extent than the wild-type sequence; thus, according to the model, this would relieve the "bottleneck" of negative supercoils between *metH*p and *gylR*p, possibly increasing promoter activity. It should be noted that *Z-form I* is not rigorously conserved (Appendix 4.4) and *Z-form II* is not conserved at all in the *Streptomyces* spp. examined so far (Paget, 1994; M.S.B. Paget and C.P. Smith, personal communication). However, these species do not have *Z-form II* and the surrounding DNA and therefore the distance between the divergent promoters is very small. In such cases the bottleneck of negative supercoils may not occur *in vivo*; Z-DNA formation would not be necessary in this case according to the above hypothesis. This could be investigated by inserting *Z-form II* or another sequence capable of forming Z-DNA into the intergenic region between *metH*p and *gylR*p, cloned from the species that lack *Z-form II*, and downstream from both promoters as well as looking at the effects of deleting *Z-form II* completely in *S. coelicolor*. Z-DNA formation could then be probed for *in situ*. The formation of Z-DNA at the sites downstream from each promoter and not in the intergenic region would demonstrate that a bottleneck of negative supercoils does not occur in these *Streptomyces* spp. Alternatively, in the case where *Z-form* DNA is inserted between the promoters, if Z-DNA is detected in the intergenic region this would suggest that the supercoiling of the region is high enough for Z-DNA formation without transcription-induced supercoiling. This would suggest that the transcription-induced change in topology predicted above has little effect on *metH*p expression *in vivo*. The *S. coelicolor* Δ*Z-form II* mutant could indicate the effect of the deletion on growth of the host; poor growth on minimal media, restored by methionine (see below), would indicate that the *Z-form II* region has a positive role. An alternative explanation, if the former proves to be the case, could be the existence of a Z-DNA binding protein that recognises *Z-form II* or has enhanced

affinity for *Z*-DNA. Such proteins or changes in DNA-protein affinity have been suggested for other systems e.g., rec1 (essential for recombination) in *Ustilago* spp. binds to *Z*-DNA 75-fold more tightly than to *B*-DNA (Kmiec *et al.*, 1985); RecA protein binding in *E. coli* is enhanced with a *Z*-DNA template *in vitro* (Kim *et al.*, 1989).

If the above experiments indicate a role for *Z*-DNA in recombinant plasmids the next step would be to investigate the *Z-form* regions on the chromosome. Results from high resolution S1 nuclease mapping indicate that *gyl*P1 expression increases in the *gylR* null-mutants; apparent transcription from *gylR*p increases 2-fold in the *gylR10* null-mutant and 6-fold in the Δ*gylR1* null-mutant (Hindle and Smith, 1994). Assuming *Z*-DNA formation at *Z-form I*, as predicted by the twin-supercoiled-domain model (see section 1.8. and below), the level of *gyl*P1 expression is unexpected; *Z*-DNA formed at *Z-form I* would probably prevent RNA polymerase initiation/binding to *gyl*P1 (Glikin *et al.*, 1991). However, the positive supercoils generated in front of the DNA::RNA polymerase complex at *gylR*p could probably diffuse towards *Z-form I* and cancel some or all of the negative supercoils that would otherwise cause *Z*-DNA formation at *Z-form I*. This could therefore relieve *gyl*P1 expression by preventing *Z*-DNA formation and allow RNA polymerase to initiate normally.

The results from the two-dimensional gel analysis indicate that *Z-form I* probably would not form *Z*-DNA *in vivo* when carried on pIJ486 (see above). However, it may do so due to the increase in negative supercoils behind the DNA::RNA polymerase complex when transcription initiates at *gyl*P1 or *gyl*P2. This is explained by the twin-supercoiled-domain model, proposed by Liu and Wang (1987) and discussed in section 1.8. The plate results

from the promoter-probing of *gyl*P1/P2-containing *gyl* DNA in pIJ486 seem to indicate that the *Z-form* regions inhibit expression from *gyl*P1/P2 (discussed in section 4.10). However, the data was inconsistent and should be further investigated, see below.

The promoter-probing of *gyl*P1/P2-containing *gyl* DNA in pIJ486 gave inconsistent data, especially when compared to other reporter systems e.g., *mel* and *xylE*. However, the cloning strategies were different and the possibility that a junction promoter was created upon sub-cloning the *gyl* DNA cannot be ignored (section 4.10). This could be investigated by high resolution S1 nuclease mapping to locate the origins of *neo* transcription in the pIJ486 constructs. Mutants have also been isolated that are no longer unconditionally repressed (Paget *et al.*, 1994); the sequence data should provide important information towards explaining this phenomenon. It is also interesting to note that the *gyl* DNA used in the *mel* and *xylE* promoter-probing experiments came from *S. coelicolor* J802, in the present study it originated from *S. coelicolor* M138. As mentioned in Chapter Four an obvious explanation for the inconsistencies between the expression of wild-type *gylR-gyl*P1/P2-containing fragments is that GylR does not bind repressively to the *gyl*P1 operator site when the fragments are cloned in pIJ486. *In vivo* footprinting of vector-borne *gyl*P1/P2 would directly address this question. Available sequence data shows that the DNA sequence of *gyl*P1/P2 is identical in both strains, but, as the available sequence does not extend to *gylR*p in J802, differences in the operator sites for GylR in the *gylR*p region or other regulatory sequences could explain the conflicting results reported for vector-borne *gylR-gyl*P1/P2 expression. The sequencing of this region in J802 is being undertaken at present. Another possible explanation for the non-reproducibility of the Km^R assay results could be variations in the copy number of

pIJ486. This has been suggested to increase during rapid growth (H. Richards, personal communication, cited in Gramajo *et al.*, 1993) and could account for differences in the level of Km^R between different experiments. Inhibition, or slowing, of growth was noted for *S. lividans* TK64 containing multiple copies of *gylR* (Paget, 1994). The determination of the copy number of pIJ486 would help to resolve the inconsistencies in both the Km^R and APHII assay data. Also, the various pIJ486 *gyl* constructs could be re-cloned in the *mel* reporter pMT3010 to overcome recombination between plasmid *gyl* DNA and the chromosome (section 4.8); *mel* is oppositely orientated to *neo* relative to the pIJ101 sequences.

The possible role of recombination (between the pIJ486 *gyl* constructs and the chromosome) in causing the different levels of vector-borne *gyl*P1/P2 expression (see sections 4.6 and 4.7) could be determined as described in section 4.10. Initial data in this study suggest that recombination between the plasmid and chromosome occurs only in the α-orientation, i.e. when *gyl*P1/P2-containing DNA is fused to *neo* in pIJ486 (section 4.8), and is possibly enhanced when *gylR*p is derepressed (this assumption is based on data from Hindle and Smith, 1994). This could be further investigated by determining expression from vector-borne *gylR*p by promoter-probing and S1 nuclease mapping. This would indicate whether or not increased expression from *gylR*p enhances recombination. The *in situ* Z-DNA probing (see above) would also determine the presence of Z-DNA and a high $-\sigma$, both of which have been implicated with recombination *in vitro* (Kim *et al.*, 1989; and references therein)

If GylR does not bind to and/or inhibit *gyl*P1 (see Chapter Four and above) but does bind at *gylR*p this could provide an explanation for the effect of the *gylR10* frameshift mutation on *gyl*P1/P2 expression. Derepressed *gylR*p activity (see above) could enhance *gyl*P1/P2 expression either topologically or by increasing the concentration of RNA polymerase in the vicinity of *gyl*P1/P2 and thus transcription initiation at *gyl*P1/P2. Other explanations as to why the *gylR10* frameshift mutation (in both *Sph*I(2)-*Kpn*I(12) and *Sma*I(4-11) fragments) increased vector-borne *gyl*P1/P2 expression 3-fold compared to vector-borne *gyl*P1/P2 expression in the *Cla*I(10)-*Sma*I(11) and *Sma*I(4-11) fragments (section 4.6) are considered below. Possibly it involved the titrating out of a repressor molecule; the *gylR10*-containing fragments have more operator sites than the *Cla*I(10)-*Sma*I(11) fragment (see section 4.5). The existence of another repressor is supported by the finding that when the *Cla*I(10)-*Sma*I(11) fragment was carried in pIJ486 glycerol kinase activity increased 3-fold compared to vector alone in the *S. lividans* 1326Δ*gylR1* host (data not shown). An alternative possibility is that the *gylR10*-containing fragments (see section 4.5) have different helical phasing compared to the wild-type and this may prevent protein binding and/or looping of the DNA in the same manner as it would on the wild-type fragment. This is in fact the case, the operator sites in wild-type *gylR-gyl*P1/P2-containing DNA are separated by almost exactly 93 helical turns (assuming a helical repeat of 10.5 bp), in *gylR10*-containing fragments they are separated by 92.57 helical turns. This is supported by similar *gyl*P1/P2 expression in the *gylR20*-containing fragments (data not shown). This frameshift mutation is the result of a 14 bp deletion; the spacing between operator sites is 91.62 helical turns. Thus, in the frameshift mutations the operator sites are on opposite sides of the DNA helix. However, as the operator sites are ca.1 kb apart writhing of the DNA (i.e. deformation of the double-helix

rather than supercoiling) may compensate for the differences in phasing of the operator sites. This has been suggested for *lac* repression by LacI when the DNA is above a certain level of negative supercoiling (Eismann and Müller-Hill, 1990). This could be investigated by altering the helical phasing in the wild-type vector-borne *gylR-gyl*P1/P2 fragment and examining vector-borne *gyl*P1/P2 expression. This could be achieved by restricting the wild-type *gylR-gyl*P1/P2-containing fragments with *Cla*I and S1 nuclease, and re-ligating the DNA. This would enable recombinant plasmids with the same spacing between the operator sites as that of the *gylR10* mutation to be screened. The existence of a second, putative, *trans*-acting repressor molecule could be investigated by *in vitro* DNaseI footprinting using whole cell extracts from a variety of sources: wild-type *S. coelicolor* MT1110; the Δ*gylR1* null-mutant MT1120; and also purified *Streptomyces* RNA polymerase. This would allow the detection of a novel footprint on the basis that it did not correspond to those caused by GylR or RNA polymerase binding within the *Sma*I(4-11) fragment.

The deletion of "*metH*" in *S. coelicolor* has so far proved impossible, suggesting that the MetH homologue is essential (M.S.B. Paget and C.P. Smith, personal communication). The natural habitat of *Streptomyces* spp., containing a relative abundance of glycerol esters, and the essential nature of *metH*, probably leads to frequent, divergent, transcription of *metH*p and *gylR*p. Thus, the intergenic region between *metH*p and *gylR*p could provide an interesting system to investigate the role of DNA supercoiling and the effect of non-*B*-DNA conformations on promoter expression *in vivo*.

Appendicies

Appendix 2.1: DNA size standards

(a) λ *Hin*dIII markers: 23.13, 9.42, 6.56, 4.4, 2.32, 2.03, 0.56, 0.12 kb.

(b) ϕX174 *Hae*III markers: 1.35, 1.08, 0.87, 0.6, 0.31, 0.28, 0.27, 0.19, 0.12, 0.07 kb.

Appendix 2.2: Beckman DU-8 program for densitometric scanning of topoisomer populations

```
SLAB GEL 04
3  λ = 0.0
8  READ AVG = 3
11 SLIT WIDTH = 1
46 LOWER SCALE = 0.000
47 UPPER SCALE = 0.25
48 CHT SPEED = 1
72 GEL SPEED = 1
73 GEL SLIT
   WIDTH = 0.2
   HEIGHT = 4.0
74 GEL START = 5.0
75 GEL END = 60.0
79 PEAK PICK
   TABULATE
80 MIN PEAK = 0.050
81 SENSITIVITY = 7
```

Appendix 2.3: Varian Cary 1 UV-Visible Spectrophotometer program for the APHII and glycerol kinase assays

The cuvette block was programmed to maintain a temperature of 25°C. OD = 340 nm.

PARAMETERS	
Photometric mode	ABS
Abscissa Mode	MIN
Ordinate (Y) Min/Max	0.0000 / 1.0000
Abscissa (X) Min/Max	0.000 / 2.000
SBW (nm)	4.0
Signal Averaging Time (sec)	0.067
Data Interval	0.0011
Scan Rate	1.000
Lamps On	VIS
Baseline Correct	OFF
Auto Scale	YES
Auto Store Data	YES
Auto Store Report	NO

Appendix 3.1: Resolution of the distributions of topoisomers by 1D ChQ gel electrophoresis

Electrophoresis was carried out as described in section 2.16.1. The concentration of ChQ used was 2.5 μg/ml. All samples were treated with TopI unless otherwise indicated.

Lanes: 1, Top 1; 2, Top 2; 3, Top 2a; 4, Top 3; 5, Top 4; 6, Top 5.

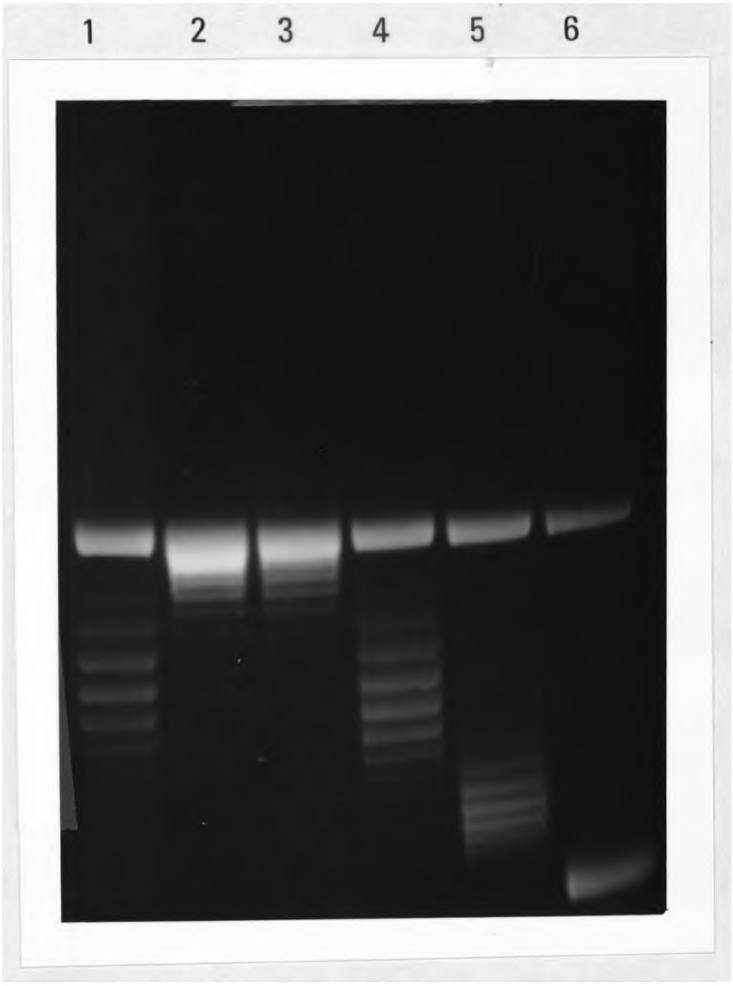

Appendix 3.2: Resolution of the distributions of topoisomers by 1D ChQ gel electrophoresis

Electrophoresis was carried out as described in section 2.16.1. The concentration of ChQ used was 10 ng/ml. All samples were treated with TopI unless otherwise indicated.

Lanes: 1, Top 1; 2, Top 2; 3, Top 2a; 4, Top 3.

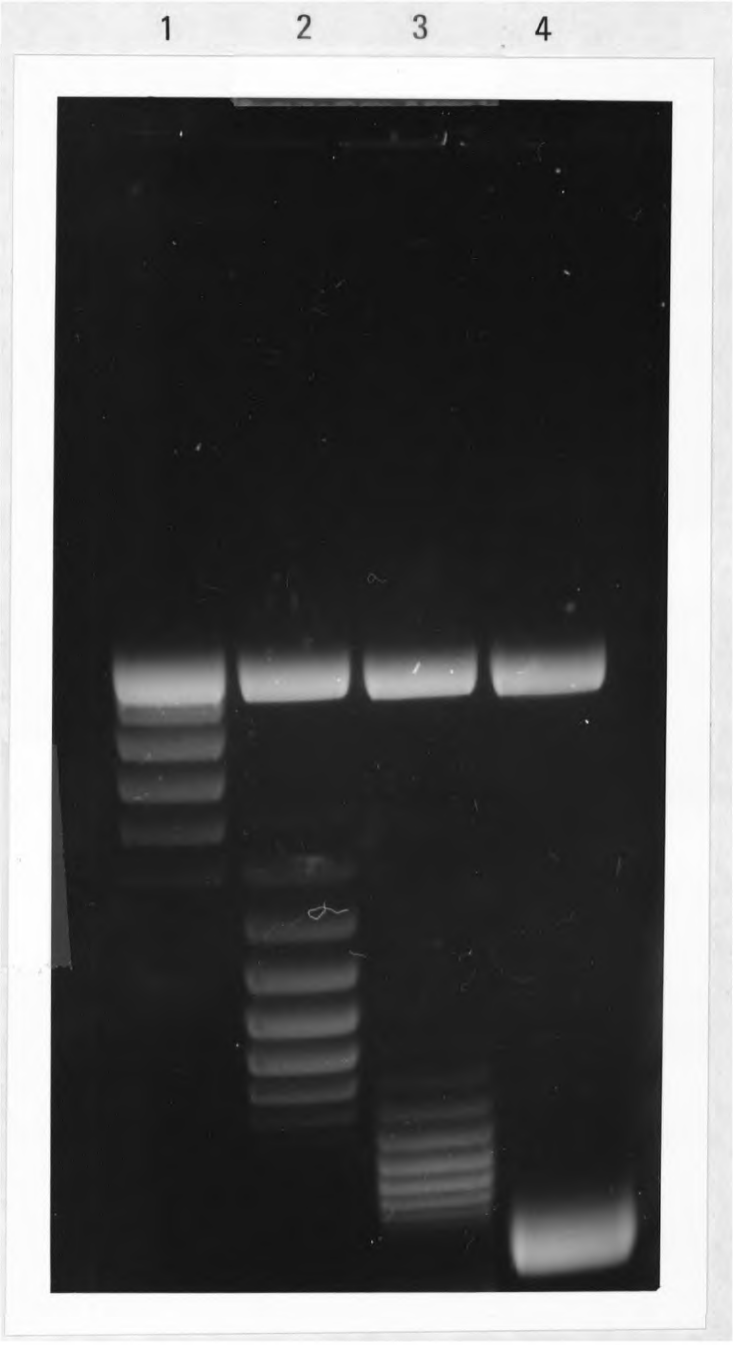

Appendix 3.3: Resolution of the distributions of topoisomers by 1D ChQ gel electrophoresis

Electrophoresis was carried out as described in section 2.16.1. The concentration of ChQ used was 10 μg/ml. All samples were treated with TopI unless otherwise indicated.

Lanes: 1, Top 3; 2, Top 4; 3, Top 5.

Appendix 3.4: Variation in superhelical density of pIJ486 across the growth curve of MT1110(pIJ486), cultured in liquid HMM

"Batch culture 1" was prepared as described in section 2.12. $\%CO_2$ evolution, pH of the medium and superhelical density of pIJ486 sampled from the culture, are shown.

Appendix 3.4

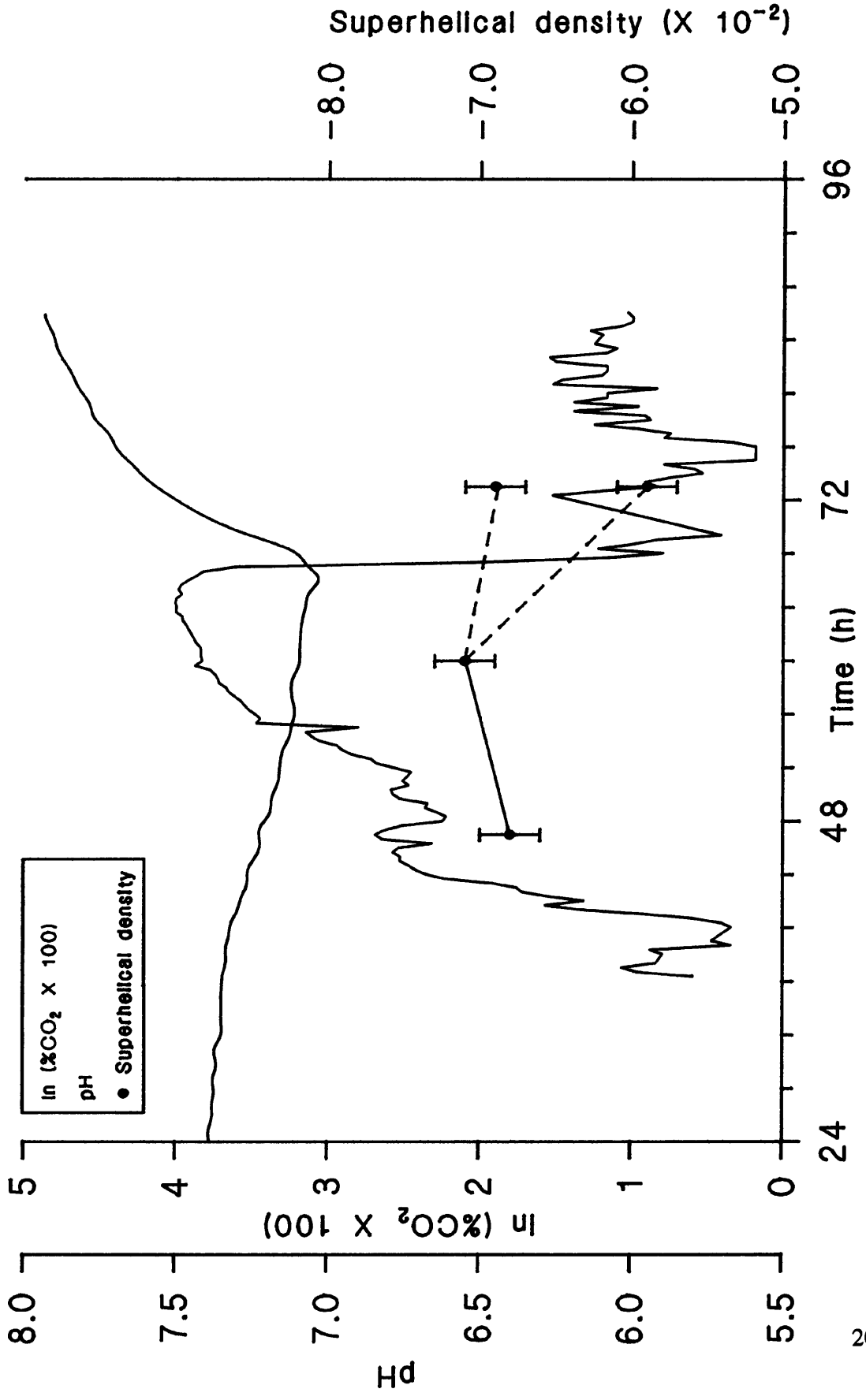
Superhelical density (X 10^{-2})
-8.0
-7.0
-6.0
-5.0
96
72
48
24
Time (h)
ln (%CO_2 X 100)
pH
• Superhelical density
5
4
3
2
1
0
8.0
7.5
7.0
6.5
6.0
5.5
pH

Appendix 3.5: Variation in superhelical density of pIJ486 across the growth curve of MT1110(pIJ486), cultured in liquid HMM

"Batch culture 2" was prepared as described in section 2.12. $\%CO_2$ evolution, pH of the medium and superhelical density of pIJ486 sampled from the culture, are shown.

Appendix 3.5

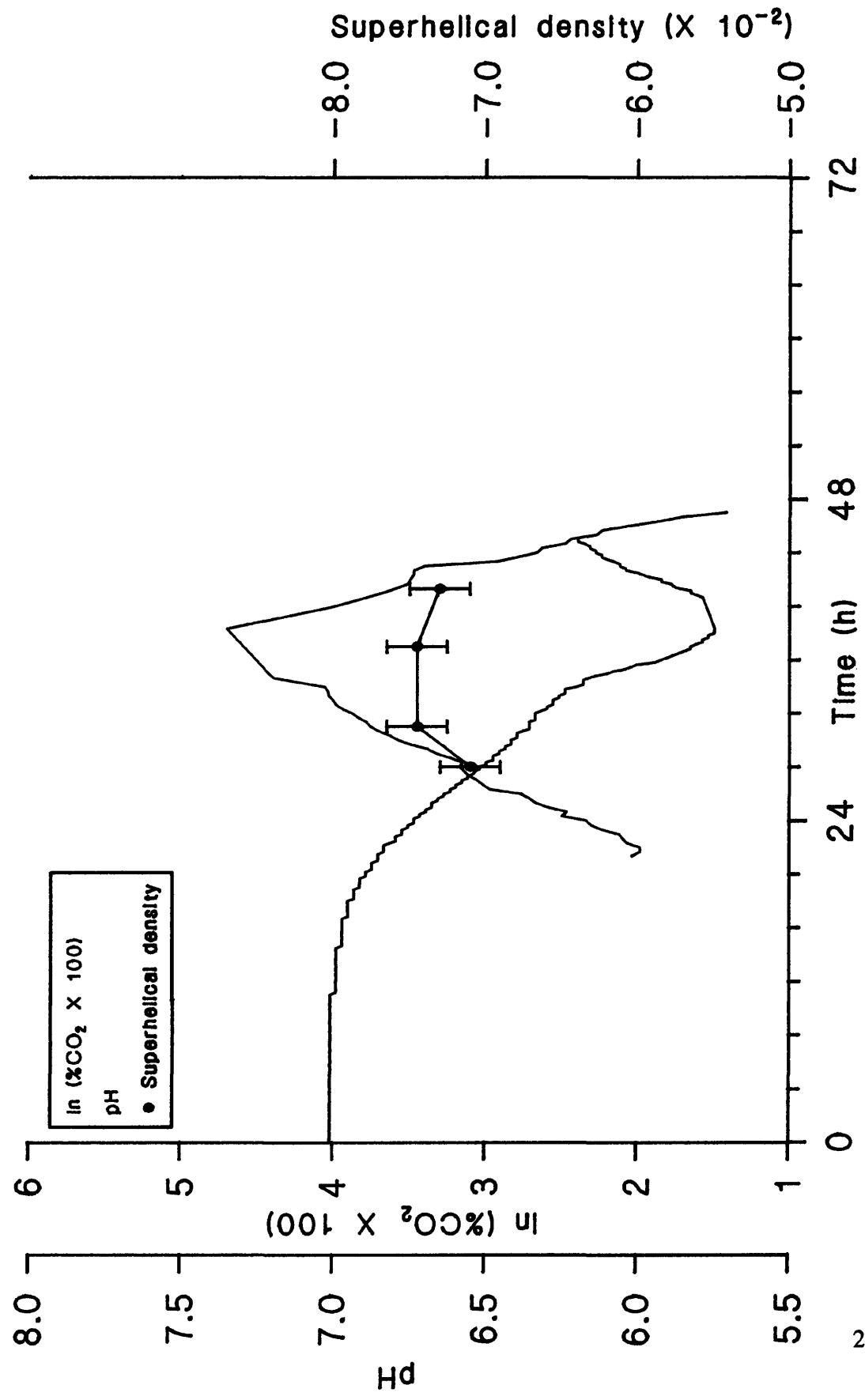
Superhelical density (X 10^{-2})
-8.0
-7.0
-6.0
-5.0
72
48
24
0
Time (h)
ln (%CO_2 X 100)
pH
• Superhelical density
6
5
4
3
2
1
ln (%CO_2 X 100)
8.0
7.5
7.0
6.5
6.0
5.5
pH

Appendix 3.6: Variation in superhelical density of pIJ486 across the growth curve of MT1110(pIJ486), cultured in liquid HMM

"Batch culture 5" was prepared as described in section 2.12. $\%CO_2$ evolution, and superhelical density of pIJ486 sampled from the culture, are shown.

Appendix 3.6

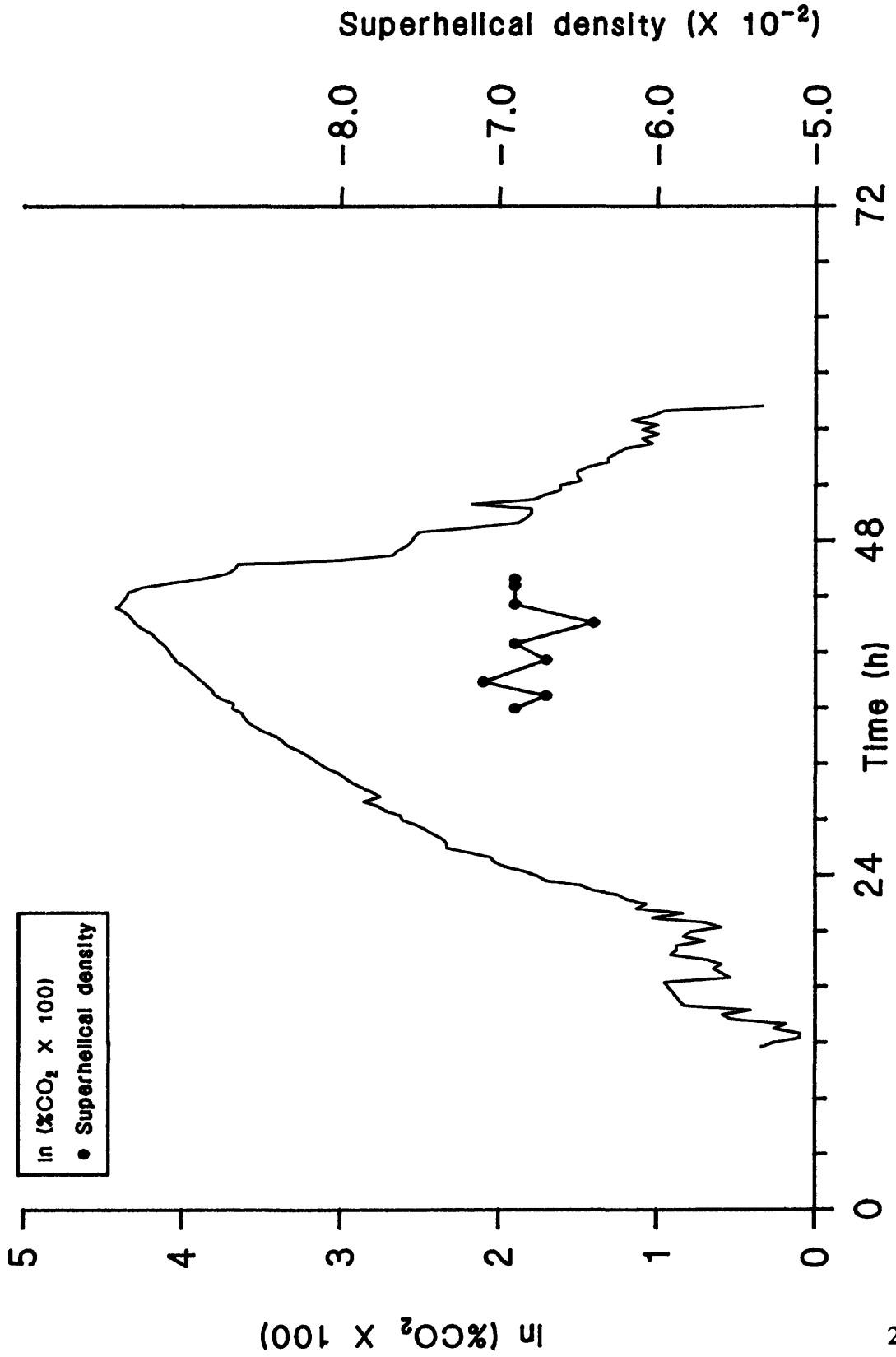
Superhelical density (X 10^{-2})
−8.0
−7.0
−6.0
−5.0
72
48
24
0
Time (h)
5
4
3
2
1
0
ln (%CO_2 X 100)
ln (%CO_2 X 100)
• Superhelical density

Appendix 3.7: Variation in the superhelical density of pIJ486 isolated from surface grown MT1110(pIJ486): experiment 1

Experiment 1, prepared as described in section 2.13, showing the dry weight, pH and variation in the σ of pIJ486 across the growth curve of the culture.

Appendix 3.7

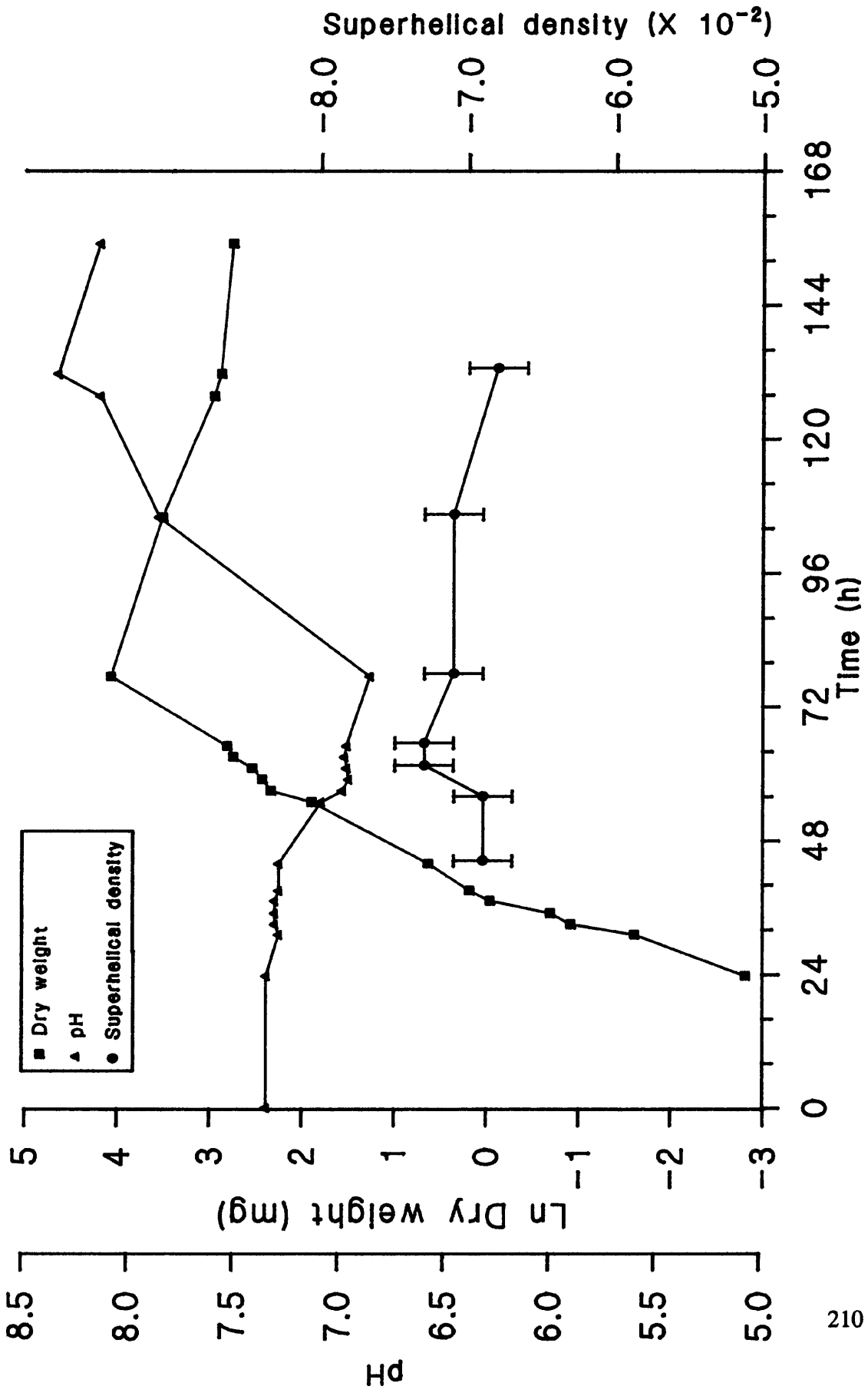
Superhelical density (X 10^{-2})
-8.0
-7.0
-6.0
-5.0
168
144
120
96
72
48
24
0
Time (h)
Dry weight
pH
Superhelical density
5
4
3
2
1
0
-1
-2
-3
Ln Dry weight (mg)
8.5
8.0
7.5
7.0
6.5
6.0
5.5
5.0
pH

Appendix 3.8: Surface grown MT1110(pIJ486) culture (experiment 1): a montage showing the transition phase, from vegetative mycelia to aerial hyphae formation

The mycelia were photographed through a X32, long focal length, microscope objective.

(a) 28 h after inoculation. Note the branched vegetative mycelium.

(b) 48.5 h after inoculation. Note the almost confluent mat of mycelium.

(c) 50 h after inoculation. Note the presence of mycelial "towers" pushed up from the basal vegetative mycelial mat, not to be confused with aerial hyphae.

(d) 54 h after inoculation. Note the appearance of aerial hyphae on one of the mycelial towers.

(e) 59 h after inoculation. Note the mass of aerial hyphae formed on one such mycelial tower; nearly all the vegetative mycelia had undergone the transition to aerial hyphae at this stage.

(f) 101 h after inoculation. Note the appearance of spores towards the tip of some of the aerial hyphae.

Appendix 3.8

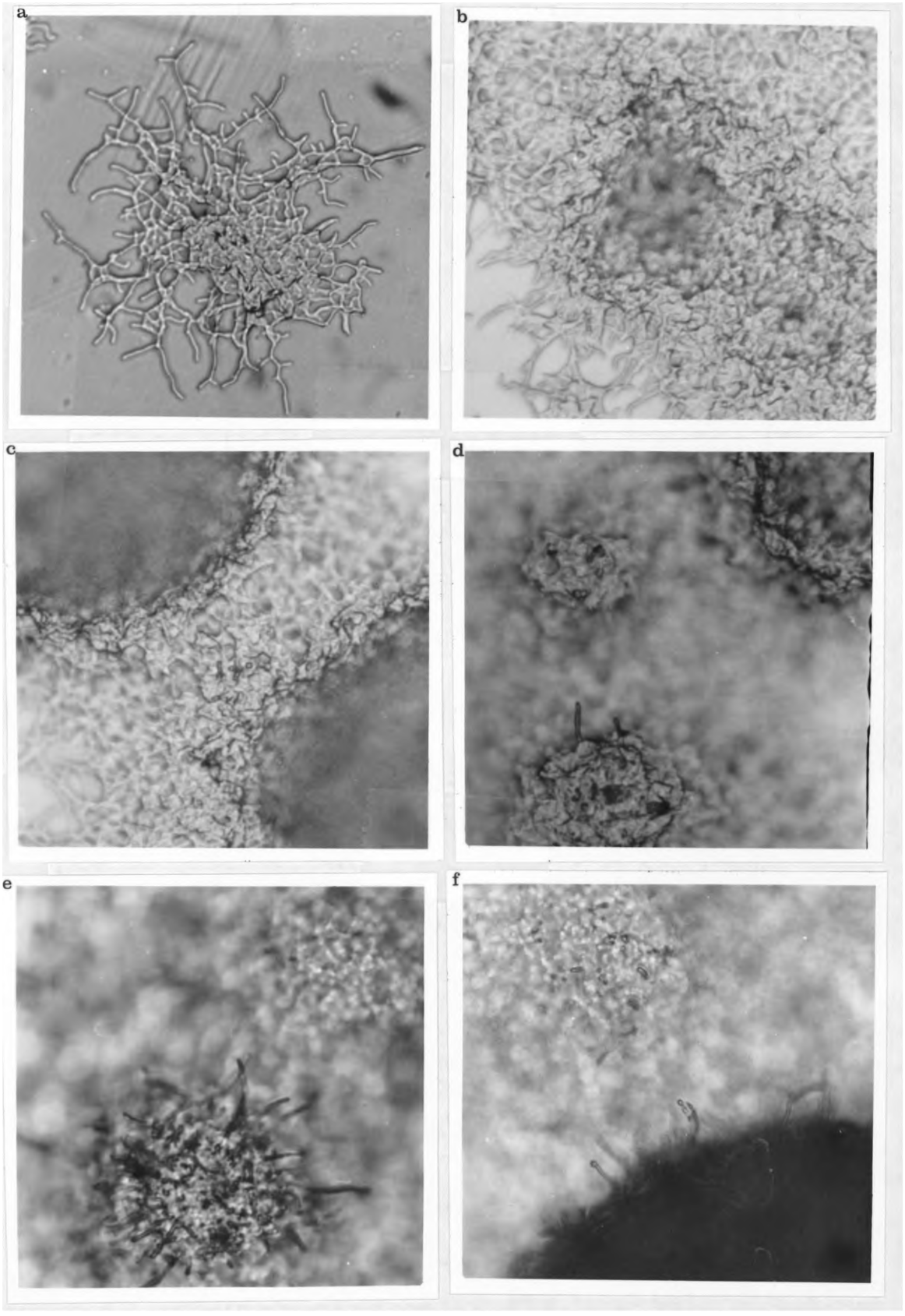

Appendix 3.9: Alignment of the biomass plots from experiments 1 and 2; to determine (by comparison), the transition phase for experiment 1

The data from experiment 2 (Figure 3.7), has been plotted over the same time period data was logged for during experiment 1 (168 h; see Appendix 3.7). As mentioned in the text (section 3.3.2.1), there appears to be a good correlation between the exponential phases and a stalling of growth (indicated by arrows), at 44 h (experiment 2), and 57 h (experiment 1).

Appendix 3.9

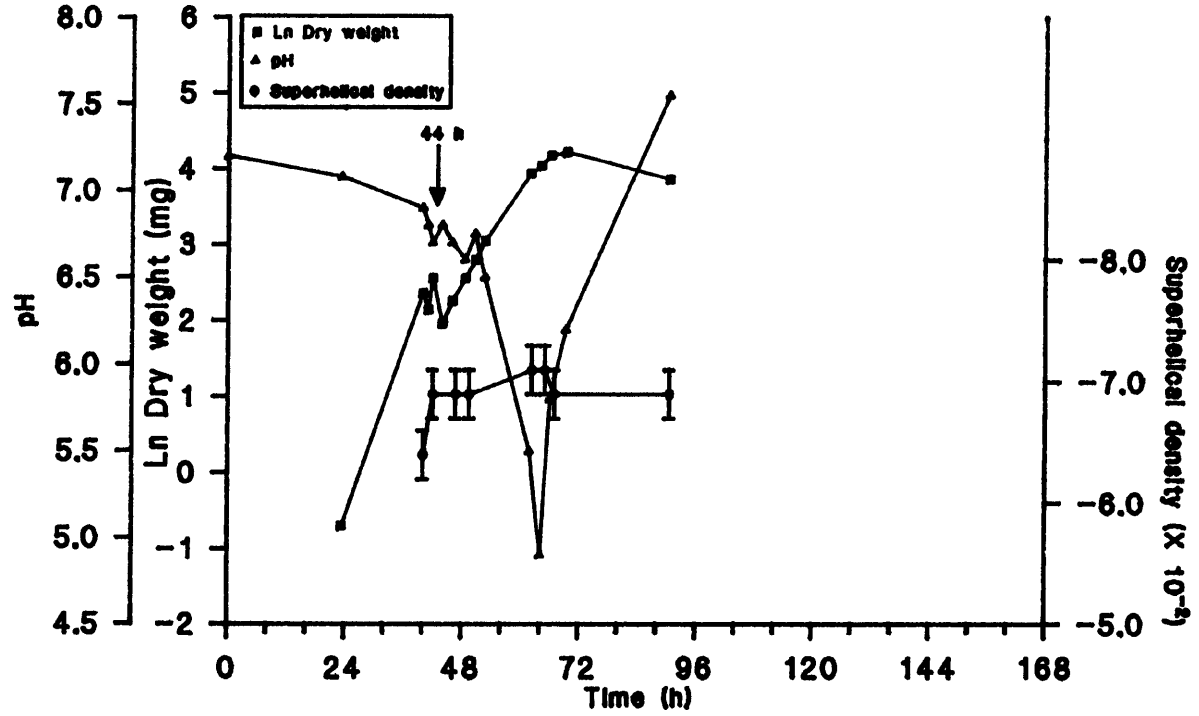
Ln Dry weight
pH
Superhelical density
44 h
pH
Ln Dry weight (mg)
Superhelical density (X 10-3)
Time (h)

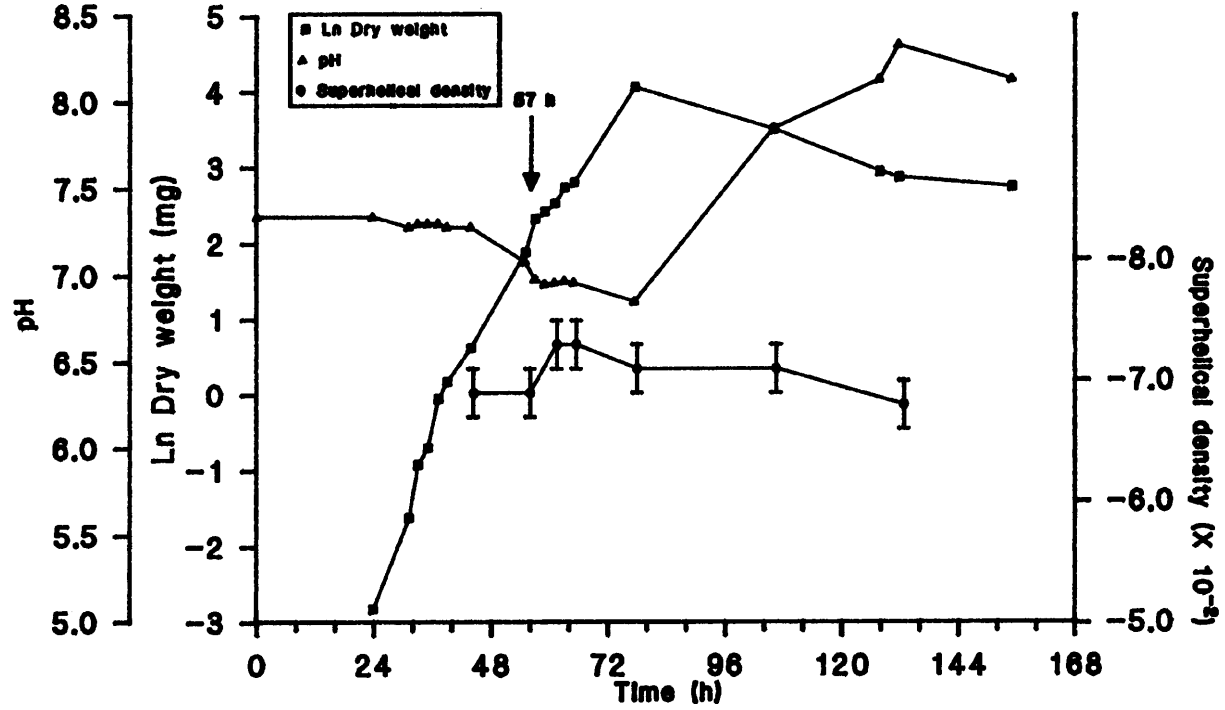
Ln Dry weight
pH
Superhelical density
67 h
pH
Ln Dry weight (mg)
Superhelical density (X 10-3)
Time (h)

Appendix 3.10: Resolution of topoisomers of pJAM180 by 2D ChQ gel electrophoresis

(a): Electrophoresis in the first dimension was carried out essentially as described in section 2.16.2. The 1% TBE gel did not contain ChQ and the topoisomers were pooled and loaded, in a volume of 8 μl, into a single well (2 mm $\varnothing$). The gel was run in 1 X TBE buffer (no ChQ), at 3.5 V/cm for 24 h in the first dimension (D1). The gel was soaked in 2 μg/ml ChQ for 6 h before being run in the second dimension (D2); 90° to the first. The gel was run in 1 X TBE buffer containing 2 μg/ml ChQ at 3 V/cm for 15 h. The gel was destained and photographed as described in section 2.16.2.

(b): 2D gel electrophoresis showing left-handed *Z*-DNA formation by a $(CG)_8$ sequence. Electrophoresis was carried out in 0.5 X TBE buffer. The first dimension (D1), was performed at 4°C in order to prevent helix opening in (A+T)-rich sequences in the plasmid. During the second dimension (D2), 1.8 μg/ml ChQ was included in the electrophoresis buffer. Note the single, co-operative transition corresponding to complete formation by the $(CG)_8$ sequence. The figure and legend are reproduced from Bowater *et al.* (1992). *Z*-DNA formation is indicated by the broken path of the topoisomers. [In D1, the $(CG)_8$ adopts *Z*-DNA and retards the topoisomers negatively supercoiled enough to permit its formation; in D2 ChQ is added, this reduces the $-\sigma$ of the topoisomers, causing the *Z*-DNA to revert to *B*-DNA, resulting in increased mobility of that topoisomer. This resolves it from the topoisomer with the same mobility in D1 (but which did not permit *Z*-DNA formation) causing the break in the path of the topoisomers (see arrow).]

Appendix 3.10

(a)

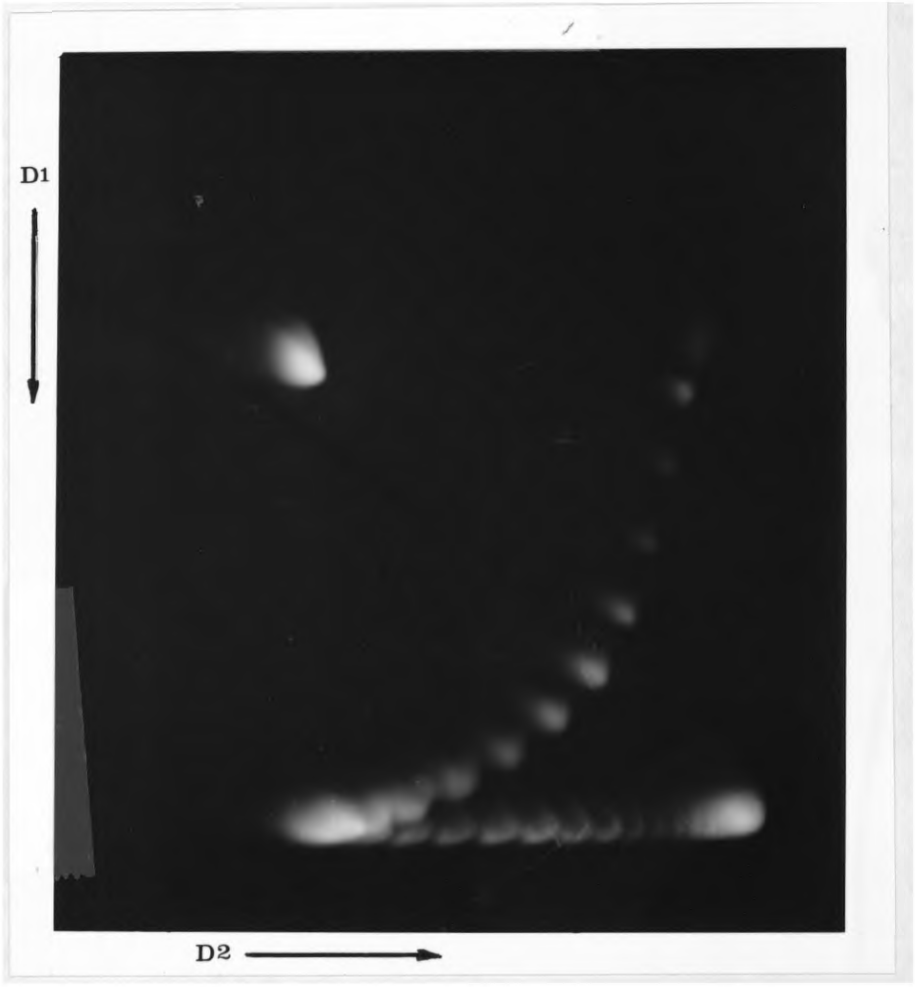

(b)

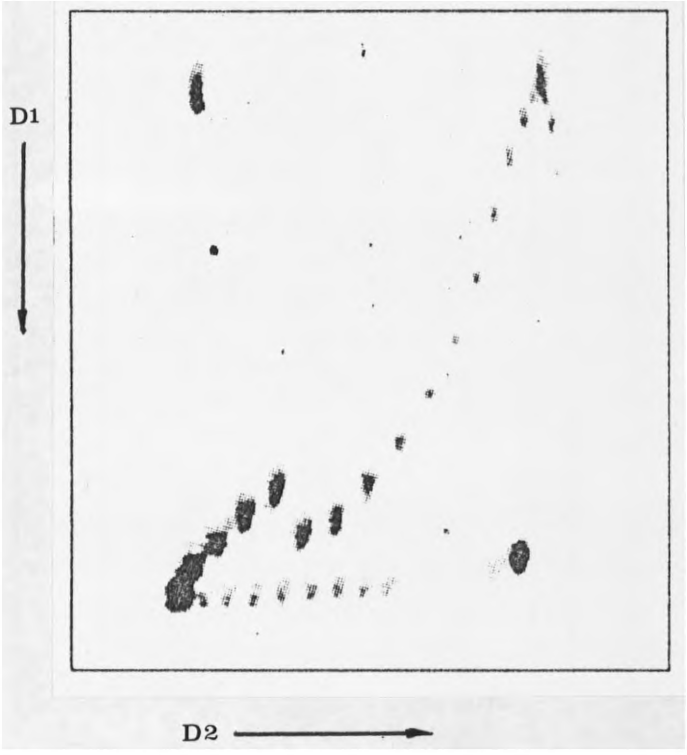

Appendix 4.1: Gradient plate assay of various *gyl*::*neo* fusions in 1326Δ*gylR1*

The gradient plate assay was performed as described in section 2.17.2. Master plates of plasmid-containing *S. lividans* 1326Δ*gylR1* were replica-plated to gradient plates containing kanamycin (0-300 μg/ml), and then to plates without kanamycin as a control for uniform growth. The medium was MMT plus 0.5% glycerol.

1. pJAM130; 2, pJAM150; 3, pJAM120; 4, pJAM135; 5, pJAM145; 6, pJAM140; 7, pJAM125; 8, pIJ486. See Table 2.2 for details of plasmids and Figures where available.

Appendix 4.2: APHII activity versus growth phase

S. lividans 1326Δ*gylR1* containing pJAM125 was pre-germinated as described previously (Hopwood *et al.*, 1985) and used to inoculate 2 l NMMP containing 0.5% glycerol in a 3 l bioreactor to a final OD_{450} of 0.05. The bioreactor conditions were the same as described in section 2.12. Mycelia were harvested at intervals throughout the growth phase and assayed for APHII activity as described in section 2.17.3. $\%CO_2$ evolution and the APHII activity are shown.

Appendix 4.2

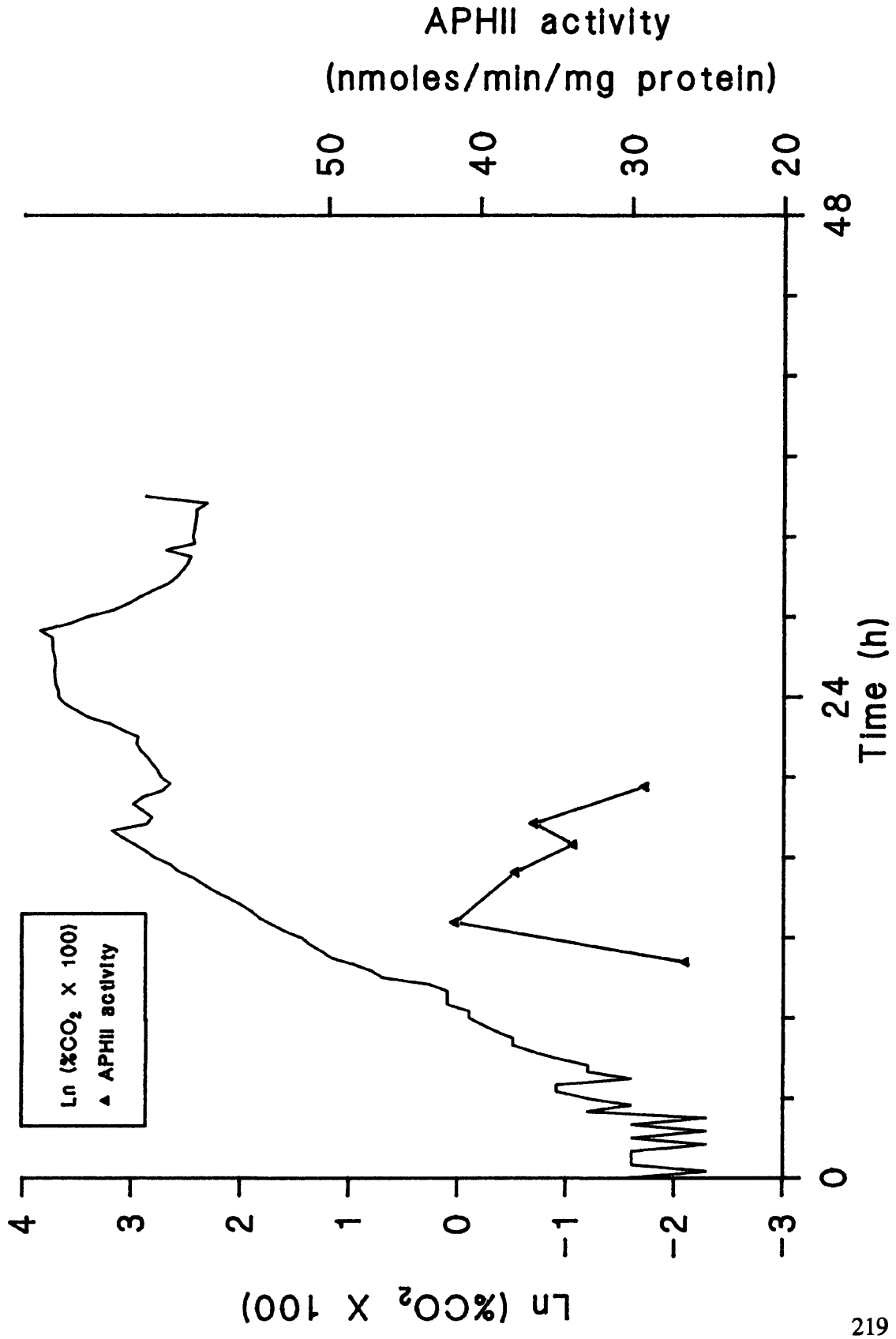
APHII activity
(nmoles/min/mg protein)
50
40
30
20
48
24
0
Time (h)
Ln (%CO2 X 100)
4
3
2
1
0
-1
-2
-3
Ln (%CO2 X 100)
▲ APHII activity

Appendix 4.3: APHII specific activity of the various plasmid constructs in MT1110
grown on solid medium

Fusion	*gylR*	*Z-form* mutant	APHII Specific activity (Units/min/mg protein)
pJAM130	NO	wt.	16.88
pJAM120	YES	wt.	24.12
pJAM135	YES	*I, II*	20.52
pJAM140	YES	*I*	28.14
pJAM145	YES	*II*	14.47
pIJ486	/	/	1.96

Notes:
1. See Table 2.2 for a detailed explanation of the plasmid fusions and Figures where available.
2. "Units" indicates nmoles NADH oxidised.

Appendix 4.4: The *gylP1* promoter region of different *Streptomyces* spp.

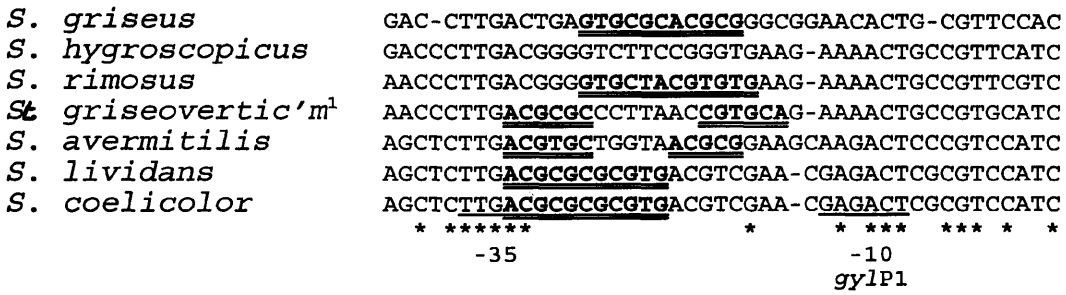

Notes:

1: *St.griseovertic'm = Streptoverticillium griseoverticillatum.*

The alternating purine-pyrimidine sequences are doubled underlined and shown in bold.

[Note that the sequence in *S. rimosus* will contain a *Z-Z* junction if it forms *Z*-DNA (section 1.8.4). *S. hygroscopicus* does not contain any *Z-form* sequences > 4 bp long.]

The -35 and -10 regions are underlined and conserved bases are indicated with a "*".

Sequence data is taken from Paget (1994).

Bibliography

Adamidis, T. and Champness, W. (**1992**). Genetic analysis of *absB*, a *Streptomyces coelicolor* locus involved in global antibiotic regulation. J. Bacteriol. *174*, 4622-4628

Angell, S., Schwarz, E. and Bibb, M. J. (**1992**). The glucose kinase gene of *Streptomyces coelicolor* A3(2): its nucleotide sequence, transcriptional analysis and role in glucose repression. Mol. Microbiol. *6*, 2833-2844

Angell, S., Lewis, C. G., Buttner, M. J. and Bibb, M. J. (**1994**). Glucose repression in *Streptomyces coelicolor* A3(2): a likely regulatory role for glucose kinase. Mol. Gen. Genet. *244*, 135-143

Babcock, M. J. and Kendrick, K. E. (**1990**). Transcriptional and translational features of a sporulation gene of *Streptomyces griseus*. Gene *95*, 57-63

Balke, V. L. and Gralla, J. D. (**1987**). Changes in the linking number of supercoiled DNA accompany growth transitions in *Escherichia coli*. J. Bacteriol. *169*, 4499-4506

Bates, A. D. and Maxwell, A. (**1993**). In Focus: DNA Topology. D. Rickwood, Ed. (IRL Press, Oxford)

Bauer, W. and Vinograd, J. (**1968**). The interaction of closed circular DNA with intercalative dyes: I. The superhelix density of SV40 DNA in the presence and absence of dye. J. Mol. Biol. *33*, 141-172

Bernan, V., Filpula, D., Herber, W., Bibb, M. and Katz, E. (**1985**). The nucleotide sequence of the tyrosinase gene from *Streptomyces antibioticus* and characterization of the gene product. Gene *37*, 101-110

Bernues, J., Beltran, R., Casanovas, J. M. and Azorin, F. (**1989**). Structural polymorphism of homopurine-homopyrimidine sequences: the secondary DNA structure adopted by a $d(GA{\cdot}CT)_{22}$ sequence in the presence of zinc ions. Embo. J. *8*, 2087-2094

Birch, A., Haüsler, A., Rüttner, C. and Hütter, R. (**1991**). Chromosomal deletion and rearrangement in *Streptomyces glaucescens*. J. Bacteriol. *173*, 3531-3538

Bliska, J. B. and Cozzarelli, N. R. (**1987**). Use of site-specific recombination as a probe of DNA structures and metabolism *in vivo*. J. Mol. Biol. *194*, 205-218

Booth, I. R. and Higgins, C. F. (**1990**). Enteric bacteria and osmotic stress: intracellular potassium glutamate as a secondary signal of osmotic stress? FEMS Microbiol. Rev. *75*, 239-246

Borowiec, J. A. and Gralla, J. D. (**1987**). All three elements of the *lac* p^s promoter mediate its transcriptional response to DNA supercoiling. J. Mol. Biol. *194*, 89-97

Borowiec, J. A. and Gralla, J. D. (**1985**). Supercoiling response of the *lac* ps promoter *in vitro*. J. Mol. Biol. *184*, 587-598

Botchan, M., Topp, W. and Sambrook, J. (**1979**). Studies on simian virus 40 excision from cellular chromosomes. Cold Spring Harbor Symp. Quant. Biol. *43*, 709-719

Bouthier de la Tour, C., Portemer, C., Huber, R., Forterre, P. and Duguet, M. (**1991**). Reverse gyrase in thermophilic eubacteria. J. Bacteriol. *173*, 3921-3923

Bowater, R., Aboul-Ela, F. and Lilley, D. M. J. (**1992**). Two-dimensional gel electrophoresis of circular DNA topoisomers. Meth. Enzymol. *212*, 105-120

Brahms, J. G., Dargouge, O., Brahms, S., Ohara, Y. and Vagner, V. (**1985**). Activation and inhibition of transcription by supercoiling. J. Mol. Biol. *191*, 455-465

Bramhill, D. and Kornberg, A. (**1988**). Duplex opening by dnaA protein at novel sequences of replication at the origin of the *E. coli* chromosome. Cell *52*, 743-755

Brown, K. L., Wood, S. and Buttner, M. J. (**1992**). Isolation and characterisation of the major vegetative RNA polymerase of *Streptomyces coelicolor* A3(2); renaturation of a sigma subunit using GroEL. Mol. Microbiol. *6*, 1133-1139

Buttner, M. J. (**1989**). RNA polymerase heterogenity in *Streptomyces coelicolor* A3(2). Mol. Microbiol. *3*, 1653-1659

Buttner, M. J., Smith, A. M. and Bibb, M. J. (**1988**). At least three different RNA polymerase holoenzymes direct transcription of the agarase gene (*dagA*) of *Streptomyces coelicolor* A3(2). Cell *52*, 599-607

Caballero, J. L., Malpartida, F. and Hopwood, D. A. (**1991**). Transcriptional organization and regulation of an antibiotic export complex in the producing *Streptomyces* culture. Mol. Gen. Genet. *228*, 372-380

Champness, W., Riggle, P., Adamidis, T. and Vandervere, P. (**1992**). Identification of *Streptomyces coelicolor* genes involved in regulation of antibiotic synthesis. Gene *115*, 55-60

Charbonnier, F. and Forterre, P. (**1994**). Comparison of plasmid DNA topology among mesophilic and thermophilic eubacteria and archaebacteria. J. Bacteriol. *176*, 1251-1259

Chater, K. F. (**1975**). Construction and phenotypes of double sporulation deficient mutants in *Streptomyces coelicolor* A3(2). J. Gen. Microbiol. *87*, 312-325

Chater, K. F. (**1989a**). Sporulation in *Streptomyces*. In Regulation of Prokaryotic Development. I. Smith, R. A. Slepecky and P. Setlow Eds. (American Society for Microbiology, Washington, DC), pp. 277-299

Chater, K. F. (**1989b**). Multilevel regulation of *Streptomyces* differentiation. Trends Genet. *5*, 372-376

Chater, K. F. (**1990**). The improving prospects for yield increase by genetic engineering in antibiotic-producing streptomycetes. Bio/Technology *8*, 115-121

Chater, K. F. (**1993**). Genetics of differentiation in *Streptomyces*. Annu. Rev. Microbiol. *47*, 685-713

Chater, K. F. and Bibb, M. J. (**1995**). Regulation of bacterial antibiotic production. In Products of Secondary Metabolism. Vol. 7. H. Kleinkauf, H. von Döhren Eds. (VCH, Weinheim, Germany), in press

Chater, K. F. and Merrick, M. J. (**1979**). Streptomycetes. In Developmental Biology of Prokaryotes. J. H. Parish Ed. (Blackwell Scientific Publications, Oxford), pp. 93-114

Chater, K. F., Bruton, C. J., Plaskitt, K. A., Buttner, M. J., Méndez, C. and Helmann, J. D. (**1989**). The developmental fate of *S. coelicolor* hyphae depends upon a gene product homologous with the motility σ factor of *B. subtilis*. Cell *59*, 133-143

Crueger, W. and Crueger, A. (**1982**). Biotechnology: a textbook of industrial microbiology. T. D. Brock, Ed. (Science Tech, Inc., Madison)

Dagert, M. and Ehrlich, S. D. (**1979**). Prolonged incubation in calcium chloride improves the competence of *Escherichia coli* cells. Gene *6*, 23-28

Davis, N. K. and Chater, K. F. (**1990**). Spore colour in *Streptomyces coelicolor* A3(2) involves the developmentally regulated synthesis of a compound biosynthetically related to polyketide antibiotics. Mol. Microbiol. *4*, 1679-1691

Dean, F., Krasnow, M. A., Otter, R., Matzuk, M. M., Spengler, S. J. and Cozzarelli, N. R. (**1983**). *Escherichia coli* type-I topoisomerases: identification, mechanism, and role in recombination. Cold Spring Harbour Symp. Quant. Biol. *47*, 769-777

Delic, I., Robbins, P. and Westphaling, J. (**1992**). Direct repeat sequences are implicated in the regulation of two *Streptomyces* chitinase promoters that are subject to carbon catabolite control. Proc. Natl. Acad. Sci. USA *89*, 1885-1889

Demain, A. L., Aharonowitz, Y. and Martin, J.-F. (**1983**). Metabolic control of secondary biosynthetic pathways. In Biochemistry and Genetic Regulation of Commercially Important Antibiotics. L. C. Vining Ed. (Addison-Wesley, London), pp. 49-72

DiNardo, S., Voelkel, K. A., Sternglanz, R., Reynolds, A. E. and Wright, A. (**1982**). *Escherichia coli* DNA Topoisomerase I mutants have compensatory mutants in DNA gyrase genes. Cell *31*, 43-51

DiNardo, S., Voelkel, K. and Sternglanz, R. (**1984**). DNA topoisomerase II mutant of *Saccharomyces cerevisiae*: topoisomerase II is required for segregation of daughter molecules at the termination of replication. Proc. Natl. Acad. Sci. USA *81*, 2616-2620

Distler, J., Ebert, A., Mansouri, K., Pissowotzki, K., Stockmann, M. and Piepersberg, W. (**1987**). Gene cluster for streptomycin biosynthesis in *Streptomyces griseus*: nucleotide sequence of three genes and analysis of transcriptional activity. Nucl. Acids Res. *15*, 8041-8056

Dorman, C. J., Barr, G. C., Ni Bhriain, N. and Higgins, C. J. (**1988**). DNA supercoiling and the anaerobic and growth phase regulation of *tonB* gene expression. J. Bacteriol. *170*, 2816-2826

Doull, J. L. and Vining, L. C. (**1990**). Nutritional control of actinorhodin production by *Streptomyces coelicolor* A3(2): suppressive effects of nitrogen and phosphate. Appl. Microbiol. Biotechnol. *32*, 449-454

Drew, H. R., Weeks, J. R. and Travers, A. A. (**1985**). Negative supercoiling induces spontaneous unwinding of a bacterial promoter. Embo. J. *4*, 1025-1032

Drlica, K. (**1992**). Control of bacterial DNA supercoiling. Mol. Microbiol. *6*, 425-433

Drlica, K. and Rouvière-Yaniv, J. (**1987**). Histone-like proteins in bacteria. Microbiol. Rev. *51*, 301-319

Drlica, K. and Snyder, M. (**1978**). Superhelical *Escherichia coli* DNA: relaxation by coumermycin. J. Mol. Biol. *120*, 145-154

Droge, P. (**1994**). Protein tracking-induced supercoiling of DNA: a tool to regulate DNA transactions *in vivo*? Bioessays *16*, 91-99

Duguet, M. (**1993**). The helical repeat of DNA at high temperature. Nucl. Acids Res. *21*, 463-468

Eckhardt, T., Strickler, J., Gorniak, L., Burnett, W. V. and Fare, L. R. (**1987**). Characterization of the promoter, signal sequence, and amino terminus of a secreted β-galactosidase from *Streptomyces lividans*. J. Bacteriol. *169*, 4249-4256

Eismann, E. R. and Müller-Hill, B. (**1990**). *lac* repressor forms stable loops *in vitro* with supercoiled wild-type *lac* DNA containing all three natural *lac* operators. J. Mol. Biol. *213*, 763-775

Fernández-Moreno, M. A., Caballero, J. L., Hopwood, D. A. and Malpartida, F. (**1991**). The *act* cluster contains regulatory and antibiotic export genes, direct targets for translational control by the *bldA* tRNA gene of *Streptomyces*. Cell *66*, 769-780

Fernández-Moreno, M. A., Martín-Triana, A. J., Martínez, E., Niemi, J., Kieser, H. M., Hopwood, D. A. and Malpartida, F. (**1992**). *abaA*, a new pleiotropic regulatory locus for antibiotic production in *Streptomyces coelicolor*. J. Bacteriol. *174*, 2958-2967

Filutowicz, M. and Jonczyk, P. (**1983**). The *gyrB* gene product functions in both initiation and chain polymerization of *Escherichia coli* chromosome replication: suppression of the initiation efficiency in *gyrB*-ts mutants a class of *rpoB* mutants. Mol. Gen. Genet. *191*, 282-287

Franklin, R. E. and Gosling, R. (**1953**). Molecular configuration in sodium thymonucleate. Nature *171*, 740-741

von Freiesleben, U. and Rasmussen, K. V. (**1992**). The level of supercoiling affects the regulation of DNA replication in *Escherichia coli*. Res. Microbiol. *143*, 655-663

Furth, M. E., Blattner, F. R., McLeester, C. and Dove, W. F. (**1977**). Genetic structure of the replication origin of bacteriophage lambda. Science *198*, 1046-1051

Gellert, M., Mizuuchi, K., O'Dea, M. H. and Nash, H. A. (**1976**). DNA gyrase: an enzyme that introduces superhelical turns into DNA. Proc. Natl. Acad. Sci. USA *73*, 3872-3876

Gladek, A. and Zakrzewska, J. (**1984**). Genome size of *Streptomyces*. FEMS Microbiol. Lett. *24*, 73-76

Glikin, G. C., Jovin, T. M. and Arndt-Jovin, D. J. (**1991**). Interactions of Drosphilia DNA topoisomerase II with left-handed *Z*-DNA in supercoiled minicircles. Nucl. Acids Res. *19*, 7139-7144

Glickman, B. W. and Ripley, L. S. (**1984**). Structural intermediates of deletion mutagenesis: a role for palindromic DNA. Proc. Natl. Acad. USA *81*, 512-516

Godden, B., Legon, T., Helvenstein, P. and Penninckx, M. (**1989**). Regulation of the production of hemicellulytic and cellulolytic enzymes by a *Streptomyces* spp. growing on lignocellulose. J. Gen. Microbiol. *135*, 285-292

Graeme-Cook, K. A., May, G., Bremer, E. and Higgins, C. F. (**1989**). Osmotic regulation of porin expression: a role for DNA supercoiling. Mol. Microbiol. *3*, 1287-1294

Gralla, J. D. (**1991**). Transcriptional control-lessons from an *E. coli* promoter database. Cell *66*, 415-418

Gramajo, H. C., Takano, E. and Bibb, M. J. (**1993**). Stationary-phase production of the antibiotic actinorhodin in *Streptomyces coelicolor* A3(2) is transcriptionally regulated. Mol. Microbiol. *7*, 837-845

Granozzi, C., Billetta, R., Passantino, R., Sollazzo, M. and Puglia, A.-M. (**1990**). A breakdown in macromolecular synthesis preceding differentiation in *Streptomyces coelicolor* A3(2). J. Gen. Microbiol. *136*, 713-716

Grau, R., Gardiol, D., Glikin, G. C. and de Mendoza, D. (**1994**). DNA supercoiling and the thermal regulation of unsaturated fatty acid synthesis in *Bacillus subtilis*. Mol. Microbiol. *11*, 933-941

Greaves, D. R., Patient, R. K. and Lilley, D. M. J. (**1985**). Facile cruciform formation by an $(A\text{-}T)_{34}$ sequence from a *Xenopus* globin gene. J. Mol. Biol. *185*, 461-478

Gumpert, J., Sarfert, E. and Zimmer, C. (**1986**). Chromosome structure and DNA-binding proteins in streptomycetes. In Biological, Biochemical and Biomedical Aspects of Actinomycetes. G. Szabó, S. Biró and M. Goodfellow Eds. (Akadémiai Kiadó, Budapest), pp. 453-463

Haber, R. and Adhya, S. (**1988**). Interaction of spatially separated protein-DNA complexes for control of gene expression: Operator conversions. Proc. Natl. Acad. Sci. USA *85*, 9683-9687

Haniford, D. B. and Pulleybank, D. E. (**1983**). Facile transition of poly[d(TG) x d(CA)] into a left-handed helix in physiological conditions. Nature *302*, 632-634

Hara, O., Horinouchi, S., Uozumi, T. and Beppu, T. (**1983**). Genetic analysis of A-factor synthesis in *Streptomyces coelicolor* A3(2) and *Streptomyces griseus*. J. Gen. Microbiol. *129*, 2939-2944

Hawley, D. K. and McClure, W. R. (**1983**). Compilation and analysis of *Escherichia coli* promoter DNA sequences. Nucl. Acids Res. *11*, 2237-2255

Heery, D. M., Gannon, F. and Powell, R. (**1990**). A simple method for subcloning DNA fragments from gel slices. Trends Genet. *6*, 173

ten Heggeler-Bordier, B., Wahli, W., Adrian, M., Stasiak, A. and Dubochet, J. (**1992**). The apical localization of transcribing RNA-polymerases on supercoiled DNA prevents their rotation around the template. Embo. J. *11*, 667-672

Higgins, C. F., Dorman, C. J., Stirling, D. A., Waddell, L., Booth, I. R., May, G. and Bremer, E. (**1988**). A physiological role for DNA supercoiling in the osmotic regulation of gene expression in *S. typhimurium* and *E. coli*. Cell *52*, 569-584

Hindle, Z. and Smith, C. P. (**1994**). Substrate induction and catabolite repression of the *Streptomyces coelicolor* glycerol operon are mediated through the GylR protein. Mol. Microbiol. *12*, 737-745

Hobbs, G., Obanye, A. I. C., Petty, J., Mason, C., Barrat, E., Gardner, D. C. J., Flett, F., Smith, C. P., Broda, P. and Oliver, S. G. (**1992**). An integrated approach to studying regulation of production of the antibiotic methylenomycin by *Streptomyces coelicolor* A3(2). J. Bacteriol. *174*, 1487-1494

Hodgson, D. A. (**1982**). Glucose repression of carbon source uptake and metabolism in *Streptomyces coelicolor* A3(2) and its perturbation in mutants resistant to 2-deoxyglucose. J. Gen. Microbiol. *128*, 2417-2430

Hodgson, D. A. (**1994**). General physiology - 1: Carbon metabolism. In Handbook of Biotechnology. *Streptomyces*. E. M. H. Wellington and D. A. Hodgson Eds. (Plenum, London), in press

Hoggarth, J. H., Cushing, K. E., Mitchell, J. I. and Ritchis, D. A. (**1994**). Induction of resistance to novobiocin in the novobiocin-producing organism *Streptomyces niveus*. FEMS Microbiol. Lett. *116*, 131-136

Hoheisel, J. D. and Pohl, F. M. (**1987**). Searching for potential *Z*-DNA in genomic *Escherichia coli* DNA. J. Mol. Biol. *193*, 447-464

Hopwood, D. A. (**1967**). A possible circular symmetry of the linkage map of *Streptomyces coelicolor*. J. Cell. Physiol. *70*, 7-10

Hopwood, D. A. (**1988**). Towards an understanding of gene switching in *Streptomyces*, the basis of sporulation and antibiotic production. Proc. R. Soc. Lond. B *235*, 121-138

Hopwood, D. A. and Kieser, T. (**1990**). The *Streptomyces* Genome. In The Bacterial Chromosome. K. Drlica and M. Riley Eds. (American Society for Microbiology, Washington, DC), pp. 147-162

Hopwood, D. A., Bibb, M. J., Chater, K. F., Kieser, T., Bruton, C. J., Kieser, H. M., Lydiate, D. J., Smith, C. P., Ward, J. M. and Schrempf, H. (**1985a**). Genetic Manipulation of *Streptomyces*. A Laboratory Manual. (The John Innes Foundation, Norwich)

Hopwood, D. A., Malpartida, F., Kieser, H. M., Ikeda, H., Duncan, J., Fujii, I., Rudd, B. A., Floss, H. G. and Omura, S. (**1985b**). Production of 'hybrid' antibiotics by genetic engineering. Nature *314*, 642-644

Hopwood, D. A., Kieser, T., Wright, H. M., Bibb, M. J. (**1983**). Plasmids, recombination and chromosome mapping in *Streptomyces lividans* 66. J. Gen. Microbiol. *129*, 2257-2269

Hopwood, D. A., Bibb, M. J., Chater, K. F. and Kieser, T. (**1987**). Plasmid and phage vectors for cloning and analysis in *Streptomyces*. Meth. Enzymol. *153*, 116-166

Horinouchi, S. and Beppu, T. (**1992**). Regulation of secondary metabolism and cell differentiation in *Streptomyces*: A-factor as a microbial hormone and the AfsR protein as a component of a two-component regulatory system. Gene *115*, 167-172

Horinouchi, S., Hara, O. and Beppu, T. (**1983**). Cloning of a pleiotropic gene that positively controls biosynthesis of A-factor, actinorhodin, and prodigiosin in *Streptomyces coelicolor* A3(2) and *Streptomyces lividans*. J. Bacteriol. *155*, 1238-1248

Hsieh, L.-S., Burger, R. M. and Drlica, K. (**1991a**). Bacterial DNA supercoiling and [ATP]/[ADP]. Changes associated with a transition to anaerobic growth. J. Mol. Biol. *219*, 443-450

Hsieh, L.-S., Rouvière-Yaniv, J. and Drlica, K. (**1991b**). Bacterial DNA supercoiling and [ATP]/[ADP]: changes associated with salt shock. J. Bacteriol. *173*, 3914-3917

Hütter, R. and Eckhardt, T. (**1988**). Genetic manipulation. In Actinomycetes in Biotechnology. M. Goodfellow, S. T. Williams and M. Mordarski Eds. (Academic Press, London), pp. 89-184

Ikeda, H., Seno, E. T., Bruton, C. J. and Chater, K. F. (**1984**). Genetic mapping, cloning and physiological aspects of the glucose kinase gene of *Streptomyces coelicolor*. Mol. Gen. Genet. *196*, 501-507

Ikeda, H. (**1990**). DNA topoisomerase-mediated illegitimate recombination. In DNA Topology and its Biological Effects. N. R. Cozzarelli and J. C. Wang Eds. (Cold Spring Harbor Laboratory Press, Cold Spring Harbor, NY), pp.341-359

Ikeda, H., Moriya, K., Matsumoto, T. (**1981**). *In vitro* study of illegitimate recombination: involvement of DNA gyrase. Cold Spring Harbor Symp. Quant. Biol. *45*, 399-408

Ikeda, H., Kawasaki, I. and Gellert, M. (**1984**). Mechanism of illegitimate recombination: common sites for recombinant and cleavage mediated by *E. coli* DNA gyrase. Mol. Gen. Genet. *196*, 546-549

Ikeda, H., Aoki, K., Naito, A. (**1982**). Illegitimate recombination mediated *in vitro* by DNA gyrase of *Escherichia coli*: structure of recombinant DNA molecules. Proc. Natl. Acad. Sci. USA *79*, 3724-3728

Janssen, G. R., Ward, J. M. and Bibb, M. J. (**1989**). Unusual transcriptional and translational features of the aminoglycoside phosphotransferase gene (*aph*) from *Streptomyces fradiae*. Genes Dev. *3*, 415-429

Janssen, G. R. and Bibb, M. J. (**1993**). Derivatives of pUC18 that have *Bgl*II sites flanking a modified multiple cloning site that retain the ability to identify recombinant clones by visual screening of *Escherichia coli* colonies. Gene *124*, 133-134

Jaworski, A., Hsieh, W.-T., Blaho, J. A., Larson, J. E. and Wells, R. D. (**1987**). Left-handed DNA *in vivo*. Science *238*, 773-777

Jaworski, A., Higgins, N. P., Wells, R. D. and Zacharias, W. (**1991**). Topoisomerase mutants and physiological conditions control supercoiling and *Z*-DNA formation *in vivo*. J. Biol. Chem. *266*, 2576-2581

Jiang, H., Zacharias, W. and Amirhaeri, S. (**1991**). Potassium permanganate as an *in situ* probe for *B-Z* and *Z-Z* junctions. Nucl. Acids Res. *19*, 6943-6948

Jones, P. G., Krah, R., Tafuri, S. R. and Wolffe, A. (**1992**). DNA gyrase, CS7.4, and the cold-shock response in *Escherichia coli*. J. Bacteriol. *174*, 5798-5802

Jyothirmai, G. and Mishra, R. K. (**1994**). Differential influence of DNA supercoiling on *in vivo* strength of promoters varying in structure and organisation in *E. coli*. FEBS. Lett. *340*, 189-192

Kato, J., Nishimura, Y., Imamura, R., Niki, H., Hiraga, S. and Suzuki, H. (**1990**). New topoisomerase essential for chromosome segregation in *E. coli*. Cell *63*, 393-404

Keller, W. (**1975**). Determination of the number of superhelical turns in simian virus 40 DNA by gel electrophoresis. Proc. Natl. Acad. Sci. USA *72*, 4876-4880

Kieser, H. M., Kieser, T. and Hopwood, D. A. (**1992**). A combined genetic and physical map of the *Streptomyces coelicolor* A3(2) chromosome. J. Bacteriol. *174*, 5496-5507

Kim, R. A. and Wang, J. C. (**1989**). Function of DNA topoisomerases as replication swivels in *Saccharomyces cerevisiae*. J. Mol. Biol. *208*, 257-267

Kim, J. I., Heuser, J. and Cox, M. M., (**1989**). Enhanced RecA protein binding to *Z*-DNA represents a kinetic perturbation of a general duplex DNA binding pathway. J. Biol. Chem. *264*, 21848-21856

Klysik, J., Stirdivant, S. M., Larson, J. E., Hart, P. A. and Wells, R. D. (**1981**). Left-handed DNA in restriction fragments and a recombinant plasmid. Nature *290*, 672-677

Kmiec, E. B., Angelides, K. J. and Holloman, W. K. (**1985**). Left-handed DNA and the synaptic pairing reaction promoted by *Ustilago* rec1 protein. Cell *40*, 139-145

Kolb, A., Busby, S., Buc, H., Garges, S. and Adhya, S. (**1993**). Transcriptional regulation by cAMP and its receptor protein. Ann. Rev. Biochem. *30*, 535-578

Kormanec, J. and Farkašovský, M. (**1993**). Differential expression of principle sigma factor homologues of *Streptomyces aureofaciens* correlates with the developmental stage. Nucl. Acids Res. *21*, 3647-3652

Krishna, P., Kennedy, B. P., Waisman, D. M., van de Sande, J. H. and McGhee, J. D. (**1990**). Are many *Z*-DNA binding proteins actually phospholipid-binding proteins? Proc. Natl. Acad. Sci. USA *87*, 1292-1295

Kutzner, H. J. and Waksman, S. A. (**1959**). *Streptomyces coelicolor* Muller and *Streptomyces violaceoruber* Waksman and Curtis, two distinctly different organisms. J. Bacteriol. *78*, 528-538

Kwakman, J. H. J. M. and Postma, P. W. (**1994**). Glucose kinase has a regulatory role in carbon catabolite repression in *Streptomyces coelicolor*. J. Bacteriol. *176*, 2694-2698

Laskey, R. A., Honda, B. M., Mills, A. D. and Finch, J. T. (**1978**). Nucleosomes are assembled by an acidic protein which binds histones and transfers them to DNA. Nature *275*, 416-420

Lawlor, E. J., Baylis, H. A. and Chater, K. F. (**1987**). Pleiotropic morphological and antibiotic deficiencies result from mutations in a gene encoding a tRNA-like product in *Streptomyces coelicolor* A3(2). Genes Dev. *1*, 1305-1310

Leith, I. R., Hay, R. T. and Russell, W. C. (**1988**). Detection of *Z*-DNA in tissue culture cells. Nucl. Acids Res. *16*, 8277-8289

Leskiw, B. K., Bibb, M. J. and Chater, K. F. (**1991**). The use of a rare codon specifically during development? Mol. Microbiol. *5*, 2861-2867

Leskiw, B. K., Mah, R., Lawlor, E. J. and Chater, K. F. (**1993**). Accumulation of *bldA*-specified tRNA is temporally regulated in *Streptomyces coelicolor* A3(2). J. Bacteriol. *175*, 1995-2005

Lilley, D. M. J. (**1986**). Bacterial Chromatin. A new twist to an old story. Nature *320*, 14-15

Lilley, D. M. J. and Hallam, L. R. (**1984**). Thermodynamics of the ColE1 cruciform. Comparisons between probing and topological experiments using single topoisomers. J. Mol. Biol. *180*, 179-200

Lin, E. C. C. (**1976**). Glycerol dissimilation and its regulation in bacteria. Annu. Rev. Microbiol. *30*, 535-578

Lin, Y.-S., Kieser, H. M., Hopwood, D. A. and Chen, C. W. (**1993**). The chromosomal DNA of *Streptomyces lividans* 66 is linear. Mol. Microbiol. *10*, 923-933

Liu, L. F. and Wang, J. C. (**1987**). Supercoiling of the DNA template during transcription. Proc. Natl. Acad. Sci. USA *84*, 7024.

Lockshon, D. and Morris, D. R. (**1983**). Positively supercoiled plasmid DNA is produced by treatment of *Escherichia coli* with DNA gyrase inhibitors. Nucl. Acids Res. *11*, 2999-3017

Lockshon, D. and Morris, D. R. (**1985**). Sites of reaction of *Escherichia coli* DNA gyrase on pBR322 *in vivo* as revealed by oxolonic acid-induced plasmid linearization. J. Mol. Biol. *181*, 63-74

Losick, R. and Straiger, P. (**1992**). Crisscross regulation of cell-type-specific gene expression during development in *B.subtilis*. Nature *355*, 601-604

Lomovskaya, N. D., Mkrtumian, N. M., Gostimskaya, N. L., and Danilenko, V. N. (**1972**). Characterization of temperate actinophage ϕC31 isolated from *Streptomyces coelicolor* A3(2). J. Virol. *9*, 258-262

Luttinger, A. (**1995**). The twisted 'life' of DNA in the cell: bacterial topoisomerases. Mol. Microbiol. *15*, 601-606

Malkhosyan, S. R., Panchenko, Y. A. and Rekesh, A. N. (**1991**). A physiological role for DNA supercoiling in the anaerobic regulation of colicin gene expression. Mol. Gen. Genet. *225*, 343-345

Margolin, P., Zumstein, P. L., Sternglanz, R. and Wang, J. C. (**1985**). The *Escherichia coli supX* locus is *topA*, the structural gene for DNA topoisomerase I. Proc. Natl. Acad. Sci. USA *82*, 5437-5441

Martin, J. F. and Demain, A. L. (**1980**). Control of antibiotic biosynthesis. Microbiol. Rev. *44*, 230-251

May, G., Dersch, P., Haardt, M., Middendorf, A. and Bremer, E. (**1990**). The *osmZ* (*bglY*) gene encodes the DNA-binding protein H-NS (H1a), a component of the *Escherichia coli* K12 nucleoid. Mol. Gen. Genet. *224*, 81-90

MacNeil , D. J., Gewain, K. M., Ruby, C. L., Dezeny, G., Gibbons, P. H. (**1992**). Analysis of *Streptomyces avermitilis* genes required for avermectin biosynthesis utilizing a novel integration vector. Gene *111*, 61-68

McClellan, J. A.,Boublikova, P., Palecek, E. and Lilley, D. M. (**1990**). Superhelical torsion in cellular DNA responds directly to environmental and genetic factors. Proc. Natl. Acad. Sci. USA *87*, 8373-8377

McCue, L. A., Kwak, J., Babock, M. J. and Kendrick, K. E. (**1992**). Molecular analysis of sporulation in *Streptomyces griseus*. Gene *115*, 173-179

McLaughlin, J. R., Murray, C. L. and Rabinowitz, J. C. (**1981**). Unique features in the ribosome binding site sequence of the gram-positive *Staphylococcus aureus* beta-lactamase gene. J. Biol Chem. *256*, 11283-11291

McLean, M. J., Blaho, J. A., Kilpatrick, M. W. and Wells, R. D. (**1986**). Consecutive AT pairs can adopt a left-handed DNA structure. Proc. Natl. Acad. Sci. USA *83*, 5884-5888

McLean, M. J., Lee, J. W. and Wells, R. D. (**1988**). Characteristics of *Z*-DNA helices formed by imperfect (purine-pyrimidine) sequences in plasmids. J. Biol. Chem. *263*, 7378-7385

McLean, M. J. and Wells, R. D. (**1988**). The role of sequence in the stabilization of left-handed DNA helices *in vitro* and *in vivo*. Bioc. Biop. Acta *950*, 243-254

Menzel, R. and Gellert, M. (**1983**). Regulation of the genes for *Escherichia coli* DNA gyrase: homeostatic control of DNA supercoiling. Cell *34*, 105-113

Menzel, R. and Gellert, M. (**1987**). Modulation of transcription by DNA supercoiling: a deletion analysis of the *Eschericheria coli gyrA* and *gyrB* promoters. Proc. Natl. Acad. Sci. USA *84*, 4185-4189

Miller, W. G. and Simons, R. S. (**1993**). Chromosomal supercoiling in *Escherichia coli*. Mol. Microbiol. *10*, 675-684

Miura-Masuda, A. and Ikeda, H. (**1990**). The DNA gyrase of *Escherichia coli* participates in the formation of a spontaneous deletion by *recA*-independent recombination *in vitro*. Mol. Gen. Genet. *220*, 345-352

Miyashita, K., Fujii, T. and Sawada, Y. (**1991**). Molecular cloning and characterization of chitinase genes from *Streptomyces lividans* 66. J. Gen. Microbiol. *137*, 2065-2072

Mukai, F. H. and Margolin, P. (**1963**). Analysis of unlinked suppressors of an O° mutation in *Salmonella*. Proc. Natl. Acad. Sci. USA *50*, 140-148

Murakami, T., Holt, T. G. and Thompson, C. J. (**1989**). Thiostrepton-induced gene expression in *Streptomyces lividans*. J. Bacteriol. *171*, 1459-1466

Narva, K. E. and Feitelson, J. S. (**1990**). Nucleotide sequence and transcriptional analysis of the *redD* locus of *Streptomyces coelicolor* A3(2). J. Bacteriol. *172*, 326-333

Naito, A., Naito, S. and Ikeda, H. (**1984**). Homology is not required for recombination mediated by DNA gyrase of *Escherichia coli*. Mol. Gen. Genet. *193*, 238-243

Nègre, D., Cortay, J.-C., Old, I. G., Galinier, A., Richaud, C., Girons, I. S. and Cozzone, A. J. (**1991**). Overproduction and characterisation of the *iclR* gene product of *Escherichia coli* K-12 and comparison with that of *Salmonella typhimurium* LT2. Gene *97*, 29-37

Ni Bhriain, N., Dorman, C. J. and Higgins, C. F. (**1989**). An overlap between osmotic and anaerobic stress responses: a potential role for DNA supercoiling in the co-ordinate regulation of gene expression. Mol. Microbiol. *3*, 933-942

Nicholson, W. L. and Setlow, P. (**1990**). Dramatic increase in negative superhelicity of plasmid DNA in the forespore compartment of sporulating cells of *Bacillus subtilis*. J. Bacteriol. *172*, 7-14

Nicholson, W. L., Setlow, B. and Setlow, P. (**1990**). Binding of DNA *in vitro* by a small, acid soluble, spore protein from *Bacillus subtilis* and the effect of this binding on DNA topology. J. Bacteriol. *172*, 6900-6906

Nordheim, A., Tesser, P., Azorin, F., Kwon, Y. H., Moller, A. and Rich, A. (**1982**). Isolation of *Drosophila* proteins that bind selectively to left-handed *Z*-DNA. Proc. Natl. Acad. Sci. USA *79*, 7729-7733

Okami, Y. and Hotta, K. (**1988**). Search and discovery of new antibiotics. In Actinomycetes in Biotechnology. M. Goodfellow, S. T. Williams and M. Mordarski Eds. (Academic Press, London), pp. 33-67

Paget, M. S. B. (**1994**). Gene regulation and expression vector development in *Streptomyces*. Ph.D. Dissertation (UMIST, Manchester, UK)

Paget, M. S. B., Hintermann, G. and Smith, C. P. (**1994**). Construction and application of streptomycete promoter probe vectors which employ the *Streptomyces glaucescens* tyrosinase-encoding gene as reporter. Gene *146*, 105-110

Passantino, R., Puglia, A.-M. and Chater, K. F. (**1991**). Additional copies of the *act*II regulatory gene induce actinorhodin production in pleiotropic *bld* mutants of *Streptomyces coelicolor* A3(2). J. Gen. Microbiol. *137*, 2059-2064

Pavitt, G. D. and Higgins, C. F. (**1993**). Chromosomal domains of supercoiling in *Salmonella typhimurium*. Mol. Microbiol. *10*, 685-696

Peck, L. J. and Wang, J. C. (**1981**). Sequence of the helical repeat of DNA in solution. Nature *292*, 375-378

Peck, L. J. and Wang, J. C. (**1983**). Energetics of *B*-to-*Z* transition in DNA. Proc. Natl. Acad. Sci. USA *80*, 6206-6210

Peck, L. J. and Wang, J. C. (**1985**). Transcription block caused by a negative supercoiling induced structural change in an alternating CG sequence. Cell *40*, 129-137

Pettijohn, D. E. and Pfenninger, O. (**1980**). Supercoils in prokaryotic DNA restrained *in vivo*. Proc. Natl. Acad. Sci. USA *77*, 1331-1335

Pohl, F. M. and Jovin, T. M. (**1972**). Salt-induced co-operative conformational change of synthetic DNA: equilibrium and kinetic studies with poly (dG-dC). J. Mol. Biol. *67*, 375-396

Postma, P. W., Lengeler, J. W. and Jacobson, G. R. (**1993**). Phosphoenolpyruvate:carbohydrate phosphotransferase systems of bacteria. Microbiol. Rev. *57*, 543-594

Pruss, G. J. (**1985**). DNA topoisomerase I mutants. Increased heterogeneity in linking number and other replicon-dependant changes in DNA supercoiling. J. Mol. Biol. *185*, 51-63

Pruss, G. J. and Drlica, K. (**1986**). Topoisomerase I mutants: the gene of pBR322 that encodes resistance to tetracycline affects plasmid DNA supercoiling. Proc. Natl. Acad. Sci. USA *83*, 8952-8956

Pruss, G. J., Manes, S. H. and Drlica, K. (**1982**). *Escherichia coli* DNA Topoisomerase I mutants: increased supercoiling is corrected by mutations near the gyrase genes. Cell *31*, 35-42

Rahmouni, A. R. and Wells, R. D. (**1989**). Stabilization of *Z*-DNA *in vivo* by localised supercoiling. Sci. *246*, 358-363

Rahmouni, A. R. and Wells, R. D. (**1992**). Direct evidence for the effect of transcription on local DNA supercoiling *in vivo*. J. Mol. Biol. *223*, 131-144

Raibaud, A., Zalacain, M., Holt, T. G., Tizard, R. and Thompson, C. J. (**1991**). Nucleotide sequence analysis reveals linked *N*-acetyl hydrolase, thioesterase, transport, and regulatory genes encoded by the bialaphos biosynthetic gene cluster of *Streptomyces hygroscopicus*. J. Bacteriol. *173*, 4454-4463

Ramirez, R. M. and Villarejo, M. (**1991**). Osmotic signal transduction to proU is independent of DNA supercoiling in *Escherichia coli*. J. Bacteriol. *173*, 879-885

Reverchon, S., Nasser, W. and Robert-Baudouy, J. (**1991**). Characterization of *kdgR*, a gene of *Erwinia chrysanthemi* that regulates pectin degradation. Mol. Microbiol. *5*, 2203-2216

Reznikoff, W. S., Siegele, D. A., Cowing, D. W. and Gross, C. A. (**1985**). The regulation of transcription initiation in bacteria. Ann. Rev. Genet. *19*, 355-387

Richardson, S. M. H., Higgins, C. F. and Lilley, D. M. J. (**1988**). DNA supercoiling and the *leu-500* promoter mutation of *Salmonella typhimurium*. Embo. J. *7*, 1863-1869

Richet, E. and Raibaud, O. (**1991**). Supercoiling is essential for the formation and stability of the initiation complex at the divergent *malEp* and *malKp* promoters. J. Mol. Biol. *218*, 529-542

Robbins, P. W., Overbye, K., Albright, C., Benfield, B. and Pero, J. (**1992**). Cloning and high-level expression of chitinase-encoding gene of *Streptomyces plicatus*. Gene *111*, 69-76

Roberts, J. M., Buck, L. B. and Axxel, R. (**1983**). A structure for amplified DNA. Cell *33*, 53-63

Roth, S. Y. and Allis, C. D. (**1992**). Chromatin condensation: does histone H1 dephosphorylation play a role? TIBS *17*, 93-98

Rüther, U., Koenen, M., Otto, K., and Müller-Hill, B. (**1981**). pUR222, a vector for cloning and rapid chemical sequencing of DNA. Nucl. Acids Res. *9*, 4087-4098

Saier Jr, M. H. (**1993**). Regulatory interactions involving the proteins of the phosphotransferase system in enteric bacteria. J. Cell. Biochem. *51*, 62-68

Sambrook, J., Fritsch, E. F. and Maniatis, T. (**1989**). Molecular Cloning. A laboratory manual. (Cold Spring Harbour Laboratory Press, Cold Spring Harbour, NY)

Saing, K. M., Orii, H., Tanaka, Y., Yanagisawa, K., Miura, A. and Ikeda, H. (**1988**). Formation of deletion in *Escherichia coli* between direct repeats located in the long inverted repeats of a cellular slime mold plasmid: participation of DNA gyrase. Mol. Gen. Genet. *214*, 1-5

Sanger, F., Nicklen, S. and Coulson, A. R. (**1977**). DNA sequencing with chain terminating inhibitors. Proc. Natl. Acad. Sci. USA *74*, 5463-5467

Saunders, S. E. and Burke, J. F. (**1990**). Rapid isolation of miniprep DNA for double strand sequencing. Nucl. Acids Res. *18*, 4948

Schultz, S. C., Shields, G. C. and Steitz, T. A. (**1991**). Crystal structure of a CAP-DNA complex: the DNA is bent by 90 degrees. Science *253*, 1001-1007

Seno, E. T. and Chater, K. F. (**1983**). Glycerol catabolic enzymes and their regulation in wild-type and mutant strains of *Streptomyces coelicolor* A3(2). J. Gen. Microbiol. *129*, 1403-1413

Seno, E. T., Bruton, C. J. and Chater, K. F. (**1984**). The glycerol utilization operon of *Streptomyces coelicolor*: Genetic mapping of *gyl* mutations and the analysis of cloned *gyl* DNA. Mol. Gen. Genet. *193*, 119.

Setlow, P. (**1992**). DNA in dormant spores of *Bacillus* species is in an *A*-like conformation. Mol. Microbiol. *6*, 563-567

Sheehan, B. J., Foster, T. J., Dorman, C. J., Park, S. and Stewart, G. S. A. B. (**1992**). Osmotic and growth-phase dependent regulation of the *eta*-gene of *Staphylococcus aureus*: a role for DNA supercoiling. Mol. Gen. Genet. *232*, 49-57

Shure, M., Pulleybank, D. E. and Vinograd, J. (**1977**). The problems of eukaryotic and prokaryotic DNA packaging and *in vivo* conformation posed by superhelix density heterogeneity. Nucl. Acids Res. *4*, 1183-1205

Silhavy, T. J., Benson, S. A. and Emr, S. D. (**1983**). Mechanisms of protein localization. Microbiol. Rev. *47*, 313-344

Sinden, R. R., Carlson, J. O. and Pettijohn, D. E. (**1980**). Torsional tension in the DNA double helix measured with trimethylpsoralen in living *E. coli* cells: analogous measurements in insect and human cells. Cell *21*, 773-783

Singleton, C. K., Klysik, J., Stirdivant, S. M. and Wells, R. D. (**1982**). Left-handed *Z*-DNA is induced by supercoiling in physiological ionic conditions. Nature *299*, 312-31

Singleton, C. K. and Wells, R. D. (**1982**). The facile generation of covalently closed, circular DNAs with defined superhelical densities. Anal. Biochem. *122*, 253-257

Smith, C. P. (**1986**). Molecular biology of the glycerol utilization operon of *Streptomyces coelicolor* A3(2). PhD. Dissertation. (University of East Anglia, Norwich, UK)

Smith, C. P. and Chater, K. F. (**1988a**). Cloning and transcriptional analysis of the entire glycerol utilization (*gylABX*) operon of *Streptomyces coelicolor* A3(2) and identification of a closely associated transcription unit. Mol. Gen. Genet. *211*, 129-137

Smith, C. P. and Chater, K. F. (**1988b**). Structure and regulation of controlling sequences for the *Streptomyces coelicolor* glycerol operon. J. Mol. Biol. *204*, 569-580

Smith, G. R. (**1981**). DNA supercoiling: Another level for regulating gene expression. Cell *24*, 599-600

Spiro, S. and Guest, J. R. (**1987**). Activation of the *lac* operon of *Escherichia coli* by a mutant Fnr protein. Mol. Microbiol. *1*, 53-58

Stanssens, P., Opsomer, C., McKeown, Y. M., Kramer, W., Zabeau, M. and Fritz, H.-J. (**1989**). Efficient oligo-nucleotide directed construction of mutations in expression vectors by the gapped duplex DNA method using alternative selectable markers. Nucl. Acids Res. *17*, 4441-4454

Steck, T., Franco, R. J., Wang, J.-Y. and Drlica, K. (**1993**). Topoisomerase mutations affect the relative abundance of many *Escherichia coli* proteins. Mol. Microbiol. *10*, 473-481

Strohl, W. R. (**1992**). Compilation and analysis of DNA sequences associated with apparent streptomycete promoters. Nucl. Acids Res. *20*, 961-974

Stutzman-Engwall, K. J., Otten, S. L. and Hutchinson, C. R. (**1992**). Regulation of secondary metabolism in *Streptomyces* spp. and overproduction of daunorubicin in *Streptomyces peucetius*. J. Bacteriol. *174*, 144-154

Takano, E., Gramajo, H. C., Strauch, E. and Andres, N. (**1992**). Transcriptional regulation of the *redD* transcriptional activator gene accounts for growth-phase-dependent production of the antibiotic undecylprodigiosin in *Streptomyces coelicolor* A3(2). Mol. Microbiol. *6*, 2797-2804

Tan, J., Shu, L. and Wu, H.-Y. (**1994**). Activation of the *leu-500* promoter by adjacent transcription. J. Bacteriol. *176*, 1077-1086

Tautz, D. and Renz, M. (**1983**). An optimized freeze-squeeze method for the recovery of DNA fragments from agarose gels. Anal. Biochem. *132*, 14-19

Thiara, A. S. and Cundliffe, E. (**1993**). Expression and analysis of two *gyrB* genes from the novobiocin producer, *Streptomyces sphaeroides*. Mol. Microbiol. *8*, 495-506

Titgemeyer, F., Walkenhorst, J., Cui, X, Reizer, J. and Saier Jr, M. H. (**1994**). Proteins of the phosphoenolpyruvate:phosphotransferase system in *Streptomyces*: possible involvment in the regulation of antibiotic production. Res. Microbiol. *145*, 89-92

Trifonov, E. N., Konopka, A. K. and Jovin, T. M. (**1985**). Unusual frequencies of certain purine-pyrimidine runs in natural DNA sequences: Relation to *Z*-DNA. FEBS. Lett. *185*, 197-202

Tse-Dinh, Y.-C. (**1985**). Regulation of the *Escherichia coli* DNA topoisomerase 1 gene by DNA supercoiling. Nucl. Acids Res. *13*, 4751-4763

Tupper, A. E., Owen-Hughes, T. A., Ussery, D. W., Santos, D. S., Ferguson, D. J. P., Sidebotham, J. M., Hinton, J. C. D. and Higgins, C. F. (**1994**). The chromatin-associated protein H-NS alters DNA topology *in vitro*. Embo. J. *13*, 258-268

Umek, R. M. and Kowalski, D. (**1988**). The ease of DNA unwinding as a determinant of initiation at yeast replication origins. Cell *52*, 559-567

Vinograd, J., Lebowitz, J., Radloff, R., Watson, R. and Laipis, P. (**1965**). The twisted circular form of polyoma viral DNA. Proc. Natl. Acad. Sci. USA *53*, 1104-1111

Virolle, M.-J. and Bibb, M. J. (**1988**). Cloning, characterisation, and regulation of an α-amylase gene from *Streptomyces limosus*. Mol. Microbiol. *2*, 197-208

Virolle, M.-J., Long, C. M., Chang, S. and Bibb, M. J. (**1988**). Cloning, characterisation and regulation of an α-amylase gene from *Streptomyces venezuelae*. Gene *74*, 321-334

Volff, J.-N, Vandewiele, D., Simonet, J.-M. and Decaris, B. (**1993**). Stimulation of genetic instability in *Streptomyces ambofaciens* ATCC 23877 by antibiotics that interact with DNA gyrase. J. Gen. Microbiol. *139*, 2551-2558

Wang, A. H.-J., Quigley, G. J., Kolpak, F. J., Crawford, J. L., van Boom, J. H., van der Marle, G. and Rich, A. (**1979**). Molecular structure of left-handed double helical DNA fragment at atomic resolution. Nature *282*, 680-686

Wang, J. C. (**1971**). Interaction between DNA and an *Escherichia coli* protein ω. J. Mol. Biol. *55*, 523-533

Wang, J. C. (**1985**). DNA Topoisomerases. Ann. Rev. Biochem. *54*, 665-697

Ward, J. M., Janssen, G. R., Kieser, T., Bibb, M. J., Buttner, M. J. and Bibb, M. J. (**1986**). Construction and characterisation of a series of multi-copy promoter-probe plasmid vectors for *Streptomyces* using the aminoglycoside phosphotransferase gene from Tn*5* as indicator. Mol. Gen. Genet. *203*, 468-478

Watson, J. D. and Crick, F. H. C. (**1953**). Molecular structure of deoxypentose nucleic acids. Nature *171*, 737-73

Wells, R. D., Amirhaeri, S., Blaho, J. A., Collier, D. A., Hanvey, J. C., Hsieh, W.-T., Janorski, A., Klysik, J., Larson, J. E., McLean, M. J., Wohlrab, F. and Zacharias, W. (**1988**). Unusual DNA structures and the probes used in their detection. In Unusual DNA Structures. R. D. Wells and S. C. Harvey Eds. (Springer-Verlag, New York), pp. 1-21

Westerhoff, H., O'Dea, M., Maxwell, A. and Gellert, M. (**1988**). DNA supercoiling by DNA gyrase. A static head analysis. Cell Biophys. *12*, 157-181

Westpheling, J., Ranes, M. and Losick, R. (**1985**). RNA polymerase heterogeneity in *Streptomyces coelicolor*. Nature *313*, 22-27

White, J. H. (**1969**). Self-linking and the Gauss integral in higher dimensions. Am. J. Math. *91*, 693-728

Willey, J., Santamaria, R., Guijarro, J., Geistlich, M. and Losick, R. (**1991**). Extracellular complementation of a developmental mutation implicates a small sporulation protein in aerial mycelium formation by *S. coelicolor*. Cell *65*, 641-650

Willimsky, G., Bang, H., Fischer, G. and Marahiel, M. A. (**1992**). Characterization of *cspB*, a *Bacillus subtilis* inducible cold shock gene affecting cell viability at low temperatures. J. Bacteriol. *174*, 6326-6335

Worcel, A. and Burgi, E. (**1972**). On the structure of the folded chromosome of *Escherichia coli*. J. Mol. Biol. *71*, 127-147

Wright, F. and Bibb, M. J. (**1992**). Codon usage in the G+C-rich *Streptomyces* genome. Gene *113*, 55-65

Wu, H.-Y., Shyy, S., Wang, J. C. and Liu, L. F. (**1988**). Transcription generates positively and negatively supercoiled domains in the template. Cell *53*, 433-440

Yamamoto, A. and Droffner, M. L. (**1985**). Mechanisms determining aerobic or anaerobic growth in the facultative anaerobe *Salmonella typhimurium*. Proc. Natl. Acad. Sci. USA *82*, 2077-2081

Young, M. and Cullum, J. (**1987**). A plausible mechanism for large-scale chromosomal DNA amplification in streptomycetes. FEBS Lett. *212*, 10-14

Volff, J.-N., Vandewiele, D., Simonet, J.-M. and Decaris, B. (**1993**). Stimulation of genetic instability in *Streptomyces ambofaciens* ATCC 23877 by antibiotics that interact with DNA gyrase. J. Gen. Microbiol. *139*, 2551-2558

Zacharias, W., Jaworski, A. and Wells, R. D. (**1990**). Cytosine methylation enhances *Z*-DNA formation *in vivo*. J. Bacteriol. *172*, 3278-3283

Zähner, H. (**1979**). What are secondary metabolites? Folia Microbiol. *24*, 435-443

Zell, R., and Fritz, H.-J. (**1987**). DNA mismatch-repair in Escherichia coli counteracting the deamination of 5-methyl-cytosine residues. EMBO J. *6*, 1809-1815

Zhou, X., Deng, Z., Firmin, J. L., Hopwood, D. A. and Kieser, T. (**1988**). Site-specific degradation of *Streptomyces lividans* DNA during electrophoresis in buffers contaminated with ferrous iron. Nucl. Acids Res. *16*, 4341-4352